Molecular Phylogenetics and Biogeography of Sphenomorphini (Squamata: Scincidae)

By

Charles W. Linkem
B.A., University of California Berkeley, 2004

Submitted to the Department of Ecology and Evolutionary Biology and the Faculty of the Graduate School of the University of Kansas in partial fulfillment of the requirements fro the degree of Doctor of Philosophy

Chair: _____

Committee Members: _____

_____

_____

_____

Date defended:____2 April 2010_____

The dissertation committee for Charles W. Linkem certifies that this is the approved version of the following dissertation:

Molecular Phylogenetics and Biogeography of Sphenomorphini (Squamata: Scincidae)

Chair: _____

Committee Members: _____

_____

_____

_____

Date approved:_____2 April 2012_____

Abstract

Sphenomorphini consists of 549 species in 34 genera, making it the most diverse skink tribes. Species diversity is highest in Southeast Asia with species found from the middle east, Asia, Australia, North and Central America. Taxonomic relationships among many of the genera and species within the genera are contentious due to poor morphological diagnoses. This dissertation resolves many of these issues through the examination of multiple independent molecular markers. Using traditional and new phylogenetic approaches an estimate of the relationships in Sphenomorphini is obtained. Additionally, the biogeographic history of Sphenomorphini and certain subgroups are examined under a variety of different approaches. A new taxonomy is defined for portions of Sphenomorphini and new species are described in the Philippines. These taxonomic changes and the new estimate of phylogenetic relationships of Sphenomorphini contribute a substantial step forward in the understanding of skink relationships.

Acknowledgements

This work is the result of the efforts from numerous individuals across many institutions. The scope of data sampling required for this work would simply not have been possible without the dedication of field researchers to generally collect all reptiles and amphibians, even if they did not have an interest in the group or were not even herpetologists. Some chapters contained herein have been co-authored variously with Kyle Hesed, Arvin Diesmos, and Rafe Brown. I gratefully acknowledge financial support provided by: an American Philosophical Society Lewis and Clark Fellowship; multiple University of Kansas Biodiversity Institute Panorama Grants; University of Kansas Department of Ecology and Evolutionary Biology; University of Kansas Graduate Program; the National Science Foundation grants DEB 0073199, 0640737 and EF 0334952 to R. Brown and DEB 0910341. Field work would not have been possible without the support of the Philippine, Indonesian, and Vietnamese governments. I thank all the collection managers and field researchers who provided me with samples necessary to complete this project including: R. F. Inger, and A. Resetar (FMNH), R. N. Fisher (USGS), B. Stuart (NCSM), C. Siler (KU), J. Vindum (CAS), C. Austin (LSU), J. McGuire (MVZ), B. Evans (McMaster), F. Kraus (BPBM), A. Allison (BPBM), A. Diesmos (PNM), L. Welton (KU), M. Brandley (MVZ), C. Hayden (LSU) and R. Brown (KU). Additionally, I appreciate the efforts of L. Heaney, E. Rickart, L. Duya, A. Duya, J. Esselstyn, M. Veluz, and D. Balete, who had the foresight to preserve genetic samples from skinks captured in their mammal traps.

The division of herpetology in the Biodiversity Institute has been my home for many years, and I thank all the past and present students who have made this such an enjoyable and enlightening place to work. Several individuals have aided my progress through reviewing manuscripts and offering stimulating discussions including: Anthony Barley, David Blackburn, Rafe Brown, Andrea Crowther, Matthew Davis, Bill Duellman, Jacob Esselstyn, Allison Fuiten, Jesse Grismer, Juan Manuel Guyasamin, Tracy Heath, Mark Holder, Andres Lira, Rob Moyle, Jamie Oaks, Carl Oliveros, Cameron Siler, Jeet Sukumaran, Linda Trueb, and several anonymous reviewers. I especially thank my advisor Rafe Brown and members of my Ph.D. committee Linda Trueb, Mark Holder, Town Peterson, and Stephen Benedict for their critiques of earlier drafts of this work and research proposals.

I am especially grateful to Andrea Crowther, Jamie Oaks, Melissa Callahan, Kathryn Mickle, and Anthony Barley for watching my dogs (Toby and Rudy) while traveling. Finally, I am especially grateful to my wife Gabrielle for you constant support and patience throughout the years and for being understanding of my need to travel to far away jungles for months at a time.

Table of Contents

CHAPTER 1

Species boundaries and cryptic lineage diversity in a Philippine forest skink complex (Retilia; Squamata; Scincidae: Lygosominae)

An incomplete understanding of biodiversity can result in poorly informed conservation planning, especially when conservation decisions are based on species diversity data confounded by outdated taxonomy. In the megadiverse global conservation hotspot of the Philippines, conservation and management decisions are ideally based on sound taxonomy, verified knowledge of biological diversity, and a basic understanding of the distributions of endemic species. Phylogenetic and phylogeographic analyses of widespread species complexes have the potential to inform conservation biologists and wildlife managers by elucidating hidden genetic variation and/or cryptic species and relating independent evolutionary lineages to geographic centers of endemism (Evans et al. 2003a). However, few regional or archipelago-wide phylogenetic studies of widespread species complexes have been conducted in the islands of Southeast Asia. Further, in biodiversity-rich Asian archipelagos like the Philippines, conservation planning has lagged behind the few available molecular phylogeographic studies. Instead, prioritizing areas for conservation has focused on geographic pockets where multiple endemic bird and mammal species co-occur (Utzurrum 1991; DENR 1997; Heaney and Mittermeier 1997; Collar et al. 1999; Mittermeier et al. 2000; Myers et al. 2000; Mallari et al. 2001; Diesmos et al. 2002; Ong et al. 2002). Although an informative first step, the practice of

mapping species distributions and prioritizing sites of maximal overlapping Areas of Endemism (AOEs)—the important areas for conservation approach—is only as sound as the underlying taxonomic knowledge of species included (Brown 2006). Similarly, the practice of establishing protected areas to cover AOEs and Pleistocene Aggregate Island Complexes (PAICs) (Evans et al. 2003a,b) may fail when species defy regional AOE and PAIC boundaries, as often occurs in complex island archipelagos (Brown and Diesmos 2009; Esselstyn and Brown 2009).

In this study, we use a phylogeographic analysis of mitochondrial gene variation to examine the Philippine archipelago for evolutionarily significant geographic variants in a common, widespread complex of lizards in the family Scincidae. We reject previously accepted taxonomic and biogeographic hypotheses using parametric bootstrapping and identify several unexpected centers of hidden genetic diversity and possible cryptic species. Our results suggest that both taxonomy and a Pleistocene model of biogeographic and evolutionary diversification underestimate species diversity (genetic lineage diversity). Accordingly, we recommend densely sampled empirical appraisals of widespread species' genetic diversity rather than adherence to predictions from Pleistocene geography or extrapolations from the taxonomy of other groups.

Geological history of the Philippines

The Philippines consists of over 7,000 islands, varying in size, relief, and geological history (Hall 1998, 2002; Voris 2000; Catibog-Sinha and Heaney 2006;

Brown and Diesmos 2009; Yumul et al. 2009). The archipelago contains large, geologically complex islands such as Luzon and Mindanao (Fig. 1.1), islands of moderate size, and thousands of tiny fringing islets associated with these larger landmasses. The major islands are organized into biodiversity regions or subprovinces (Brown and Diesmos 2002, 2009), based on species distributions (Dickerson et al. 1928) and knowledge of historical land connections (Heaney 1986; Voris 2000). First defined by Dickerson et al. (1928), Kloss (1929), and Inger (1954), these Pleistocene Aggregate Island Complexes (PAICs; Brown and Diesmos 2002) are the result of oscillating sea-levels during Pleistocene climatic cycling (Heaney 1986; Voris 2000). Islands separated by shallow channels merged to form large aggregate islands during low sea-level stands, allowing range expansions of flora and fauna through dispersion and dispersal (Brown and Guttman 2002; Roberts 2006a,b). These PAICs are characterized by high levels of endemism in mammals and birds (Heaney 1985; Kennedy et al. 2000; Esselstyn et al. 2004; reviewed by Brown et al. 2002) with much of the speciation or diversification in the archipelago being associated with colonization or dispersal between PAICs (Heaney and Rickart 1990). These observations in mammals and birds have failed to explain the modern diversity and species distributions for amphibians and reptiles (McGuire and Kiew 2000; Brown and Guttman 2002; Evans et al. 2003b). Recent phylogenetic studies of several taxa contradict the Pleistocene model of PAIC-level structuring of Philippine biodiversity (Jones and Kennedy 2008; Brown and Diesmos 2009; Esselstyn and Brown 2009; Esselstyn et al. 2009). Additionally, distributions of many taxa span

multiple PAICs (e.g., *Polypedates leucomystax*, *Draco spilopterus*, *Lamprolepis smaragdina*, *Sphenomorphus cumingi*). These examples may represent the high end of the relative dispersal-ability scale, species capable of repeatable and predictable over-water dispersal.

Predictions of biodiversity partitioning among and across PAICs

The geologic history of the Philippines tells us that (1) the Philippine islands (except Palawan) are oceanic and have always been separate from the continent and (2) that some of the islands were connected to one another during the Pleistocene when sea-levels were lower, forming larger aggregate islands. The combined geologic history of the PAICs unites the evolutionary history of the organisms living on those islands and forms hypotheses of relationships (Brown et al. 2002). This history predicts that each PAIC will have a different lineage (genus, species, subspecies, population, etc.) that can be diagnosed using genetic data (in this case mtDNA) and that multiple individuals from the same PAIC will have a shared genetic history (ie. form a clade of mtDNA haplotypes). There are at least two ways that a widely distributed endemic Philippine lineage could fail to meet the predictions of the Pleistocene model and thereby reject the PAIC structuring of Philippine biodiversity. The PAIC model could be rejected by (1) the topology of a phylogenetic analysis, or (2) an incompatible temporal framework for diversification. The PAIC model predicts monophyly of within-PAIC populations (assuming haplotype coalescence has occurred in time), due to shared history of island connectivity. Although we would not consider a few

dispersal events outside the geographic confines of a PAIC to offshore islands to be strong evidence for rejecting the PAIC model, wholesale deviation from the prediction of PAIC monophyly necessitates rejection of this hypothesis. Additionally, the PAIC model predicts relatively recent (mid- to late-Pleistocene) divergences between suites of closely related and minimally divergent taxa. If a time-calibrated phylogeny revealed evidence of numerous ancient lineages that pre-dated Pleistocene sea-level fluctuations, and if those divergences were statistically inconsistent with a Pleistocene framework for diversification, we would reject the PAIC model (eg. Jansa et al. 2006). We will explore the former in this paper.

Taxonomic review of the Sphenomorphus abdictus, S. coxi, and S. jagori species groups

The lygosomine genus *Sphenomorphus* is widespread, with high diversity in Southeast Asia. At least 145 species are recognized worldwide (EMBL reptile database, 2009), with 26 species currently recognized in the Philippines (Brown and Alcala 1980; Brown et al. 1995; Brown et al. 1999; Linkem et al. 2010a).

In their 1980 monograph *Philippine Lizards of the Family Scincidae*, Brown and Alcala arranged Philippine *Sphenomorphus* into six non-phylogenetic groups. Their Group 5, which they judged "to probably be a natural evolutionary group," included *S. llanosi* Taylor, *S. jagori* (Peters) and *S. coxi* Taylor. To this group, Brown and Alcala added a new species, *S. abdictus* (type locality: Camiguin Sur Island).

Sphenomorphus abdictus, *S. coxi*, and *S. jagori* are moderately large terrestrial skinks, inhabiting riparian, and open forested habitats. They share similar color patterns and characters of scalation, and co-occur across many islands of the Philippines (Brown and Alcala 1980; Fig. 2). A variety of morphological features were used by Brown and Alcala (1980) to define and to distinguish these species; unfortunately, these characters overlap both between subspecies of a single species and between the three species themselves (Table 1). In practice, the single feature most heavily relied upon to distinguish *S. abdictus* from *S. jagori* is the presence of two "very prominent dark bars" beneath the eye in *S. jagori* (Fig. 3C). However, a cursory examination of large numbers of specimens reveals that this character varies widely among both *S. abdictus* and *S. jagori* (unpublished data). At one end of the spectrum are animals that show complete absence of suborbital barring; at the other end of this range of variation are animals with highly prominent suborbital bars (as figured in Brown and Alcala 1980). Intermediate ranges of barring prominence are commonly observed (Fig. 1.3C) yet were discounted by Brown and Alcala (1980).

In some cases, the distributions of *S. abdictus* and *S. jagori* coincide with PAIC predictions of species diversity. *Sphenomorphus abdictus abdictus* is found on the Mindanao PAIC and nearby Camiguin Sur Island (Fig. 1.3B); *S. abdictus aquilonius* is limited to the Luzon PAIC; and *S. jagori grandis* is limited to the Visaya PAIC. However, *S. jagori jagori* is reported to occur on the Mindanao PAIC, the Luzon PAIC, and Mindoro Island. Although three of these four subspecies are restricted to a single PAIC and nearby islands, each of the two

species (*S. abdictus* and *S. jagori*) displays a distribution across multiple PAICs (Brown and Alcala 1980). The existing taxonomy and distributions circumscribed for these taxa clearly represent a pattern that is ripe for phylogenetic study and explicit hypothesis testing.

In this study we evaluate Brown and Alcala's (1980) enumeration of taxonomic diversity in this common group of Philippine forest skinks. Using a molecular phylogenetic analysis and parametric bootstrap simulations, we re-assess relationships in these species, and compare our results to previous taxonomy and the biogeographic expectations from the PAIC paradigm. Finally, we suggest future directions for estimating true species diversity in widespread Philippine species.

Materials and methods

Taxon sampling

Taxon sampling for this study comprised 168 vouchered tissue samples, including 156 samples of the six ingroup subspecies and 12 outgroup samples (Appendix 1). Ingroup sampling included collections from 38 sites in 19 provinces in the Philippines. Samples from type localities (or as close to these locations as possible) of the six nominal subspecies (*Sphenomorphus abdictus abdictus*, *S. abdictus aquilonius*, *S. coxi coxi*, *S. coxi divergens*, *S. jagori grandis*, and *S. jagori jagori*) were included. Voucher specimens were identified to subspecies based on the following criteria from Brown and Alcala (1980): frontoparietal fused (*S. coxi*) or divided (*S. abdictus* and *S. jagori*); subdigital

lamellae on toe IV between 20–25 (*S. abdictus*), or between 24–30 (*S. jagori*). Subspecies of *S. abdictus* were identified based on locality, number of large supraoculars, and number of midbody scale rows. Subspecies of *S. coxi* were identified based on locality and number of large supraoculars. The number of midbody scale rows and number of paravertebral scales identified subspecies of *S. jagori*. Specimens with a divided frontoparietal and toe IV lamellae counts of 24 or 25 were challenging to identify to species; in the few cases in which these numbers of scales were found, midbody scale row number or paravertebral scale number helped unequivocally to assign samples to subspecies.

The 12 outgroup samples include other *Sphenomorphus* species (*S. fasciatus*, *S. jobiensis*, *S. leucospilos*, *S. llanosi*, and *S. steerei*) as well as species of the genera *Scincella* (*S. potanini*, *S. rupicola*, and *S. tsinlingensis*) and *Eutropis* (*E. multifasciata*). *Sphenomorphus llanosi* was determined by Brown and Alcala (1980) to be morphologically similar to the three species under investigation here. We included additional species representing a range of diversity in the genus to ensure that the taxa under examination were properly rooted.

Molecular data collection and alignment

Whole genomic DNA was extracted from liver or muscle tissue using a Guanidine Thiocyanate protocol that was adapted from the Puregene protocol (Esselstyn et al. 2008). The mitochondrial gene encoding NADH dehydrogenase subunit 2 (ND2) was amplified by Polymerase Chain Reaction (PCR) using overlapping primers modified from Macey et al. (1997). The primer sequences

used for PCR are: METF6 5'—AAGCTTTCGGGCCCATACC—3' and SphenoR 5'—TAGGYGGCAGGTTGTAGCCC—3'. These primers amplify the protein coding gene only, and not the associated tRNAs. Amplification followed standard PCR protocols (Palumbi, 1996) with the following thermal cycling conditions: 5 min. at 95ºC, followed by 30 cycles of 95ºC for 30 sec., 50ºC for 30 sec., and 72ºC for 1:30 sec., and a final extension at 72ºC for 7 min. Amplified samples were purified using Exonuclease I and Shrimp Alkaline Phosphatase (ExoSAPit, USB corp.). Purified PCR products were sequenced directly using Big Dye Terminator sequencing reaction mix following manufacturer's protocols (Applied Biosystems). The PCR primers and an additional sequencing primer (ND2SPHR 5'—CTCTTDTTTGTRGCTTTGAAGGC—3') were used for multiple coverage of each base. Cycle-sequencing products were visualized on an ABI 3130 automated sequencer. Sequences were edited using Sequencher v4.2 and aligned with MUSCLE v3.6 (Edgar 2004) using default settings. Coding frame was verified by gene translation in MacClade v4.07 (Maddison and Maddison 2005). There were no adjustments needed for the original alignment, and all characters were included in analyses (Treebase.org: project number SN4928). Corrected sequence divergences were calculated in PAUP* with the GTR model.

Phylogenetic analysis

Bayesian phylogenetic analyses were performed in MrBayes v3.1.2 (Huelsenbeck and Ronquist 2001). The best-fit nucleotide substitution model for each of the three partitions was determined using MrModelTest 2.2 (Nylander

2004). Data were partitioned by codon position to allow for variation in evolutionary rate. Each Bayesian analysis was run for 20 million generations, sampling from the chain every 1000 generations. The output files were examined in Tracer v1.4 (Rambaut and Drummond 2007) to determine the number of generations to exclude as burn-in and to ensure that all parameters converged. Additionally, we used Are We There Yet (AWTY: Nylander et al. 2007; Wilgenbush et al. 2004) to ensure that the multiple runs converged and that sampling was sufficient. The sump and sumt commands were executed in MrBayes, summing over the multiple convergent runs.

Hypothesis Testing

When inferring a phylogenetic tree, we may conceive of a particular topology or set of *a priori* relationships of interest. If these relationships are not represented in the best estimate of the phylogeny, it is often interesting to know if our *a priori* hypotheses reside within the possibilities of the data. In such cases, hypothesis testing is warranted. Previous examination (Brown and Alcala 1980) of the taxa studied herein found all three species to be closely related based on morphology. In addition, each species has two recognized subspecies. Given current interpretations of subspecies, we expect that each of those subspecies should represent distinct lineages. We tested each hypothesis of species monophyly and subspecies monophyly independently when they conflicted with our preferred topology.

To test these *a priori* hypotheses we implemented the Swofford-Olsen-

Wadell-Hillis (SOWH) parametric bootstrapping method (Swofford et al., 1996). The SOWH test has been found to have more power and lower occurrence of Type I error than other hypothesis testing methods (e.g., AU-test, SH-test, KH-test), when accurate simulation models are used (Goldman et al. 2000; Shi et al. 2006). A reduced data set representing 37 unique ingroup samples from all six subspecies and representative outgroups was used to expedite computation. A maximum likelihood analysis of the reduced dataset, with no partitions, was run in GARLI V0.6 (Zwickl 2006) under the GTR + I + G model with the hypothesis as a constraint on the phylogeny. The best of 10 runs was chosen as the tree for simulation, using the model scores from GARLI. These scores were used in Mesquite V2.5 in the Batch Architect Package (Maddison and Maddison 2004) to simulate 1000 datasets on the best tree under the constraint. For each dataset two heuristic parsimony searches were performed with 100 random addition-sequence replicates and TBR branch swapping. The first search was used to find the optimal tree consistent with the constraint, and the second search was used to find the unconstrained optimal tree. The frequency of difference in tree length between the first and second tree for each replicate dataset represents the expected distribution of the hypothesis. The observed differences between the best tree under the constraint and the best unconstrained tree were then compared to the distribution for the hypothesis to evaluate significance. The use of a complex model for dataset simulation (GTR + G + I, with parameters estimated from the empirical dataset) and a simpler model for the tree search (parsimony) renders our test more conservative, further reducing the possibility of type I error.

Additionally, we applied a sequential Bonferroni procedure to adjust alpha values for hypothesis rejection under multiple tests (Rice, 1989).

Results

Phylogenetic analyses

The unambiguously aligned dataset included 1038 nucleotides, representing the entirety of the ND2 gene. Each of the three partitions individually fit the GTR + G + I model. Our partitioned Bayesian analysis produced a consensus tree with a negative harmonic mean likelihood of 11531.25, which was summed from four independent runs. All parameters converged in all 4 runs, examination of which was accomplished both in Tracer and AWTY. Burn-in was estimated at 2 million generations, giving a posterior distribution of 18,000 trees per run. A 50% majority-rule consensus tree of the posterior distribution from the four independent runs is presented in Figure 1.3A. Clade posterior probability is shown for each split above 50%. We represent clades with less than 50% support collapsed into polytomies.

Deep nodes in our preferred tree exhibited poor support, although there is good resolution at the nodes of interest for the current study. The relationship between *Scincella* and *Sphenomorphus* shows paraphyly, but support for the node is low and may be an artifact of data limitations or taxon sampling. The polytomy of *Scincella*, *Sphenomorphus fasciatus*, and the rest of the Philippine *Sphenomorphus* species render the Philippine clade unresolved. We cannot determine whether Philippine *Sphenomorphus* represents a monophyletic assemblage, and it would be premature to assume such a conclusion based on the

incomplete taxon sampling used in the current study. The clade labeled "Philippine *Sphenomorphus*" forms a highly supported monophyletic group. Within this clade there is a sister-taxon relationship between *Sphenomorphus steerei* and *Sphenomorphus leucospilos*, representing Species Groups 2 and 3, respectively. These species together form the sister-taxon to Brown and Alcala's (1980) Group 5.

Relationships among Sphenomorphus in Group 5

Our preferred phylogenetic hypothesis (Fig. 1.3A) suggests that *Sphenomorphus llanosi* is the sister-taxon to *S. abdictus abdictus* to the exclusion of *S. abdictus aquilonius*, thus rendering populations referred to *S. abdictus* paraphyletic. We also find that populations referred to *S. coxi* are paraphyletic, but that populations referred to *S. jagori* are a monophyletic group. *Sphenomorphus coxi coxi* is the sister-taxon to a clade consisting of *S. jagori*, *S. abdictus aquilonius*, and *S. coxi divergens.* Within *S. jagori* there are four major clades that are distinguished by biogeographic region (Fig. 1.2; 1.3A, B). The Luzon PAIC is the only region that is not monophyletic within this taxon. Samples from the volcanic mountains on southern Luzon (the Bicol Peninsula; Fig. 1.2) are more closely related to samples from the Mindanao PAIC than to the remainder of the *S. jagori jagori* diversity in the Luzon PAIC. The other clade from the Luzon PAIC comprises members of islands off the coast of Luzon, Polillo and Catanduanes, which were connected to Luzon during the Pleistocene. These samples are the sister-taxon to the remaining populations of *S. jagori*. The fourth clade of *S. jagori* corresponds to the

subspecies *S. j. grandis*. This clade is restricted to the Visayas PAIC and is monophyletic. *Sphenomorphus jagori* is the sister-taxon to a clade including *S. abdictus aquilonius* and *S. coxi divergens,* neither of which is monophyletic. The clade containing the type locality *S. a. aquilonius* (Subic Bay) is the sister-taxon to *S. coxi divergens* from the type locality (Mt. Makiling) of the latter subspecies. The clade containing the type locality of *S. a. aquilonius* has a disjunct distribution, occurring in the southwestern part of Luzon and in the islands off the north coast of Luzon, but has not been detected in intervening areas. There are two divergent clades of *S. abdictus aquilonius* and one clade of *S. coxi divergens* that, based on topology tests, are significantly different from samples from the type localities. *Sphenomorphus a. aquilonius* from Polillo Island and Mt. Isarog (S.E. Luzon) form the sister-taxon to the clade of *S. a. aquilonius* and *S. coxi divergens* mentioned above. Individuals in this clade from Polillo Island are sympatric with *S. jagori jagori*.

Sequence divergence across clades

Corrected sequence divergence was calculated for all clades within this complex (Table 1.2). Genetic diversity within *S. abdictus abdictus* on the one island sampled is less than 1%, but is over 12% when compared to all other clades. *Sphenomorphus coxi coxi* has over 7% genetic variation within the subspecies and is at least 11% divergent from all other clades. Within the clade of *S. jagori* there is lots of genetic diversity. The samples of *S. jagori jagori* from Luzon (clades 3 and 6) show 8–10.2% sequence divergence. The Luzon samples (clade 3) that

form the sister-taxon to Mindanao samples (clade 4) are 3.5–5.7% divergent. This sister-group relationship is the only one with low support (posterior probability = 80) for what we are designating distinct clades. The subspecies *S. j. grandis* has 0–5.9% sequence divergence within the subspecies and is over 5% divergent from all other clades. The two clades of *S. coxi divergens* (clades 7 and 9) are over 12.9% divergent. The samples within *S. c. divergens* (clade 9) from Mindoro and Luzon are less than 1% divergent. Clade 9 is over 5.8% divergent from other subspecies including its sister clade, *S. a. aquilonius*. There is between 6.8–11.6% sequence divergence between the three clades of *S. a. aquilonius*.

Hypothesis testing

Hypothesis A (Fig. 1.4A) postulates the monophyly of populations curently referred to *Sphenomorphus abdictus* and assumes that *S. a. abdictus* and *S. a. aquilonius* form a monophyletic assemblage. Although we do not have tissue samples of *S. a. abdictus* from its type locality (Camiguin Sur Island), we do have readily identifiable *S. a. abdictus* from the nearby island of Dinagat (Fig. 1.2B), and these samples are more closely related to *S. llanosi* from Samar Island than they are to any other member of the *S. jagori-abdictus-coxi* complex. Not surprisingly, our data reject the monophyly of *S. abdictus* and suggest that the species represents at least four distinct evolutionary lineages.

Hypothesis B (Fig. 1.4B) postulates the monophyly of just the populations assigned to the subspecies *S. abdictus aquilonius*. Our preferred tree (Fig. 1.3A), however, includes three genetically divergent clades referable to this taxon, one of which (including samples from the type locality of Subic Bay) is more closely

related to *S. coxi divergens* from its type locality (Mt. Makiling, S. Luzon) and Mindoro Island. Again, our data reject the hypothesis of monophyly of *S. a. aquilonius* and suggest that this subspecies represents at least three distinct evolutionary lineages..

Hypothesis C (Fig. 1.4C) assumes the monophyly of *S. coxi* (including *S. c. coxi* and *S. c. divergens*). With *S. c. coxi* known from Mindanao (and smaller associated islands like Camiguin Sur) and *S. c. divergens* known from southern Luzon (type locality: Mt. Makiling), Panay, and Mindoro, and since these populations are widely disparate in our preferred tree (Fig. 3A), it is not surprising that our data soundly reject the monophyly of this species and suggest that this species is actually composed of at least three evolutionary lineages.

Hypothesis D (Fig. 1.4D) postulates the monophyly of the subspecies *S. coxi divergens*. This taxon was described by Taylor (1922a) as a subspecies of *S. jagori* on the basis of specimens from Mt. Makiling, and we sequenced specimens from this locality, Panay, and Mindoro. Brown and Alcala (1980) subsequently moved this subspecies to *S. coxi*. Although Mindoro and Mt. Makiling populations occur within the same clade in the preferred tree, this clade is separated from the Panay population by samples of *S. a. aquilonius*; our data reject the monophyly of specimens referable to *S. coxi divergens* and suggest that this subspecies is composed of two distinct evolutionary lineages (one from Panay and another from southern Luzon and Mindoro).

Finally, in Hypothesis E (Fig. 1.4E) we test the monophyly of populations of the *S. jagori* complex from the Luzon PAIC (including Luzon, Polillo, and

Catañduanes Islands). Our preferred phylogenetic tree includes two non-sister clades of Luzon PAIC members of the complex: one clade situated on the Bicol Peninsula and another on the offshore islands of Polillo and Catañduanes.

Discussion

Phylogenetic relationships and the PAIC model of Philippine biogeography

If processes such as sea-level fluctuations and known patterns of intra-PAIC island connectivity have been responsible for the partitioning of Philippine biodiversity in a manner akin to the widely accepted paradigm of Philippine biogeography (e.g., Dickerson et al. 1928; Kloss 1929; Inger 1954; Brown et al. 2002; Heaney 1985, 1986; Heaney et al. 1998, 2005), we would expect today's patterns of species distributions to reflect PAIC-level predictions (Brown and Guttman 2002; Evans et al. 2003; Esselstyn and Brown 2009; Siler et al. 2010). Similarly, if the PAIC-level processes structure species distributions, one might expect similar partitioning of genetic diversity *within* widely-distributed species (e.g., Evans et al. 2003a; Esselstyn et al. 2009). In accordance with the PAIC model of Pleistocene diversification of Philippine biodiversity (e.g., Brown et al. 2002; Heaney and Mittermeier 1997; Heaney and Regalado 1998; Catibog-Sinha and Heaney 2006), we might expect the Luzon, Mindoro, western Visayan, and Mindanao PAICs each to contain one or more monophyletic evolutionary lineages (Fig 1.1), but we would not expect to find a large number of lineages spanning PAIC boundaries (Esselstyn and Brown 2009; Siler et al. 2010). It is important to note that many earlier workers have noted selected taxa or distribution patterns

which represent exceptions to a strict PAIC-based structuring of Philippine biodiversity (Dickerson et al. 1928; Inger 1954; Collar et al. 1999; Kennedy et al. 2000; Heaney and Rickart 1990; Heaney et al. 1998, 2005; Roberts 2006a, 2006b; Jansa et al. 2006; Jones and Kennedy 2008); recent studies have provided some of the first statistical tests of the model predictions (Evans et al. 2003; Esselstyn and Brown 2009; Siler et al. 2010). Strong statistical rejection of some tenants of the PAIC model of diversification in recent studies have thus confirmed earlier workers' empirically observed deviations from strict adherance to a PAIC model (Heaney and Rickart 1990; Heaney et al. 1998, 2005; Steppan et al. 2003; Brown and Diesmos 2009).

Our empirical findings and statistical tests of experimental topologies strongly reject some topological predictions based on these biogeographic expectations, suggesting that other, possibly equally pervasive processes bear explanatory value in light of current species distributions. One unexpected finding that we have revealed is the tendency for several morphologically and genetically divergent lineages to coexist at multiple areas throughout the archipelago. The first case involves the island of Polillo (and probably adjacent mainland Quezon Province of Luzon) where *S. jagori jagori* (Clade 6) and *S. abdictus aquilonius* (Clade 10) occur together. The second case is on a volcano, Mt. Isarog (possibly other Bicol Peninsula massifs will be documented to support sympatric lineages in future studies) where Clade 3 of *S. jagori jagori* co-occurs with members of Clade 10 of *S. abdictus aqilonius* (Figs. 1.2, 1.3).

The documentation of sympatric lineages contributes to knowledge of species diversity, but in and of itself does not reject the PAIC paradigm. However, the two large clades revealed in our phylogenetic analysis strongly contradict predictions derived from the PAIC model. In the *S. jagori* clade, the species spans Luzon, western Visayan, and Mindanao faunal regions, with parametric bootstrapping rejecting the hypothesis of monophyly of lineages on Luzon. Within this clade, the subspecies *S. j. grandis* in western Visaya is the only genetic lineage that captures taxonomy accurately. *Sphenomorphus j. jagori* was considered to be a widespread species, but it is clear from our results that there are at least two, and possibly three genetic lineages within this currently recognized subspecies. In the scenario with two additional lineages, a single lineage would span Luzon and Mindanao (Clades 3 and 4), thereby crossing a PAIC boundary, and a separate lineage would occur on the Luzon PAIC but only on offshore islands. This scenario would separate the clades with more than 5% sequence divergence. If we accept three separate lineages, the lineages on the Mindanao and Luzon PAICs would be recognized as distinct with over 3.5% sequence divergence, and there would be two separate lineages on the Luzon PAIC. Both of these scenarios involve newly recognized diversity and a deviation from the PAIC paradigm but rely on decisions either based on sequence divergence levels or low support on the tree, neither of which is ideal. The large clade containing *S. a. aquilonius* and *S. c. divergens* spans Luzon and Mindoro faunal regions and many deepwater islands. Each of these subspecies as currently defined rejects the PAIC predictions for relationships. Within *S. c. divergens*, the

clade spanning Luzon and Mindoro was originally proposed by Taylor (1922a) when he described the subspecies. The morphological similarity Taylor recognized in samples from these localities corresponds to the genetic results (less than 1% sequence divergence) and thereby supports our finding of strong conflict in the prediction of PAIC relationships for this subspecies. *Sphenomorphus a. aquilonius* samples are found predominately from Luzon, representing three allopatric clades. As each of these clades has related samples on neighboring islands, they could therefore represent dispersals from the Luzon PAIC and not necessarily wholesale deviations from the PAIC predictions. What is clear is that the samples currently identified as *S. a. aquilonius* from Luzon do not form a monophyletic group and therefore, the Luzon PAIC harbors three clades with over 6.8% sequence divergence within this subspecies.

Past studies fall into two categories with regard to deviations from the PAIC model of diversification. Some studies have provided empirical observations inconsistent with the PAIC model (e.g., Brown and Guttman 2002; Steppan et al. 2003; Jansa et al. 2006; Jones and Kennedy 2008). Others have provided findings inconsistent with PAIC-derived predictions, and additionally demonstrated with statistical analyses that their data strongly reject predictions of the PAIC model of Pleistocene diversification (e.g., Evans et al. 2003b; Roberts 2006a, b; Esselstyn and Brown 2009; Esselstyn et al. 2009; Siler et al. 2010). We find the latter studies more compelling because they have provided robust statistical tests of *a priori* predictions within the context of phylogenetic analyses and clearly articulated hypotheses. Whatever the approach preferred by

respective investigators, it is clear that our findings contribute to a growing body of literature that demonstrates the tendency of empirical data to deviate markedly from a widely accepted quarter-century-old theoretical paradigm on the dominating processes of evolutionary diversification in the model island archipelago of the Philippines.

Lineage diversity and taxonomic implications

Our phylogenetic analyses of mitochondrial DNA sequence data and tests of experimental topologies from taxonomic expectations reject former hypotheses of diversity on two hierarchically nested levels. First, our data are inconsistent with (and reject with strong statistical significance) the taxonomic hypotheses of three species (*S. jagori*, *S. coxi*, and *S. abdictus*). Second, our data strongly reject the hypothesis of the existence of only six taxa (i.e., six named subspecies). In contrast to previous taxonomic arrangements, we find evidence of at least eleven highly divergent and monophyletic lineages.

The question remains: how many evolutionary lineages (i.e., species) exist within the *S. jagori-coxi-abdictus* complex in the Philippines? Do our highly divergent and monophyletic mitochondrial gene lineages identify species? A liberal application of the Evolutionary Species Concept (Simpson 1961; Wiley 1978; Frost and Hillis 1990; de Queiroz 1998) focusing on apparent lineage cohesion, diagnosability, allopatry of morphologically similar forms, and/or sympatry of morphologically distinguishable forms might suggest to us that all Philippine subspecies need to be elevated to the species level and an additional

five species should be recognized. In contrast, a more conservative approach might be to recognize only the most divergent clades in our analysis, requiring the recognition of five species, namely *S. abdictus* from Dinagat, *S. coxi* from the Mindanao PAIC, *S. c. divergens* from Panay (with a new name), and two widely distributed species: *S. jagori* throughout the Philippines and *S. aquilonius* from Luzon, the Babuyan Islands, and Mindoro. The problem with both of these scenarios is that they would be applied on the basis of arbitrarily assigned divergence levels and would not incorporate biogeographic information or diagnoses based on morphology. Accordingly, we do not recommend *carte blanche* acceptance of either arrangement or the explicit use of divergence level cut-offs for diagnosing species.

Rather than make seemingly arbitrary decisions based on levels of divergence and/or branching pattern in our phylogeny, we prefer to make taxonomic decisions based on the identification of evolutionary lineages and diagnostic characters (e.g., morphology, coloration, ecology, etc.) in combination with biogeography. We note that in two cases, readily diagnosable forms have been shown to occur in sympatry. As noted above, we have documented two cases of sympatric, morphologically diagnosable, and genetically highly distinct entities involving three haplotype clades. In our opinion, each of these must be recognized as a species, and we suspect that the majority of systematists will agree. The remaining eight divergent lineages occur in apparent allopatry, whether on separate islands, in small biogeographically subscribed subsets (i.e., isolated mountain ranges, formerly separate peninsulas), or within larger islands.

The fact that these isolated geologic and/or habitat islands contain highly divergent, haplotype clades is strong evidence in support of the hypothesis of lineage cohesion and the expectation that each amounts to a unique evolutionary lineage with a recoverable evolutionary history and predictable evolutionary fate —i.e., species (Wiley 1978; Frost and Hillis 1990; de Queiroz 1998).

The fact that all eleven highly divergent lineages detected here occur either (1) in sympatry where they are clearly diagnosable as separate morphologically-defined entities or (2) allopatrically with no evidence of gene flow or introgression, suggests to us that we may indeed have uncovered an instance of eleven full evolutionary lineages, and that future taxonomic work likely will reveal at least this many candidate species. Thus, although we strongly suspect that further work will justify recognizing not three, but at least eleven species, we hold taxonomic decisions in abeyance until a formal taxonomic revision is possible. A comprehensive analysis of morphological variation in this complex is now underway (Linkem, Diesmos, and Brown, unpublished data).

Implications for conservation planning

The results of this study contribute to a growing body of literature emphasizing the surprisingly complex patterns of biodiversity partitioning in the Philippines (e.g., Brown and Guttman 2002; Heaney et al. 2005; Roberts 2006a,b; Jones and Kennedy 2008; Esselstyn et al. 2009). Brown et al. (2000) have emphasized that patterns of biodiversity partitioning in amphibians and reptiles often show much finer-scale differentiation than those exhibited in volant mammals (bats) and birds

(e.g., Heaney et al. 1998; Kennedy et al. 2000); non-volant mammals may exhibit differentiation on a scale eqivalent to amphibians and reptiles. However, to date, no analyses of these patterns have been provided. Whatever the case, Brown et al. (2000) emphasized that conservation planning might best be served by embracing patterns of differentiation at the finest scales at which they occur (Brown and Diesmos 2009). The results of this study exhibit that even in common, widespread species complexes of some of the most abundant Philippine scincid lizards, multiple evolutionarily significant units for conservation exist within taxonomically recognized entities (species and even within subspecies). If our results are corroborated by future studies of additional taxa, the conservation priority-setting exercise of identifying centers of geographic endemism based on traditional taxonomy will have to be abandoned in favor of new data from empirical studies with accurate assessments of evolutionarily significant diversity.

Conclusion

The results of this study indicate that the current taxonomic arrangement of three nominal species—*S. jagori*, *S. coxi*, and *S. abdictus*—incorrectly represents the relationships and diversity of these Philippine forest skinks as inferred from mitochondrial sequence data. Species definitions based on widely varying morphological characters and biogeographically unrealistic distributions have obscured at least eleven divergent mitochondrial lineages with distinct geographic ranges. Each of these lineages either occurs in sympatry with other morphologically diagnosable lineages or occurs as an isolated, allopatric endemic

entity (i.e., candidate species). Additionally, our robust phylogeny estimated from molecular data is an important step toward elucidating the evolutionary relationships of members of the Philippine Scincidae; future goals include updating scincid taxonomy to reflect phylogenetic diversity. Although a thorough study of morphological data will need to be combined with our results in order to provide evidence necessary for making taxonomic decisions, it is clear that current taxonomy underestimates lineage diversity in this complex of Philippine skinks. If even the most common and widespread species groups are underestimated for species diversity, future conservation prioritization will benefit greatly from access to data from enhanced and more accurate biodiversity studies.

Table 1.1 Scale counts and character presence (+)/absence (0) for each subspecies in the *abdictus-jagori-coxi* species complex as defined by Brown and Alcala (1980). Character abbreviations correspond to: snout–vent length (SVL), number of mid-body scale rows (MBSR), number of paravertebral scales between the parietals and cloaca (PV).

Taxon	SVL (mm)	MBSR	PV	4th toe lamellae	Frontoparietal (F) fused; (D) divided	Supralabial barring	# of supraoculars
S. a. abdictus	81–98	36–42	63–74	21–25	D	0	5
S. a aquilonius	55–95.5	34–38	62–73	20–25	D	0	4
S. coxi coxi	53–85	32–38	62–72	19–26	F	0	5
S. coxi divergens	63–90	34–40	64–75	21–26	F	0	4
S. jagori grandis	71–108	38–44	68–80	24–30	D	+	4
S. jagori jagori	71–108	32–42	63–73	24–30	D	+	4

Table 1.2. Comparison of corrected sequence divergence (GTR) within and across the clades in figure 3 of *S. jagori*, *S. abdictus,* and *S. coxi*. Values in the table are minimum and maximum percentages of the corrected sequence divergences from PAUP*.

	clade 1	clade 2	clade 3	clade 4	clade 5	clade 6	clade 7	clade 8	clade 9	clade 10	clade 11
clade 1	0–0.68										
clade 2	12.480 – 14.402	0– 7.877									
clade 3	13.543 – 14.136	12.800 – 13.836	0– 2.113								
clade 4	13.409 – 14.744	13.801 – 15.597	3.470– 5.693	0– 3.730							
clade 5	14.125 – 15.239	12.757 – 14.796	5.292– 6.359	5.077– 6.934	0– 5.912						
clade 6	15.222 – 16.260	11.821 – 14.746	8.601– 10.185	8.462– 11.745	9.323– 11.182	0– 6.277					
clade 7	15.996 – 16.308	15.098 – 15.882	12.577 – 12.787	10.824 – 14.142	12.271 – 13.274	12.525 – 13.983	—				
clade 8	14.160 – 15.419	13.465 – 16.816	9.540– 11.557	10.795 – 13.913	9.618– 12.864	11.339 – 13.931	11.333 – 12.860	0– 6.731			
clade 9	13.844 – 14.715	12.973 – 15.217	10.363 – 11.240	10.579 – 13.022	10.266 – 11.989	11.576 – 13.136 7	12.932 – 13.022	5.789– 8.404	0– 1.174		
clade 10	13.702 – 15.820	13.117 – 15.599	9.515– 11.511	10.056 – 14.147	9.456– 12.273	10.850 – 13.547	11.399 – 12.497	6.873– 9.971	7.751– 9.216	0– 5.750	
clade 11	12.990 – 14.891	12.251 – 13.945	8.926– 10.862	9.550– 12.415	9.595– 12.415	9.890– 11.769	10.698 – 13.077	8.323– 11.623	8.622– 10.028	7.455– 10.183	0– 2.640

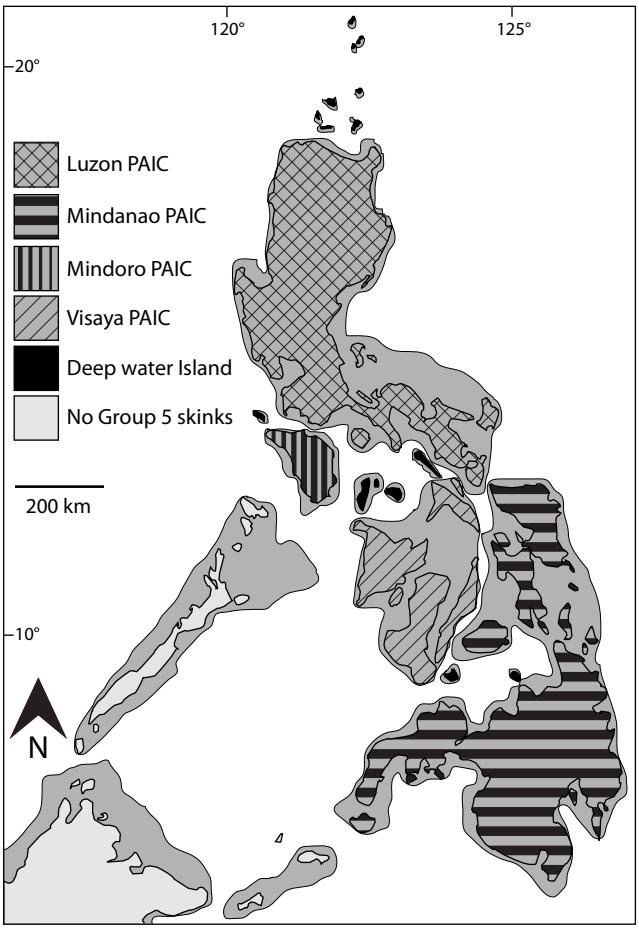

Figure 1.1 The expected geographic distribution of lineages in this group if the diversification followed the predictions made by the PAIC paradigm. Each PAIC Island would harbor a lineage, with subdivisions existing between inter-PAIC islands. The samples from different PAICs would be reciprocally monophyletic for mitochondrial haplotype clades. Samples from deepwater islands may be associated with founder PAIC populations through random dispersal.

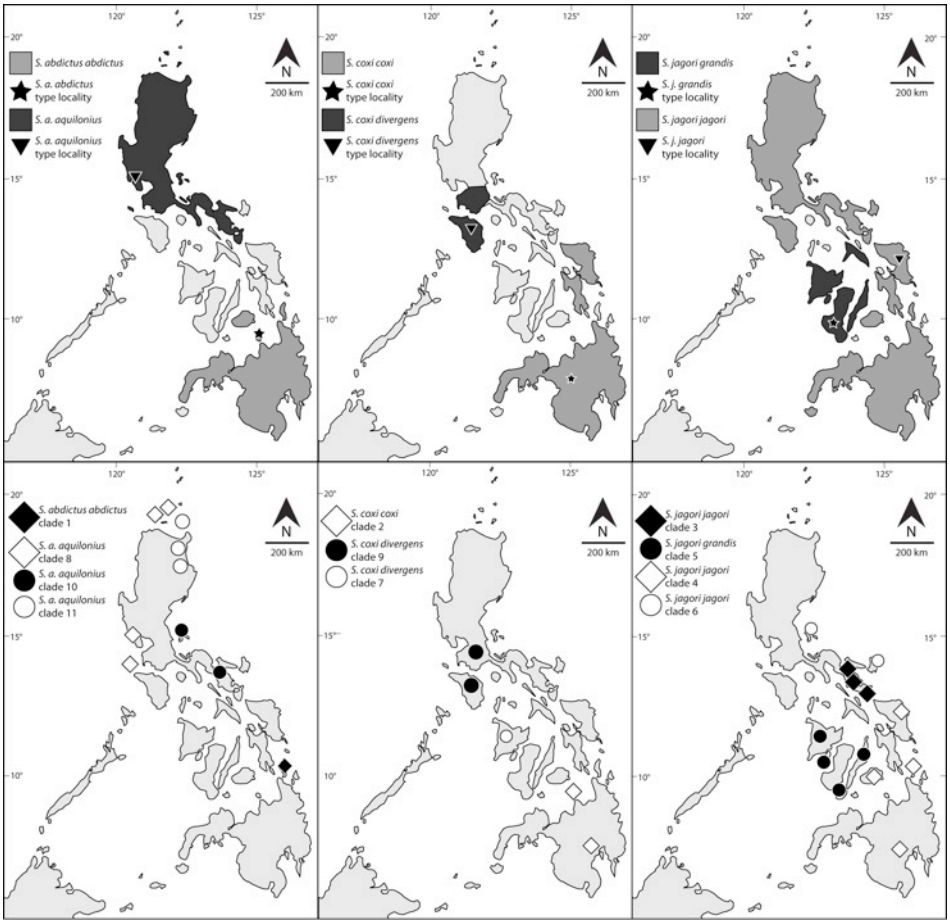

Figure 1.2 Top row depicts the predicted distribution of each species (*S. abdictus*, *S. coxi*, and *S. jagori*) and the subspecies therein from left to right as explained by Brown and Alcala (1980). Bottom row shows the geographic location of samples in each subspecies, with genetic clades distinguished from one another.

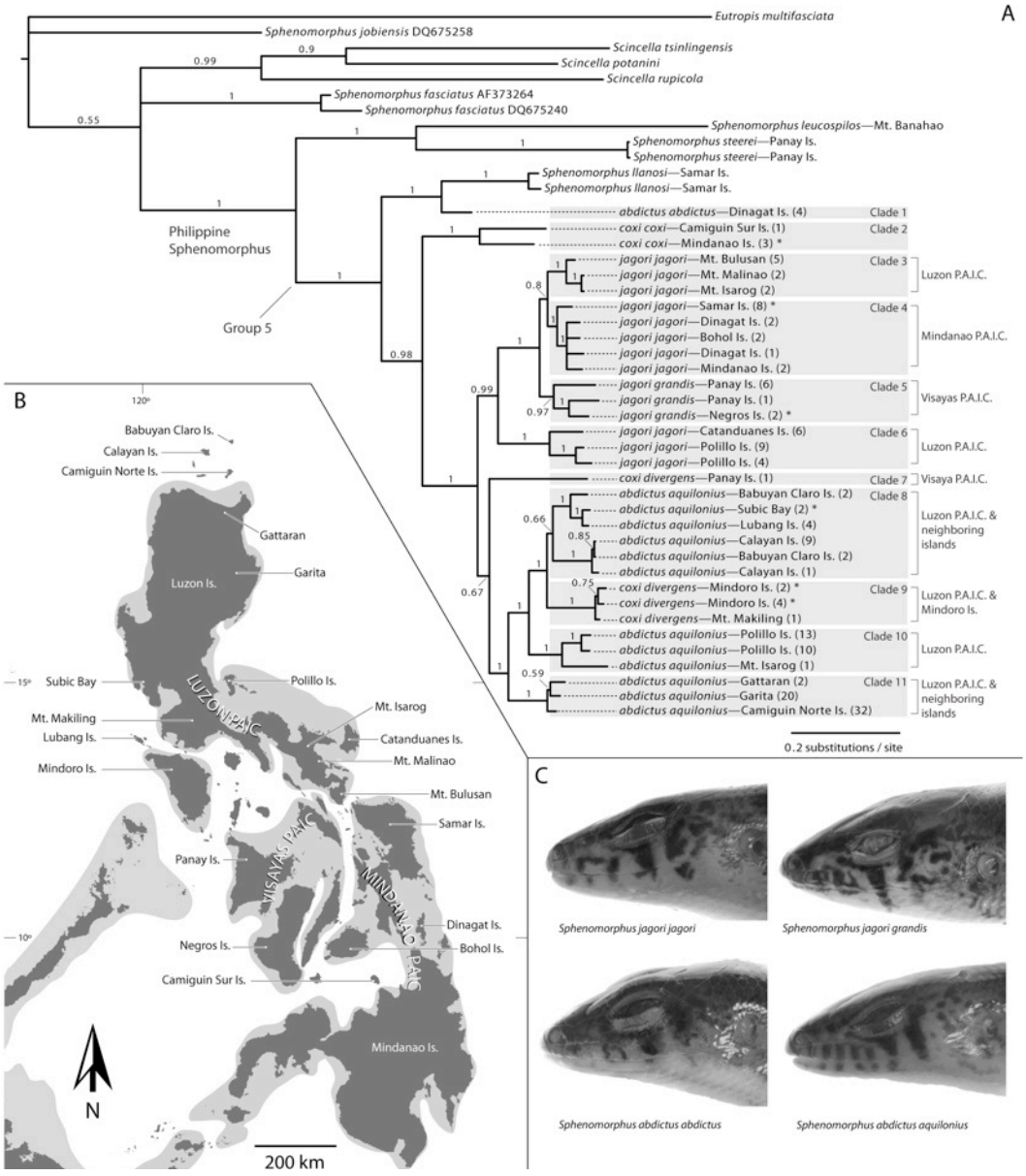
A
Eutropis multifasciata
Sphenomorphus jobiensis DQ675258
Scincella tsinlingensis
Scincella potanini
Scincella rupicola
Sphenomorphus fasciatus AF373264
Sphenomorphus fasciatus DQ675240
Sphenomorphus leucospilos—Mt. Banahao
Sphenomorphus steerei—Panay Is.
Sphenomorphus steerei—Panay Is.
Sphenomorphus llanosi—Samar Is.
Sphenomorphus llanosi—Samar Is.
abdictus abdictus—Dinagat Is. (4) Clade 1
coxi coxi—Camiguin Sur Is. (1) Clade 2
coxi coxi—Mindanao Is. (3) *
jagori jagori—Mt. Bulusan (5) Clade 3
jagori jagori—Mt. Malinao (2)
jagori jagori—Mt. Isarog (2)
Luzon P.A.I.C.
jagori jagori—Samar Is. (8) * Clade 4
jagori jagori—Dinagat Is. (2)
jagori jagori—Bohol Is. (2)
jagori jagori—Dinagat Is. (1)
jagori jagori—Mindanao Is. (2)
Mindanao P.A.I.C.
jagori grandis—Panay Is. (6) Clade 5
jagori grandis—Panay Is. (1)
jagori grandis—Negros Is. (2) *
Visayas P.A.I.C.
jagori jagori—Catanduanes Is. (6) Clade 6
jagori jagori—Polillo Is. (9)
jagori jagori—Polillo Is. (4)
Luzon P.A.I.C.
coxi divergens—Panay Is. (1) Clade 7 Visaya P.A.I.C.
abdictus aquilonius—Babuyan Claro Is. (2) Clade 8
abdictus aquilonius—Subic Bay (2) *
abdictus aquilonius—Lubang Is. (4)
abdictus aquilonius—Calayan Is. (9)
abdictus aquilonius—Babuyan Claro Is. (2)
abdictus aquilonius—Calayan Is. (1)
Luzon P.A.I.C. & neighboring islands
coxi divergens—Mindoro Is. (2) * Clade 9
coxi divergens—Mindoro Is. (4) *
coxi divergens—Mt. Makiling (1)
Luzon P.A.I.C. & Mindoro Is.
abdictus aquilonius—Polillo Is. (13) Clade 10
abdictus aquilonius—Polillo Is. (10)
abdictus aquilonius—Mt. Isarog (1)
Luzon P.A.I.C.
abdictus aquilonius—Gattaran (2) Clade 11
abdictus aquilonius—Garita (20)
abdictus aquilonius—Camiguin Norte Is. (32)
Luzon P.A.I.C. & neighboring islands
0.2 substitutions / site
Philippine Sphenomorphus
Group 5
B
120°
15°
10°
Babuyan Claro Is.
Calayan Is.
Camiguin Norte Is.
Gattaran
Garita
Luzon Is.
Subic Bay
Polillo Is.
LUZON P.A.I.C.
Mt. Makiling
Lubang Is.
Mindoro Is.
Mt. Isarog
Catanduanes Is.
Mt. Malinao
Mt. Bulusan
Samar Is.
Panay Is.
VISAYAS P.A.I.C.
MINDANAO P.A.I.C.
Dinagat Is.
Negros Is.
Bohol Is.
Camiguin Sur Is.
Mindanao Is.
N
200 km
C
Sphenomorphus jagori jagori
Sphenomorphus jagori grandis
Sphenomorphus abdictus abdictus
Sphenomorphus abdictus aquilonius

Figure 1.3 The preferred phylogenetic hypothesis (A) generated by Bayesian and Likelihood analysis of the ND2 gene. Highly divergent mitochondrial lineages and clades (diagnosing presumptive evolutionary species) are highlighted with gray shaded boxes. Pleistocene Aggregate Island Complexes (PAICs) are included to the right of clades for reference. A map of the Philippines (B) with 120 m underwater bathymetric contours highlighted in gray is included, along with labelled collection localities and PAIC identities. Specimens (C) exhibiting ranges of variation in the suborbital bar character are included for comparison.

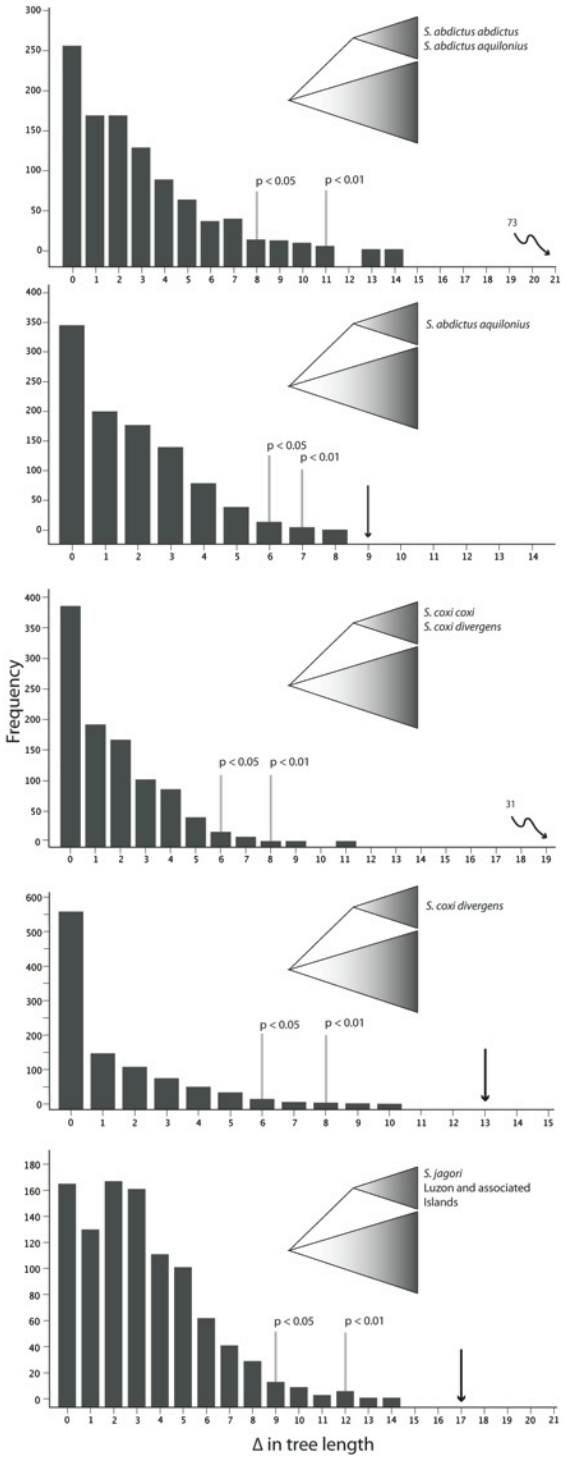

Figure 1.4 Five taxonomic hypotheses (based on Brown and Alcala, 1980) tested in the study using Parametric Bootstrapping and the Swofford-Olsen-Wadell-Hillis (SOWH) test of tree topology (Swofford et al. 1996). See text for discussion.

CHAPTER 2

Molecular systematics of the Philippine forest skinks (Squamata: Scincidae: *Sphenomorphus*): testing morphological hypotheses of interspecific relationships

The majority of lizard species in the family Scincidae are found in the subfamily Lygosominae, which is divided into three groups (Greer 1979). The *Sphenomorphus* group is one of the largest assemblages of squamates on earth, including approximately 30 genera and 500 species defined by the shared presence of several morphological synapomorphies (Greer 1979). Of these, *Sphenomorphus* Fitzinger is the most species rich genus (145 species) but the definition of this taxon remains enigmatic due to the lack of clear synapomorphies. Greer and Shea (2003) stated "*Sphenomorphus* is undiagnosable and is almost certainly not monophyletic" and Myers and Donnelly (1991) referred to *Sphenomorphus* as "a plesiomorphic taxon not at present definable by derived characters." Originally named by Fitzinger (1843), *Sphenomorphus* was not recognized by Boulenger (1887) in his catalog of lizards, but was later designated as a section of *Lygosoma* by Smith (1937). Mittleman (1952) redefined *Sphenomorphus* as a genus based on the presence of large prefrontals, paired frontoparietals, enlarged precloacals, exposed auricular openings, and large limbs. Mittleman's definition of the taxon is only slightly improved from Boulenger's (1887) definition of *Lygosoma*, and only includes plesiomorphic characters. Since that time, the genus has been gradually

partitioned, as new taxa defined by novel, apomorphic characters have been described (*Ctenotus* Storr 1969; *Eremiascincus* Greer 1979; *Lankascincus* Greer 1991; *Leptoseps* Greer 1997; *Oligosoma* Girard 1857; *Parvoscincus* Ferner et al. 1997; *Sigaloseps* Sadlier 1987). However, other genera (*Otosaurus, Insulasaurus, Ictiscincus, Parotosaurus*) have been combined with *Sphenomorphus* (Loveridge 1948; Mittleman 1952; Greer and Parker 1967). Though the composition of the genus has changed through time, species diversity remains high due to the lack of diagnostic characters, which results in many new species being artificially assigned to *Sphenomorphus*. Currently, *Sphenomorphus* occur in Southeast Asia, Asia, Indochina, and Central America.

Two series of taxonomic revisions of Philippine *Sphenomorphus* provided an initial insight into the diversity of this assemblage. Taylor (1922a,b,c, 1923, 1925) recognized 19 species of Philippine forest skinks in the genera *Otosaurus, Insulasaurus*, and *Sphenomorphus*. In their review of Philippine scincids, Brown and Alcala (1980) followed Greer and Parker (1967) in placing *Otosaurus* and *Insulasaurus* in synonymy with *Sphenomorphus*. In addition, they synonymized several species recognized by Taylor and described four new species (reviewed by Brown et al. 2010). Six additional species were described (Brown 1995; Brown et al. 1999, 2010; Linkem et al. 2010a), and one species was moved to the genus *Parvoscincus* (Ferner et al. 1997). Twenty-eight endemic species are recognized as a result of these revisions and descriptions, making *Sphenomorphus* the most diverse squamate genus in the Philippines (Brown et al. 2010).

Taxonomy and Biogeography of Philippine Sphenomorphus

Species diversity in the Philippine archipelago is intrinsically linked to the geologic history of the region (Heaney 1986; Brown and Diesmos 2002, 2009). The Philippine archipelago formed during the last 15 My as continental plate movement and volcanism caused the emergence of multiple large oceanic islands (Hall 1998). During low sea-level stands of the Pleistocene, islands separated by shallow channels were connected by land allowing for faunal and floral range expansion through dispersion and dispersal (Fig. 2.1: Brown and Guttman 2002; Roberts 2006a,b). These connected islands are often referred to as Pleistocene Aggregate Island Complexes (PAICs). Species are commonly endemic to a single PAIC, though some species span multiple PAICs. *Sphenomorphus atrigularis*, *Sphenomorphus beyeri, Sphenomorphus boyingi, Sphenomorphus diwata, Sphenomorphus hadros, Sphenomorphus igorotorum, Sphenomorphus kitangladensis, Sphenomorphus laterimaculatus*, *Sphenomorphus lawtoni, Sphenomorphus leucospilos, Sphenomorphus luzonensis, Sphenomorphus tagapayo*, *Sphenomorphus traanorum, Sphenomorphus wrighti,* and *Sphenomorphus victoria* only occur on one island. *Sphenomorphus acutus, Sphenomorphus arborens, Sphenomorphus bipartalis*, *Sphenomorphus fasciatus, Sphenomorphus llanosi, Sphenomorphus mindanensis,* and *Sphenomorphus variegatus* are endemic to a single PAIC and can be found on multiple islands within that PAIC. *Sphenomorphus abdictus, Sphenomorphus coxi*, *Sphenomorphus cumingi*, *Sphenomorphus decipiens, Sphenomorphus jagori*, and

Sphenomorphus steerei have widespread distributions occurring on more than one PAIC.

In addition to the 28 endemic species, three species are partitioned into two subspecies: *Sphenomorphus abdictus abdictus, Sphenomorphus abdictus aquilonius, Sphenomorphus coxi coxi, Sphenomorphus coxi divergens, Sphenomorphus jagori grandis* and *Sphenomorphus jagori jagori*. These 31 taxonomic units are organized into six groups in the foundational work of Brown and Alcala (1980); although not created in a phylogenetic framework, these groups have served as convenient phenotypic categories for diagnoses of new species (e.g., Brown et al. 1995, 1999, 2010; Ferner et al. 1997; Linkem et al. 2010a) and as the basis for hypotheses of evolutionary relationships (Linkem et al. 2010b). Each group is diagnosed by a combination of morphological features. Some Philippine groups are similar to *Sphenomorphus* species groups that occur outside of the Philippines (Greer and Parker 1967). The species in each of the Brown and Alcala (1980) groups are summarized below.

Group 1 *Sphenomorphus* are distinguished by moderate body size, high numbers of paravertebral scales (> 88), and a preference for high elevation, montane habitats (Table 2.1). Brown and Alcala (1980) placed two species in Group 1, *Sphenomorphus beyeri* and *Sphenomorphus diwata*, but a recent taxonomic revision (Brown et al. 2010) identified three additional species in this group—*Sphenomorphus boyingi*, *Sphenomorphus hadros*, and *Sphenomorphus igorotorum*. Most species in Group 1 are Luzon endemics, the only exception being *Sphenomorphus diwata*, which is restricted to eastern Mindanao (Fig. 2.1).

Group 2 comprises small species with small digits (Table 2.1). Brown and Alcala (1980) described Group 2 as "a somewhat artificial assemblage," but specified that *Sphenomorphus atrigularis, Sphenomorphus lawtoni,* and *Sphenomorphus steerei* were closely related, and that *Sphenomorphus biparietalis* was most similar to *Sphenomorphus hallieri* from Borneo. The authors also included *Sphenomorphus luzonensis* and *Sphenomorphus palawanensis* in Group 2. The discovery of *Parvoscincus sisoni* led to the movement of *Sphenomorphus palawanensis* to the genus *Parvoscincus* (Ferner et al. 1997). Because the two species of *Parvoscincus* resemble Group 2 species morphologically, we conditionally consider them as members of this group for the purpose of this review of phenotypic variation. The most recent species added to Group 2 was *Sphenomorphus tagapayo* (Brown et al. 1999; for a total of 8 species in Group 2). Most species in this group have limited distributions, with *Sphenomorphus lawtoni, Sphenomorphus luzonensis,* and *Sphenomorphus tagapayo* occurring only in limited regions of Luzon Island; *Sphenomorphus atrigularis* in western Mindanao; *Sphenomorphus biparietalis* in the Sulu Archipelago; *Parvoscincus palawanensis* on Palawan Island; and *Parvoscincus sisoni* on Panay Island. *Sphenomorphus steerei* ranges throughout the archipelago.

Group 3 consists of small-to-intermediate–sized, slender-bodied species with midbody scale rows 30–40, and lamellae beneath toe IV 15–20 (Table 2.1). Group 3 was considered most similar to Bornean *Sphenomorphus murudensis* and *Sphenomorphus kinabaluensis*, which are part of the Greer and Parker (1967) *variegatus* group. Brown and Alcala (1980) partitioned Philippine species of

Greer and Parker's (1967) *variegatus* group into Groups 3 and 4 (see below) based on the ratio of midbody scale rows to lamellae beneath toe IV, which were on average fewer in Group 3 species than Group 4 species. Brown and Alcala (1980) placed the following species in Group 3: *Sphenomorphus leucospilos, Sphenomorphus mindanensis, Sphenomorphus victoria, Sphenomorphus laterimaculatus,* and *Sphenomorphus acutus. Sphenomorphus acutus* does not fit into any of Brown and Alcala's (1980) groups, but resembles Groups 3 and 4, and was subsequently placed in Group 3 by Brown and Alcala. The Group 3 species occur in disparate parts of the archipelago, with *Sphenomorphus laterimaculatus* and *Sphenomorphus leucospilos* occurring on Luzon Island, *Sphenomorphus victoria* on Palawan Island, and *Sphenomorphus mindanensis* and *Sphenomorphus acutus* broadly distributed on Mindanao, Samar, and Leyte. Since Brown and Alcala's review (1980), Brown (1995) described another Group 3 species, *Sphenomorphus kitangladensis*, from eastern Mindanao (Brown 1995).

Brown and Alcala's (1980) Group 4 contains most Philippine members of Greer and Parker's (1967) *variegatus* group, defined by midbody scale rows 36–54 and lamellae beneath toe IV 20–28 (Table 2.1). This group includes the following species: *Sphenomorphus arborens, Sphenomorphus cumingi, Sphenomorphus decipiens, Sphenomorphus variegatus,* and *Sphenomorphus wrighti*. A new species was recently described in Group 4—*Sphenomorphus traanorum* (Linkem et al. 2010a). Two Group 4 species are widespread in the archipelago, *Sphenomorphus cumingi* and *Sphenomorphus decipiens*. The others have more limited distributions, with *Sphenomorphus wrighti* and

Sphenomorphus traanorum occurring on Palawan Island, *Sphenomorphus arborens* on Negros, Panay and Masbate, and *Sphenomorphus variegatus* on Mindanao, Samar, Leyte and Bohol.

Brown and Alcala's (1980) Group 5 was the only group which the authors considered a natural assemblage. It includes large (snout-vent > 53 mm) species with midbody scale rows 32–44, and > 20 toe IV subdigital lamellae (Table 2.1). Brown and Alcala (1980) placed *Sphenomorphus abdictus abdictus, Sphenomorphus abdictus aquilonius, Sphenomorphus jagori grandis, Sphenomorphus jagori jagori, Sphenomorphus coxi coxi, Sphenomorphus coxi divergens,* and *Sphenomorphus llanosi* in this group. Linkem et al. (2010b) corroborated the monophyly of Group 5, but demonstrated that many of the species and subspecies within the group do not correspond to the clades identified in phylogenetic analysis of mitochondrial DNA sequence data, thereby suggesting the need for a comprehensive review.

Brown and Alcala's (1980) Group 6 was considered a member of Greer and Parker's (1967) *fasciatus* group and contains only one species, *Sphenomorphus fasciatus*, found on Mindanao, Bohol, Camiguin Sur, Dinagat, Samar, and Leyte Islands.

Here we test whether Brown and Alcala's cohesive and largely unchallenged phenotypic groupings represent natural assemblages (but see Brown et al. 1995, 2010). First, we assess whether there is statistically significant phylogenetic support for the morphological species classifications of Brown and Alcala (1980). We then determine whether these supraspecific assemblages are

natural monophyletic groups or whether these apparently cohesive phenotypic clusters of taxa represent instances of morphological convergence. In the context of these broad goals, we address three specific questions: (1) Are the morphologically cohesive, phenotypically defined species groups of Brown and Alcala (1980) natural, monophyletic units or has convergent evolution obscured and confounded our understanding of evolutionary trends in Philippine *Sphenomorphus*? (2) Are Philippine *Sphenomorphus* species derived from a single common ancestor, or is this diversity the product of multiple invasions from Asian and/or Papuan sources? (3) Is our current understanding of *Sphenomorphus* species diversity accurate (28 species), or is species diversity as grossly underestimated as suggested by recent studies (Linkem et al. 2010b; Brown et al. 2010)?

Materials and Methods

Taxon Sampling

To adequately examine the relationships among Philippine *Sphenomorphus*, we included 131 samples of lygosomine skinks, representing 64 described species (Appendix 2). Sampling is predominantly from the *Sphenomorphus* group (53 species), with representatives from the *Eugongylus* (6 species) and *Mabuya* groups (5 species). We also incorporate representatives from the "Scincinae" genus *Plestiodon* (*P. anthracinus, P. fasciatus,* and *P. quadrilineatus*), and from the families Xantusiidae (*Xantusia vigilis*), and Lacertidae (*Tachydromus sexilineatus*).

We include samples from the following *Sphenomorphus* group genera: *Lipinia, Papuascincus, Scincella, Glaphyromorphus, Eulamprus, Eremiascincus,* and *Hemiergis*. The latter four genera are part of the Australian clade of the *Sphenomorphus* group, which is an assemblage of 15 genera previously shown to be well supported (Reeder 2003; Skinner 2007; Rabosky et al. 2007). We do not include all of the previously published data for this Australian clade because previous studies have found it to have high support, though these analyses lacked adequate outgroup sampling. We have run preliminary analyses (not shown) of our sampling in combination with all the Australian clade genera and found the Australian clade maintains high support. Thus we excluded members of the Australian clade to reduce the computational burden associated with this large dataset.

We collected 27 of the 28 currently recognized species of Philippine *Sphenomorphus* and included samples of the three subspecies for a total of 30 taxonomic units sampled from the archipelago. We could not sample the species *Sphenomorphus biparietalis* because it occurs in the Sulu Archipelago, a region inaccessable to researchers. Similarly, *Parvoscincus palawanensis* has not been observed by researchers since its original collection and no genetic samples are available. For two widespread species (*Sphenomorphus decipiens* and *Sphenomorphus steerei*), we incorporate samples from multiple populations to maximize geographic coverage across known biogeographic boundaries such as mountain ranges and marine channels (Brown and Diesmos 2002, 2009). Sampling comprises each of the 11 clades of the *Sphenomorphus abdictus*–

Sphenomorphus coxi–Sphenomorphus jagori complex of Linkem et al. (2010b). We included available non-Philippine *Sphenomorphus* from Borneo, Sulawesi, Indochina, China, the Solomon Islands, Central America, and Palau (Appendix 2). Sampling for *Sphenomorphus* and the *Sphenomorphus* group are far from inclusive, but are sufficient to address the questions that are the focus of this study.

Morphological Data and Analyses

Brown and Alcala (1980) based their morphological groupings on a combination of (1) snout–vent length, (2) number of scales around the mid-body, (3) paravertebral scales, and (4) subdigital lamellae of the fourth toe of the right foot (Table 2.1). Because we sought to determine whether Brown and Alcala's classification reflects natural phenotypic variation in the characters that vary among Philippine *Sphenomorphus*, we measured and counted the same characters on adults for all species of Philippine *Sphenomorphus* (see Brown et al. 2010 for a list of specimens examined). Scale counts, except mid-body scale rows, were taken on the right side of the body and the average value of each species was used for subsequent multivariate analyses (Table 2.2). Morphological data were analyzed in the R statistical package and in JMP8 (©SAS Institute Inc.). We used the unweighted pair group method with arithmetic mean (UPGMA: Sokal and Michner 1958) to create a phenogram of the morphological characters. Principal components analysis (PCA) was conducted using a correlation matrix on the raw scale counts for midbody scale rows and subdigital lamellae and log-transformed

paravertebral scale rows and snout–vent length. Log-transformation was needed for the last two variables to achieve a normal distribution. The use of a correlation matrix standardized the variables with a zero mean and unit standard deviation, which is important when variable are not all of the same scale.

Gene Choice and Data Collection

Tissue samples were extracted using a guanidine thiocyanate protocol modified from the PureGene© protocol (Esselstyn et al. 2008, based on a protocol developed by M. Fujita, *pers. comm.*). Each extraction was amplified for the genes of interest (Table 2.3) through standard PCR protocols (Palumbi 1996). PCR products were purified with ExoSAPit (USB corp.) with a 20% dilution of stock ExoSAPit, incubated for 30 min at 37 ºC and then 80 ºC for 15 min. Cleaned PCR products were dye-labeled using Big-Dye terminator 3.1 (Applied Biosystems), purified using Sephadex (NC9406038, Amersham Biosciences, Piscataway, NJ), and sequenced on an ABI 3730 automated capillary sequencer. Raw sequence data were processed using Sequencing Analysis Software (Applied Biosystems). Individual sequence chromatograms were examined in Sequencher v4.2 and individual single-stranded fragments were assembled into contiguous consensus reads for subsequent analysis. Consensus sequences for each individual for each gene were aligned using MUSCLE v3.6 (Edgar 2004) with default settings. By-eye adjustment of alignments and verification of coding frame was done in Se-Al v.2.0a11 (http://tree.bio.ed.ac.uk/software/seal). RNA

alignments were adjusted to maintain correct secondary struture based on the structure profile of skinks in Brandley et al. (2005)

We chose a variety of mitochondrial and nuclear genes to resolve the phylogeny of this group (Table 2.3). We sequenced the mitochondrial genes NADH dehydrogenase subunit 2 (ND2: 1095 base pairs) and subunit 4 (ND4: 705 base pairs), and ribosomal 12S (447 base pairs) and 16S (518 base pairs) genes as well as two nuclear genes, nerve growth factor beta polypeptide (NGFB: 567 base pairs) and RNA fingerprint protein 35 (R35: 689 base pairs). These genes were sequenced for the majority of our novel samples (Appendix 2), though some sample and gene combinations could not be amplified and were coded as missing data in the matrix. We do not have samples of the Australian group taxa and could therefore only include previously published data, which is limited to 12S, 16S, and ND4. Simulation and empirical studies have suggested that robust estimates of phylogeny can still be obtained despite the presence of missing data, especially when many characters are sampled (Wiens 2003; Philippe et al. 2004; Wiens and Moen 2008), therefore we are not worried about the missing data in out dataset.

All data are available on genbank (JF497855–JF498576) and alignments can be downloaded from Dryad (http://datadryad.org/)

Gene Concatenation, Partitioning Strategy, Model Choice, and Phylogenetic Analyses

Our mitochondrial gene sampling is very similar to other studies on skinks allowing us to make some assumptions in regard to concatenation and partitioning. In addition to two mitochondrial genes (12S, 16S) used in Brandley et al. (2005), we sequenced ND2 and ND4, which have been informative in *Sphenomorphus* group skinks (Linkem et al. 2010; Reeder 2003). We assume that these mitochondrial genes share a single evolutionary history due to matrilineal inheritance and the lack of recombination of the mitochondrion. Brandley et al. (2005) found that the best partitioning strategy for mitochondrial genes was to partition by gene, codon, and ribosomal secondary structure. We therefore concatenate our mitochondrial genes following the partitioning strategy of Brandley et al. (2005) for an 11 partition mitochondrial dataset. The nuclear genes we sampled have not been used in skink phylogenetics, so we tested whether they should be partitioned by codon or analyzed as a continuous gene. We analyzed each gene in MrModelTest v2.2 (Nylander 2004) to estimate the best-fit nucleotide subtition model, using the Akiake Information Criterion (AIC) to select the appropriate model. When multiple models had similar scores, we chose the most parameter rich model within 10 AIC units of the best AIC model (Table 2.4). We assume that partitions within genes (codons and ribosomal secondary structure) have the same overall model as the entire gene because simulations show that choosing the correct model may be difficult with a few hundred characters (Posada and Crandall 2001).

In order to combine the nuclear and mitochondrial data we tested for statistically significant incongruent phylogenetic relationships among the gene

trees to ensure each gene tracks the same evolutionary history. We conducted partitioned Bayesian phylogenetic analyses using MrBayes v3.2 (Huelsenbeck and Ronquist 2001) of each nuclear gene and the mitochondrial dataset separately. Each dataset was run with four independent analyses for 20 million generations sampling every 1000 generations. Partitioned Bayesian analyses were completed with rates across partitions unlinked and the prior on branch lengths adjusted to exponential base 100 (Marshall et al. 2006; Marshall 2010). Chain convergence on the same posterior distribution was assessed using Tracer v1.5 (Rambaut and Drummond 2007) and Are We There Yet (AWTY: Nylander et al. 2007; Wilgenbush et al. 2004). The *compare* function in AWTY was used to ensure split frequencies were similar across separate runs insuring topological congruence. Majority rule consensus topologies of the posterior distributions from the multiple runs were summarized using the "sumt" command in MrBayes v3.2. We found no statistically significant incongruent phylogenetic relationships among gene trees ($PP \geq 0.95$; Huelsenbeck and Rannala 2004) so we combined the nuclear and mitochondrial genes into a single dataset for subsequent phylogenetic analysis.

Our combined dataset was analyzed with two different partitioning schemes, varying the partitioning of the nuclear data: P14, nuclear genes partitioned by codon; P17 nuclear genes partitioned by gene and codon (Table 2.5). We compared these partitioning strategies using Bayes Factors (Nylander et al. 2004; Brandley et al. 2005). Analyses of the combined data used the same protocol as the individual genes mentioned above. All four analyses of the

combined datasets for each partitioning strategy converged on the same posterior distribution within 2 million generations.

Testing Alternative Phylogenetic Hypotheses

We use a Bayesian approach to test alternative phylogenetic relationships not represented in our consensus tree. We calculated a 95% credibility set of unique trees in the posterior distribution using the *sumt* command in MrBayes. We reject the alternative phylogenetic hypothesis if it is absent from any tree in the 95% credible set.

Results

Morphological Groups

Our statistical analyses of the four morphological variables used by Brown and Alcala (1980) corresponded to most of their phenotypic groupings (Fig. 2.2). Each of Groups 1, 2, and 5 form morphological clusters in the UPGMA tree, equivalent to the findings of Brown and Alcala (1980). Groups 3 and 4 did not form morphological clusters; however, this seems to reflect the morphological divergence of *Sphenomorphus acutus* and *Sphenomorphus cumingi* (Fig. 2.2). Morphological clustering places these two species as morphologically divergent from all other Philippine *Sphenomorphus*. The other species that do not fit within morphological clusterings of Group 3 and 4 are *Sphenomorphus traanorum*, which Linkem et al. (2010a) placed in Group 4, and *Sphenomorphus decipiens*, which Brown and Alcala considered part of Group 4.

Morphological variation of the four variables is summarized with PCA (Table 2.6). Most of the variation among species is explained by size (69%). Principal Component 2 explains 22% of the morphological variation and is primarily a shape axis of variation in paravertebral scales and midbody scale rows in relation to size. Groups 1, 2, and 5 are separated by PC Axis 1 and moderately separate on PC Axis 2 (shape). Groups 3 and 4 have a region of broad overlap, with most of the variation for Group 4 being the result of size and that of Group 3 the result of shape. Group 6 falls within Group 4. The range of variation for Group 4 would be smaller if the outlying point at the far right of PC1 were not included. This point is represented by the very large species *Sphenomorphus cumingi*. Similarly, Group 3 would be more compact if the morphologically disparate species, *Sphenomorphus acutus*, was not included. Comparing the morphological species classifications mapped onto the PCA plot and our best estimate of phylogeny, it is clear that the morphologically cohesive phenotypic classifications of Brown and Alcala (1980) are predominated by evolutionary convergence, with the only exception being Group 5, which is monophyletic.

Molecular Phylogenetic Results

We did not find any incongruent clades above 95% posterior probability between the nuclear and mitochondrial gene trees. Therefore, we concatenated the data into one matrix totaling 4096 nucleotides, in which 155 characters were ambiguous to align and excluded (from 12S and 16S). Each partition was fit to its best-fit model of evolution and summarized for number of parsimony informative

characters, number of invariant characters and number of uninformative characters (Table 2.4).

We performed two different partitioning strategy analyses on the full dataset, one with the nuclear genes partitioned by gene and codon (P17) and the other with the nuclear genes partitioned by codon position (P14: Table 2.5). Bayes factor comparisons demonstrated that the more partitioned model is the best model of evolution. Our preferred phylogenetic tree is therefore based on the analysis of the full, 17-partition model (Table 2.5).

The resulting consensus tree from the Bayesian phylogenetic analyses of the fully partitioned dataset has high (≥ 0.95) posterior probability for almost all nodes (Fig 2.2). This includes support for Lygosominae and the *Sphenomorphus* group. Other, non-*Sphenomorphus* genera in the *Sphenomorphus* group included in this study render *Sphenomorphus* paraphyletic; these include *Scincella, Lipinia, Papuascincus, Parvoscincus,* and the genera from the diverse radiation of Australian skinks of the *Sphenomorphus* group (*Eremiascincus, Eulamprus, Glaphyromorphus, Hemiergis*).

Philippine *Sphenomorphus* are more diverse phylogenetically than originally expected, with multiple, highly divergent and independent clades defined here. One large radiation is represented by 19 of the 28species found in the Philippines (Fig. 2.3, clade I). This diverse assemblage is in a polytomy with the Australian *Sphenomorphus* group radiation and with *Sphenomorphus cumingi*. Outside of this large Philippine clade, other Philippine species of *Sphenomorphus*

are dispersed throughout the tree, all representing separate invasions of the Philippines. *Sphenomorphus atrigularis*, for example, is nested within a clade of species from Borneo, Sulawesi, and Peninsular Malaysia. *Sphenomorphus variegatus* is nested within a clade of Bornean species. *Sphenomorphus arborens, Sphenomorphus wrighti, Sphenomorphus traanorum,* and *Sphenomorphus victoria* are related to *Lipinia*, which is a widespread genus in Southeast Asia, and *Papuascincus*, a genus found on Papua New Guinea. *Sphenomorphus fasciatus* is nested within a clade of species from Papua New Guinea and the Solomon Islands. These separate clades represent six invasions of the Philippines, which occured primarily via the western island arc of the Philippines.

Discussion

Morphological Variation

Sphenomorphus are often thought of as skinks without morphological novelty (Myers and Donnelly 1991; Greer and Shea 2003). When morphological novelties, or derived apomorphic character differences, were found within species assigned to *Sphenomorphus*, the taxa were recognized as different genera (e.g. Greer 1979; Greer and Simon 1982; Greer 1991; Greer 1997; Ferner et al. 1999). Our results suggest that these morphological novelties represent multiple evolutionary transitions from a generalized pleisiomorphic ancestor, repeated independently throughout the range and evolutionary history of the *Sphenomorphus* group. One such example invloves the transition from a scaly lower eyelid to a transparent "window" in the lower eyelid. Within our sampling

the transparent "window" is found in *Lipinia, Scincella,* and *Papuascincus* (clades C and D). It is also found in *Sphenomorphus assatus* and northern populations of *Sphenomorphus cheerei*, however southern populations of *Sphenomorphus cheerei* have a scaley eyelid. Clade E is nested within this group of transparent "window" taxa, but the taxa in clade E have the pleisiomorphic state of a scaley eyelid. Since *Sphenomorphus cheerei* and clade E both have the pleisomoprhic state, there are two equally parsimonious reconstructions of this character within these taxa, one requiring two reversals to the pleisomorphic state and one requiring a convergence of the derived character and one reversal. These convergences and reversals of complex characters have contributed to the complexity of taxonomic and historical evaluations of the *Sphenomorphus* group.

In the case of Brown and Alcala's (1980) taxonomic groups, it seems that the characters employed for most of the groups have evolved convergently, having arisen in multiple clades; therefore, their groupings based on those characters do not reflect phylogenetic history (Fig. 2.2). The one exception is the *Sphenomorphus abdictus–Sphenomorphus coxi–Sphenomorphus jagori* complex, Group 5, which corresponds to a clade.

It is not surprising that the phenotypic assemblages of Brown and Alcala (1980) do not correspond to phylogenetic clades since Brown and Alcala (1980) emphasized the doubtful phylogenetic validity of the groups they defined. Nevertheless, their identification of diagnostic characters has proven effective for identifying and describing new species. We have shown that Brown and Alcala's (1980) species groups do form phenotypically defined statistical clusters, but that

they are not necessarily the most closely related congeners. Our results therefore suggest that the characters used to define phenotypic assemblages in Philippine *Sphenomorphus* are convergent within the archipelago.

Similarly, our results indicate that changes in body size have occurred repeatedly in Philippine *Sphenomorphus*. Our results suggest that small body size evolved early within clade K (*Sphenomorphus steerei, Sphenomorphus decipiens, Parvoscincus sisoni, Sphenomorphus lawtoni, Sphenomorphus leucospilos, Sphenomorphus luzonensis, Sphenomorphus tagapayo*) of Philippine species, with a later reversal to increased body size, forming a group of "giant-dwarfs" (*Sphenomorphus beyeri, Sphenomorphus hadros, Sphenomorphus igorotorum, Sphenomorphus boyingi, Sphenomorphus cf. decipiens* sp. 4, and *Sphenomorphus laterimaculatus*). All of these "giant-dwarf" taxa have proportionally more scales than other *Sphenomorphus* in the Philippines—a fact that may be explained by scales being proportionally smaller in miniaturized *Sphenomorphus* (Linkem, pers. obs.) and an increase in scale number as body size increases (Greer and Parker 1974). We speculate the increase in body size may have been necessary for the shift to high-elevation, moist cloud forest inhabited by the group of "giant-dwarfs" on Luzon.

Geographic Patterns of Species Relationships

Biogeographic relationships found in Philippine *Sphenomorphus* represent novel patterns never before inferred by phylogenetic analyses of other Philippine vertebrate taxa (Brown and Diesmos 2009; Esselstyn et al. 2010). In particular,

our results unequivocally demonstrate that the complex southern and western Philippine communities of forest skinks are assembled from multiple regions of Southeast Asia and the Papuan realm (Fig. 2.3). The finding that these separate invasions have primarily been restricted to clades occupying the southwestern portion of the archipelago is expected given the geographically proximate potential sources of dispersal (Inger 1954; Brown and Alcala 1970). Invasions seem to have originated from different directions, including two potential invasions from Borneo into Mindanao (*Sphenomorphus atrigularis,* and *Sphenomorphus variegatus*), one potential invasion from an unknown source into Palawan and Panay (*Sphenomorphus arborens, Sphenomorphus traanorum, Sphenomorphus victoria, Sphenomorphus wrighti*), and one potential invasion from the New Guinea faunal region into Mindanao (*Sphenomorphus fasciatus*). *Sphenomorphus variegatus* was conspecific with *Sphenomorphus multisquamatus*, *Sphenomorphus sabanus*, and *Sphenomorphus simus* (Inger 1958), the first two species, sampled in this study, are from Borneo, the latter is not sampled and from Papua New Guinea. We infer that *Sphenomorphus variegatus* is derived from Borneo, but future sampling of *Sphenomorphus simus* may show this to be incorrect. The largest clade (clade I) of Philippine species forms a polytomy with the diverse Australian *Sphenomorphus* group radiation and another Philippine species, *Sphenomorphus cumingi*. This finding is biogeographically unexpected and may be due to our missing-taxon sampling from Papua New Guinea and/or Indonesia, or due to phylogenetic misplacement because of our limited gene sampling of the Australian taxa. Outside of the

Philippine taxa, clades tend to be geographically restricted, with the caveat that our sampling is taxonomically sparse in these regions (Fig. 2.3). Additional clades identified in our analysis include: Clade A of Malaysia, Borneo, Sulawesi, and Mindanao species; Clade B of Indochina, Borneo, and Mindanao species; Clade F of Papuan and Mindanao species; Clade G of Australian species; and Clade I of Philippine species.

It is clear that some Philippine *Sphenomorphus* have evolved from multiple independent origins. Only two Clades (E, I) show signs of within-archipelago speciation, with Clade I diversifying to a much greater extent than Clade E. The species in Clade E are located on the Visayan PAIC (Panay, Negros, Masbate, Guimaras) and on Palawan Island. The islands of the Visayan PAIC and Palawan are geographically distant, with more than 150 km of intervening open water.

In a recent paper Blackburn et al. (2010) presented the "Palawan Ark Hypothesis" and the supposition that the portion of the island arc now consisting of Palawan, southern Mindoro, and northern Panay was potentially emergent for the last 30 million years as it drifted southeast from continental Asia. Clade E *Sphenomorphus* on Panay and Palawan present a possible extension of this hypothesis, though lack of fossil calibrations prevents reliable divergence time estimation. Our current taxon sampling makes it difficult to infer if clade E is closely related the species in Asia, Borneo, or elsewhere in Southeast Asia. Clade I shows some biogeographic patterns similar to those seen in other Philippine animals (Heaney 1985; Kennedy et al. 2000; Brown and Diesmos 2002, 2009),

with speciation events occurring across PAIC boundaries, although there are many speciation events within PAICs. The biogeography of Clade H is discussed in detail by Linkem et al. (2010b). Generally, widespread species in Clade H do not conform to PAIC predictions and there are multiple instances of divergent clades within a species occurring sympatrically. On Luzon Island, there are multiple instances of speciation on the island within Clade K—cases of potential allopatry across mountain ranges. The most obvious example of this is the clade of *Sphenomorphus beyeri, Sphenomorphus boyingi, Sphenomorphus cf. decipiens* sp. 4*, Sphenomorphus hadros, Sphenomorphus igorotorum,* and *Sphenomorphus laterimaculatus*. All of these species are high-elevation endemics found on different mountain ranges on Luzon. (Brown et al. 2010). The *Sphenomorphus decipiens* complex may be another example, but the putative new species have not yet been described.

Species Relationships

This study confirms a long-held suspicion of researchers interested in the relationships of skinks of the *Sphenomorphus* group—viz., that the genus *Sphenomorphus* is widely paraphyletic with respect to a number of lygosomine taxa (Honda et al. 2000; Greer and Shea 2003; Reeder 2003). Nevertheless, the degree of paraphyly is surprising given that every genus of the *Sphenomorphus* group sampled is nested within *Sphenomorphus sensu lato*. One explanation for this problem is that *Sphenomorphus* was never properly defined with diagnostic characters (Myers and Donnelly 1991; Greer and Shea 2003). Thus, species were

placed in the genus if they possessed generalized pleisiomorphic character states or if their phylogenetic affinities were unclear (Grismer et al. 2009b).

Clade A is a group of small skinks represented here by *Sphenomorphus aesculeticola, Sphenomorphus parvus, Sphenomorphus hallieri,* and *Sphenomorphus atrigularis*. These leaf-litter specialists occur in Borneo, Sulawesi, Borneo, and Mindanao, respectively. When describing *Sphenomorphus aesculeticola*, Inger et al. (2001) hypothesized that it was most closely related to the Philippine species *Sphenomorphus atrigularis, Sphenomorphus biparietalis,* and *Sphenomorphus luzonensis*, the Bornean species *Sphenomorphus buettikoferi* and *Sphenomorphus hallieri*, and the Malaysian species *Sphenomorphus malayanus* and *Sphenomorphus butleri*. Because we lack samples of *Sphenomorphus buettikoferi, Sphenomorphus malayanus,* and *Sphenomorphus butleri*, we cannot comment on the relationships of those species, but the others are closely related, except *Sphenomorphus luzonensis*. Recently, numerous small, diminutive species have been described from Malaysia (Grismer 2006, 2007a,b; Grismer et al. 2009a,b). In the recent description of *Sphenomorphus temengorensis*, Grismer et al. (2009b) summarized the eight species of diminutive skinks in Peninsular Malaysia, all of which are morphologically and ecologically similar to the species in Clade A. We also expect that diminuative species in Indonesia: *Sphenomorphus temmincki, Sphenomorphus schlegeli, Sphenomorphus sanana, Sphenomorphus textus, Sphenomorphus necopinatus*, and *Sphenomorphus vanheurni* to be part of this clade based on morphological similarity. Expanded taxon sampling to include these other diminutive species

will hopefully resolve their relationships to Clade A, or elucidate part of another convergent lineage.

The genera *Lipinia, Scincella,* and *Papuascincus* are all nested within a clade of *Sphenomorphus* species from Indochina, Borneo, and the Philippines (Clades B, C, D, E). The Central American *Sphenomorphus* species *Sphenomorphus cheerei* and *Sphenomorphus assatus* are nested within *Scincella* and closely related to *Scincella lateralis*. *Lipinia* is monophyletic and sister to *Papuascincus*. There is low support for the monophyly of *Lipinia* (posterior probability = 0.83), but we note that we only include *Lipinia noctua* and *Lipinia pulchella*. More sampling may increase support for this genus. Pustulated structures on the surface of the eggshells in three species of *Lobulia* skinks led Allison and Greer (1986) to describe *Papuascincus*. These structures are unique among skinks and may represent a reliable synapomorphy for this clade. Also, Greer (1974) hypothesized that *Lipinia, Lobulia,* and *Prasinohaema* were related. Given the hypothesis of Greer (1974) and that *Papuascincus* was previously included in *Lobulia*, we expect that *Lobulia* and *Prasinohaema* will be related to Clade D of *Lipinia* and *Papuascincus*.

Clade B consists of one Philippine species, *Sphenomorphus variegatus*, which is closely related to a clade of the Bornean species *Sphenomorphus multisquamatus, Sphenomorphus sabanus,* and *Sphenomorphus cyanolaemus*. Both *Sphenomorphus multisquamatus* and *Sphenomorphus sabanus* were considered *Sphenomorphus variegatus* until Inger (1958) distinguished them. The species in Clade B are part of Greer and Parker's (1967) *variegatus* group, which

was defined based on external morphology. These skinks are considered surface dwellers and Greer and Parker (1967) included a diverse array of species in the group. The *variegatus* group is not monophyletic in our phylogeny, with representatives in Clade B, E, G and K. We speculate that with increased sampling, we will find that most of the species in the *variegatus* group belong to Clade B. However, given the placement of some species in the *variegatus* group in other clades, it seems premature to assign unsampled species to clades identified here on the basis of overall morphological gestalt.

We do not have a sample of *Sphenomorphus melanopogon*, the type species of the genus *Sphenomorphus*. There are few samples of this species in museums and the type series contains multiple species, raising the question of the true identity of *Sphenomorphus melanopogon* (Linkem, *pers. obs*.). The type series for *Sphenomorphus melanopogon* contains species that are morphologically similar to species in Clade B and Clade F. There is one sample of *Sphenomorphus melanopogon* sequenced and available through GenBank from the work of Schmitz (2003), which is related to species in Clade F (not shown). A revision of *Sphenomorphus melanopogon* is in progress (G. Shea, *pers. comm*.), which will resolve the placement of the type species of *Sphenomorphus*. Until then, it is unclear whether *Sphenomorphus sensu stricto* is our Clade B or Clade F.

Papua New Guinea and the islands of the West Pacific are the most diverse regions for *Sphenomorphus*. Our sampling from these regions is limited in this phylogeny, but all species sampled are closely related in Clade F. Thus, we suspect that most of the Papuan and West Pacific diversity of *Sphenomorphus* will

be related to Clade F. Greer and Parker (1967) divided Papuan *Sphenomorphus* into the *variegatus* and the *fasciatus* groups. Part of the *fasciatus* group was later put in the *maindroni* group based on a synapomorphic scale character (Greer and Shea 2004). We have shown that the *variegatus* group is non-monophyletic, and the one species (*Sphenomorphus concinnatus*) from the Papuan region that we sampled appears in Clade F. However, other species in the *variegatus* group fall into different clades. Members of the *maindroni* group (*Sphenomorphus cranei, Sphenomorphus fasciatus, Sphenomorphus solomonis,* and *Sphenomorphus scutatus*) form a clade based on the four species sampled (of the 22 species in the group). Our results suggest that the *maindroni* group may be a monophyletic assemblage, whereas the *variegatus* group should be revised.

The *Sphenomorphus* group is most diverse in Australia, where it is represented by 15 genera (Reeder 2003; Skinner 2007). In these studies of the Australian genera, outgroup sampling for the *Sphenomorphus* group included only limited sampling of Papuan *Sphenomorphus* species. We find that the Australian group forms a polytomy with Philippine species in Clade I + *Sphenomorphus cumingi*, and not closely related to Papuan species. The Australia + Philippines polytomy has a posterior probabaility of 1.0, rejecting all possabilities for alternative Australian clade relationships given our current sampling and analyses. We cannot reject the hypothesis that the Australia group is sister to clade I + *Sphenomorphus cumingi*, since these groups collapse to a polytomy (Table 2.7). Increased gene sampling from the Australian clade and inclusion of more taxa from Papua and Indonesia may help to resolve this set of relationships.

Most of the Philippine species are found in Clade I, which can be subdivided into Clades H and J. If *Sphenomorphus mindanensis* is removed from Clade H, the lineage is the same as Brown and Alcala's (1980) Group 5 and the same group examined in Linkem et al. (2010b). The relationship between the *Sphenomorphus abdictus–Sphenomorphus coxi–Sphenomorphus jagori* group are similar to those found in Linkem et al. (2010b), but one of the clades identified in that study (*Sphenomorphus abdictus aquilonius* 8) is not monophyletic with the increased gene sampling in this study. *Sphenomorphus abdictus aquilonius* 8 is a large clade with a disjunct geographic distribution in the southwest of Luzon and the islands north of Luzon. Finding that the populations in these geographic regions differ with the analysis of more data is not surprising, showing that even the division of widespread taxa in Linkem et al. (2010b) may still be insufficient to explain the diversity in the *Sphenomorphus abdictus–Sphenomorphus coxi–Sphenomorphus jagori* group. *Sphenomorphus mindanensis* was not included in the Linkem et al. (2010b) analysis of Group 5. It is interesting that we uncover *Sphenomorphus mindanensis* as sister to group 5 because it has nearly identical coloration to *Sphenomorphus coxi coxi*, but is smaller. *Sphenomorphus mindanensis* is part of Brown and Alcala's (1980) Group 3, and based on our morphological analyses of scale counts does not resemble members of the morphologically cohesive Group 5.

The placement of *Sphenomorphus acutus* and *Sphenomorphus diwata* is tenuous. Clade J, supporting these species as sister to Clade K, has low support (posterior probability = 0.77). Morphologically, it is also difficult to ascertain

where these species might fit best within the Philippine taxa. *Sphenomorphus acutus* is morphologically unique, with a body shape most similar to *Emoia*, a distantly related genus. It does not resemble *Sphenomorphus diwata*, or any of the other species in the Philippines. Based on its unique appearance, we expected that it would be related to species outside the Philippines, but clearly our assumptions were incorrect. *Sphenomorphus diwata* has been considered part of Group 1, and morphologically similar to the Luzon high-elevation species *Sphenomorphus beyeri, Sphenomorphus boyingi, Sphenomorphus hadros,* and *Sphenomorphus igorotorum*; however, *Sphenomorphus diwata* clearly is not related to these taxa. Increased gene sampling will probably help to resolve the relationship of these two Mindanao species with respect to the rest of Clade I in the Philippines.

We sampled multiple populations for two widespread species that we suspected contained cryptic genetic lineages. *Sphenomorphus steerei* is abundant on all the major Philippine islands except Palawan, where it is absent, and our analyses infer two highly divergent clades on Luzon, four divergent clades on Mindanao, and four clades on the Visayan PAIC. In some cases, these divergent clades occur in sympatry (*Sphenomorphus cf. steerei* sp. 5 & 6 on Panay; *Sphenomorphus cf. steerei* sp. 4 & 5 on Negros; *Sphenomorphus cf. steerei* sp. 1 & 7 on Mt. Banahao on Luzon) thereby suggesting that these may be exclusive lineages in need of species recognition. Because *Sphenomorphus steerei* is a diminutive skink it is difficult to find externally diagnosable characters for these separate lineages. Populations of *Sphenomorphus decipiens* also show significant

levels of genetic divergence; unlike *Sphenomorphus steerei*, there are pronounced morphological differences between clades. The most divergent population (*Sphenomorphus cf. decipiens* sp. 4) occurs at high elevations on Mt. Banahao and Mt. Palali on Luzon Island. Genetically, this population is most similar to the other high-elevation species—*Sphenomorphus beyeri, Sphenomorphus boyingi, Sphenomorphus hadros, Sphenomorphus igorotorum,* and *Sphenomorphus laterimaculatus*. Scale counts and the size of *Sphenomorphus cf. decipiens* sp. 4 diagnose it as *Sphenomorphus decipiens*; however, these resemblances clearly are convergences because these populations of skinks are genetically so distinct from other *Sphenomorphus decipiens*. *Sphenomorphus decipiens* and *cf. decipiens* species 1, 2, & 3 form a clade, but there are morphological differences among these subclades. Additionally, *Sphenomorphus cf. decipiens* sp. 1, 2, & 4 all occur on Mt. Banahao on Luzon, with *Sphenomorphus cf. decipiens* sp. 1 & 2 occuring in sympatry and *Sphenomorphus cf. decipiens* sp. 4 occurring at a higher elevation on the mountain.

We were surprised to find that the diminutive, high-elevation *Parvoscincus sisoni* on Panay Island is sister to the small, high-elevation *Sphenomorphus tagapayo* on Luzon Island. These miniaturized species seem to have limited ranges on the mountains on which they occur; thus, it is difficult to ascertain relationships between these distant populations, especially given the suspected low probability of detection in intervening forested regions.

Taxonomic Revision

Our analyses reveal that *Sphenomorphus* is not monophyletic with large portions of its diversity more closely related to a variety of other skink genera. Paraphyly has been shown in other studies of lygosomine skinks (Honda et al. 2003), but far less trenchant than that characterizing our results. Although most of our sampling is from species in the genus *Sphenomorphus*, and primarily from the Philippines, every other genus of the *Sphenomorphus* group included in this study renders *Sphenomorphus* paraphyletic.

Given the apparent wholesale paraphyly characterizing the *Sphenomorphus* group, we will avoid some taxonomic changes until future analyses incorporate more taxon sampling (Linkem et al. unpublished data). However we agree with Graybeal and Cannatella (1995) that phylogenetic definitions of taxon names are often best viewed as works in progress, allowing for some well-substantiated changes to be made as evidence justifying such changes becomes available. To that end, we implement a few taxonomic changes that are clearly warranted on the basis of our current results. These changes are an initial step toward a generic revision for the *Sphenomorphus* group and primarily affect the species from the Philippines, where our sampling is robust (Fig 2.4).

Our fully partitioned Bayesian tree presents six separate invasions of the Philippines, each of which is a monophyletic, historical unit. Future taxonomic work will benefit from the recognition of these units as independent from *Sphenomorphus sensu stricto*. Previously defined names are available for most of the lineages defined herein. *Insulasaurus* and *Otosaurus* are revalidated and

Scincella and *Parvoscincus* are extended to include clades defined here. We define two new genera based on phylogenetic results and apply stem-based names to these groups.

New Genera

Tytthoscincus *New genus*

Type species: *Tytthoscincus hallieri* (Lidth de Jeude 1905).

Definition: The clade comprising *Tytthoscincus hallieri* (Lidth de Juede 1905) and all species that share a more recent common ancestor with *Tytthoscincus hallieri* than with *Anomalopus verreauxii, Calyptotis scutirostrum, Coeranoscincus frontalis, Coggeria naufragus, Ctenotus taeniolatus, Eremiascincus richardsonii*, *Eulamprus quoyiii, Glaphyromorphus isolepis, Gnypetoscincus queenslandiae, Hemiergis decresiensis, Insulasaurus wrighti, Lerista lineata, Lipinia pulchella, Nangura spinosa, Notoscincus ornatus, Ophioscincus australis, Otosaurus cumingi, Papuascincus stanleyanus, Parvoscincus sisoni, Pinoyscincus jagori, Prasinohaema flavipes, Saiphos equalis, Scincella lateralis, Sphenomorphus melanopogon*.

Etymology: From the Greek *tytthos,* meaning "small" and the Latin *scincus* for lizard, the combination refers to the small sizes of the species in this genus.

Suggested common name: Diminutive Asian Skink

Description: *Tytthoscincus* can be identified by the following characters: (1) Body size diminutive, usually less than 45 mm SVL; (2) temporal scales small, same size and shape as lateral body scales (Fig. 2.5); and (3) digits small, toe IV slightly longer than, or equal to, toe III.

Included species: *aesculeticolus* (Inger, Lian, Lakim & Yambun 2001), *atrigularis* (Stejneger 1905), *biparietalis* (Taylor 1918), *hallieri* (Lidth de Juede 1905), and *parvus* (Boulenger 1897).

Comment: This clade of diminutive species has unique features that diagnoses it from all other skinks of the *Sphenomorphus* group. Although we lack genetic data for *T. biparentialis*, we nonetheless include it in this genus because it shares the unique presence of divided parietal scales with *T. hallieri*. The diminutive skinks of Malaysia (Grismer et al. 2009) should probably also be placed in this new genus, although we prefer to leave that decision in abeyance until a morphological and genetic examination of those taxa are complete. *Tytthoscincus parvus* (Boulenger 1897) is one of three species of diminutive skinks described from Sulawesi Island. It is likely that the other diminutive species on Sulawesi, *Sphenomorphus temmincki*, and *Sphenomorphus textus* are also part of *Tytthoscincus*. Future examination of temporal scales on small skinks in Southeast Asia should reveal the species composition of *Tytthoscincus*.

Pinoyscincus *New genus*

Type species: *Pinoyscincus jagori* (Peters 1864)

Definition: The clade comprising *Pinoyscincus jagori* (Peters 1864) and all species that share a more recent common ancestor with *Pinoyscincus jagori* than with *Anomalopus verreauxii, Calyptotis scutirostrum, Coeranoscincus frontalis, Coggeria naufragus, Ctenotus taeniolatus, Eremiascincus richardsonii*, *Eulamprus quoyii, Glaphyromorphus isolepis, Gnypetoscincus queenslandiae, Hemiergis decresiencsis, Insulasaurus wrighti, Lerista lineata, Lipinia pulchella, Lobulia elegans, Nangura spinosa, Notoscincus ornatus, Ophioscincus australis, Otosaurus cumingi, Papuascincus stanleyanus, Parvoscincus sisoni, Prasinohaema flavipes, Saiphos equalis, Scincella lateralis, Sphenomorphus melanopogon, Tytthoscincus hallieri*.

Etymology: The word *pinoy* is a commonly used Tagalog term of endearment among Filipinos, referring to an individual Filipino or the nation as a whole. We use it here in conjunction with the Latin *scincus*, meaning lizard, to name a clade of skinks found on the Philippine Archipelago. Suggested common name: Filipino skinks.

Description: *Pinoyscincus* can be identified by the following combination of characters: (1) Body size medium to large (> 42 mm SVL); (2) paravertebral scale rows 56–80; (3) midbody scale rows 30–44; and (4) subdigital lamellae 17–26. In addition to these scale characters, species in this genus share a unique morphology of the hemipenis. The main shaft of the hemipenis, before the

bifurcation, is wide with a large bulbous lobe on each lateral side of the shaft (Fig. 2.6).

Included species: *abdictus* (Brown and Alcala 1980), *coxi* (Taylor 1915), *jagori* (Peters 1864), *llanosi* (Taylor 1919), and *mindanensis* (Taylor 1922).

Comment: This morphologically cohesive genus includes Brown and Alcala's (1980) Group 5 and *Pinoyscincus mindanensis*. All of these species are easily diagnosable among the Philippine skink fauna. The morphology of the hemipenis in this genus has been observed in *Pinoyscincus mindanensis, Pinoyscincus abdictus, Pinoyscincus jagori,* and *Pinoyscincus llanosi* and has not been observed in any other Philippine skink examined (*Otosaurus cumingi*, *Insulasaurus arborens, I. traanorum*, *Parvoscincus beyeri, Parvoscincus decipiens*, *Sphenomorphus fasciatus*, *Sphenomorphus variegatus*). We have not examined the hemipenis of *Sphenomorphus acutus* or *Sphenomorphus diwata* yet to see if they share the *Pinoyscincus* character so we prefer to leave them *incerta sedis* until a more thorough examination can be performed.

Generic Resurrection

Insulasaurus *Taylor* 1922

Type species *Insulasaurus wrighti* Taylor 1922.

Definition: The clade comprising *Insulasaurus wrighti* Taylor 1922 and all species that share a more recent common ancestor with *Insulasaurus wrighti* than

with *Anomalopus verreauxii, Calyptotis scutirostrum, Coeranoscincus frontalis, Coggeria naufragus, Ctenotus taeniolatus, Eremiascincus richardsonii*, *Eulamprus quoyii, Glaphyromorphus isolepis, Gnypetoscincus queenslandiae, Hemiergis decresiencsis, Lerista lineata, Lipinia pulchella, Lobulia elegans, Nangura spinosa, Notoscincus ornatus, Ophioscincus australis, Otosaurus cumingi, Papuascincus stanleyanus, Parvoscincus sisoni, Pinoyscincus jagori, Prasinohaema flavipes, Saiphos equalis, Scincella lateralis, Sphenomorphus melanopogon, Tytthoscincus hallieri*.

Description: *Insulasaurus* is diagnosed by the following combination of characters: (1) Medium body size, 45–64 mm SVL; (2) paravertebral scale rows 62–78; (3) midbody scale rows 29–41; and (4) subdigital lamellae 15–25.

Included species: *arborens* (Taylor 1917)*, traanorum* (Linkem, Diesmos, & Brown 2010)*, wrighti* Taylor 1925*,* and *victoria* (Brown & Alcala 1980).

Comment: The monotypic genus *Insulasaurus* was described by Taylor (1925) based on the presence of a divided frontonasal scale. Greer and Parker (1967) found this character to be variable within *Insulasaurus wrighti*, and subsequently placed *I. wrighti* in the *variegatus* group and synonymized *Insulasaurus* with *Sphenomorphus*. We found that *I. wrighti*, *I. victoria*, *I. traanorum* (all from Palawan Island) and *I. arborens* (Panay Island) are monophyletic, and distinct from other Philippine skinks. Our phylogeny suggests that this small, unique, and biogeographically circumscribed clade is more closely related to the genera

Lipinia and *Papuascincus*, but separate from both, and therefore worthy of designation as a unique genus.

At this time, we have no data suggesting that other *Sphenomorphus* species would be properly placed in the genus *Insulasaurus*, although species in Borneo (e.g. *Sphenomorphus kinabaluensis* and *Sphenomorphus murudensis*) are potential candidates should future phylogenetic studies determine that they are more closely related to *Insulasaurus*, than they are to *Sphenomorphus s.s.*

Otosaurus *Gray* 1845

Type species *Otosaurus cumingi* Gray 1845.

Definition: The clade comprising *Otosaurus cumingi* (Gray 1845) and all species that share a more recent common ancestor with *Otosaurus cumingi* than with *Anomalopus verreauxii, Calyptotis scutirostrum, Coeranoscincus frontalis, Coggeria naufragus, Ctenotus taeniolatus, Eremiascincus richardsonii*, *Eulamprus quoyii, Glaphyromorphus isolepis, Gnypetoscincus queenslandiae, Hemiergis decresiencsis, Insulasaurus wrighti, Lerista lineata, Lipinia pulchella, Lobulia elegans, Nangura spinosa, Notoscincus ornatus, Ophioscincus australis, Papuascincus stanleyanus, Parvoscincus sisoni, Pinoyscincus jagori, Prasinohaema flavipes, Saiphos equalis, Scincella lateralis, Sphenomorphus melanopogon, Tytthoscincus hallieri*.

Description: *Otosaurus* is diagnosed by the following combination of characters: (1) Body large and robust, with adults being longer than 115 mm SVL; (2) large supranasal scales in contact medially, occluding frontonasal contact with the rostral; and (3) supraoculars 7 or 8.

Included species: *cumingi* Gray 1845.

Comments: The species *Otosaurus cumingi* Gray 1845 has always been a morphological outlier to the other Philippine skinks. Being the only *Sphenomorphus* group skink in the region to have large supranasal scales and having an average body-size double that of other species (Gray 1845; Taylor 1922, Brown and Alcala 1980), it has been recognized as phenotypically distinct and unique among Philippine skinks. Our genetic and morphological results confirm its uniqueness among other lineages. Historically, this species was placed in the genus *Otosaurus* Gray 1845 because of its distinctive morphology. Because *O. cumingi* is the type species for the genus *Otosaurus* and is found to be both morphologically and genetically distinct, and our phylogenetic analyses place it in a polytomy with the Australian genera of the *Sphenomorphus* group and with the clade of *Parvoscincus* and *Pinoyscincus*, we re-establish *Otosaurus* as a monotypic genus, moving *cumingi* from *Sphenomorphus* to *Otosaurus.*

Generic Revision

Parvoscincus *Ferner, Brown, & Greer* 1999

Type species *Parvoscincus sisoni* Ferner, Brown, & Greer 1999.

Definition: The clade comprising *Parvoscincus sisoni* (Ferner, Brown, & Greer 1999) and all species that share a more recent common ancestor with *Parvoscincus sisoni* than with *Anomalopus verreauxii, Calyptotis scutirostrum, Coeranoscincus frontalis, Coggeria naufragus, Ctenotus taeniolatus, Eremiascincus richardsonii*, *Eulamprus quoyii, Glaphyromorphus isolepis, Gnypetoscincus queenslandiae, Hemiergis decresiencsis, Insulasaurus wrigthi, Lerista lineata, Lipinia pulchella, Lobulia elegans, Nangura spinosa, Notoscincus ornatus, Ophioscincus australis, Otosaurus cumingii, Papuascincus stanleyanus, Pinoyscincus jagori, Prasinohaema flavipes, Saiphos equalis, Scincella lateralis, Sphenomorphus melanopogon, Tytthoscincus hallieri*.

Description: *Parvoscincus* is diagnosed by the following combination of characters: (1) Body size usually small (< 55 mm SVL) but larger in high-elevation species (46 mm < SVL < 86 mm); (2) four enlarged supraoculars; (3) paravertebral scales 51–110; (4) midbody scale rows 23–46; and (5) subdigital lamellae 10–20.

Included species: *beyeri* (Taylor 1922)*, boyingi* (Brown et al. 2010)*, decipiens* (Boulenger 1894)*, hadros* (Brown et al. 2010), *igorotorum* (Brown et al. 2010), *laterimaculatus* (Brown & Alcala 1980)*, leucospilos* (Peters 1872)*, lawtoni* (Brown & Alcala 1980)*, luzonensis* (Boulenger 1894)*, kitangladensis* (Brown 1995), *palawanensis* (Brown & Alcala 1961)*, sisoni* (Ferner et al. 1999), *steerei* (Stejneger 1908)*,* and *tagapayo* (Brown et al. 1999).

Comments: The recently described genus *Parvoscincus* (Ferner et al. 1999) is nested within a large clade of Philippine *Sphenomorphus* (Clade K). Represented in our phylogeny by the type species, *Parvoscincus sisoni*, it is clear that this genus is not phylogenetically distinct from other Philippine *Sphenomorphus* as originally proposed (Ferner et al. 1999). The other species in this genus, *Parvoscincus palawanensis*, was not sampled; therefore, it is uncertain if it would be related to *Parvoscincus sisoni*, but we assume it is until contrary evidence is presented. Clade K is clearly a unique and supported group of mostly small species of Philippine *Sphenomorphus*. Because *Parvoscincus* is placed within this clade, we recommend that the name *Parvoscincus* be expanded to include the other small-bodied species in this Philippine clade (*Parvoscincus leucospilos, Parvoscincus tagapayao, Parvoscincus luzonensis, Parvoscincus lawtoni, Parvoscincus kitangladensis, Parvoscincus laterimaculatus, Parvoscincus steerei, Parvoscincus decipiens*) in addition to the secondarily enlarged, montane forest species (*Parvoscincus beyeri, Parvoscincus boyingi, Parvoscincus igorotorum,* and *Parvoscincus hadros*). Two species (*Sphenomorphus acutus* and *Sphenomorphus diwata*) in the Philippines are not diagnosable to either *Parvoscincus* or *Pinoyscincus*. These morphologically distinct species are genetically most similar to *Parvoscincus*, but this relationship has low phylogenetic support. We prefer to leave these species *incerta sedis* until a more thorough examination can be performed.

Scincella *Mittleman* 1950

Type species *Scincus lateralis* Say 1823.

Definition: The clade comprising *Scincella lateralis* (Say 1823) and all species that share a more recent common ancestor with *Scincella lateralis* than with *Anomalopus verreauxii, Calyptotis scutirostrum, Coeranoscincus frontalis, Coggeria naufragus, Ctenotus taeniolatus, Eremiascincus richardsonii*, *Eulamprus quoyii, Glaphyromorphus isolepis, Gnypetoscincus queenslandiae, Hemiergis decresiencsis, Insulasaurus wrighti, Lerista lineata, Lipinia pulchella, Lissonota maculata, Lobulia elegans, Nangura spinosa, Notoscincus ornatus, Ophioscincus australis, Otosaurus cumingii, Papuascincus stanleyanus, Parvoscincus sisoni, Pinoyscincus jagori, Prasinohaema flavipes, Saiphos equalis, Sphenomorphus melanopogon, Tytthoscincus hallieri*.

Description: *Scincella* can be diagnosed by the following combination of characters: (1) Body size medium (SVL usually < 65 mm); (2) alpha palate (Greer 1974) with 9 premaxillary teeth; (3) long, thin postorbital bone usually present; and (4) with a transparent window in a movable lower eyelid. Transparent window may be lacking in southern populations of *Scincella cheerei*.

Included species: *apraefrontalis* Nguyen, Nguyen, Bohme & Ziegler 2010, *assata* (Cope 1864)*, barbouri* (Stejneger 1925), *boettgeri* (Van Denburgh 1912), *capitanea* Oubeter 1986, *caudaequinae* (Smith 1951), *cheerei* (Cope 1893)*, doriae* (Boulenger 1887), *forbesora* (Taylor 1937), *formosensis* (Van Denburgh 1912), *gemmingeri* (Cope 1864), *inconspicua* (Müller 1894), *incerta*

(Stuart 1940)*, kikaapoa* Garcia-Vazquez, Canseco-Marquez & Nieto-Montes de Oca 2010, *lateralis* (Say 1823), *macrotis* (Steindachner 1867), *melanosticta* (Boulenger 1887), *modesta* (Günther 1864), *monticola* (Schmidt 1927), *ochracea* (Bourret 1937), *potanini* (Günther 1896), *przewalskii* (Bedriaga 1912), *punctatolineata* (Boulenger 1893), *rara* (Darevsky & Orlov 1997), *rarus* Myers & Donnelly 1991, *reevesi* (Gray 1838), *rufocaudatus* Darevsky & Nguyen 1983, *rupicola* (Smith 1927), *schmidti* (Barbour 1927), *silvicola* (Taylor 1937), *tsinglingensis* (Hu & Djao 1966), *vandenburghi* (Schmidt 1927), and *victoriana* (Shreve 1940).

Comment: The New World species *Scincella cherrei* and *Scincella assata* are nested within the genus *Scincella*, sister to the North American species *Scincella lateralis*. We predict that *Scincella rarus,* and *Scincella incertus* also will be members of this clade. When Greer (1974: pg 33) revised the genus *Leiolepisma*, he provided detailed comments about the potential relationships of these Central American skinks. Morphologically, these species are a mix of *Sphenomorphus* and *Scincella*, with *Scincella assatus* and *Scincella incertus* lacking a postorbital bone but possessing a window in the lower eye (characters of *Scincella*) and *Scincella cherrei* possessing a postorbital bone but having population variation in the presence of the lower eyelid window. Greer (1974) inferred that *Scincella cherrei* was the primitive form of the Central American radiation owing to the possession of the postorbital bone and placed these species in *Sphenomorphus*. He noted that this did not make sense biogeographically because it inferred a separate migration across the Bering Bridge, but he argued it was more plausible

than the re-evolution of the postorbital bone in *Scincella cherrei*. Our molecular evidence shows that the Central American species are part of the same radiation as North American *Scincella*, following the biogeographic expectation. It is therefore reasonable to move these Central American skinks to the genus *Scincella*.

Conclusions

This study, along with several other recent works, demonstrates the need for thorough systematic revision of Scincidae, the largest monophyletic family of squamates. We have shown that the largest genus of skinks in Scincidae is highly paraphyletic. Based on our phylogeny, morphological convergence in scale characters and body size are common within Philippine *Sphenomorphus*; these phenomena clearly have confounded past supraspecific taxonomic treatments. Taxonomic revisions based on robust molecular phylogenies may avoid misdiagnosing phylogenetic relationships due to high levels of homoplasy in some morphological characters. However, it is clear that many of these same morphological characters are useful for identifying new species. We have shown that species composition varies on different islands, with Luzon and Palawan being composed of closely related species, and the Mindanao faunal region being composed of an assembled fauna, derived from multiple separate invasions of the archipelago. Widespread species in the Philippines continue to show divergent relationships both within and between islands, and divergent clades often occur in sympatry. It is likely that morphological examination of subclades of these

widespread species may reveal greater species diversity than currently recognized. If so, a more comprehensive understanding of Philippine *Sphenomorphus* group skinks will require a deeper knowledge of the diversity of the skinks in this unique archipelago.

Table 2.1 Taxonomic groups based on Brown and Alcala (1980) and the characters used to diagnose them.

Species group	Species included	Character support for group
Group 1	*S. beyeri, S. boyingi, S. diwata, S. hadros, S. igorotorum*	Moderate size, > 88 paravertebral scales
Group 2	*S. atrigularis, S. biparietalis, S. lawtoni, S. luzonensis, S. steerei, S. tagapayo, P. palawanensis, P. sisoni*	Small size, with small digits
Group 3	*S. acutus, S. laterimaculatus, S. leucospilos, S. kitangladensis, S. mindanensis, S. victoria*	Midbody scales 30–40, toe IV lamellae 15–20
Group 4	*S. arborens, S. cumingi, S. decipiens,S. traanorum, S. variegatus, S. wrighti*	Midbody scales 36–54, toe IV lamellae 20–28
Group 5	*S. abdictus abdictus, S. abdictus aquilonius, S. coxi coxi, S. coxi divergens, S. jagori grandis, S. jagori jagori, S. llanosi*	Large size, midbody scales 32–44, toe IV lamellae > 20
Group 6	*S. fasciatus*	Limbs do not overlap, midbody scales < 36

Table 2.2 Morphological data used for principal components analysis and morphological clustering. Values are averages for each species. See Brown et al. (2010) for list of specimens examined.

Species	SVL	PV	MBSR	SDL
Parvoscincus palawanensis	31.2	51.0	23.0	11.0
Parvoscincus sisoni	30.1	65.0	25.0	11.5
Sphenomorphus abdictus	86.2	68.5	39.0	23.0
Sphenomorphus abdictus aquionius	87.1	67.5	36.0	22.5
Sphenomorphus acutus	69.6	57.0	28.0	32.0
Sphenomorphus arborens	55.5	69.5	37.5	20.0
Sphenomorphus atrigularis	32.0	56.5	29.0	9.5
Sphenomorphus beyeri	65.4	95.0	40.0	19.5
Sphenomorphus biparietalis	33.7	64.5	32.0	10.0
Sphenomorphus boyingi	56.4	92.0	39.5	20.0
Sphenomorphus coxi coxi	75.0	67.0	35.0	22.5
Sphenomorphus coxi divergens	76.5	69.5	39.0	23.5
Sphenomorphus cumingi	135.8	82.5	51.0	24.5
Sphenomorphus decipiens	38.1	61.5	35.0	16.0
Sphenomorphus diwata	55.0	91.5	40.0	15.0
Sphenomorphus fasciatus	69.9	84.0	30.0	22.0
Sphenomorphus hadros	80.1	109.5	46.0	20.0
Sphenomorphus igorotorum	54.7	102.0	44.5	20.0
Sphenomorphus jagori grandis	90.2	74.0	41.0	25.0
Sphenomorphus jagori jagori	89.9	68.0	38.0	27.0
Sphenomorphus kitangladensis	53.5	74.5	36.0	16.0
Sphenomorphus laterimaculatus	49.6	78.5	36.0	17.5
Sphenomorphus lawtoni	40.1	61.0	28.5	13.5
Sphenomorphus leucospilos	53.5	65.5	31.0	17.0
Sphenomorphus llanosi	80.5	68.5	40.0	22.0
Sphenomorphus luzonensis	43.9	69.0	28.0	10.5
Sphenomorphus mindanensis	49.0	72.0	31.0	18.5
Sphenomorphus steerei	31.2	58.0	30.0	11.5
Sphenomorphus tagapayo	27.6	57.5	29.0	10.0
Sphenomorphus traanorum	50.6	65.5	31.0	16.0
Sphenomorphus variegatus	56.3	71.0	41.0	22.0
Sphenomorphus victoria	46.1	65.0	31.0	19.0
Sphenomorphus wrighti	59.0	74.5	39.0	23.5

Table 2.3 Primer sequences used in this study.

Gene	Primer name	Sequence: 5'–3'	Citation
ND2	Metf6	AAGCTTTCGGGCCCATACC	Macey et al., 1997
	SphenoR	TAGGYGGCAGGTTGTAGCCC	Linkem et al., 2010b
	ND2sphR	CTCTTDTTTGTRGCTTTGAAG GC	Linkem et al., 2010b
12S	12S.H1478	GAGGGTGACGGGCGGTGTGT	Kocher et al., 1989
	12S.L1091	AAACTGGGATTAGATACCCCA CTAT	Kocher et al., 1989
16S	16SF.SKINK	TGTTTACCAAAAACATAGCCT TTAGC	Whiting et al., 2003
	16SR.SKINK	TAGATAGAAACCGACCTGGAT T	Whiting et al., 2003
ND4	ND4	CACCTATGACTACCAAAAGCT CATGTAGAAGC	Arevalo et al., 1994
	tHis	ATCCTTTAAAAGTGARGRGTC T	T. Reeder (pers. comm.)
NGFB	NGFBF_F2	GATTATAGCGTTTCTGATYGG C	Townsend et al., 2008
	NGFBR_R2	CAAAGGTGTGTGTWGTGGTG C	Townsend et al., 2008
R35	R35F	GACTGTGGAYGAYCTGATCAG TGTGGTGCC	Leaché, 2009
	R35R	GCCAAAATGAGSGAGAARCG CTTCTGAGC	Leaché, 2009

Table 2.4 Summary of the model of evolution selected using MrModelTest for each partition. Partitions within genes are assumed to share the partition of the whole gene (see text for justification).

Gene partition	Model of substition based on AIC	Informative characters	Uninformative characters	Constant characters	Total
ND2	GTR + I + G	703	56	270	1029
12S	GTR + I + G	216	29	200	445
16S	GTR + I + G	195	51	266	512
ND4 + tRNA	GTR + I + G	503	56	287	846
NGFB	GTR + I + G	230	55	282	567
R35	GTR + I + G	307	60	322	689
Total		2154	307	1627	4088

Table 2.5 Different partitioning strategies employed for concatenated Bayesian phylogenetic analyses. The last column shows the Bayes Factor (BF) difference between the two partitioning strategies.

Partitioning strategy	Gene Type	Partitions	BF difference to P14
P14	Mitochondrial + Nuclear	12Sstems, 12Sloops, 16Sstems, 16Sloops, ND2pos1, ND2pos2, ND2pos3, ND4pos1, ND4pos2, ND4pos3, tRNA, nucDNApos1, nucDNApos2, nucDNApos3	—
P17	Mitochondrial + Nuclear	12Sstems, 12Sloops, 16Sstems, 16Sloops, ND2pos1, ND2pos2, ND2pos3, ND4pos1, ND4pos2, ND4pos3, tRNA, NGFBpos1, NGFBpos2, NGFBpos3, R35pos1, R35pos2, R35pos3	53.72

Table 2.6 Results of PCA analysis.

Variable	PC1	PC2	PC3	PC4
log(PV)	0.42098	0.70214	0.57273	-0.042
MBSR	0.53437	0.28797	-0.72137	0.33339
SDL	0.48329	-0.56911	0.38239	0.54435
log(SVL)	0.55105	-0.31652	-0.07338	-0.76862
Eigenvalue	2.7976	0.8726	0.2251	0.1047
Percent of variation	69.94	21.81	5.628	2.618

Table 2.7 Tests of multiple phylogenetic hypotheses using the most partitioned (P17) analysis. The presence of any trees within the 95% confidence set of unique trees that are congruent with the hypothesized relationship specifies the hypothesis cannot be rejected by the data.

Phylogenetic hypothesis	**Number of congruent trees**
Total # of trees in 95% CI	14426
S. cumingi + Clade I – Clade G	4619
group 1	0
group 2	0
group 3	0
group 4	0
Monophyly of Philippine taxa	0

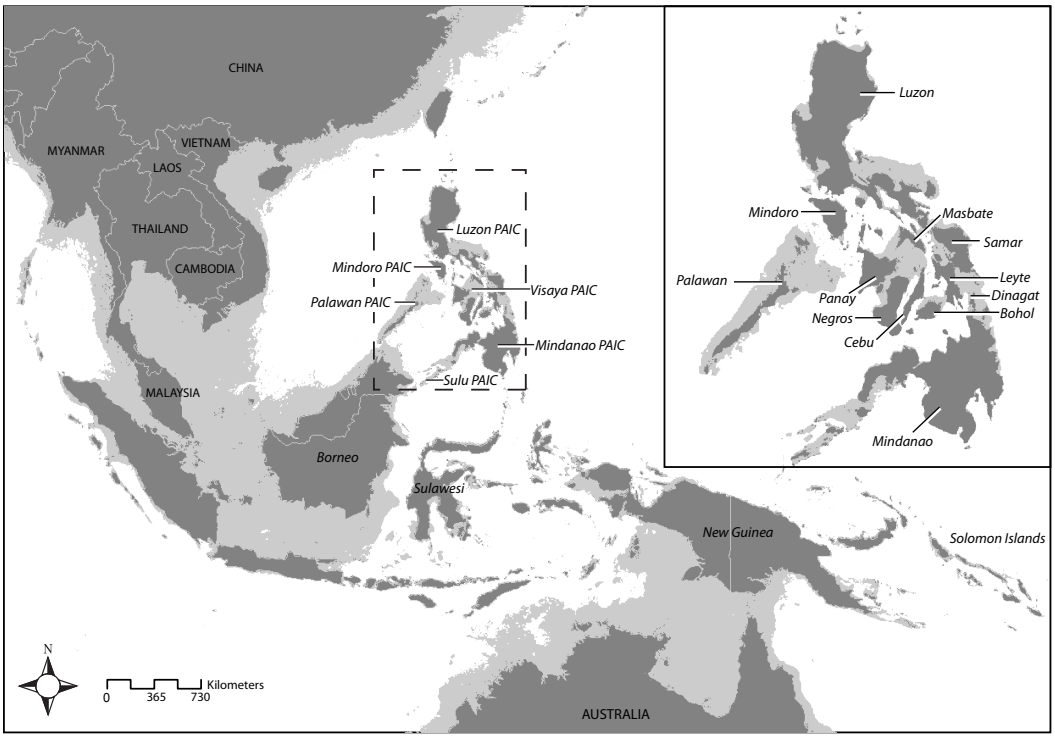

Figure 2.1 A map of the Philippine Islands with the major landmasses labeled. The light gray areas depicts the 120 m bathymetric contour which joined some neighboring islands into Pleistocene aggregate island complexes (PAICs).

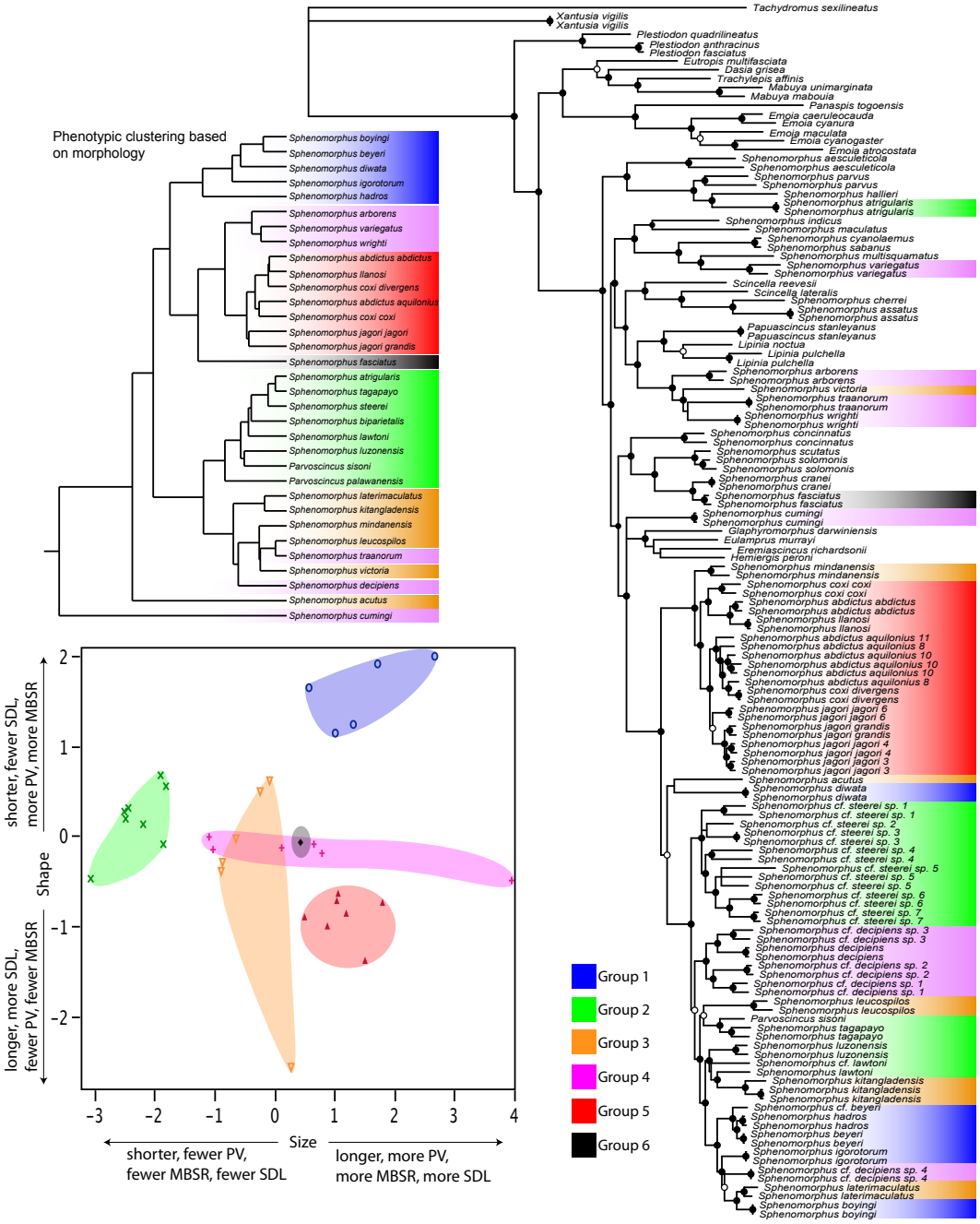
Phenotypic clustering based on morphology
Sphenomorphus boyingi
Sphenomorphus beyeri
Sphenomorphus diwata
Sphenomorphus igorotorum
Sphenomorphus hadros
Sphenomorphus arborens
Sphenomorphus variegatus
Sphenomorphus wrighti
Sphenomorphus abdictus abdictus
Sphenomorphus llanosi
Sphenomorphus coxi divergens
Sphenomorphus abdictus aquilonius
Sphenomorphus coxi coxi
Sphenomorphus jagori jagori
Sphenomorphus jagori grandis
Sphenomorphus fasciatus
Sphenomorphus atrigularis
Sphenomorphus tagapayo
Sphenomorphus steerei
Sphenomorphus biparietalis
Sphenomorphus lawtoni
Sphenomorphus luzonensis
Parvoscincus sisoni
Parvoscincus palawanensis
Sphenomorphus laterimaculatus
Sphenomorphus kitangladensis
Sphenomorphus mindanensis
Sphenomorphus leucospilos
Sphenomorphus traanorum
Sphenomorphus victoria
Sphenomorphus decipiens
Sphenomorphus acutus
Sphenomorphus cumingi
Tachydromus sexilineatus
Xantusia vigilis
Xantusia vigilis
Plestiodon quadrilineatus
Plestiodon anthracinus
Plestiodon fasciatus
Eutropis multifasciata
Dasia grisea
Trachylepis affinis
Mabuya unimarginata
Mabuya mabouia
Panaspis togoensis
Emoia caeruleocauda
Emoia cyanura
Emoia maculata
Emoia cyanogaster
Emoia atrocostata
Sphenomorphus aesculeticola
Sphenomorphus aesculeticola
Sphenomorphus parvus
Sphenomorphus parvus
Sphenomorphus hallieri
Sphenomorphus atrigularis
Sphenomorphus atrigularis
Sphenomorphus indicus
Sphenomorphus maculatus
Sphenomorphus cyanolaemus
Sphenomorphus sabanus
Sphenomorphus multisquamatus
Sphenomorphus variegatus
Sphenomorphus variegatus
Scincella reevesii
Scincella lateralis
Sphenomorphus cherrei
Sphenomorphus assatus
Sphenomorphus assatus
Papuascincus stanleyanus
Papuascincus stanleyanus
Lipinia noctua
Lipinia pulchella
Lipinia pulchella
Sphenomorphus arborens
Sphenomorphus arborens
Sphenomorphus victoria
Sphenomorphus traanorum
Sphenomorphus traanorum
Sphenomorphus wrighti
Sphenomorphus wrighti
Sphenomorphus concinnatus
Sphenomorphus concinnatus
Sphenomorphus scutatus
Sphenomorphus solomonis
Sphenomorphus solomonis
Sphenomorphus cranei
Sphenomorphus cranei
Sphenomorphus fasciatus
Sphenomorphus fasciatus
Sphenomorphus cumingi
Sphenomorphus cumingi
Glaphyromorphus darwiniensis
Eulamprus murrayi
Eremiascincus richardsonii
Hemiergis peronii
Sphenomorphus mindanensis
Sphenomorphus mindanensis
Sphenomorphus coxi coxi
Sphenomorphus coxi coxi
Sphenomorphus abdictus abdictus
Sphenomorphus abdictus abdictus
Sphenomorphus llanosi
Sphenomorphus llanosi
Sphenomorphus abdictus aquilonius 11
Sphenomorphus abdictus aquilonius 8
Sphenomorphus abdictus aquilonius 10
Sphenomorphus abdictus aquilonius 10
Sphenomorphus abdictus aquilonius 10
Sphenomorphus abdictus aquilonius 8
Sphenomorphus coxi divergens
Sphenomorphus coxi divergens
Sphenomorphus jagori jagori 6
Sphenomorphus jagori jagori 6
Sphenomorphus jagori grandis
Sphenomorphus jagori grandis
Sphenomorphus jagori jagori 4
Sphenomorphus jagori jagori 4
Sphenomorphus jagori jagori 3
Sphenomorphus jagori jagori 3
Sphenomorphus acutus
Sphenomorphus diwata
Sphenomorphus diwata
Sphenomorphus cf. steerei sp. 1
Sphenomorphus cf. steerei sp. 1
Sphenomorphus cf. steerei sp. 2
Sphenomorphus cf. steerei sp. 3
Sphenomorphus cf. steerei sp. 3
Sphenomorphus cf. steerei sp. 4
Sphenomorphus cf. steerei sp. 4
Sphenomorphus cf. steerei sp. 5
Sphenomorphus cf. steerei sp. 5
Sphenomorphus cf. steerei sp. 5
Sphenomorphus cf. steerei sp. 6
Sphenomorphus cf. steerei sp. 6
Sphenomorphus cf. steerei sp. 7
Sphenomorphus cf. steerei sp. 7
Sphenomorphus cf. decipiens sp. 3
Sphenomorphus cf. decipiens sp. 3
Sphenomorphus decipiens
Sphenomorphus decipiens
Sphenomorphus cf. decipiens sp. 2
Sphenomorphus cf. decipiens sp. 2
Sphenomorphus cf. decipiens sp. 1
Sphenomorphus cf. decipiens sp. 1
Sphenomorphus leucospilos
Sphenomorphus leucospilos
Parvoscincus sisoni
Sphenomorphus tagapayo
Sphenomorphus tagapayo
Sphenomorphus luzonensis
Sphenomorphus luzonensis
Sphenomorphus cf. lawtoni
Sphenomorphus lawtoni
Sphenomorphus kitangladensis
Sphenomorphus kitangladensis
Sphenomorphus kitangladensis
Sphenomorphus cf. beyeri
Sphenomorphus hadros
Sphenomorphus hadros
Sphenomorphus beyeri
Sphenomorphus beyeri
Sphenomorphus igorotorum
Sphenomorphus igorotorum
Sphenomorphus cf. decipiens sp. 4
Sphenomorphus cf. decipiens sp. 4
Sphenomorphus laterimaculatus
Sphenomorphus laterimaculatus
Sphenomorphus boyingi
Sphenomorphus boyingi
Group 1
Group 2
Group 3
Group 4
Group 5
Group 6
shorter, fewer SDL, more PV, more MBSR
longer, more SDL, fewer PV, fewer MBSR
Shape
2
1
0
−1
−2
−3
−2
−1
0
1
2
3
4
Size
shorter, fewer PV, fewer MBSR, fewer SDL
longer, more PV, more MBSR, more SDL

Figure 2.2 Molecular phylogeny, morphological UPGMA clustering, and principal components analysis plot for Philippine *Sphenomorphus*. The molecular phylogeny is the Bayesian maximum consensus tree from the combined 17-partition analysis. Posterior probability values equal or greater than 0.95 are black circles, above 0.75 are white circles and below 0.75 are not shown. Morphological UPGMA clustering was calculated in JMP using average distances. The PCA plot is for PC1 and PC2 in Table 7. Species groups from Brown and Alcala (1980) are color-coded. Morphological UPGMA clustering shows species groups are morphologically congruent, but the phylogeny shows that these morphologies are convergent.

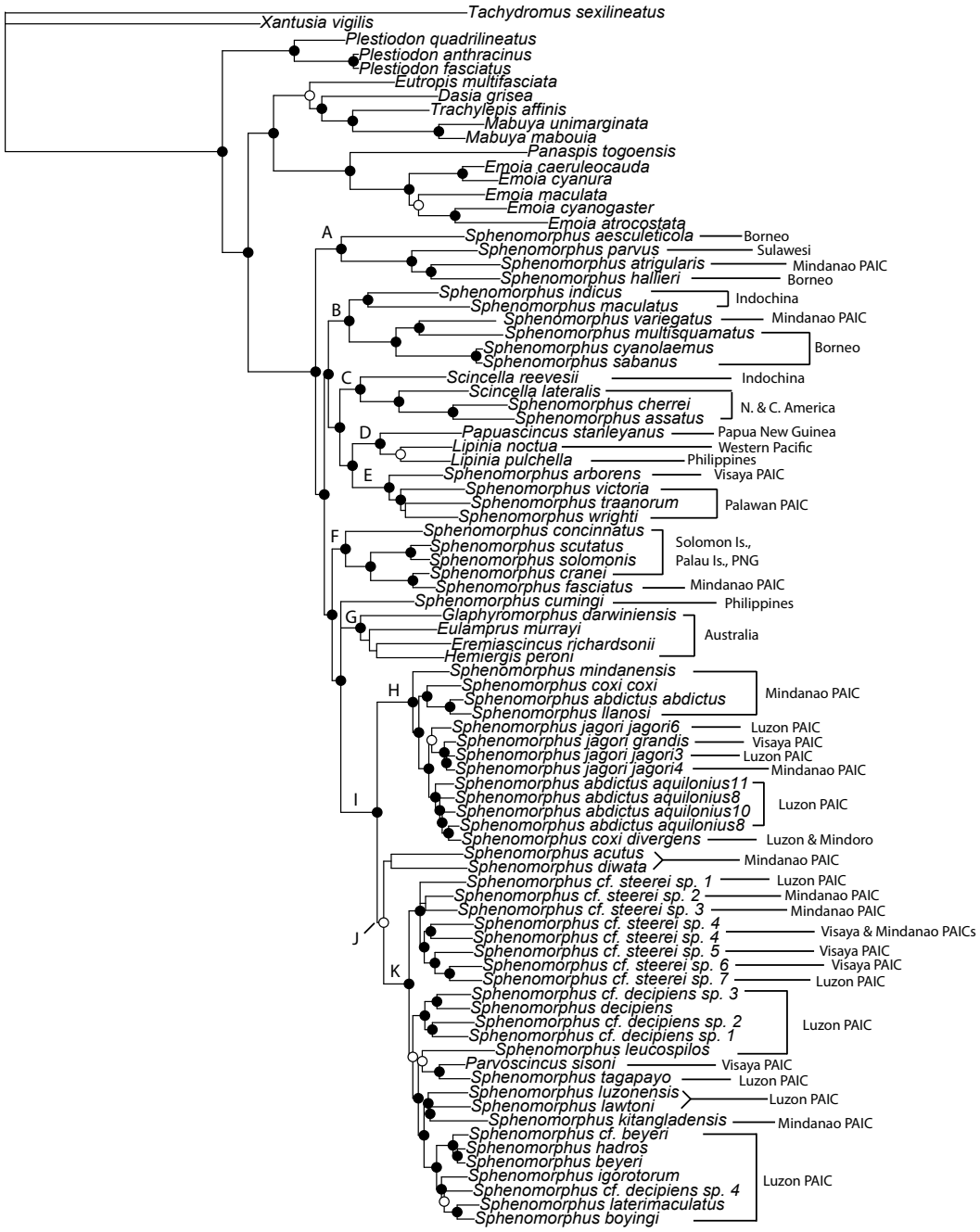

Figure 2.3 Molecular phylogeny from Figure 2 with sampling reduced to one sample per species. Support same as Figure 2. Biogeographic ranges for *Sphenomorphus* species are marked on the phylogeny. Clades discussed in the text are denoted with letters A–K.

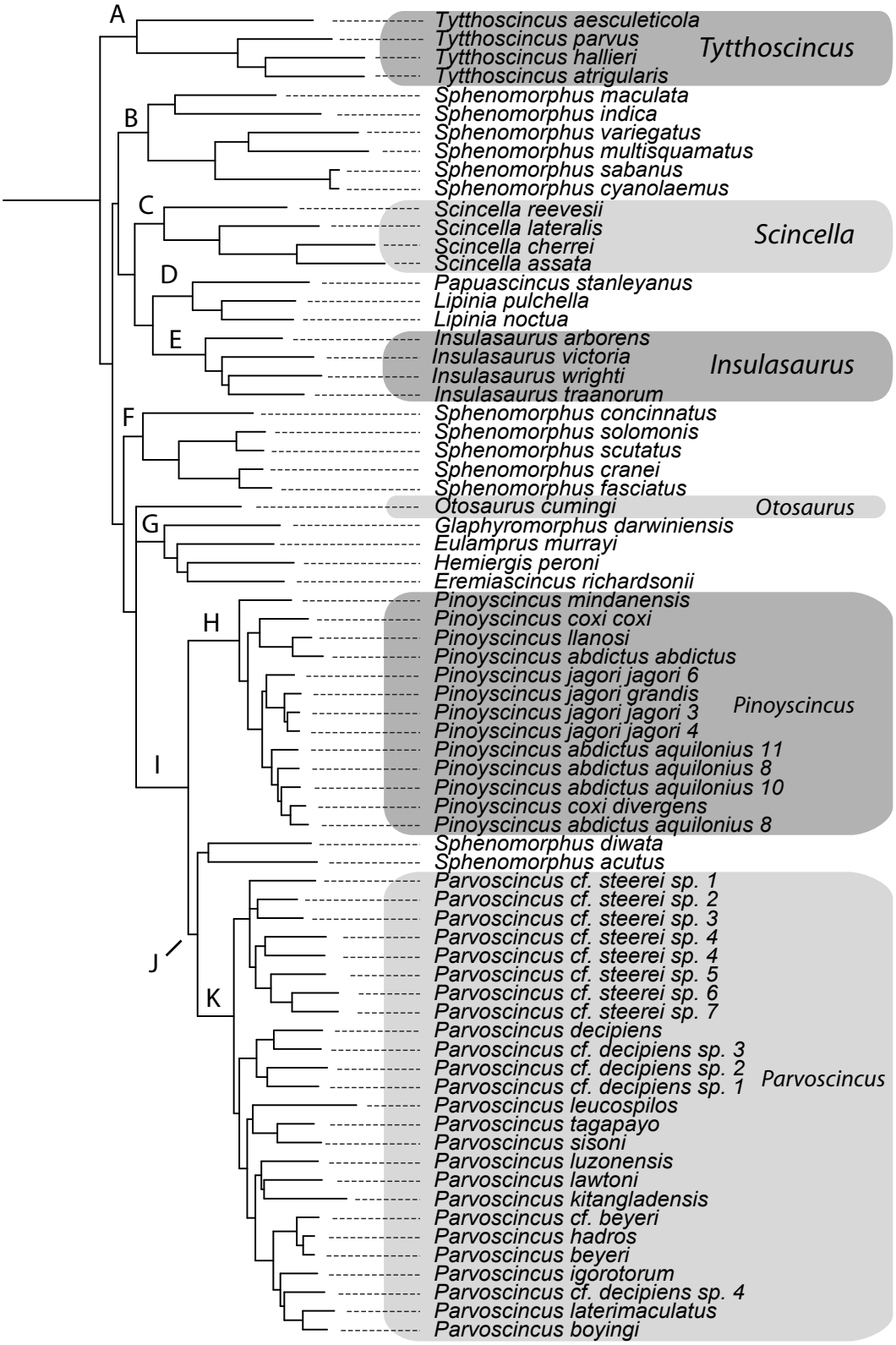

Figure 2.4 Molecular phylogeny from Figure 3 with the species names changed to reflect our new generic taxonomy.

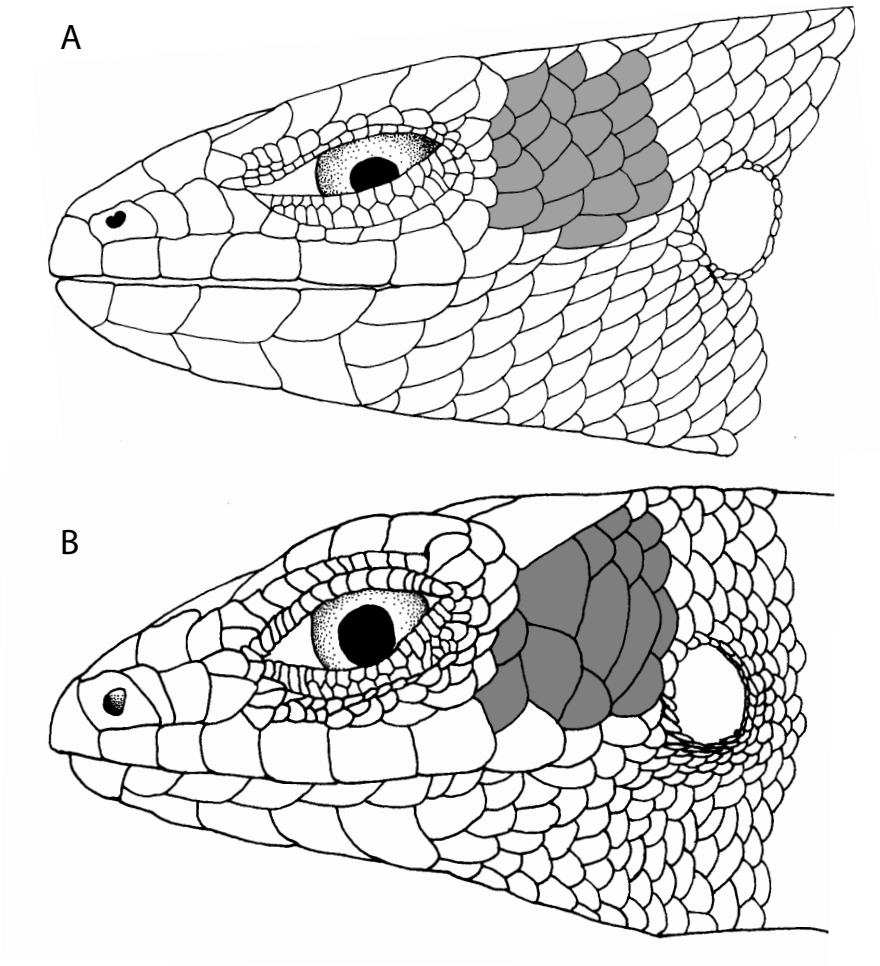

Figure 2.5 Lateral view of the heads of *Tytthoscincus hallieri* (A :redrawn from Inger et al. 2001:Fig 4) and of *Parvoscincus cf. decipiens* 1 (B). The temporal scales (highlighted in gray) of the new genus *Tytthoscincus* are small and blend in with the body scales which is different from the typical shield-like temporal scales (B).

Figure 2.6 Sulcate, lateral, and asulcate views of *Pinoyscincus abdictus abdictus* hemipenis showing (arrows) the unique bulge structures on the lateral region of the main shaft before the bifurcation. Scale bar equals 5 mm.

CHAPTER 3

Southeast Asian biogeography and the origin of skinks in the Sphenomorphini (Squamata: Scincidae: Lygosominae)

Scincidae is the largest family of squamate lizards with more than 1450 species, ~26% of all lizards (Uetz 2011). This global family of lizards exhibits a diverse array of morphological variation, species richness, and behavioral adaptations (Greer 1970). Skinks range from 24 mm to more than 49 cm in length and have diverse morphological adaptations, including multiple transitions to a snake-like body form and repeated evolution of ovoviviparity and keeled scales. Unusual behavioral adaptations include monogamy and communal nest building. The morphological diversity in this family is interesting from an evolutionary perspective but has made proper classification based on morphological characters difficult and often incorrect (Greer 1974, 1979; Greer and Shea 2003).

Skinks in the subfamily Lygosominae have their highest species richness in tropical Asia and are ubiquitously distributed across all of the region's major landmasses; thus, these skinks are an ideal system for studying Southeast Asian biogeography. Lygosominae is composed of five phylogenetic groups (*Mabuya, Lygosoma, Eugongylus, Egernia,* and *Sphenomorphus*), which share common distributional patterns. The *Sphenomorphus* Group (referred to here as the tribe Sphenomorphini) is the most diverse of these groups with more than 500 species (33% of all skinks). It is almost entirely restricted to Asia and Australia (except one clade in Central America), and represents a significant portion of the reptile diversity in these regions. Sphenomorphini species occur as far west as parts of

the Middle East, through India and Sri Lanka, China, Japan, Indochina, Southeast Asia, the Philippines, the West Pacific islands, and Australasia. Most species are restricted to a single biogeographic area (broadly defined, as discussed below), reducing the potential for ambiguity associated with biogeographic analyses. Until now, a poor understanding of the taxonomic relationships within this tribe has hampered analyses of biogeographic history and morphological character evolution. Many of ~30 genera within the tribe are defined without morphological synapomorphies, making inference of species relationships difficult (Linkem et al. 2011). Additionally, the genus *Sphenomorphus* has been treated indiscriminately as a pleisiomorphic taxonomic receptacle for species in Asia and Southeast Asia that do not fit the characters of the other genera in the region.

Recent molecular phylogenetic studies of the Sphenomorphini have begun to resolve some taxonomic issues, revealing the discrepancy between morphological taxonomy and phylogenetic relationships (Honda et al. 2001; Reeder 2003; Honda et al. 2006; Skinner 2007; Skinner et al. 2010; Linkem et al. 2011). Honda et al. (2001) presented a phylogeny of Lygosominae based on mitochondrial DNA and found that *Sphenomorphus* was not monophyletic. Honda et al. (2005) focused on the genus *Tropidophorus* and found that this genus also was not monophyletic, despite a study a year prior (Greer and Biwas 2004) defining a putative new morphological synapomorphy for the genus. A series of papers on the Australian Sphenomorphini by Reeder (2003) and then Skinner (2007) found that many of the Australian genera were not monophyletic, and the Australian radiation was found to be a single radiation that diversified rapidly. Skinner et al. (2011) focused on the Lygosominae and found that the tribe

Sphenomorphini is highly supported. The most recent study by Linkem et al. (2011) focused on *Sphenomorphus* from the Philippines, including the largest sampling of species of the genus to date. *Sphenomorphus* was found to be highly paraphyletic, with many other genera nested within it. Based on the phylogenetic results, Linkem et al. (2011) revised the taxonomy of Philippine Sphenomorphini, resolving some relationships in the tribe. In general, phylogenetic studies of the Sphenomorphini have recovered paraphyly of some genera and some species, demonstrating that morphological variation and convergence have obscured phylogenetic relationships at multiple levels of Sphenomorphini classification. Despite the frustrating taxonomic miscues, convergence in underlying morphological traits makes this tribe particularly interesting for evolutionary study.

This study aims to present the most complete phylogeny of Sphenomorphini to estimate biogeographical patterns and timing of diversification across the geologically complex template of Southeast Asia and the Pacific. Data were assembled from five nuclear and four mitochondrial genes for 447 individuals (294 species) in Sphenomorphini, including at least one individual of all described genera except *Leptoseps*, to reconstruct the evolutionary relationships and estimate the divergence times within the tribe. Multiple methods of divergence time estimation and ancestral range reconstruction were used to estimate the origins of Sphenomorphini diversity and routes of colonization through Southeast Asia.

Materials and Methods

Data Sources

Data in this study are primarily from novel taxon sampling, expanding from the taxon sampling in Linkem et al. (2011). Additional sampling was obtained from Genbank using the PhyLoTa browser (Sanderson et al. 2008) of Genbank public release No. 176 downloaded 22 July 2011. Gene clusters on PhyLoTa that were identified as being the same as genes sequenced for the novel taxon sampling were downloaded and labeled with their gene name for all Scincoidea (Scincidae, Gerrhosauridae, Cordylidae). Gene clusters that had the same gene name were combined if possible. Custom Python scripts were used to: extract the longest single sequence per species for each gene cluster; align the sequences within each gene cluster; and output files necessary for phylogenetic analyses. Another Python script was used to reduce taxon sampling for each gene cluster to include only species in Sphenomorphini and outgroup samples necessary for fossil calibrations and rooting (described below). Gene clusters and new sampling collected for this study that overlapped in identity were combined and aligned (described below). Python scripts are available on github or from the author.

Taxon Sampling

Taxon sampling was restricted to the Scincomorpha, including the outgroup *Xantusia vigilis*. Within Scincidae, samples include two genera from the paraphyletic "Scincinae," *Brachymeles* and *Plestiodon*. Within Lygosominae, sampling focused on the sister clades to the Sphenomorphini, the Eugongylini, the Lygosomini, and the Mabuyini. Samples from the Egernini were included from Genbank. From the Eugongylini, samples from *Emoia,* and *Panaspis* were

combined with *Oligosoma* from Genbank. Samples from *Mabuya, Trachylepis,* and *Eutropis* as well as *Dasia* were included as representative of the Mabuyini. The Lygosomini is represented by two species of *Lygosoma*. The Genbank samples of the Egernini are primarily from Gardner et al. (2009) and use the taxonomic changes therein.

Complete taxon sampling within the Sphenomorphini is critical owing to the paraphyly among many genera revealed by previous studies (Reeder 2003; Skinner 2007; Linkem et al. 2011). Additionally, having a complete phylogeny of the group will provide more power for later statistical analyses of character evolution over the phylogeny. A total of 447 individuals in the Sphenomorphini representing 294 species were included. The goal was to sample two individuals per species whenever possible to improve phylogenetic accuracy and verify species monophyly. Genbank samples were limited to one sample per species. The final dataset included 525 samples for 367 species in the Scincomorpha.

DNA sequencing and Alignment

DNA was extracted from tissue samples using a guanidine thiocyanate protocol modified from the PureGene protocol (Esselstyn et al. 2008, based on a protocol developed by M. Fujita, pers. comm.). Each DNA extraction was amplified for the genes of interest using gene specific primers (Table 3.1) and standard PCR protocols (Palumbi 1996). PCR products were visualized on 1% agarose gels and purified using a 20% dilution of EXOSAPit (USB corp.). EXOSAPit PCR cleaning is an enzymatic purification using endonuclease 1 and shrimp alkaline phosphatase to remove small DNA fragments and extraneous nucleotides. When

diluted, an increased incubation time from 15 minutes to 30 minutes in needed to ensure purification is complete.

Purified PCR products were dye-labelled using Big-Dye terminator 3.1 (Applied Biosystems) with the same primers as in PCR, except for ND2, where a different reverse primer is used for sequencing. Sequencing reactions were visualized using an ABI 3730 automated capillary sequencer. The program SEQUENCHER v.4.8 was used to examine individual chromatograms and assemble fragments into contiguous consensus reads for subsequent analysis. Consensus sequences were grouped by gene and aligned using the L-INS-I algorithm in MAFFT v6.717b (Katoh et al. 2005). This algorithm assumes there is only one align-able region in the fragment and is especially useful for rRNA fragments that have hard to align loop regions. Protein coding genes were adjusted by-eye to verify coding frame using Se-Al v2.0a11 (http://tree.bio.ed.ac.uk/software/seal). Individual gene alignments were combined into one concatenated matrix using a Python script written by CWL available on github. The combined matrix was used for all subsequent analyses and is available on Dryad (http://www.datadryad.org). Individual gene fragments are available on genbank.

Data Exploration and Program Settings

The primary goal of this study is a robust estimate of phylogenetic relationships among taxa. Preliminary analyses showed that the size and complexity of the dataset (525 taxa and > 6300 characters) would render traditional approaches to phylogeny estimation computationally challenging. Initial, exploratory analyses

resulted in parameter interaction, taxonomic instability resulting from missing data, low bootstrap support for well-established relationships, and failure for posterior distributions to converge.

Rogue taxa.—Our initial data matrix included numerous samples from Genbank that were not as complete for gene sampling as were data collected by us (from tissue samples); this introduced missing data to our supermatrix. Despite previous studies that suggest missing data may not be a problem for phylogenetic accuracy (Wiens 1998; 2003; 2006), recent studies have found that missing data can cause an unstable placement of taxa in a phylogeny and that these "rogue taxa" may lower support for nodes in the tree (Sanderson and Shaffer, 2002; Thomson and Shaffer 2010; Moyle et al. 2012). Identification of rogue taxa was accomplished through screening 1000 RAxML (Stamatikus 2006) rapid bootstrap replicates in Mesquite (Maddison and Maddison 2010) for taxonomic instability among trees. Taxa that had highly variable phylogenetic placement among the 1000 replicates were removed from subsequent analyses.

Data partitioning and evolutionary model selection.—The finalized dataset includes four mitochondrial and five nuclear genes that represent a large number of potential partitioning strategies. Seven of these genes are protein coding and could be divided by codon position, making 21 partitions plus two additional partitions for the rRNA and tRNA genes. Preliminary analyses in MrBayes (Huelsenbeck and Ronquist 2001) failed to converge after 30 million generations, thereby precluding the use of the posterior distribution of runs needed for Bayes Factor comparison to determine the optimal partitioning strategy (Nylander et al. 2004; Brandley et al. 2005). As an alternative, we tested

different partitioning strategies by running each in RAxML (Stamatikus 2006). Each partitioning strategy (Table 3.2) was run using the GTR + G model for all partitions and Akaike Information Criterion (AIC) or Bayesian Information Criterion (BIC) were used to compare the partitioning schemes. Identification of the optimal molecular evolutionary model for each data partition used the AIC or BIC implemented in the program jModelTest v2.0.2 (Posada 2008). The partitioning scheme with the best BIC score and optimal models based on BIC were chosen for subsequent Bayesian analyses.

Bayesian Phylogenetic Analysis: MrBayes and PhyloBayes

Given the size of our dataset, standard approaches to Bayesian phylogenetic inference failed to converge during multiple preliminary attempts. A variety of changes to the MCMC parameters were attempted with variable success. Analyses were run in MrBayes v3.2.1 (Huelsenbeck and Ronquist 2001) and PhyloBayes v3.3 (Lartillot et al. 2009).

In MrBayes v3.1.2 two separate datasets were prepared. The first dataset included all the data mentioned previously, and the second dataset was reduced by 200 Genbank samples, primarily the Australian species. Removing these taxa should not affect analyses because previous studies have shown that the Australian clade is monophyletic (Reeder 2003; Skinner 2007). Both datasets were partitioned based on the optimal strategy from the ML searches and optimal models from model testing were employed. Both datasets were run with the parallel version of MrBayes utilizing multiple concurrent runs. The smaller dataset was run with two concurrent analyses for 50 million generations sampling

every 5000 generations; the larger dataset was run for 100 million generation. Owing to the size of these datasets, default Markov chain Monte Carlo (MCMC) parameters were not sufficient to provide proper mixing of the chains. The number of metropolis coupling chains was increased to eight—one cold chain and seven hot chains—and the heating was decreased to 0.01 to increase the probability of a swap being accepted. The chain swap proposal frequency was increased from on to two proposals per generation. These MCMC changes were shown to be effective in other studies with large data matrices (Moyle et al. 2012). Rates across partitions were unlinked and the prior for branch lengths was adjusted to exponential base 100 (Marshall et al. 2006; Marshall 2010). Chain convergence of the posterior distribution was assessed using TRACER v1.5 (Rambaut and Drummond 2007) and Are We There Yet (AWTY: Wilgenbusch et al. 2004; Nylander et al. 2007). If convergence of the posterior distributions between runs was reached, majority rule consensus trees of the posterior distribution of trees from the two runs were summarized in MrBayes.

Analyses run in PhyloBayes v3.3 do not need apriori partitioning. PhyloBayes uses a variety of models to account for site-specific rate variation beyond that available in other programs. Analyses in PhyloBayes of the 525-sample dataset used the non-parametric Dirichlet Process (-ratecat) which models the specific rate of each site and bins sites of similar rates together (Huelsenbeck and Suchard 2007). This process partitions the data into rate groups as part of the MCMC search, allowing the data to inform the partitioning scheme. The composition and quantity of sites in each partition change throughout the MCMC search and at termination of the run there is a posterior distribution of partitions

and rates that can be summarized. The 525-sample dataset was analyzed through eight independent MCMC chains with random starting conditions run for 50 days. Convergence of the parameters in the posterior distribution was assessed in Tracer after using a python script to reformat the PhyloBayes output. Topological convergence across runs was assessed using AWTY, which also required converting the PhyloBayes output to a readable format. A majority rule consensus tree was summarized from the posterior distribution of trees from all eight runs using the program Sumtrees.py in the Dendropy library (Sukumaran and Holder 2010).

Divergence Time Estimation

Divergence time estimation was conducted in BEAST v1.6 (Drummond and Rambaut 2007) using fossil calibrations. Fossil skinks are scarce, especially within Sphenomorphini; therefore outgroup fossils were used to calibrate the tree. Fossils in Egernini and Eugongylini were used to set minimum time bounds on clades in which the fossils belong. A series of fossils from the early to mid-miocene Dwornamor local fauna of riversleigh includes representatives of *Bellatorias*, *Egernia*, and *Tiliqua* (Hutchinson 1992; Shea and Hutchinson 1992), indicating that these clades diverged prior to the mid-miocene (c. 16.4 Ma). Fossils of *Egernia hosmeri* and *Tiliqua scincoides* are represented in the Bluff Downs local fauna of Northeastern Queensland (Mackness and Hutchinson 2000), providing a hard lower bound of 3.6 Ma for the divergence of *Egernia* and *Tiliqua*. A soft upper bound of 26 Ma (mean = 2.55, standard deviation = 0.3) is based on the putative stem taxon of the Egernini—*Proegernia palankarinnensis*—

described from the late Oligocene Minikina Local Fauna of South Australia (Martin et al. 2004).

Based on size, pre-Pleistocene fossils from New Zealand are intermediate between *Oligosoma zelandicum* and *Oligosoma infrapunctatum*, and are definitively placed within the clade of *Oligosoma* and *Cyclodinia*, demonstrating that this clade was present on New Zealand prior to 16 Ma (Lee et al. 2009). Genbank taxon sampling of *Oligosoma* includes the breadth of diversity in this clade (Chapple et al. 2009) and provides a hard lower bound on this clade of 16 Ma. A soft upper bound of 23 Ma is based on the evidence that New Zealand was marine inundated until and inclusive of the late Oligocene (Landis et al. 2008).

The age of Scincomorpha (represented here by skinks, Cordylidae, Gerrhosauridae, and Xantusiidae) was calibrated using the age (Berriasian) of the fossil *Sakurasaurus* (Evans and Manabe 1999; Conrad 2008). A lognormal distribution was chosen; thus the earliest possible sampled age corresponds to 138 Ma and the older 97.5% CI encompasses the earliest age of the root (151 Ma; mean = 0, standard deviation = 1.309; Wiens et al. 2006; Hugall et al. 2007). This node is the root node of the taxon sampling in this study.

Estimation of divergence time on this large dataset involved reducing the taxon sampling and reducing the number of parameters. For these analyses, the 322-sample dataset from the MrBayes analyses was used and the ML tree from RAxML was used as a starting tree. The dataset was partitioned by gene and each gene was run under an HKY + G model of evolution. All nine gene partitions were linked under a single uncorrelated lognormal clock estimated based on the fossil calibrations. To account for the rate variation between genes within the

single clock, rate multipliers were added to the xml code. These rate multipliers are written into the xml code by BEAUTi when partitioning by codon position, but are not an option when partitioning by gene under a single clock. Adding rate multipliers in partitioned Bayesian analyses has been shown to help reduce overestimation of tree length (Marshall 2010) and therefore, should help account for rate heterogeneity between genes in divergence time estimation. The use of the rate multipliers under one clock instead of the use of multiple uncorrelated lognormal clocks significantly reduces the number of parameters estimated in the analysis. Each gene was assigned a rate multiplier weighed by the length of the gene and all rate multipliers were linked. Convergence of the posterior distribution of independent runs was assessed in Tracer and AWTY. Trees were combined using LogCombiner v1.6.1 and summarized using TreeAnnotator v. 1.6.1. The maximum clade credibility tree with median node heights was set as the target tree for summary.

Ancestral Area Reconstruction

Areas were grouped into biogeographic areas that are consistent with previous studies (Brown and Stuart in press) of Southeast Asian fauna and flora (Fig. 1). Species are classified as being "Asian" if they occur in India, the Middle East, China, Japan, Indochina, and the islands of the Sunda Shelf. Species are Philippine if they occur on the Philippine islands, including Palawan. Wallacean species occur on the islands between Wallace's line (Wallace 1863) and Lydekker's line (Lydekker 1896). Species were classified as New Guinean if they occur on New Guinea or any islands in the West Pacific. Australian species are

those restricted to Australia. Any species not occurring in one of these areas were classified as "other"; within Sphenomorphini, this included *Scincella* in North and Central America. Ancestral ranges were estimated using two different approaches, LAGRANGE (Ree and Smith 2008) and Bayesian Binary MCMC (BBM: Yu et al. 2012).

LAGRANGE uses a dispersal-extinction-cladogenesis (DEC) model to estimate the ancestral ranges of nodes. The model treats dispersal and local extinction as stochastic processes that cause range expansion and contraction. It assumes only a single local extinction or dispersal event can happen in an instance of time and that rates of geographic range evolution and speciation occur independently. In addition to estimating the ancestral ranges, dispersal rates between areas and extinction rates within areas also are estimated (Ree and Sanmartin 2009). For Sphenomorphini, ancestral areas were limited to two regions and estimated on the maximum clade credibility tree from the divergence time estimation analysis.

BBM uses a hierarchical Bayesian approach to estimate the ancestral range at nodes. The analysis is available in the program RASP (Yu et al. 2012). The posterior distribution of trees from the divergence time analysis was imported into RASP and a consensus tree was constructed from 100 random trees. The number of ancestral ranges was restricted to two; this restriction is justified by the observation that all the species sampled in Sphenomorphini only occur in one of the defined ranges. We ran the MCMC chain for 50,000 cycles with 10 chains for 2 independent runs. The root distribution was set to NULL to limit the biasing of ancestral range at the basal nodes.

Results

Sequencing, Alignment, Model Selection, and Partitioning

Sequencing of the mitochondrial and nuclear genes was successful for most taxa and with the inclusion of Genbank data there is 51% missing data. The dataset after alignment is 6313 bp with 3256 informative characters across the nine gene regions (Table 3.2). jModelTest v2.0.2 designated GTR + G as the model of evolution for each of the genes when using AIC; slightly less parameterized models were chosen with the BIC (Table 3.2). The invariants sites model was excluded from the possible models owing to interactions with the G parameter in preliminary analyses. Optimal models of evolution also were tested for each of the subgene (codon) partitions. The more conservative models (BIC) were used for subsequent phylogenetic analyses in MrBayes.

The dataset was partitioned using five different strategies based on genes and codon positions of protein coding genes. The partitioning strategies varied from nine to twenty-three partitions. Each partitioning scheme was analyzed in RAxML and the ML was compared between runs. The fully partitioned (23) model was preferred based on AIC and the 18-partition model was preferred based on the BIC (Table 3.2). The BIC is a more conservative measure, with a higher penalty for increased parameterization. The model chosen from BIC was used for partitioning in MrBayes analyses.

Bayesian phylogenetic analyses

MrBayes.—The 525-sample dataset failed to converge on the same posterior distribution after 60 million generations, despite trying multiple parameterizations and varying the MCMC chain temperature. This was largely the result of poor swapping among hot and cold chains. The two independent chains made multiple large jumps in likelihood after 10 and 35 million generations but maintained an average standard deviation of split frequencies of 0.17, well outside the range for convergence. Convergence likely would never occur for this dataset, given that the swap acceptance was so poor in the run (i.e., not likely to jump to the same peak in different runs). The temperature was dropped to 0.01 and the number of chains increased to eight (7 cold and 1 hot) and swapping did not improve. The number of swap proposals is high, but swaps with the cold chains are rarely accepted, which decreases the ability for the analysis to explore the parameter space effectively (Moyle et al. 2012).

The reduced dataset experienced similar difficulty in finding the same posterior parameter space between independent runs. Swap acceptance was improved in the reduced dataset with the increased number of chains and the reduced heating. At 25 million generations the chains still sampled different likelihood space, though all the parameters had converged among runs except the topologies.

PhyloBayes.—The eight independent runs from PhyloBayes converged quickly (~5000 generations) on the same posterior parameter space, and when combined, had estimated sample sizes greater than 200 for all parameters. The posterior estimate for the number of rate categories (partitions) had a mean of 65.9. A majority rule consensus tree of the posterior distribution of topologies

showed good resolution across most of the tree and results consistent with the ML tree from RAxML and previous studies (Fig. 3.2).

Phylogenetic Relationships

Outgroup relationships are similar to those of other analyses (Townsend et al. 2004; Brandley et al. 2005), in which Xantusiidae is found to be sister to the remaining Scincomorpha (Fig. 2a). As in previous analyses, Cordylidae is sister to Gerrhosauridae, and these families are sister to Scincidae. Scincidae is monophyletic with the "Scincinae" paraphyletic. Lygosominae is monophyletic with strong support. The Sphenomorphini is sister to the other four tribes, as found in previous studies (Honda et al. 2000; Reeder 2003; Skinner 2007; Skinner et al. 2011). Lygosomini is sister to Egernini. The Lygosomini / Egernini clade is sister to the Eugongylini. The Eugongylini / Lygosomini / Egernini clade is sister to the Mabuyini (Fig. 3.2a). Two species of *Sphenomorphus* are resolved within the Eugongylini—*S. louisiadensis* and *S. bignelli*. The Sphenomorphini genus *Lankascincus*, described by Greer (1991) and restricted to Sri Lanka, is sister to the Mabuyini with low support and can be rejected as being part of the Sphenomorphini.

Within Sphenomorphini, *Scincella*, *Lipinia*, *Sphenomorphus*, and *Tropidophorus* are paraphyletic (Fig 2b–d). *Lipinia* species appear in three clades; one consists of the small earless species *L. quadrivittata* and *L. infralineolata*, one consists of the type species *L. pulchella*, and the species *L. noctua, L. rouxi, and L. longiceps*, and the third consists of the species *L. leptosoma*. The monophyly of *Lipinia* was not recovered from any trees in the posterior distribution. Most

species of *Scincella* emerge in a single poorly supported (pp = 0.69) clade. One species, *Scincella victoriana* is separate from its congeners and more closely related to *Kaestlea*, *Ateuchosaurus* and *Ablepharus*. The monophyly of *Scincella* also is rejected. The paraphyly of *Tropidophorus* has been shown in previous studies (Honda et al. 2006). The current results are interesting in that the clade with the type species *Tropidophorus cocincinensis* is distinct from all other Sphenomorphini skinks; no other genera were found to be part of this clade with the increased taxon sampling. The remaining *Tropidophorus* clade on the other hand is related to *Sphenomorphus stellatus* and *Sphenomorphus praesignus* ,and is more closely related to the rest of Sphenomorphini than to other *Tropidophorus* (Fig. 3.2b).

The remaining Sphenomorphini clades are primarily organized by biogeographic region. One large *Sphenomorphus* clade consists of species from Asia, Indochina, and Wallacea, with one species from the Philippines and one species from Papua New Guinea. The second large clade of *Sphenomorphus* species consists of species from New Guinea Island, the Solomon Islands, the islands of the West Pacific, and one species from the Philippines (Fig. 3.2b).

Previous revisions of the taxonomy of *Sphenomorphus* remain supported, including the genera *Insulasaurus*, *Otosaurus*, *Pinoyscincus*, *Parvoscincus*, and *Tytthoscincus*. Increased taxon sampling places many of the small Malaysian species of *Sphenomorphus* in the clade currently defined as *Tytthoscincus*; these taxa also fit the morphological definition of the genus (Linkem et al. 2011).

The clade of Australian Sphenomorphini species is sister to a large radiation of Philippine species of Sphenomorphini, not the more geographically

proximate Papua New Guinea species. There is strong support for the sister relationship between the Australian and Philippine clades.

The New Guinea genera *Papuascincus*, *Lobulia*, *Fojia*, and *Prasinohaema* are closely related and are sister to the *Lipinia* clade of *Lipinia pulchella, L. noctua, L. rouxi*, and *L. longiceps*. This radiation is separate from the large New Guinea *Sphenomorphus* radiation.

Most of the species for which two individuals are included are monophyletic. The exceptions include *Tropidophorus misaminius*, *Tytthoscincus temmincki*, *Sphenomorphus variegatus*, *Sphenomorphus auruensis*, *Sphenomorphus jobiensis*, *Sphenomorphus solomonis*, and *Sphenomorphus maindroni*. These species may represent taxonomic problems and reexamination of vouchers is necessary to confirm species identity.

Ancestral range reconstruction

The two different ancestral range estimation methods produced markedly similar results (Fig. 3.3). The general pattern of ancestral ranges shows an origin in Asia with progressive and independent movements of divergent groups east through Wallacea and the Philippines toward New Guinea and Australia. The basal nodes up to 45 mya were identified as Asian for both analyses except for one split in LANGRANGE inferred at 50 mya as being Asia | Philippines. There are multiple dispersals from Asia to the Philippines in *Tropidophorus*, *Insulasaurus* / *Lipinia*, and *Otosaurus* / *Pinoyscincus* / *Parvoscincus* clades of Sphenomorphini. One dispersal event from Wallacea back to Asia (*Tytthoscincus*) stands in contrast to all others, which are invariably from west to east.

The BBM model appears more conservative with estimating node areas, especially for nodes subtending single dispersal events where the ancestral range is always preferred. In LAGRANGE all nodes were inferred with one predominate ancestral area (i.e., there were no 50/50 probabilities between two areas).

Discussion

Genbank Data in Need of Verification

Inclusion of Genbank data for the same species that have new vouchered sampling in this study allows for the verification of some Genbank sample identities. Many of the samples on Genbank are consistent with the vouchered species included in this study (and are considered reliably identified). Within *Tropidophorus*: *T. cocincinensis*, *T. grayi*, *T. partelloi, T. robinsoni*, and *T. misaminius* are similar between Genbank and new samples here. Samples within an identified species that differ between Genbank and this study include *T. sinicus* and *T. berdmorei*. Genbank *T. berdmorei* and *T. sinicus* are from Honda et al. (2005). *T. sinicus* lists a voucher specimen (KUZR 37673) that will allow for taxonomic verification, *T. berdmorei* does not include a locality or voucher for the tissue used. The vouchered samples of these species newly sequenced by us do not appear to be any of the previously identified Genbank species sampled.

Phylogeny of the Sphenomorphini

Support for the Sphenomorphini is not as high in the PhyloBayes and BEAST tree as has been found in previous studies (Skinner et al. 2011). This may

be the result of limited gene sampling from Genbank of some samples (*Kaestlea*, *Ateuchosaurus*, *Ablepharus*) that are sister to the remaining Sphenomorphini; the sampling might limit the confident placement of these taxa in our tree. These samples were not identified as "rogue," though statistics that might be utilized to determine whether a single taxon is significantly unstable currently are unavailable. Interestingly, there is strong support for the small, limb-reduced *Sphenomorphus tridigitus* from Cambodia and Vietnam being a unique lineage, separate from all other clades. The species, originally in the genus *Saiphos* was redescribed by Greer et al. (2006) and moved to *Sphenomorphus*. The species was compared to a number of small, derived taxa that share characters with the genera *Parvoscincus*, *Larutia*, and *Leptoseps*. The current results can rule out *Sphenomorphus tridigitus* being a member of *Larutia* and *Parvoscincus*. There are no genetic samples of *Leptoseps* included here, but we speculate that this genus will be related to *Sphenomorphus tridigitus* given the similarities in body shape and limb reduction.

The paraphyly of *Tropidophorus* has been known in the literature since Honda et al. (2005). Our results also show this genus to be paraphyletic, but we find that *Sphenomorphus praesignus* is sister to a different clade of *Tropidophorus* than the one hypothesized by Honda et al. (2005), who inferred that *Sphenomorphus praesignus* was related to "true" *Tropidophorus*, including the type species *T. cocincinensis*. Our results suggest that *Sphenomorphus praesignus* is related to *Sphenomorphus stellatus* and that these species are sister to the *Tropidophorus* clade primarily consisting of Indochinese species. This leaves "true" *Tropidophorus* a unique lineage separate from all *Sphenomorphus*. Greer

and Biswas (2004) diagnosed *Tropidophorus* based on a character of the eye scales that seemed to be unique among Sphenomorphini species. The derived eyelid character can also be found in some *Cophoscincopus durus*, which is part of Eugongylini. Greer and Biswas (2004) considered this a potential derived character useful for semi-aquatic species that seem to have converged in both clades of *Tropidophorus* and *Cophoscincopus*. Other semi-aquatic species examined (*Parvoscincus leucospilos* and *Sphenomorphus acutus*) lack this eye-scale feature; thus, it may not be necessary for living in semi-aquatic environments.

Another limb-reduced genus of skinks in the Sphenomorphini, *Larutia*, is sister to *Sphenomorphus cameronicus*, a species with a similar semi-fossorial life history to that of *Larutia* but having a body form that is more similar to other *Sphenomorphus*. *Sphenomorphus cameronicus* is from the Cameron Highlands of Malaysia, which fits geographically for a relationship with *Larutia*, which is found in Thailand, Peninsular Malaysia, Sumatra, and Borneo (J. Grismer et al. 2003). *Larutia* was described by Böhme (1981) to separate the species from *Lygosoma*. Their morphology is reminiscent of *Brachymeles* (a Philippine Scincine; Taylor 1917; Siler and Brown 2010) both in body shape and scalation, a clear convergence of morphology for a fossorial lifestyle. Our data fail to resolve any phylogenetic structure within *Larutia*.

Sphenomorphus cryptotis from China and Vietnam is sister to a clade of species primarily from Indochina and Wallacea. This clade consists of medium to large species distributed from India through Wallacea and the Philippines. One species in this clade, *Sphenomorphus simus* occurs on New Guinea. This clade

consists of what will be considered *Sphenomorphus* after the identity of the type species for the genus *Sphenomorphus melanopogon* is resolved (Shea in review). This will change *Sphenomorphus florensis* to *Sphenomorphus melanopogon* and will designate this clade as the nominate clade for the genus *Sphenomorphus*. These species share a morphological character under their hind foot, which will serve in future studies to diagnosis this clade.

Samples of *Scincella* form a clade in the analyses, but support for the relationships are poor. The recently described *Sphenomorphus tonkinensis* (Nguyen et al. 2011) is nested within *Scincella*. The New World species of *Scincella* are a clade, but an apparently undescribed Chinese species is nested within them. This may represent a data quality issue with the Genbank sample of *Scincella gemmingeri*, which also includes few genes.

One *Lipinia* clade, consisting of *Lipinia infralineolata* and *Lipinia quadravittata* is sister to the genus *Insulasaurus* (Linkem et al. 2011). Another clade of *Lipinia* (*L. pulchella*, *L. rouxi*, *L. longiceps*, *L. noctua*) is sister to the Papua New Guinea genera *Prasinohaema*, *Lobulia*, *Fojia*, and *Papuascincus*. The third clade of *Lipinia* represented by *Lipinia leptosoma* is sister to a large clade of primarily Papuan *Sphenomorphus*. These three separate groupings of this genus make sense in light of morphology. *Lipinia infralineolata* and *L. quadravittata* are both small skinks with short legs and scaled-over ear openings whereas *Lipinia pulchella*, *L. noctua*, *L. rouxi* and *L. longiceps* have well-developed legs and elongate bodies. *Lipinia leptosoma* originally was described as a separate genus (*Aulacoplax*).

The species in the *Sphenomorphus maindroni* Group designated by Greer and Shea (2003) are closely related in one of the large clades within the Papuan radiation, save for *S. darlingtoni*, which is not part of the *S. maindroni* Group clade. The New Guinea clade of *Sphenomorphus* requires revision. The *S. maindroni* Group could be designated as a genus and there are multiple available names within the synonymies of species in the clade consisting of *S. pratti*, *S. mulleri*, and *S. jobiensis*.

The Australian clade of Sphenomorphini is well supported and includes samples of *Eremiascincus* from East Timor, indicating relatively recent dispersal out of Australia. The Australian clade is sister to the main radiation of Philippine species in the genera *Otosaurus*, *Pinoyscincus*, *Sphenomorphus*, and *Parvoscincus*. The sister relationship between the species in these regions was first shown in Chapter 2 (Linkem et al. 2011), with the expectation that increased taxon sampling in New Guinea would split this relationship. The sampling is increased dramatically here, including endemic New Guinea genera and multiple New Guinea species. Some taxon sampling is still missing, though most of the missing species should be related to the New Guinea *Sphenomorphus* clade based on morphology. The sister relationship between the Philippines and Australia is biogeographically anomalous. There was never a time when these regions were close together or not separated by New Guinea to the north of Australia (Hall 1997). The biogeography of these taxa will be addressed in more detail below.

Lizard colonization from Asia

The ancestral area reconstructions show a trend of movement from ancestral areas in Asia toward the Philippines, Wallacea, New Guinea, and Australia. All Australian species are nested within the rest of the Sphenomorphini and are inferred to be a single colonization event from a Philippines | Australian ancestor. The sister relationship between Australian taxa and Philippine taxa was shown in Chapter 2. In that chapter, it was unclear whether increased taxon sampling of New Guinea fauna would show a different pattern, linking these two regions with New Guinea in between. With the increased sampling here, this has not been shown to be the case. The MRCA of Australia and the Philippines is inferred to have occurred 44 mya [36–50], which is older than previous estimates for skinks of the Sphenomorphini in Australia (25 mya: Skinner et al 2011) and agamid lizards (30 mya: Hugall and Lee 2004), but not outside the possible age for these regions. The first appearance of Philippine land masses were 50 mya, making it plausible that skinks might have colonized this piece of land as it formed off the coast of Borneo. At this time, Australia was farther south near Antarctica, though it had already separated and was drifting northward. Lizards would have needed to disperse longer distances than found today to colonize Australia from the Philippines and still bypass New Guinea, which is attached to the Sahul Plate north of Australia. The link between Australia and the Philippines seems implausible without relatives in New Guinea, and there is still the potential that these relatives exist, given that unsampled species remain on New Guinea. That said, most of the unsampled lineages on New Guinea are expected to be related to the taxa sampled and represented in the New Guinea clade of *Sphenomorphus*.

More investigation into the relationship of the Australian and Philippine fauna is needed.

New Guinea and its associated islands have been colonized three times by members of the Sphenomorphini. There is a single colonization event of *Sphenomorphus simus* from Wallacea, a colonization of the "window-eyed" skinks potentially from the Philippines, and a colonization of *Sphenomorphus* from the Philippines or Asia. The "window-eyed" skinks of the genus *Lipinia* "back-dispersed" to the Philippines (*Lipinia pulchella*). The ancestral range of this clade may be skewed to the Philippines as a result of taxon sampling in *Lipinia*, which is a wide-ranging genus in Southeast Asia. Increased taxon sampling may reveal a New Guinea ancestral range for this *Lipinia* clade, which is more consistent with prior expectations.

The Philippines has been colonized many times and also seems to be a source for some of the more eastern radiations in this group. Most Philippine colonizations have come from Asia, though there is dispersal from Wallacea to the Philippines with *Tytthoscincus atrigularis* and dispersal from New Guinea to the Philippines with *Sphenomorphus fasciatus* and *Lipinia pulchella*. Timing of dispersal into the Philippines is estimated to be as old as 40–50 mya, when the Philippine islands were a small area of land off the coast of Borneo. This piece of land moved north away from Borneo and became isolated in the South China Sea. Colonization this early would require the land to remain subaerial up through current day. An additional piece of Philippine land broke away from the Asian continent near China, giving rise to Palawan, part of Panay, and some small islands north of Panay (the Romblon group). This piece of land that rafted from

Asia is inferred to be subaerial and has been termed the Palawan Ark (Blackburn et al. 2010). One of the three colonizations of the Philippines is consistent with the Palawan ark hypothesis, the *Insulasaurus–Lipinia quadravittata* clade. Ancestral range reconstruction shows that this radiation shared an ancestral range with Asia slightly more than 40 mya. This is consistent with isolation on Palawan before rafting of the Palawan ark began. By 40 mya, the radiation is inferred to be completely Philippine, which is just prior to the isolation of the Palawan block. *Insulasaurus* is restricted to Palawan and Panay, and *Lipinia* in this clade is found on Panay, Negros, and Palawan. This scenario is consistent with the findings in *Barbourula* toads (Blackburn et al. 2010) and Philippine *Gekko* (Siler et al. 2012) and demonstrates a third example of colonization through the Palawan ark.

Wallacea was colonized later than the other regions, probably because of the variable nature of the island formation in this region. The first inferred ancestral range in Wallacea is 37–42 mya for a clade of *Sphenomorphus* endemic to Sulawesi. This is the largest and oldest of the Wallacean islands and portions of the island are inferred to be subaerial for 40 mya. At this time period, the southwestern peninsula and central core of Sulawesi were connected to eastern Borneo and *Sphenomorphus* may have gotten to the island via range expansion, followed by a vicariance event when the Sulawesi block separated from the Sunda Shelf. Sulawesi *Tytthoscincus* is estimated to have colonized Sulawesi Island about 25 mya, which would have required dispersal to the island from Asia. Increased taxon sampling in both Sulawesi clades should help to resolve the origins of these groups (discusses in next chapter). The Wallacean endemic *Sphenomorphus florensis* is nested within the clade of Asian *Sphenomoprhus*.

LAGRANGE infers a shared ancestral range of Wallacea and Asia more than 40 mya, though none of the Lesser Sunda Islands where *S. florensis* occurs was present this early. There are unsampled taxa in both Asia and Wallacea that may break this long-branch and result in a more plausible timing for the Wallacean *Sphenomorphus*. The phylogenetic results and ancestral range analysis document the origin of this radiation came from Asian *Sphenomorphus*.

Conclusions

Increased taxon sampling has shown that our previous understanding of the Sphenomorphini was incomplete. Many genera are paraphyletic and revisions are needed. As has been shown previously (Linkem et al. 2011) morphological characters consistent with the molecular phylogeny can be used to diagnose these new or resurrected genera. Skink diversity in Asia and Australasia seems to have originated in Asia and spread progressively eastward. As lineages arrived on new islands with potential new niches, they diversified, sometimes rapidly as in the case on Australia. Now that we have a phylogenetic estimate for Sphenomorphini we will be able to better understand to evolution of complex characters such as body size, limb reduction, and reproductive mode.

Table 3.1 Primers used for PCR and sequencing with citations for sources.

Gene	Primer name	sequence	Citation
ND2	Metf6	AAGCTTTCGGGCCCATACC	Macey et al. 1997
	SphenoR	TAGGYGGCAGGTTGTAGCCC	Linkem et al. 2010b
	ND2sphR	CTCTTDTTTGTRGCTTTGAAGGC	Linkem et al. 2010b
12S	12S.H1478	GAGGGTGACGGGCGGTGTGT	Kocher et al. 1989
	12S.L1091	AAACTGGGATTAGATACCCCACTAT	Kocher et al. 1989
16S	16SF.SKINK	TGTTTACCAAAAACATAGCCTTTAGC	Whiting et al. 2003
	16SR.SKINK	TAGATAGAAACCGACCTGGATT	Whiting et al. 2003
ND4	ND4	CACCTATGACTACCAAAAGCTCATGTAGAAGC	Arevalo et al 1994
	tHis	ATCCTTTAAAAGTGARGRGTCT	T. Reeder (pers. comm.)
NGFB	NGFBF_F2	GATTATAGCGTTTCTGATYGGC	Townsend et al. 2009
	NGFBR_R2	CAAAGGTGTGTGTWGTGGTGC	Townsend et al. 2009
R35	R35F	GACTGTGGAYGAYCTGATCAGTGTGGTGCC	Leache 2009
	R35R	GCCAAAATGAGSGAGAARCGCTTCTGAGC	Leache 2009
PTGER4	PTGER4_f1	GACCATCCCGGCCGTMATGTTCATCTT	Townsend et al. 2009
	PTGER4_r5	AGGAAGGARCTGAAGCCCGCATACA	Townsend et al. 2009
ADNP	ADNP_f5	ATTGAAGACCATGARCGYATAGG	Townsend et al. 2009
	ADNP_r2	GCCATCTTYTCHACRTCATTGA	Townsend et al. 2009
MKL1	MKL1_f1	GTGGCAGAGCTGAAGCARGARCTGAA	Townsend et al. 2009
	MKL1_r2	GCRCTCTKRTTGGTCACRGTGAGG	Townsend et al. 2009

Table 3.2 Comparison of Maximum Likelihood runs in RAxML under 5 different partitioning schemes. AIC based on the formula AIC=-2*ln(likelihood) + 2*K and BIC based on BIC = -2*ln(L) + K*ln(n). The number of parameters does not include the branch lengths since they are number is the same across all runs. The smallest AIC and BIC are preferred (bold)

Partitioning	# parameters (K)	Likelihood	AIC	BIC
9 partitions	81	-205391.064859	410944.1297	411490.6009
13 partitions	117	-202270.898492	404775.797	405565.1442
16 partitions	144	-202093.846647	404475.6933	405447.1976
18 partitions	162	-201751.787779	403827.5756	**404920.5178**
23 partitions	207	-201686.160226	**403786.3205**	405182.8578

Table 3.3 Partitions and the optimal model of evolution estimated by jModelTest under BIC and AIC criterion.

Partition	BIC	AIC
12S	GTR + G	GTR + G
16S	GTR + G	GTR + G
ND2	GTR + G	GTR + G
ND4 + tRNA	GTR + G	GTR + G
ADNP	K80 + G	GTR + G
NGFB	HKY + G	GTR + G
MKL1	GTR + G	GTR + G
PTGER4	GTR + G	GTR + G
R35	GTR + G	GTR + G
ND2pos1	GTR + G	GTR + G
ND2pos2	GTR + G	GTR + G
ND2pos3	GTR + G	GTR + G
ND4pos1	GTR + G	GTR + G
ND4pos2 + tRNA	GTR + G	GTR + G
ND4pos3	GTR + G	GTR + G
ADNPpos1,2	HKY + G	GTR + G
ADNPpos3	HKY + G	GTR + G
NGFBpos1,2	HKY + G	HKY + G
NGFBpos3	SYM + G	SYM + G
PTGER4pos1,2	HKY + G	GTR + G
PTGER4pos3	JC + G	GTR + G
MKL1pos1,2	SYM + G	SYM + G
MKL1pos3	GTR + G	GTR + G
R35pos1,2	K80 + G	GTR + G
R35pos3	GTR + G	GTR + G

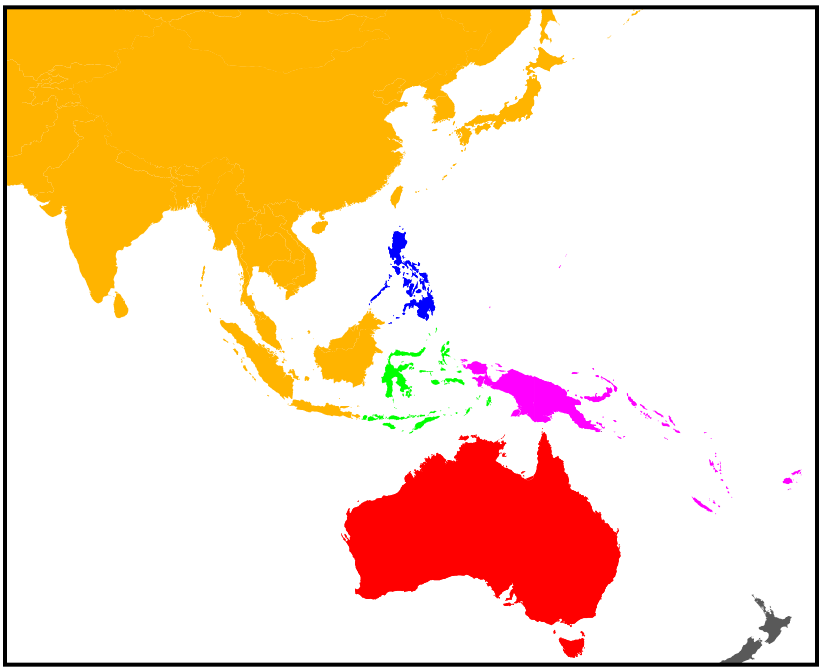

Figure 3.1 Map of Asia, Southeast Asia, and Australia with the biogeographic regions used in this study color-coded to match the tree and ancestral area reconstruction.

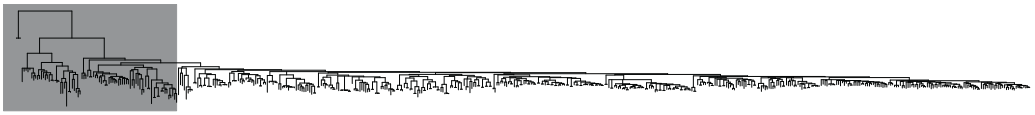

A

Figure 2b

Asia
Philippines
Wallacea
New Guinea
Australia
Other

Lygosominae

Scincidae

Emoia atrocostata RMB6017
Emoia cyanogaster RMB6957
Emoia maculata RMB6855
Emoia caeruleocauda RMB6876
Emoia cyanura RMB1711
ti105737 Oligosoma nigriplantare polychroma
ti538569 Oligosoma longipes
ti105733 Oligosoma microlepis
ti105740 Oligosoma smithi
Sphenomorphus louisiadensis BPBM20312
Sphenomorphus louisiadensis BPBM20313
Sphenomorphus bignelli RMB6888
Sphenomorphus bignelli RMB6911
Panaspis togoensis KU290440
Eugongylus group

Lygosoma quadrupes LSUHC8002
Lygosoma quadrupes LSUHC8403
Lygosoma bowringii LSUHC6970
Lygosoma group

Mabuya mabouia KU214970
Mabuya unimarginata KU291283
Trachylepis affinis EBG969
Dasia grisea CDS2086
Eutropis multifasciata CDS145
Mabuya group

ti245627 Lankascincus fallax
Lankascincus taprobanensis CCA1730
ti245673 Ristella rurkii

ti261943 Liopholis guthega
ti261951 Liopholis montana
ti161945 Liopholis whitii
ti261949 Liopholis margaretae personata
ti261948 Liopholis margaretae margaretae
ti261950 Liopholis modesta
ti261945 Liopholis kintorei
ti261956 Liopholis striata
ti261944 Liopholis inornata
ti261952 Liopholis multiscutata
ti261954 Liopholis pulchra longicauda
ti71010 Tiliqua scincoides
ti96725 Tiliqua gigas
ti155307 Tiliqua nigrolutea
ti220768 Tiliqua adelaidensis
ti245668 Tiliqua rugosa asper
ti96718 Bellatorias frerei
ti261946 Bellatorias major
ti261955 Egernia saxatilis
Egernia group

Plestiodon anthracinus CAS325
Plestiodon fasciatus KU289462
Plestiodon quadrilineatus KU311490
Brachymeles boulengeri CDS1118
Brachymeles makusog CDS2369
Brachymeles tridactylus CDS1561
Scincinae

ti143504 Gerrhosaurus nigrolineatus
ti219631 Gerrhosaurus multilineatus auritus
ti174278 Gerrhosaurus flavigularis
ti219623 Angolosaurus skoogi
ti126622 Gerrhosaurus typicus
ti219618 Gerrhosaurus validus maltzahni
ti219619 Gerrhosaurus validus validus
ti219625 Cordylosaurus subtesselatus
ti126624 Tetradactylus seps
ti219628 Tetradactylus tetradactylus
ti219629 Tetradactylus africanus fitzsimonsi
ti219620 Gerrhosaurus major major
ti219621 Gerrhosaurus major bottegoi
ti174280 Gerrhosaurus major
ti174283 Zonosaurus karsteni
ti219626 Zonosaurus laticaudatus
ti174284 Zonosaurus ornatus
ti143654 Zonosaurus brygooi
ti174285 Zonosaurus rufipes
ti174286 Zonosaurus trilineatus
ti143662 Zonosaurus madagascariensis
ti174273 Tracheloptychus madagascariensis
ti211473 Tracheloptychus petersi
Gerrhosauridae

ti126626 Pseudocordylus capensis
ti357131 Pseudocordylus microlepidotus
ti126612 Cordylus tropidosternum
ti126610 Cordylus oelofseni
ti126606 Cordylus macropholis
ti94417 Cordylus cordylus
ti126609 Cordylus niger
ti52175 Platysaurus capensis
Cordylidae

Xantusia vigilis KU220088
Xantusia vigilis KU220090
Xantusia vigilis KU220089
Xantusiidae

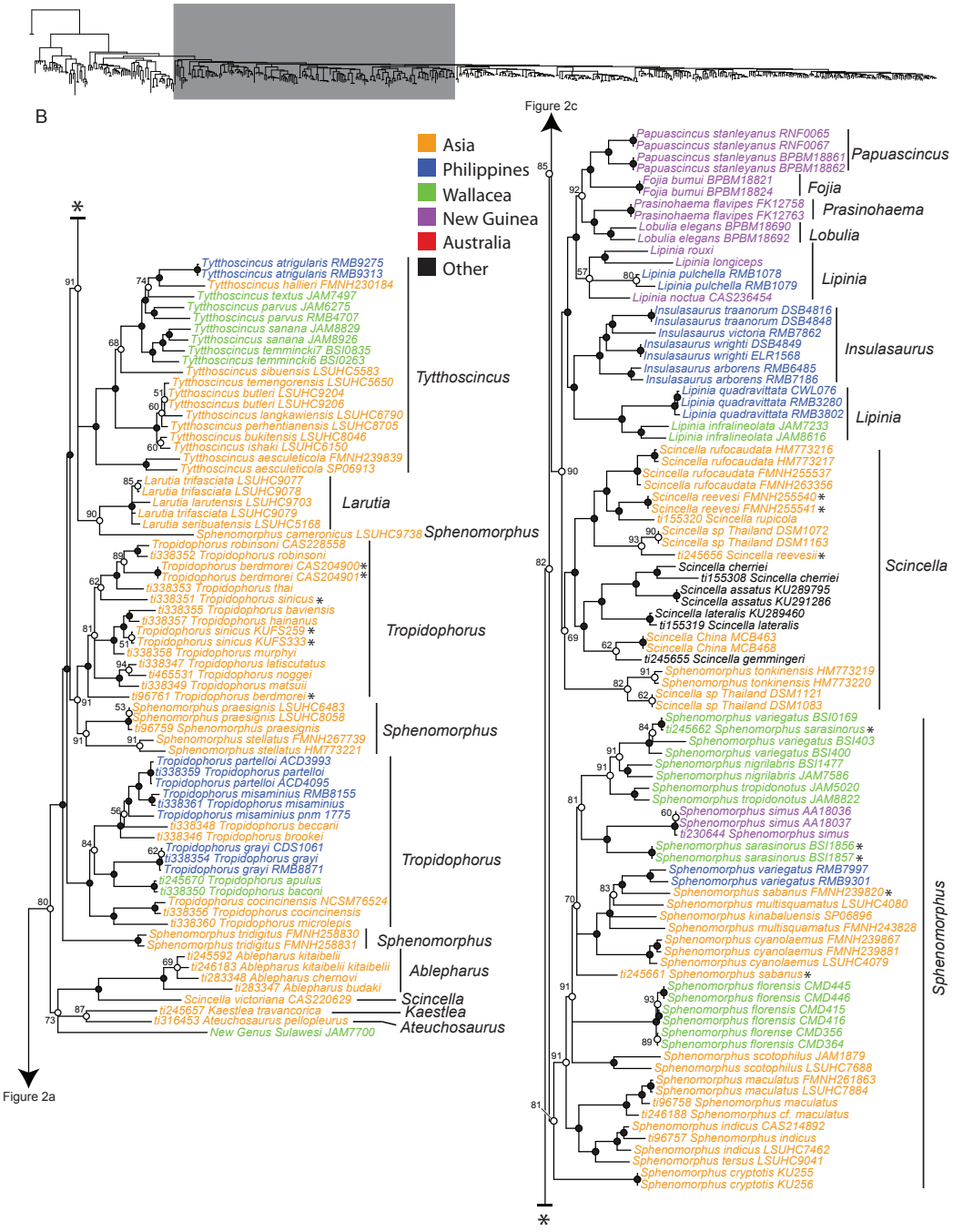
B
Asia
Philippines
Wallacea
New Guinea
Australia
Other
Figure 2c
Figure 2a
Tytthoscincus
Larutia
Sphenomorphus
Tropidophorus
Sphenomorphus
Tropidophorus
Sphenomorphus
Ablepharus
Scincella
Kaestlea
Ateuchosaurus
Papuascincus
Fojia
Prasinohaema
Lobulia
Lipinia
Insulasaurus
Lipinia
Scincella
Sphenomorphus

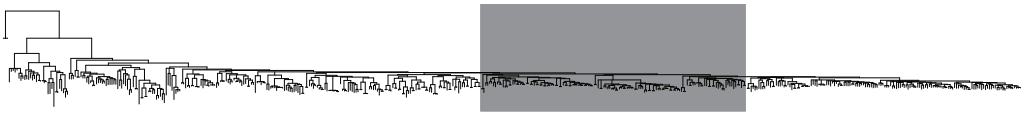

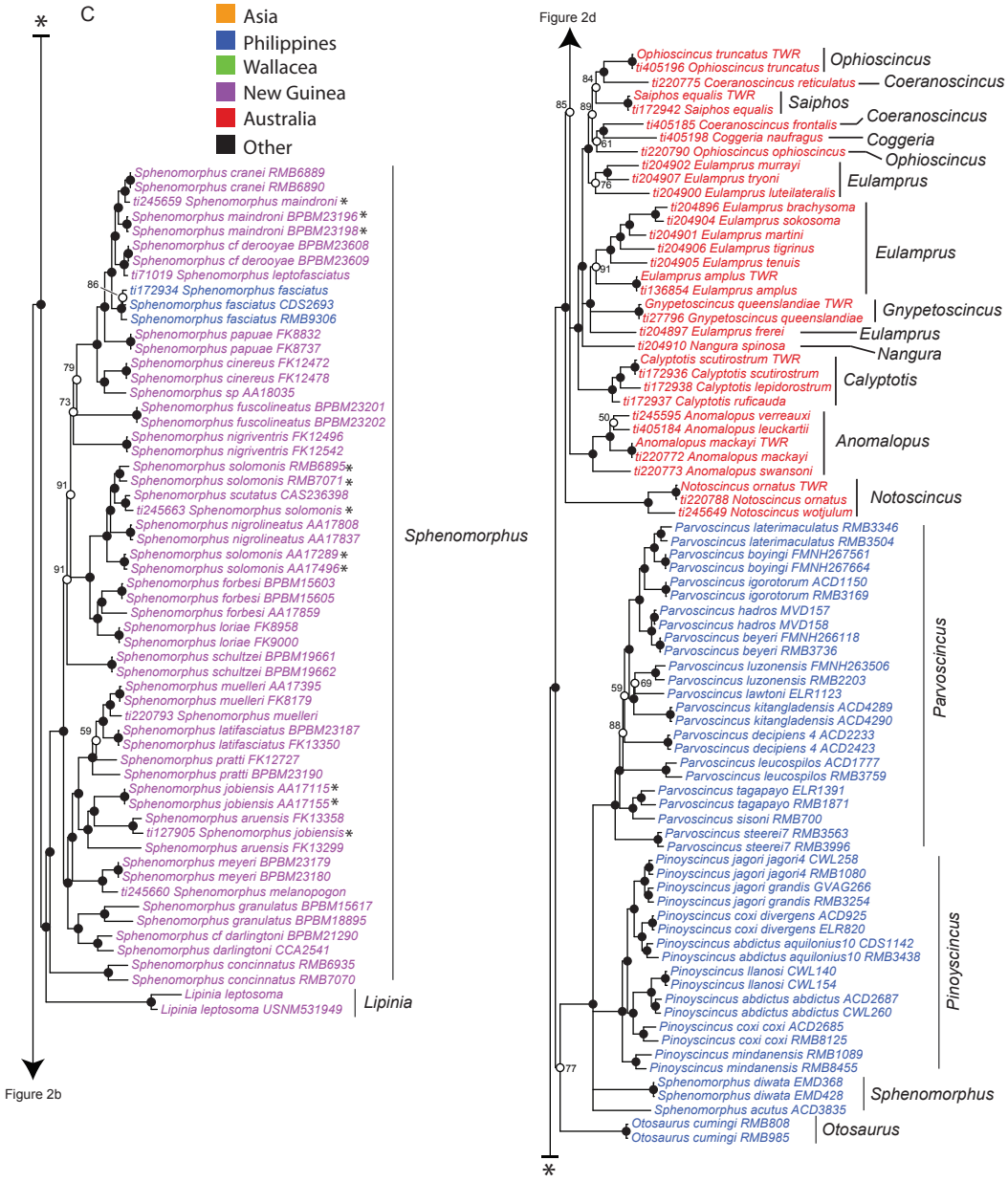
C
Asia
Philippines
Wallacea
New Guinea
Australia
Other
Sphenomorphus cranei RMB6889
Sphenomorphus cranei RMB6890
ti245659 Sphenomorphus maindroni
Sphenomorphus maindroni BPBM23196
Sphenomorphus maindroni BPBM23198
Sphenomorphus cf derooyae BPBM23608
Sphenomorphus cf derooyae BPBM23609
ti71019 Sphenomorphus leptofasciatus
ti172934 Sphenomorphus fasciatus
Sphenomorphus fasciatus CDS2693
Sphenomorphus fasciatus RMB9306
Sphenomorphus papuae FK8832
Sphenomorphus papuae FK8737
Sphenomorphus cinereus FK12472
Sphenomorphus cinereus FK12478
Sphenomorphus sp AA18035
Sphenomorphus fuscolineatus BPBM23201
Sphenomorphus fuscolineatus BPBM23202
Sphenomorphus nigriventris FK12496
Sphenomorphus nigriventris FK12542
Sphenomorphus solomonis RMB6895
Sphenomorphus solomonis RMB7071
Sphenomorphus scutatus CAS236398
ti245663 Sphenomorphus solomonis
Sphenomorphus nigrolineatus AA17808
Sphenomorphus nigrolineatus AA17837
Sphenomorphus solomonis AA17289
Sphenomorphus solomonis AA17496
Sphenomorphus forbesi BPBM15603
Sphenomorphus forbesi BPBM15605
Sphenomorphus forbesi AA17859
Sphenomorphus loriae FK8958
Sphenomorphus loriae FK9000
Sphenomorphus schultzei BPBM19661
Sphenomorphus schultzei BPBM19662
Sphenomorphus muelleri AA17395
Sphenomorphus muelleri FK8179
ti220793 Sphenomorphus muelleri
Sphenomorphus latifasciatus BPBM23187
Sphenomorphus latifasciatus FK13350
Sphenomorphus pratti FK12727
Sphenomorphus pratti BPBM23190
Sphenomorphus jobiensis AA17115
Sphenomorphus jobiensis AA17155
Sphenomorphus aruensis FK13358
ti127905 Sphenomorphus jobiensis
Sphenomorphus aruensis FK13299
Sphenomorphus meyeri BPBM23179
Sphenomorphus meyeri BPBM23180
ti245660 Sphenomorphus melanopogon
Sphenomorphus granulatus BPBM15617
Sphenomorphus granulatus BPBM18895
Sphenomorphus cf darlingtoni BPBM21290
Sphenomorphus darlingtoni CCA2541
Sphenomorphus concinnatus RMB6935
Sphenomorphus concinnatus RMB7070
Lipinia leptosoma
Lipinia leptosoma USNM531949
Sphenomorphus
Lipinia
Figure 2b
Figure 2d
Ophioscincus truncatus TWR
ti405196 Ophioscincus truncatus
ti220775 Coeranoscincus reticulatus
Saiphos equalis TWR
ti172942 Saiphos equalis
ti405185 Coeranoscincus frontalis
ti405198 Coggeria naufragus
ti220790 Ophioscincus ophioscincus
ti204902 Eulamprus murrayi
ti204907 Eulamprus tryoni
ti204900 Eulamprus luteilateralis
ti204896 Eulamprus brachysoma
ti204904 Eulamprus sokosoma
ti204901 Eulamprus martini
ti204906 Eulamprus tigrinus
ti204905 Eulamprus tenuis
Eulamprus amplus TWR
ti136854 Eulamprus amplus
Gnypetoscincus queenslandiae TWR
ti27796 Gnypetoscincus queenslandiae
ti204897 Eulamprus frerei
ti204910 Nangura spinosa
Calyptotis scutirostrum TWR
ti172936 Calyptotis scutirostrum
ti172938 Calyptotis lepidorostrum
ti172937 Calyptotis ruficauda
ti245595 Anomalopus verreauxi
ti405184 Anomalopus leuckartii
Anomalopus mackayi TWR
ti220772 Anomalopus mackayi
ti220773 Anomalopus swansoni
Notoscincus ornatus TWR
ti220788 Notoscincus ornatus
ti245649 Notoscincus wotjulum
Parvoscincus laterimaculatus RMB3346
Parvoscincus laterimaculatus RMB3504
Parvoscincus boyingi FMNH267561
Parvoscincus boyingi FMNH267664
Parvoscincus igorotorum ACD1150
Parvoscincus igorotorum RMB3169
Parvoscincus hadros MVD157
Parvoscincus hadros MVD158
Parvoscincus beyeri FMNH266118
Parvoscincus beyeri RMB3736
Parvoscincus luzonensis FMNH263506
Parvoscincus luzonensis RMB2203
Parvoscincus lawtoni ELR1123
Parvoscincus kitangladensis ACD4289
Parvoscincus kitangladensis ACD4290
Parvoscincus decipiens 4 ACD2233
Parvoscincus decipiens 4 ACD2423
Parvoscincus leucospilos ACD1777
Parvoscincus leucospilos RMB3759
Parvoscincus tagapayo ELR1391
Parvoscincus tagapayo RMB1871
Parvoscincus sisoni RMB700
Parvoscincus steerei7 RMB3563
Parvoscincus steerei7 RMB3996
Pinoyscincus jagori jagori4 CWL258
Pinoyscincus jagori jagori4 RMB1080
Pinoyscincus jagori grandis GVAG266
Pinoyscincus jagori grandis RMB3254
Pinoyscincus coxi divergens ACD925
Pinoyscincus coxi divergens ELR820
Pinoyscincus abdictus aquilonius10 CDS1142
Pinoyscincus abdictus aquilonius10 RMB3438
Pinoyscincus llanosi CWL140
Pinoyscincus llanosi CWL154
Pinoyscincus abdictus abdictus ACD2687
Pinoyscincus abdictus abdictus CWL260
Pinoyscincus coxi coxi ACD2685
Pinoyscincus coxi coxi RMB8125
Pinoyscincus mindanensis RMB1089
Pinoyscincus mindanensis RMB8455
Sphenomorphus diwata EMD368
Sphenomorphus diwata EMD428
Sphenomorphus acutus ACD3835
Otosaurus cumingi RMB808
Otosaurus cumingi RMB985
Ophioscincus
Coeranoscincus
Saiphos
Coeranoscincus
Coggeria
Ophioscincus
Eulamprus
Eulamprus
Gnypetoscincus
Eulamprus
Nangura
Calyptotis
Anomalopus
Notoscincus
Parvoscincus
Pinoyscincus
Sphenomorphus
Otosaurus

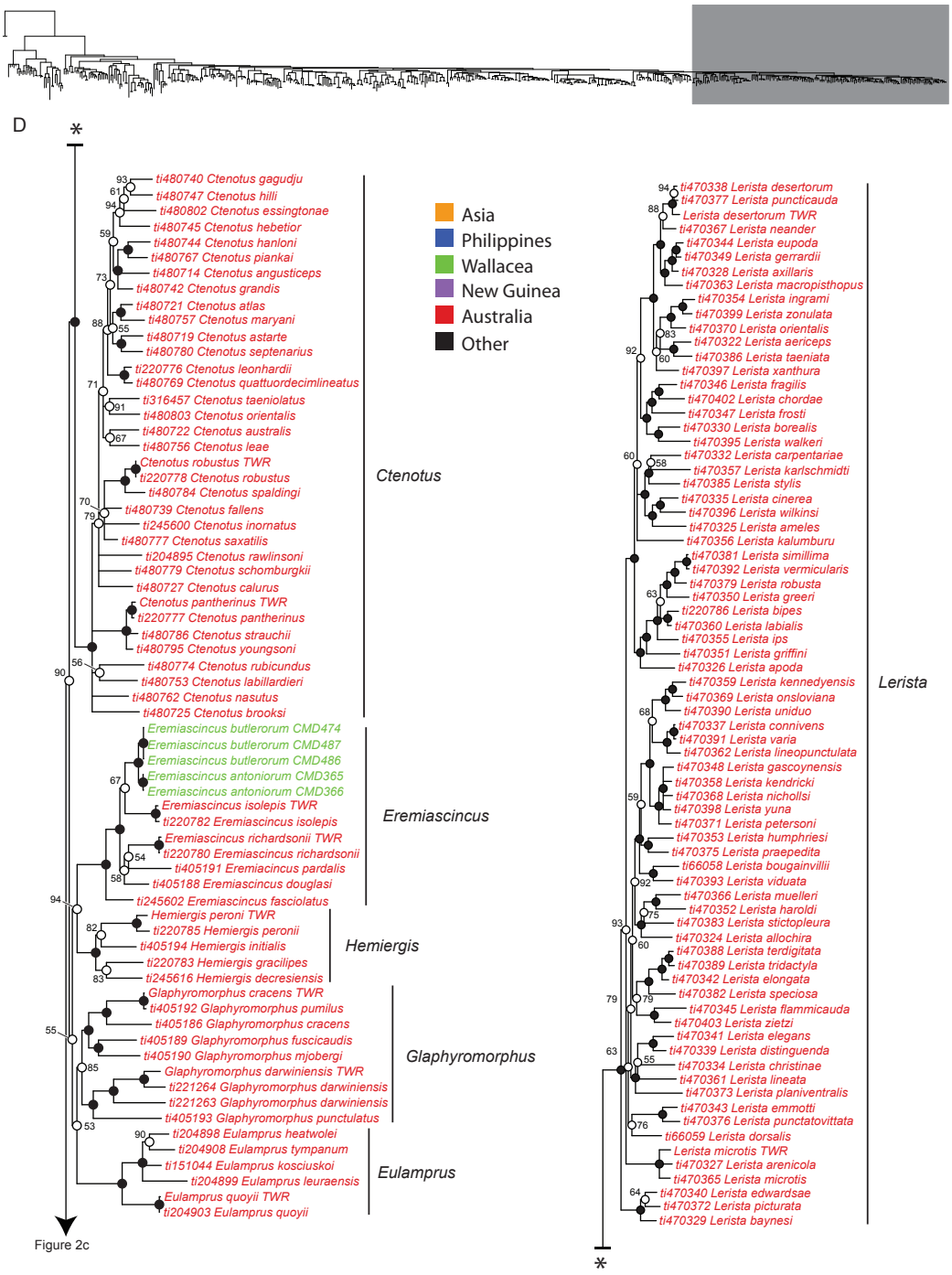
D
Asia
Philippines
Wallacea
New Guinea
Australia
Other
Ctenotus
Eremiascincus
Hemiergis
Glaphyromorphus
Eulamprus
Lerista
ti480740 Ctenotus gagudju
ti480747 Ctenotus hilli
ti480802 Ctenotus essingtonae
ti480745 Ctenotus hebetior
ti480744 Ctenotus hanloni
ti480767 Ctenotus piankai
ti480714 Ctenotus angusticeps
ti480742 Ctenotus grandis
ti480721 Ctenotus atlas
ti480757 Ctenotus maryani
ti480719 Ctenotus astarte
ti480780 Ctenotus septenarius
ti220776 Ctenotus leonhardii
ti480769 Ctenotus quattuordecimlineatus
ti316457 Ctenotus taeniolatus
ti480803 Ctenotus orientalis
ti480722 Ctenotus australis
ti480756 Ctenotus leae
Ctenotus robustus TWR
ti220778 Ctenotus robustus
ti480784 Ctenotus spaldingi
ti480739 Ctenotus fallens
ti245600 Ctenotus inornatus
ti480777 Ctenotus saxatilis
ti204895 Ctenotus rawlinsoni
ti480779 Ctenotus schomburgkii
ti480727 Ctenotus calurus
Ctenotus pantherinus TWR
ti220777 Ctenotus pantherinus
ti480786 Ctenotus strauchii
ti480795 Ctenotus youngsoni
ti480774 Ctenotus rubicundus
ti480753 Ctenotus labillardieri
ti480762 Ctenotus nasutus
ti480725 Ctenotus brooksi
Eremiascincus butlerorum CMD474
Eremiascincus butlerorum CMD487
Eremiascincus butlerorum CMD486
Eremiascincus antoniorum CMD365
Eremiascincus antoniorum CMD366
Eremiascincus isolepis TWR
ti220782 Eremiascincus isolepis
Eremiascincus richardsonii TWR
ti220780 Eremiascincus richardsonii
ti405191 Eremiascincus pardalis
ti405188 Eremiascincus douglasi
ti245602 Eremiascincus fasciolatus
Hemiergis peroni TWR
ti220785 Hemiergis peronii
ti405194 Hemiergis initialis
ti220783 Hemiergis gracilipes
ti245616 Hemiergis decresiensis
Glaphyromorphus cracens TWR
ti405192 Glaphyromorphus pumilus
ti405186 Glaphyromorphus cracens
ti405189 Glaphyromorphus fuscicaudis
ti405190 Glaphyromorphus mjobergi
Glaphyromorphus darwiniensis TWR
ti221264 Glaphyromorphus darwiniensis
ti221263 Glaphyromorphus darwiniensis
ti405193 Glaphyromorphus punctulatus
ti204898 Eulamprus heatwolei
ti204908 Eulamprus tympanum
ti151044 Eulamprus kosciuskoi
ti204899 Eulamprus leuraensis
Eulamprus quoyii TWR
ti204903 Eulamprus quoyii
ti470338 Lerista desertorum
ti470377 Lerista puncticauda
Lerista desertorum TWR
ti470367 Lerista neander
ti470344 Lerista eupoda
ti470349 Lerista gerrardii
ti470328 Lerista axillaris
ti470363 Lerista macropisthopus
ti470354 Lerista ingrami
ti470399 Lerista zonulata
ti470370 Lerista orientalis
ti470322 Lerista aericeps
ti470386 Lerista taeniata
ti470397 Lerista xanthura
ti470346 Lerista fragilis
ti470402 Lerista chordae
ti470347 Lerista frosti
ti470330 Lerista borealis
ti470395 Lerista walkeri
ti470332 Lerista carpentariae
ti470357 Lerista karlschmidti
ti470385 Lerista stylis
ti470335 Lerista cinerea
ti470396 Lerista wilkinsi
ti470325 Lerista ameles
ti470356 Lerista kalumburu
ti470381 Lerista simillima
ti470392 Lerista vermicularis
ti470379 Lerista robusta
ti470350 Lerista greeri
ti220786 Lerista bipes
ti470360 Lerista labialis
ti470355 Lerista ips
ti470351 Lerista griffini
ti470326 Lerista apoda
ti470359 Lerista kennedyensis
ti470369 Lerista onsloviana
ti470390 Lerista uniduo
ti470337 Lerista connivens
ti470391 Lerista varia
ti470362 Lerista lineopunctulata
ti470348 Lerista gascoynensis
ti470358 Lerista kendricki
ti470368 Lerista nichollsi
ti470398 Lerista yuna
ti470371 Lerista petersoni
ti470353 Lerista humphriesi
ti470375 Lerista praepedita
ti66058 Lerista bougainvillii
ti470393 Lerista viduata
ti470366 Lerista muelleri
ti470352 Lerista haroldi
ti470383 Lerista stictopleura
ti470324 Lerista allochira
ti470388 Lerista terdigitata
ti470389 Lerista tridactyla
ti470342 Lerista elongata
ti470382 Lerista speciosa
ti470345 Lerista flammicauda
ti470403 Lerista zietzi
ti470341 Lerista elegans
ti470339 Lerista distinguenda
ti470334 Lerista christinae
ti470361 Lerista lineata
ti470373 Lerista planiventralis
ti470343 Lerista emmotti
ti470376 Lerista punctatovittata
ti66059 Lerista dorsalis
Lerista microtis TWR
ti470327 Lerista arenicola
ti470365 Lerista microtis
ti470340 Lerista edwardsae
ti470372 Lerista picturata
ti470329 Lerista baynesi

Figure 2c

Figure 3.2 Molecular phylogeny from PhyloBayes for the 525-sample dataset. Taxon names are color coded to match biogeographic range in Figure 3.1. Nodes with > 95% posterior probability are black circles; nodes < 95% have white circles and the posterior probability shown. An asterisk next to the taxon name indicates the positions of multiple samples with the same identification coming out in different places in the tree.

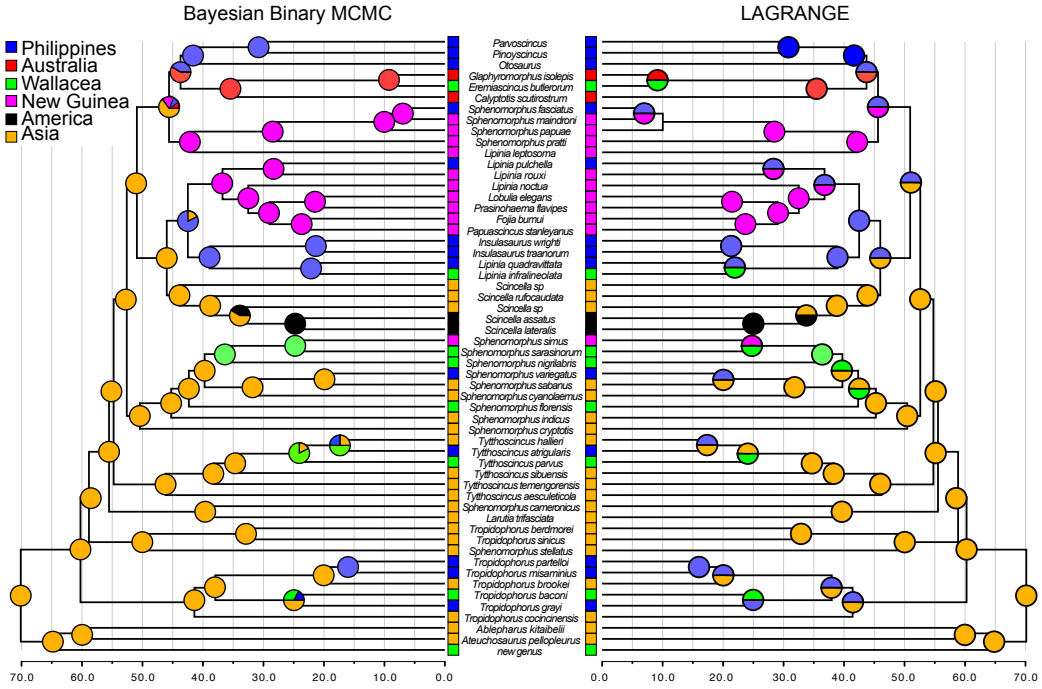

Figure 3.3 For BBM the pie charts represent the percent probability of that area being the ancestral area, which was ~ 100 for many of the nodes. In LAGRANGE, ancestral areas are inferred to be single areas or shared areas. If the ancestral area is shared, then it is shown with a half circle for each of the shared regions. The analysis was limited to two ancestral areas per node, which is why the nodes only have half circle splits or full circles. Nodes with an asterisk had a probability less than 0.95 for the preferred ancestral area, the color of the asterisk represent the other area inferred.

CHAPTER 4

Colonization of Sulawesi through dispersal and/or vicariance: parameterization of the molecular Clock in BEAST

Wallacea is a region of islands between the Asian and Australian continental plates (Dickerson et al. 1928) bordered to the north by the Philippines (Heaney et al. 2005). Sulawesi is the largest and most geologically complex island in Wallacea (Wallace 1863, Hall 2001) with a diverse endemic fauna. The majority of the fauna on Sulawesi is of Asian origin (Sarasin and Sarasin 1901; Whitmore 1987; Whitten et al. 2002), which is consistent with its closer geographic proximity to the Asian continent. Wallacea is the center of collision between the Asian and Australian continental plates, which have been coming together since the Miocene. Sulawesi is a composite island at the center of this collision zone formed by the coalescence of multiple continental and volcanic blocks of land (Hall 2009). During the late cretaceous (> 65 mya), western Sulawesi was connected to the Asian plate until rifting led to the Makassar Strait, which separated western Sulawesi from Asia in the Eocene (~ 45 mya) (Fig. 1: Hall 2009). This geologic scenario for the history of western Sulawesi offers the theoretical possibility of a vicariant origin of taxa from the Asian continent on Sulawesi (Fig. 1: Hall 2009; 2011; Spakman and Hall 2010).

A recent study by Stelbrink et al. (2012) compared the biogeographic relationships of 20 different taxa that occur on Sulawesi, combining new geological evidence with divergence time estimation to determine if there is evidence for a vicariant origin of taxa on Sulawesi. Due to a lack of congruence

between divergence time and geologic history they inferred that 80% of the taxa studied dispersed to Sulawesi. The divergence times in two taxa, mite harvestman and water beetles, could not reject a hypothesis of vicariance. Additionally, they inferred that speciation on Sulawesi did not occur prior to the Miocene (< 25 mya), which coincides with an increase in island size from collisions of other blocks of land (Hall, 2009) and changes in climate related to mid-Miocene sea-level lowstands (De Graciansky et al. 1998). The study of Stelbrink et al. (2012) provides compelling evidence for the history of Sulawesi biodiversity, but may not represent the history of all groups. The results of their study rely on the estimation of divergence times from molecular data without fossil calibrations and with limited exploration of model parameterization, which could lead to improper estimation of time. With these limitations in mind, we explore the biogeographic origins of two endemic clades of scincid lizards on Sulawesi under a variety of divergence time estimation models to estimate whether divergence times in the clades are consistent with dispersal or vicariance and what effect model parameterization has on diversification time.

SULAWESI FOREST SKINKS

Previous examinations of forest skinks in Southeast Asia (Linkem et al. 2011; Chapter 3) found there are two clades on Sulawesi. Divergence time analyses of the Sphenomorphini in Chapter 3 found that *Tytthoscincus* and *Sphenomorphus* colonized Sulawesi around 25 and 35 mya respectively, which is older than many of the taxa in Stelbrink et al. (2012) but consistent with their predictions. The divergence time analysis in Chapter 3 required reducing the parameterization of the clock model and molecular rate variation in order to get convergence between

runs, which may affect divergence time estimation. To establish a more rigorous estimate of the divergence times for Sulawesi *Tytthoscincus* and *Sphenomorphus* we sampled additional species from Sulawesi Island and the neighboring regions of Indochina, Papua New Guinea, and the Philippines. We then sought to address the following questions: 1) What is the time of colonization and subsequent diversification of these lineages on Sulawesi? 2) Is the timing of colonization consistent with dispersal or vicariance? 3) Did species diversification predate the Miocene?

Materials and Methods

Taxon Sampling and Molecular Data Collection

During multiple expeditions to Sulawesi, collections of forest skinks were made representing almost all of the 10 known species of *Tytthoscincus* and *Sphenomorphus* on the island. Two high elevation species (*Sphenomorphus zimmeri* and *Sphenomorphus celebense*) are still unsampled. A number of unique lineages were also discovered that represent new species. We include samples of the described and undescribed species on Sulawesi to estimate the timing of colonization and diversification on the island. Sampling from other regions includes species from the Philippines, Borneo, Indochina, and Papua New Guinea based on relationships in Chapter 3. Outgroups from the *Eugongylus* group (*Emoia* and *Oligosoma*) are included to aid in divergence time analyses.

The mitochondrial genes 12s, 16s, ND2, and ND4, as well as the nuclear genes ADNP, NGFB, PTGER4, R35, and MKL1 were sampled for all Sulawesi lineages. Many of the sequences are from Chapter 3, with samples of Sulawesi

lineages added. All genes were amplified from genomic DNA using primers in Chapter 3. Sequencing was performed on an ABI 3730 automated capillary sequencer. Individual chromatograms were annotated and assembled in Sequencher v4.8, grouped by gene region and aligned using MAFFT v6.717b (Katoh et al. 2005). Protein coding genes were transformed into protein sequence to verify coding frame alignment and ensure genes are not pseudocopies using the program Se-Al v2.0a11 (http://tree.bio.ed.ac.uk/software/seal). Genes were concatenated using a Python script available on github. The concatenated data matrix was used for all analyses and is available on the Dryad data repository (http://www.datadryad.org).

Model Selection and Data Partitioning for Bayesian Phylogenetic Analyses

The final dataset of 94 taxa consists of four mitochondrial and five nuclear genes with 6394 base-pairs of DNA. Identification of the optimal molecular evolutionary model for each data partition used the Akaike information criterion (AIC) as implemented in the program MrModelTest v2.3 (Nylander 2004). Five different partitioning strategies were run based on different combinations of codon positions and genes. Each partitioning strategy was run in parallel MrBayes v3.2.1 (Huelsenbeck and Ronquist 2001) for 50 million generations sampling every 5000 generations. Parameters for the Markov Chain Monte Carlo (MCMC) chain heating and swapping were left default. Among partition rate variation was set to variable to account for different rates of evolution between partitions and the prior for the branch lengths was adjusted to exponential base 100 (Marshall et al. 2006; Marshall 2010). Convergence of the posterior distribution was assessed

using Tracer v1.5 (Rambaut and Drummond 2007) and Are We There Yet (AWTY: Wilgenbusch et al. 2004; Nylander et al. 2007). The harmonic mean of the posterior distribution of log likelihoods for all partitioning strategies were compared using the Bayes Factor in Tracer v1.5 under both the log base 10 and natural log. The partitioning strategy with the fewest parameters not rejected by Bayes Factors from the more parameter rich models was chosen as the optimal model.

Divergence Time Estimation

Terminology.—In divergence time analyses there are multiple clocks and rates that can be adjusted and it is important that terminology is consistent to reduce confusion. Here are explanations of the terminology used in this paper.

Rate calibrated: molecular clock calibrated with a prior rate of evolution based on a previous study or rate estimated on another group.

Fossil calibrated: molecular clock calibrated by using a fossil in the analysis to place a constraint on the age of the tree. The molecular clock is estimated from the data, the other rate parameters and the fossil calibrations.

Strict clock: a strict molecular clock assumes an equal rate of evolution over every branch of the tree. In this study the strict clock is either rate calibrated or fossil calibrated.

UCLN clock: uncorrelated relaxed lognormal molecular clock allows for a different rate of molecular evolution on each branch and rates are not correlated with ancestors. In this study the UCLN clock is either rate calibrated or fossil calibrated.

Linked clock: separate partitions of data that have their own rate variation model (i.e. GTR + G) but share a single molecular clock. When linking clocks we use a rate multiplier between partitions to allow for among partition rate variation.

Calibration Choice: Fossil or Rate.—Estimating divergence time without a fossil record for the ingroup taxa is not a trivial task. The closest fossil to the Sphenomorphini is found in the Eugongylini, a diverse sister clade. In the Eugongylini, there are fossils of *Oligosoma* on New Zealand dated to 16 mya, which places a minimum age on the origin of the New Zealand *Oligosoma* clade (Lee et al., 2009). This fossil was used in Chapter 3 as an external calibration to the Sphenomorphini. The use of only external fossil calibrations (fossil not within the ingroup) has not been thoroughly explored in the literature, though the use of improper calibration is known to be a problem (Graur and Martin, 2004). An alternative approach suggested by Near et al. (2011) is to use the outgroup fossil to estimate the clock rate in the outgroup clade, in this case the Eugongylini, and then use this rate to calibrate the molecular clock in the ingroup, assuming that there is not a rate shift between the groups. Both of these possibilities were explored by running all analyses of divergence time with either the fossil calibration or the rate calibration from a separate analysis of the Eugongylini.

Estimated clock from Eugongylini fossil.—To get an estimate of the rate for the mitochondrial molecular clock for the Eugongylini, 12s, 16s, ND2, and ND4 data were downloaded from Genbank for the genera *Oligosoma*, *Carlia*,

Cyclodinia, *Eugongylus*, and *Emoia*. The taxon sampling was chosen to be inclusive of the diversity in the Eugongylini and resulting in the *Oligosoma* clade being well nested. The fossil *Oligosoma* was used to place a minimum constraint on the crown *Oligosoma* clade at 16 mya. The dataset for divergence time analysis was prepared in BEAUTI v1.6 (Drummond and Rambaut 2007) and run in BEAST v1.6 (Drummond and Rambaut, 2007). Two different clocks were used, an UCLN clock and a strict clock to see which fit the data better and if the clock rate was robust to different clock parameters. The xml code from BEAUTI was changed to add rate multiplier parameters between the mitochondrial genes. The use of rate multipliers was shown to be important for proper estimation of branch lengths in Bayesian Phylogenetic analyses (Marshall et al. 2006). The use of rate multipliers between genes has not been implemented in BEAUTI, but adding them to the xml code is straightforward. The effect of rate multipliers is explored more below. Analyses with each type of clock were run two times to ensure convergence in all parameters, and topologies. The estimate of molecular clock rate from the posterior distribution of trees was used as the molecular clock distribution for the Sphenomorphini.

Linked Clocks or Unlinked Clocks

It is well established that different genes, or subsets within genes, have different rates of evolution and that accounting for rate variation is critical to accurate estimation of phylogeny (Yang 1996). This rate variation can be accommodated by partitioning the data into different rate categories, typically by different genes and/or codon positions within protein coding genes (Brandley et al. 2005). Properly accounting for the variations in rate within the data are critical

to the proper estimates of branch lengths, and subsequently divergence time (Drummond et al. 2006). In divergence time analyses, in addition to the partitioning of data, substitution rate parameters, and gamma rate variation parameters, there are also clock parameters which estimate the rate either over the whole tree (strict clock) or over each individual branch (UCLN clock). Additionally, data partitions can either have linked or unlinked clocks, with separate clocks for each partition. The choice between using linked or unlinked clocks and the effect on estimation of divergence time has not been explored. The dataset used herein has 4 mitochondrial genes and 5 nuclear genes that can be partitioned in a variety of different ways to account for rate variation.

To evaluate the difference in divergence time estimation under different clock parameterizations, multiple parameter setting were used in BEAUTI. The DNA data was partitioned by gene and each gene was assigned the HKY + G model of sequence evolution. These parameters were kept the same for all clock variations to standardize the number of partitions and rate model between analyses. Clocks were linked in three different ways, all genes linked under one clock, mitochondrial genes linked and nuclear genes linked for two clocks, or mitochondrial genes linked and each nuclear gene with its own clock for 6 clocks. Clocks were either strict clocks or UCLN clocks. When clocks were linked between genes, rate multipliers were used to allow for rate variation between genes, within the clock. When using the rate calibrated clock the rate from the Eugongylini was used as the prior distribution of the mean rate for the mitochondrial data set as a normal distribution (mean = 0.0067; standard deviation 7.04 E-4) and all other clocks were estimated from the data.

Comparing Divergence time parameterization in BEAST

The dataset was parameterized using the combinations of parameters mentioned above, resulting in 12 different types of analyses. Each parameterization of the data was run 6 independent times using BEAST v1.6 for 30 million generations, sampling ever 4000 generations. Chain convergence of the posterior distribution was assessed using Tracer v1.5, ensuring estimated sample sizes were > 200. Runs that converged were combined using LogCombiner. Comparisons of likelihood scores and root node ages were made in Tracer. Posterior distributions of trees were compared between runs with AWTY to assess the effect of rate parameterization on tree topology.

Results

Bayesian Phylogenetic Analyses and Partitioning Choice

Analyses were run with 9, 13, 16, 18, and 23 partitions. Each partition was run with the optimal model of evolution, GTR + G, based on the results of MrModelTest. Convergence of the posterior distribution for the independent runs was assessed in TRACER and AWTY. Parameters for all analyses converged after 1.0×10^6 generations and were combined using the sump and sumt commands in MrBayes 3.2. Bayes Factor comparisons found that the p23 partitioning strategy was marginally preferred over the other strategies (Table 4.1) when using the natural log BF. The posterior distributions of topologies for each partitioning scheme converged and the topologies between the 18 and 23 partition runs

converged. The 18 partition model was chosen as optimal and phylogenetic relationships are based on this tree (Fig. 4.2).

Phylogenetic relationships

Our estimate of phylogeny is consistent with relationships estimated in Chapter 3 (Fig 4.2). Increased taxon sampling within the Sulawesi *Tytthoscincus* has changed some species relationships within Sulawesi taxa from Chapter 3, though many of the basal nodes in the clade are poorly supported. Sulawesi *Tytthoscincus* is well support with *T. atrigularis* and *T. hallieri* nested within the Sulawesi radiation. *Tytthoscincus sibuensis* is poorly supported (posterior probability = 65) as the sister taxon to the Sulawesi radiation, similar to the phylogeny in Chapter 3. Ancestral area reconstruction for the MRCA of Sulawesi *Tytthoscincus* (Node B) estimates the ancestral area to be Sulawesi with 98% posterior probability.

Sulawesi *Sphenomorphus* species are strongly supported as a clade and are nested within the Asian *Sphenomorphus* radiation similar to estimates in Chapter 3. *Sphenomorphus simus* from Papua New Guinea is sister to *Sphenomorphus sarasinorum,* nested within the Sulawesi radiation. Ancestral area reconstruction of the MRCA of Sulawesi *Sphenomorphus* (Node E) estimates the ancestral areas to be Sulawesi with 98% posterior probability. Six nodes in Figure 2 labeled A–F are discussed in detail in relation to divergence time estimation and colonization of Sulawesi.

Eugongylini diversification rate

Broad sampling of the Eugongylini was accomplished using data found on Genbank. A lognormal prior on the age of the *Oligosoma* clade with a minimum age of 16 million years was used to calibrate the analyses. The analyses were run under a strict clock with a uniform prior U[0,4] and a relaxed clock with a uniform prior U[0,4]. The molecular rates from these analyses were pulled from the posterior distributions of the clock rate parameters, which were largely overlapping. The strict clock estimated a mean rate of 0.00639 (range 0.00536–0.00718) and the UCLN clock estimated a mean rate of 0.00686 (range 0.00577–0.00838). For analyses of the Sphenomorphini a clock spanning the range from both the strict clock estimate and UCLN clock estimate was used.

Divergence Time Analyses in BEAST

Model Selection.—We used the 18 partition model and optimal model of evolution for each partition, GTR + G, for preliminary divergence time analyses in BEAST. These analyses did not converge after 50 million generations and 6 independent runs and many of the parameters had insufficient effective sample sizes. Parameterization was reduced to partitioning by gene (9 partitions) and using the HKY + G model for each data subset and convergence was achieved. This parameterization was used for subsequent analyses and for testing clock parameters.

Fossil calibrations or rate calibration.—Analyses of the dataset in this study were completed under a variety of different clock models that are typically used in divergence time estimation. Because there is no prior information that would help direct which set of clocks or calibrations are most appropriate,

explorations of all were performed. In total, we ran 12 different sets of analyses with varying parameterizations including strict clocks or uncorrelated log normal clocks, linked clocks versus unlinked clocks, and fossil calibrations versus rate calibration.

Despite rejecting a strict molecular clock in PAUP*, we ran analyses with strict clocks in comparison to analyses with uncorrelated lognormal (UCLN) clocks. Comparison of likelihood scores (Figure 4.3) shows that UCLN clocks have a much higher likelihood than strict clocks and are preferred when compared using Bayes Factors (Table 4.2). All combinations of strict clocks with either linked or unlinked clocks between genes (1 clock, 2 clocks, 6 clocks) result in the same likelihood distribution (Figure 3). Within the UCLN clock models, six unlinked clocks are preferred over a single linked clock or two unlinked clocks with rate multipliers (Table 4.2).

Using an external fossil as calibration results in a more consistent estimate of divergence time across alternative rate parameterizations (Figure 4.4A, B). All UCLN clocks and the strict clocks resulted in a similar distribution of root node heights when the fossil calibration was used. The strict clocks have a narrower posterior density than the UCLN clocks. When using the rate calibration from the fossil in the Eugongylini, the estimate of the root node height was highly affected by the clock model chosen (Figure 4.4C, D). A single linked clock estimated the root node age younger than the other estimates, either with a UCLN clock or strict clock, and younger than analyses using the fossil directly (Fig. 4.4). The use of two linked clocks estimated a root node age slightly older than the fossil calibrated UCLN clock and older than the strict clock. The use of six unlinked

strict clocks gave the same root node age estimate as using two unlinked strict clocks (Fig. 4.4D), but drastically overestimated the root age when using UCLN clocks (Fig. 4.4C). The age estimated with six UCLN clocks is older than the age of squamates. Another analysis was performed with a prior on the root node age consistent with the study of Skinner et al. (2011) for the two unlinked and six unlinked UCLN clock analyses. The posterior distribution of the age of the root node for the two unlinked clock analysis matched the prior distribution of the root node. The posterior distribution for the age of the root node for the six unlinked UCLN clocks analysis still diverged older than the prior, though was more consistent with the prior. Based on comparison of the distribution of the likelihood in each of these different analyses, the six unlinked UCLN clocks model without the root node prior has the highest likelihood with either a fossil calibration or rate calibration. The rate calibration analysis gave the most unrealistic set of divergence times and the fossil calibrated analysis gave times consistent with other studies (Skinner et al. 2011).

Estimation of Topology in BEAST

We compared the posterior distributions of topologies for strict clocks, UCLN clocks, linked clocks, unlinked clocks, fossil calibrated clocks, and rate calibrated clocks in AWTY using the compare function. The compare function plots the frequency of splits between two different posterior distributions. If the runs converge then the split frequencies will line up along a diagonal from 0 to 100.

When using fossil calibrations or molecular clock calibrations, choosing between linked and unlinked clocks will result in slightly different posterior distributions of topology (Figure 4.5). The compare plots show spread away from the diagonal, indicating that the posterior distribution of trees did not converge between runs. Many split frequencies are similar, especially when split frequency is high (above 90) or low (below 10). Comparison of maximum clade credibility trees across runs shows that the differences are between some basal nodes that have short internodes.

Posterior estimation of topology was also significantly different when using a strict clock or UCLN clock (Fig. 4.6). This was the case whether calibrating using a rate or a fossil (Fig. 4.6). There are many splits sharing similar frequencies when strongly supported (above 90), but there are also a lot of splits with high frequency using a strict clock and absent using a UCLN clock and vice-versa. Strong support for nodes that are absent in other analyses are prevalent throughout different linked or unlinked clocks and different calibration strategies (Fig. 4.6).

Topologies are much more similar between the use of a fossil calibration and a rate calibration (Fig. 4.7). When using 6 unlinked UCLN clocks the use of a fossil versus a molecular rate results in very similar topology estimates. The difference in topology estimates is greatest when using two unlinked UCLN clocks, where there are multiple high frequency nodes that are absent in the other calibration type. Using one linked UCLN clock results in very similar topology estimates between calibration types, though there are three nodes that have high

frequency in one calibration analysis but are absent in the other (Fig. 4.7). Strict clocks have the same topology estimation regardless of calibration used (Fig. 4.8).

Linked Clocks or Unlinked clocks

Bayes factor comparisons give strong support to the 6 unlinked UCLN clock model with either the fossil or clock calibration (Table 4.2). The 6 unlinked UCLN clock model with clock calibration gave the most unrealistic divergence times (Fig. 4.4). The date of the root node (Lygosominae) has a mean age of 257 mya, which is older than the estimated age of all skinks and most Squamates. All other relaxed clock estimates of the root node age, either using the fossil calibration or molecular rate, were at a more realistic mean between 99 and 111 mya, which overlaps with previous estimates of Lygosominae divergence times. The use of the fossil calibration with the 6 unlinked UCLN clocks gave the highest likelihood and consistent estimates of divergence time (Skinner et al. 2011).

Dating the colonization of Sulawesi

All analyses show that Sulawesi was colonized by two different clades of forest skinks. The timing of these arrivals varies depending on the calibration and clock model choice. The mean age and 95% highest posterior densities for Nodes A–F were calculated in sumtrees.py (Table 4.3). Different clock parameterizations result in maximum timing of Sulawesi colonization (Nodes A and D) between 26.9–70.2 mya and minimum timing of Sulawesi colonization (Nodes B and E) between 24.3–63.9 mya, not including the uncertainty among trees in the 95%

highest posterior density of node ages. Diversification on Sulawesi (Nodes C and F) occurred between 17.5 and 47 mya depending on the clock model used. Proper parameterization of the clock models is critical to interpreting the history of colonization of these clades on Sulawesi.

Discussion

Colonization of Sulawesi: Dispersal or Vicariance

Our results show that *Sphenomorphus* and *Tytthoscincus* skinks colonized Sulawesi from Asia during times that are estimated to overlap. Whether we can interpret this colonization event as vicariance or dispersal depends on which parameterization of the data we choose to use. In this case, the model with six unlinked UCLN clocks has the highest likelihood and should therefore be preferred over other models. The likelihoods for analyses with a fossil calibration or rate calibration were identical (Fig. 4.3) but the differences in divergence times were large (Fig. 4.4; Table 4.3). Node ages when using the rate calibration were twice as old as when using the fossil calibration for the six unlinked UCLN clock model (Table 4.3). Because the ages from the molecular rate analysis are unrealistic, we use the six unlinked UCLN clock model with fossil calibration as the preferred estimate of divergence time (Fig. 4.9).

The maximum ages for the origin of the Sulawesi *Tytthoscincus* and Sulawesi *Sphenomorphus* have a mean of 30.7 and 32.0 mya respectively, which are both younger than the estimated timing of the rifting that separated the Sulawesi block from the Sunda Shelf (Hall 2009). If we take the 95% highest posterior density into account then we cannot reject the possibility that

colonization of Sulawesi was through vicariance in both genera. Diversification on Sulawesi started 21 [10–35] and 18 [7.6–29] mya for *Tytthoscincus* and *Sphenomorphus* respectively. This coincides with the estimates of Stelbrink et al. (2012) for diversification increasing on Sulawesi during the Miocene as the island increased in area from coalescence of land and sea-level lowering. These results rely on complete sampling of the diversity in each of the clades to ensure that the inferred ancestral node is the most recent common ancestor of all the species and not just a subclade. Despite missing a few known species in the *Sphenomorphus* clade, our taxon sampling is robust and we do not expect the most recent common ancestor of the Sulawesi clades to be pushed back farther in the tree. Both the *Tytthoscincus* and *Sphenomorphus* clades have a long branch before diversification on the island, with the *Sphenomorphus* branch being longer. Diversification on Sulawesi, once started, proceeded fairly quickly with multiple branches diversifying early in the radiation (Fig. 4.9).

The Link Between Clocks and Topology

The results of these various analyses show that the choice of clock, calibration, and linking of clocks not only can affect the estimation of branch lengths, and subsequently divergence time (Fig 4.4; Table 4.3), but also affects the estimation of topology (Figs. 4.5–4.8). It is therefore critical that one explores multiple sets of parameters to ensure that their results are robust. If you reject the strict clock you should not use it since the results here show that the topology can be very different than if using a UCLN clock. Brown and Yang (2011) found that for recent lineages the strict clock outperforms the UCLN clock and should be

used if not rejected. Our results show that the strict clock is very robust to variation in parameter settings in consistent estimates of likelihood, divergence times, and topology, but is outperformed by UCLN clocks for this dataset. The affect of other clocks (correlated lognormal, random clocks) on topology estimation also need to be explored and is an avenue of necessary future research.

Conclusions

Our results show that model choice in divergence time estimation is an important consideration that can affect estimates of node ages as well as estimates of topology. We recommend that researchers explore multiple clocks and partitions to ensure that rate variation is accurately accommodated. This may not be trivial for large datasets, such as Chapter 3, where analyses with more parameters do not converge between runs. It is clear that more testing for the effect of model parameterization in divergence time analyses is needed.

Table 4.1 Bayes factor comparison among different partitioning strategies run in MrBayes.

Partitioning strategy	P9	P13	P16	P18	P23
P9	—				
P13	1106.67	—			
P16	1289.60	182.93	—		
P18	1565.10	458.44	275.50	—	
P23	1581.23	474.56	291.63	16.13	—

Table 4.2 Bayes Factor comparison between different clocks and calibrations. The 6 UCLN clock is preferred (gray highlight) and is significantly better than other clocks.

	Ln likelihood	1 UCLN Fossil	1 UCLN Rate	1 Strict Fossil	1 Strict Rate	2 UCLN Fossil	2 UCLN Rate	2 Strict Fossil	2 Strict Rate	6 UCLN Fossil	6 UCLN Rate	6 Strict Fossil	6 Strict Rate
1 UCLN Fossil	-89058.432	—	5.494	124.019	124.429	-202.959	-209.441	124.366	124.444	-242.243	-241.788	124.467	124.438
1 UCLN Rate	-89071.082	-5.494	—	118.525	118.935	-208.453	-214.935	118.872	118.95	-247.737	-247.282	118.973	118.944
1 Strict Fossil	-89343.997	-124.019	-118.525	—	0.41	-326.978	-333.46	0.347	0.424	-366.262	-365.807	0.447	0.419
1 Strict Rate	-89344.94	-124.429	-118.935	-0.41	—	-327.388	-333.869	-0.063	0.015	-366.672	-366.216	0.038	0.009
2 UCLN Fossil	-88591.102	202.959	208.453	326.978	327.388	—	-6.482	327.325	327.402	-39.284	-38.829	327.425	327.397
2 UCLN Rate	-88576.177	209.441	214.935	333.46	333.869	6.482	—	333.807	333.884	-32.802	-32.347	333.907	333.878
2 Strict Fossil	-89344.796	-124.366	-118.872	-0.347	0.063	-327.325	-333.807	—	0.077	-366.609	-366.154	0.1	0.072
2 Strict Rate	-89344.974	-124.444	-118.95	-0.424	-0.015	-327.402	-333.884	-0.077	—	-366.687	-366.231	0.023	-0.006
6 UCLN Fossil	-88500.647	242.243	247.737	366.262	366.672	39.284	32.802	366.609	366.687	—	0.455	366.71	366.681
6 UCLN Rate	-88501.695	241.788	247.282	365.807	366.216	38.829	32.347	366.154	366.231	-0.455	—	366.254	366.225
6 Strict Fossil	-89345.027	-124.467	-118.973	-0.447	-0.038	-327.425	-333.907	-0.1	-0.023	-366.71	-366.254	—	-0.029
6 Strict Rate	-89344.961	-124.438	-118.944	-0.419	-0.009	-327.397	-333.878	-0.072	0.006	-366.681	-366.225	0.029	—

Table 4.3 Median node ages and 95% highest poster for nodes A–F in Figure 4.2 & 4.9.

	Node-A	Node-B	Node-C	Node-D	Node-E	Node-F
1UCLN fossil	51.6 [33.6–75.5]	45.9 [30–67.3]	35.2 [23–51]	52.4 [34.6–75.4]	48.4 [31.8–69.8]	31.2 [20.2–45.6]
1UCLN rate	29.6 [22.4–37.3]	25.1 [19–32.1]	19.5 [14.9–24.7]	29.2 [21.9–36.9]	27.1 [20.2–34.3]	17.5 [12.8–22.5]
1 strict fossil	53.9 [46.5–63.8]	48.7 [41.8–57.6]	36.1 [31.1–42.7]	55.5 [47.8–65.4]	52.5 [45.1–61.9]	31.6 [27.1–37.4]
1 strict rate	26.9 [21.5–33.1]	24.3 [19.2–29.8]	18.0 [14.3–22.0]	27.7 [21.9–33.7]	26.1 [20.8–32.0]	18.9 [12.5–19.3]
2 UCLN fossil	48.6 [26.4–72.4]	44.1 [24.3–66.9]	34.4 [19.2–50.9]	49.5 [28.6–74.7]	45.8 [26.2–69.1]	29.8 [15.9–44.9]
2 UCLN rate	64.1 [48.0–81.7]	54.3 [40.2–69.2]	41.8 [31.5–52.7]	61.6 [47–78.1]	57.4 [43.1–72.8]	35.8 [25.9–46.6]
2 srict fossil	53.7 [44.4–64.0]	48.5 [40.1–57.8]	35.9 [29.6–42.8]	55.3 [45.7–65.7]	52.3 [43.3–62.3]	31.4 [25.8–37.5]
2 strict rate	56.1 [44.5–68.7]	50.8 [40.6–62.3]	37.6 [29.8–46.0]	57.8 [46.1–70.9]	54.7 [43.1–66.6]	32.9 [26.2–34.4]
6 UCLN fossil	30.7 [13.7–50.6]	25.4 [11.7–41.8]	21.4 [10.0–35.7]	32.0 [14.3–52.1]	29.0 [12.9–47.6]	17.9 [7.6–29.5]
6 UCLN rate	67.3 [48.2–86.4]	55.7 [40.5–72.8]	47.0 [34.7–61.3]	70.2 [51.1–90.6]	63.9 [47.1–82.9]	39.5 [27.7–52.5]
6 strict fosil	52.0 [43.3–61.2]	46.9 [38.9–55.1]	34.9 [29.3–41.1]	53.6 [44.9–62.7]	50.7 [42.6–59.7]	30.5 [25.3–35.8]
6 strict rate	53.8 [43.7–65.8]	48.6 [38.9–58.8]	36.1 [29.1–43.7]	55.4 [45.0–67.2]	52.4 [42.6–63.8]	31.5 [25.1–38.1]
Comment	Maximum origin of Sulawesi *Tythoscincus*	Minimum origin of Sulawesi *Tythoscincus*	MRCA of Sulawesi radiation	Maximum origin of Sulawesi *Sphenomorphus*	Minimum origin of Sulawesi *Sphenomorphus*	MRCA of Sulawesi radiation

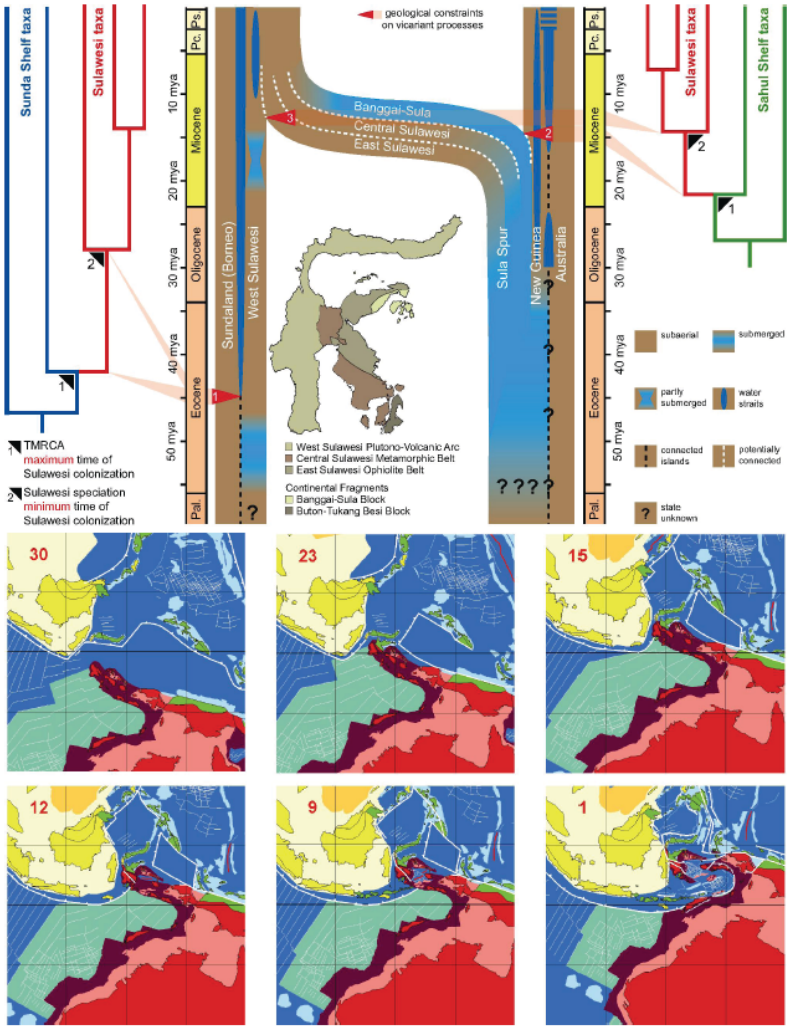

Figure 4.1 Geological reconstruction and predictions of timing for vicariance from Stelbrink et al. (2012). The phylogeny on the left denotes the expectations of divergence time for vicariance from Asia. The brown denotes land and the blue water. The reconstruction shows that western Sulawesi was connected to Asia up until the opening of the Makassar straight (red arrow 1), after which dispersal would be required to colonize Sulawesi. The lower six maps show paleo-reconstructions of island extent and position for the last 30 million years.

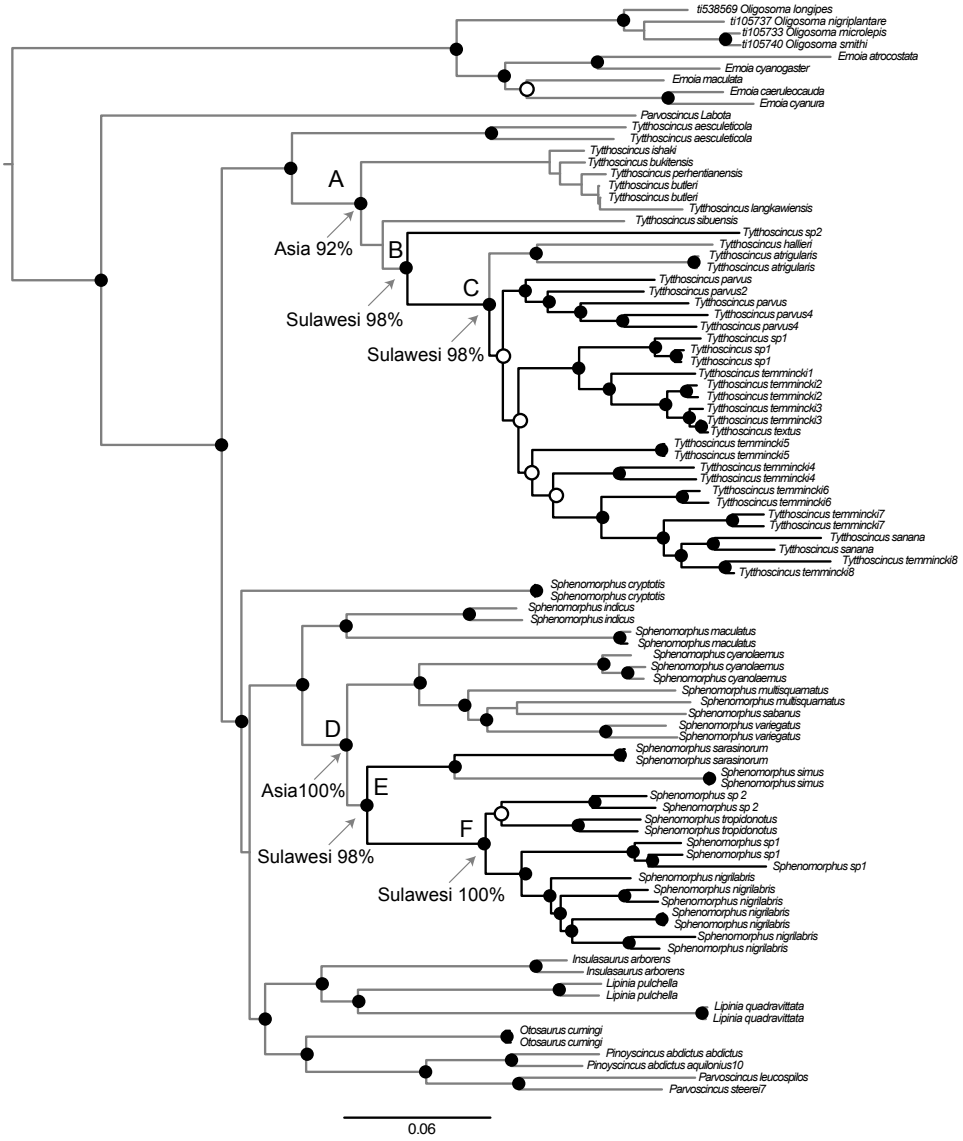

Figure 4.2 Partitioned Bayesian majority rule consensus estimate of molecular phylogeny from the 18 partition model. Node posterior probabilities above 0.95 are black circles and below 0.95 are open circles. Nodes A and D are the maximum time of Sulawesi colonization (unsampled stem lineage) and nodes B and E are the minimum time of Sulawesi colonization. Nodes C and F represent the most recent common ancestor of all Sulawesi species. Ancestral area reconstructions for these nodes are labeled with the probability of the reconstructed Area.

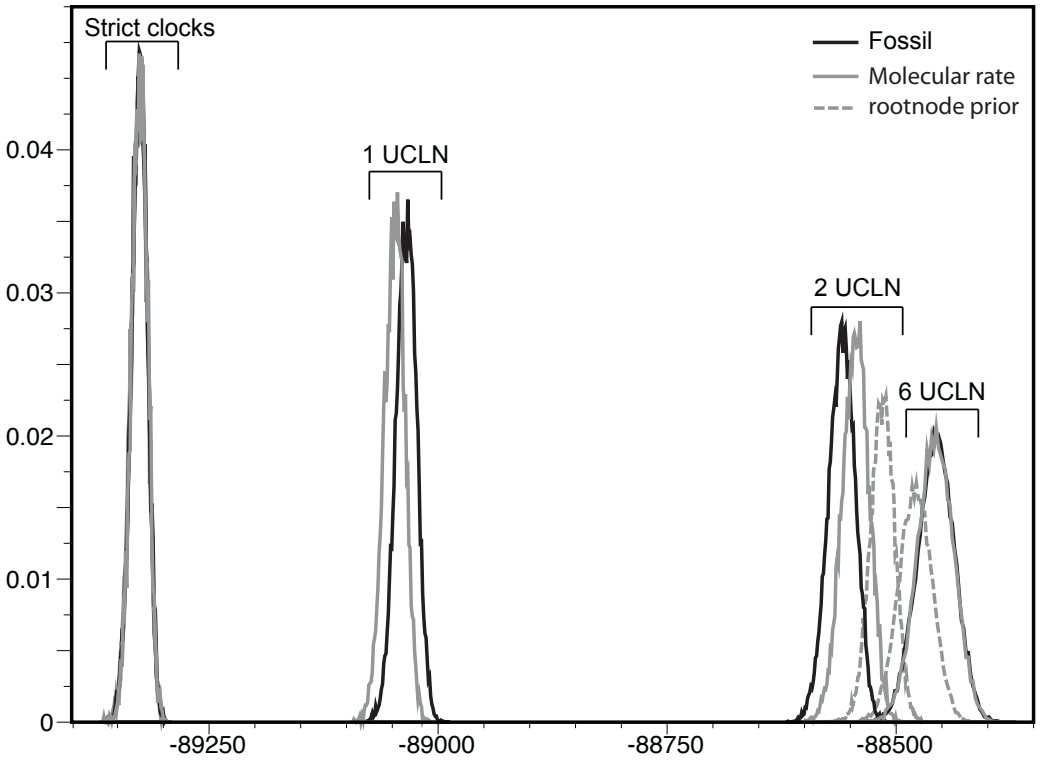

Figure 4.3 Summary of the posterior distribution of LnL from different parameterizations of rate estimation in BEAST. Unlinked clocks have a higher likelihood than linked clocks, though the difference is marginally significant between the 2 linked clocks versus the 6 unlinked clocks and non-significant when a prior is placed on the age of the rootnode. A strict clock resulted in the same posterior distribution of LnL regardless of the calibration or number of linked clocks. Likelihoods were equal between fossil calibration and molecular clock calibration.

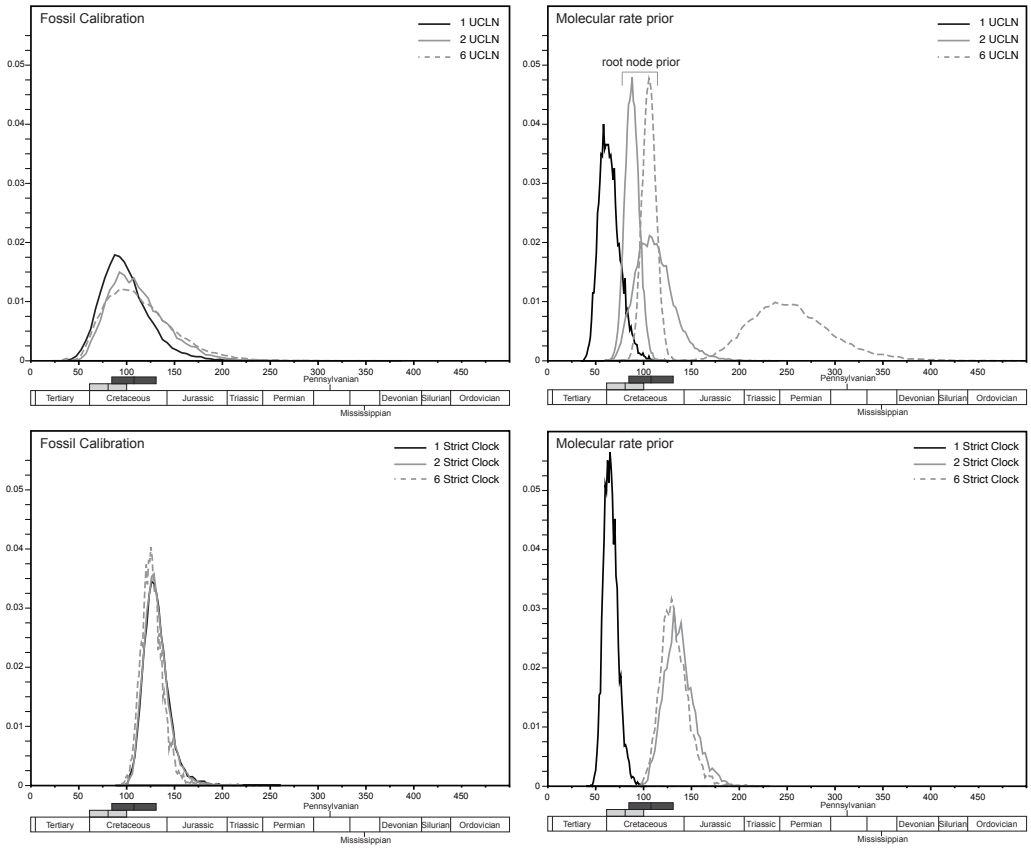
Fossil Calibration
1 UCLN
2 UCLN
6 UCLN
Molecular rate prior
root node prior
1 UCLN
2 UCLN
6 UCLN
Fossil Calibration
1 Strict Clock
2 Strict Clock
6 Strict Clock
Molecular rate prior
1 Strict Clock
2 Strict Clock
6 Strict Clock
Pennsylvanian
Mississippian
Tertiary
Cretaceous
Jurassic
Triassic
Permian
Devonian
Silurian
Ordovician

Figure 4.4 These plots are summaries of the posterior distribution of rootnode ages for different rate parameterizations run in BEAST. The x-axis is time in millions of years and the y-axis is proportion sampled. Geological periods are added to the x-axis for reference. The light gray bar is the prior age of the root node from Skinner et al. (2011) and the dark gray bar is the estimate for the age of Scincidae from Brandley et al (2011). Fossil caibration resulted in consistent estimates of the root node age for UCLN and strict clocks, with UCLN clocks placing the posterior root node age as expected from previous studies. The strict clock with fossil calibration was estimated slightly older than expected. Calibration with a molecular clock resulted in very different estimates of root node age depending on the clock models chosen. Linked clocks resulted in a younger estimate than unlinked clocks, with the 6 UCLN clock analyses estimating the age of Lygosominae to be older than all Squamates. Placing a prior on the root node for the 2 linked and 6 unlinked UCLN clocks resulted in better estimates, though the 6 UCLN clock still pushed older than the prior. Strict clocks with molecular rates were slightly older for 2 linked and unlinked clocks than for 1 linked clock.

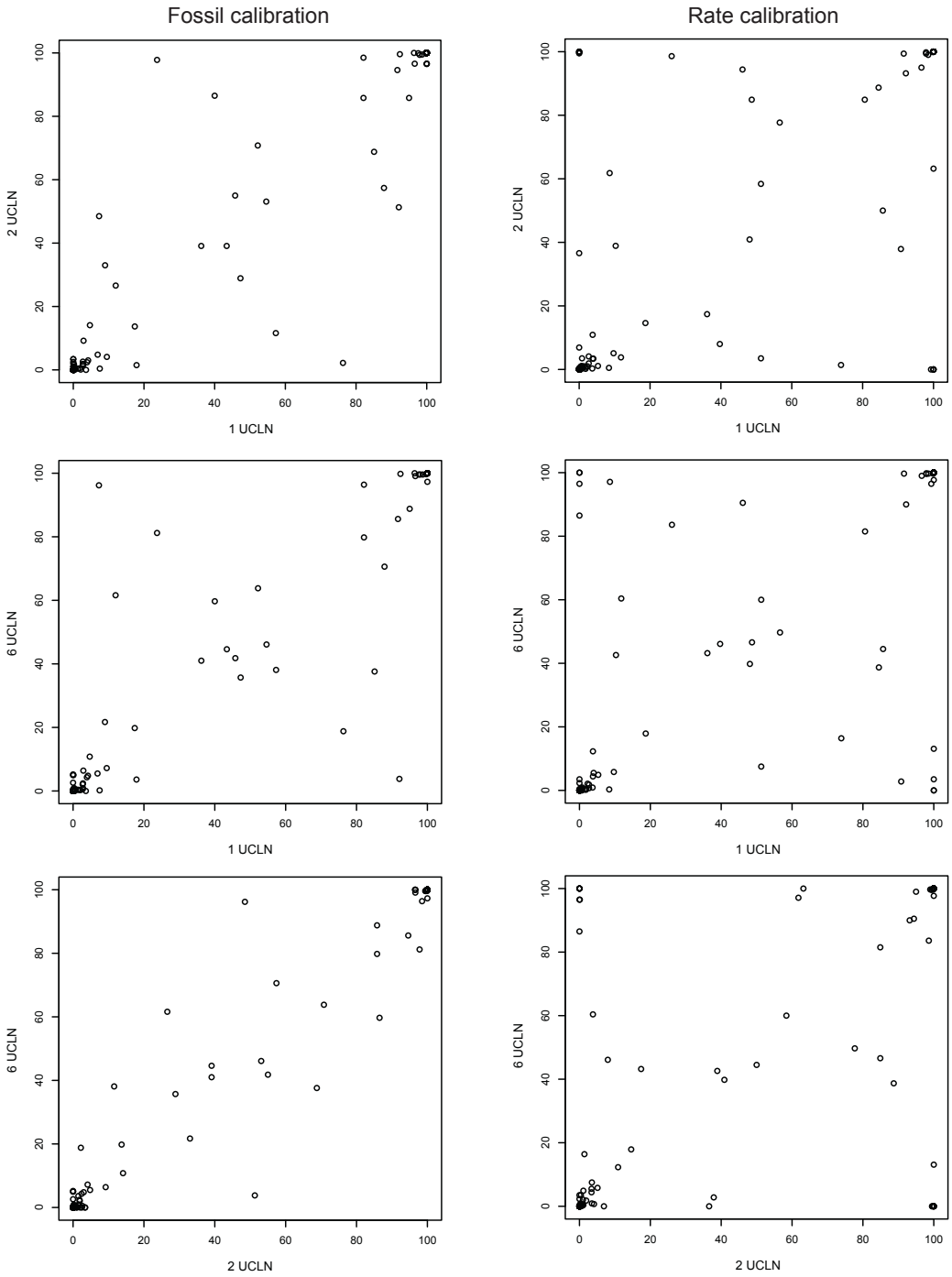

Figure 4.5 Compare plots of the split frequencies from the posterior distribution of trees for fossil calibrated and molecular rate calibrated analyses. These comparisons in each plot are between the use of a single clock (1 UCLN), two clocks (2 UCLN), or six clocks (6 UCLN). These plots show that using different numbers of UCLN clocks will result in different estimates of topology.

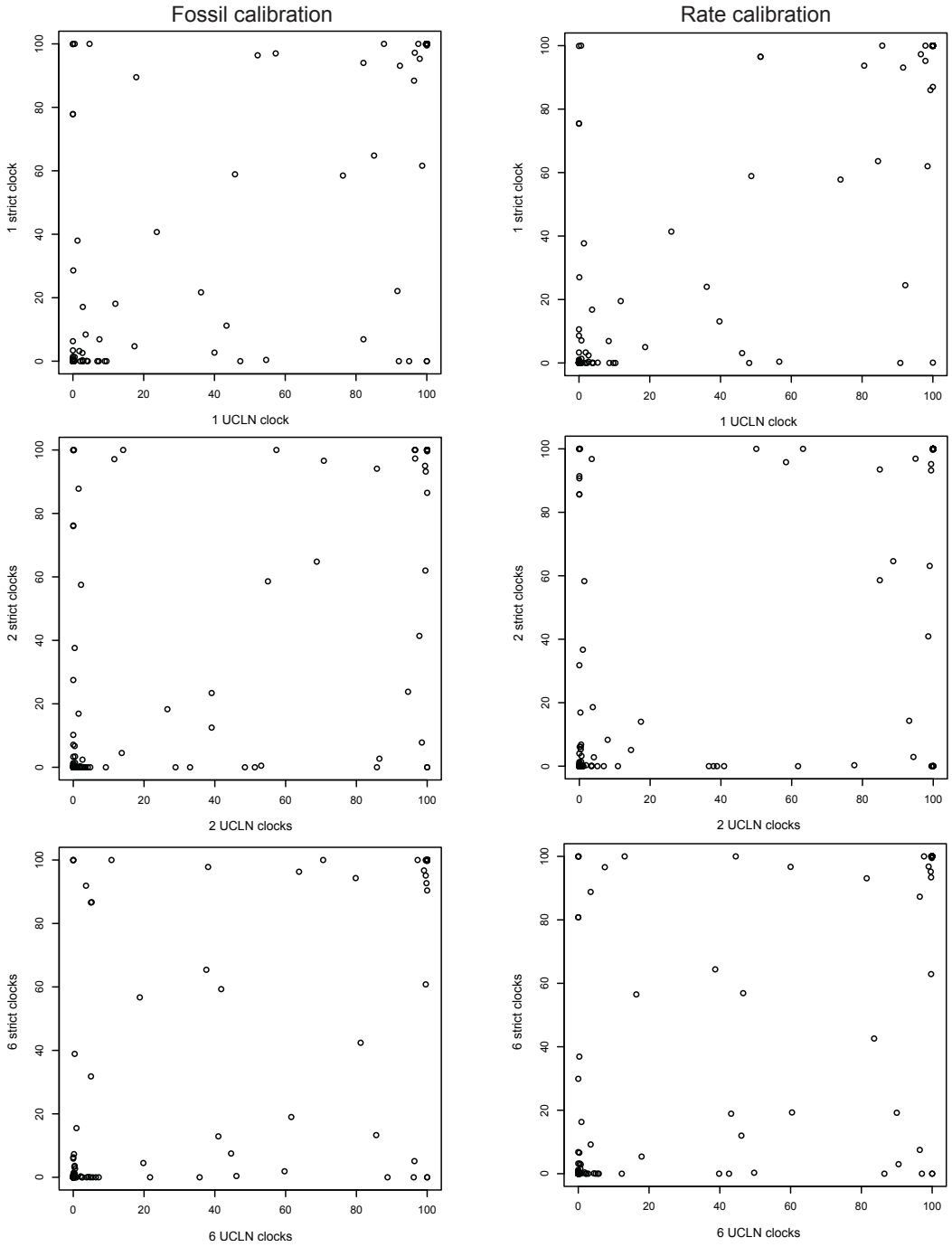

Figure 4.6 Compare plots of the split frequencies from the posterior distribution of trees for fossil calibrated and molecular rate calibrated analyses. The comparisons in each plot are between the use of an UCLN clock or a strict clock. These plots show that analyses with UCLN clocks and strict clocks result in different estimates of topology.

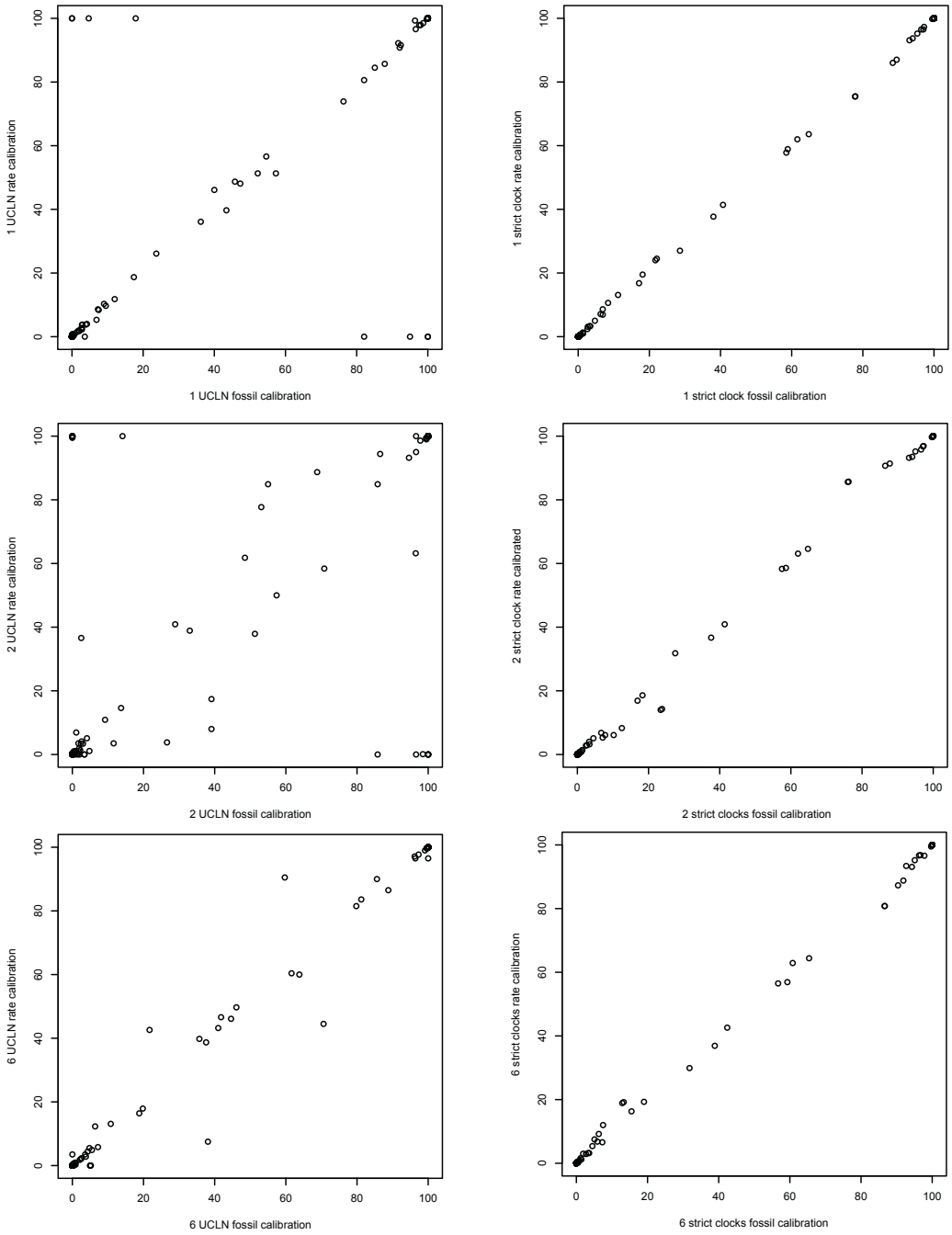

Figure 4.7 Compare plots of split frequencies from the posterior distribution of trees for strict clocks and UCLN clocks. The comparison in each plot is between analyses using fossil calibration or molecular rate calibration. Calibration choice does not seem to matter for strict clocks. Calibration has an affect on topology when using UCLN clocks. The difference is less when using 1 clock or 6 clocks, with 6 clocks producing the most similar topologies.

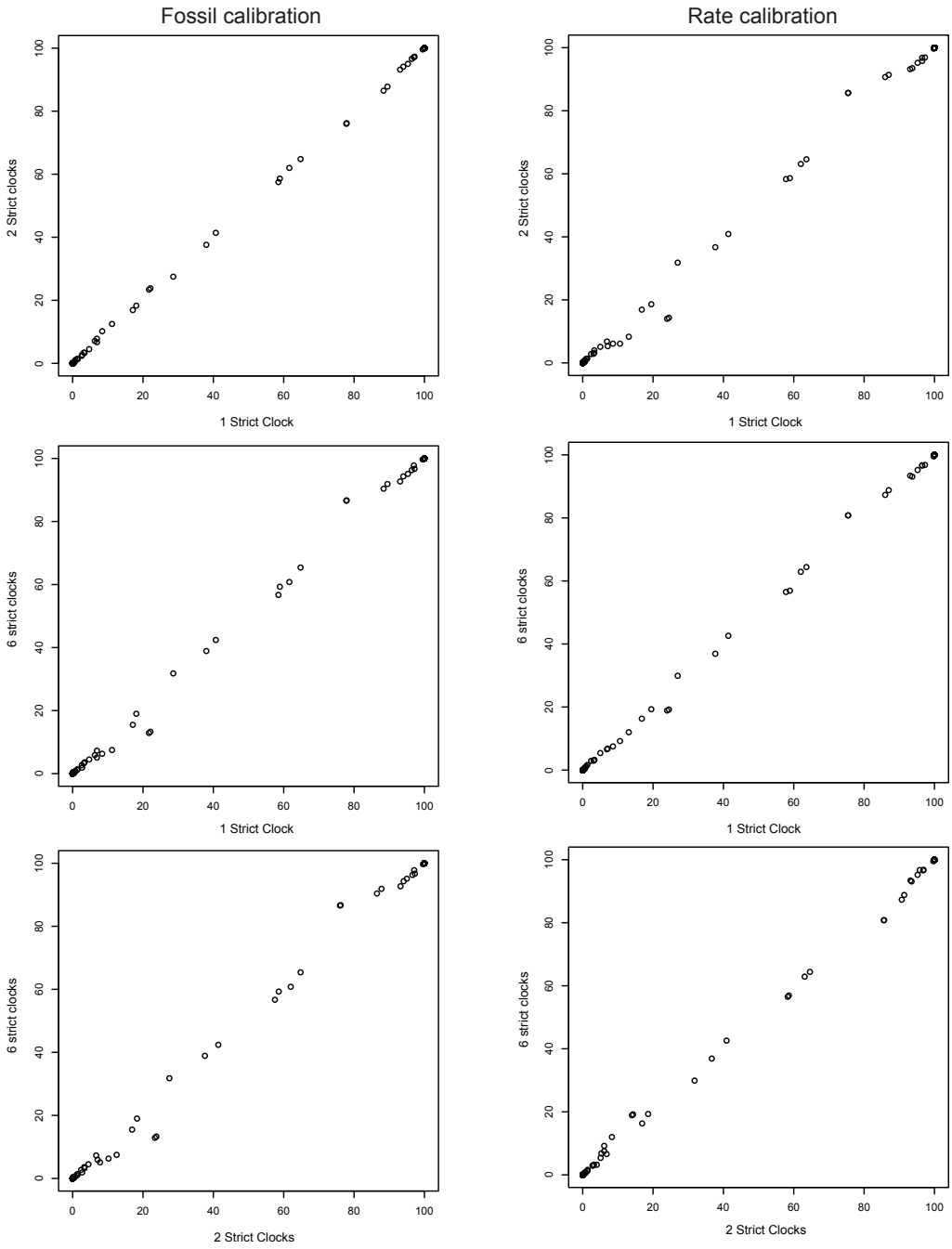

Figure 4.8 Compare plots of split frequencies from the posterior distribution of trees for fossil calibrated and molecular rate calibrated analyses using strict molecular clocks. The comparisons in each plot are between the use of a single strict clock, two strict clocks, or six strict clocks. These plots show that using a different number of strict molecular clocks will not change the estimate of topology.

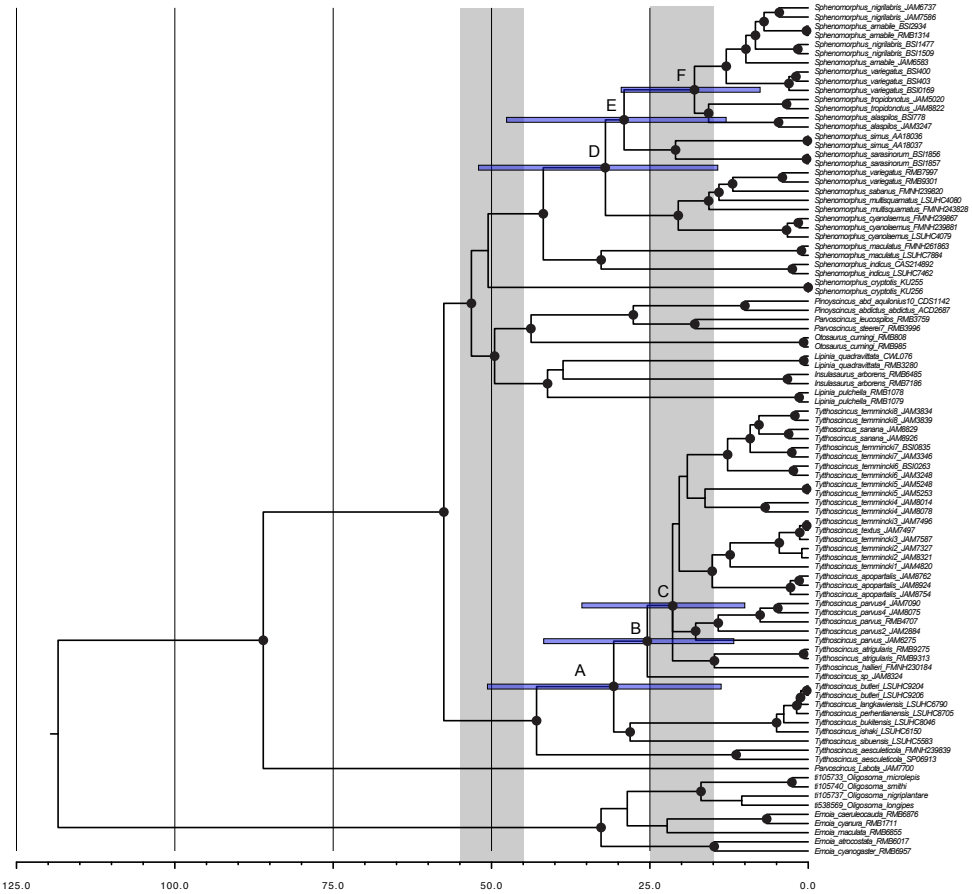

Figure 4.9 Phylogeny from the preferred diversification rate model (6 UCLN clocks with fossil calibration). The x axis is in millions of years and the time period for vicariance and the Miocene are highlighted in gray. The 95% highest posterior density of node ages overlaps with the timing of potential vicariance. Diversification on Sulawesi coincides with changes in climate, sea-level and island size in the Miocene.

CHAPTER 5

Taxonomic revision of *Parvoscincus decipiens* (Boulenger 1894) (Squamata: Scincidae: Lygosominae): Descriptions of six new species

The first major revision of lizards in the Philippines was done by Taylor (1922a) and included descriptions of numerous skink species. Taylor (1922a,b,c, 1923, 1925) recognized 19 Philippine species in the genera *Otosaurus*, *Insulasaurus*, and *Sphenomorphus*. In their revision, Brown and Alcala (1980) enumerated 23 species of *Sphenomorphus*, and no longer recognized *Otosaurus* and *Insulasaurus*. These genera have been resurrected in the interim, and three other genera have been described (Ferner et al. 1997; Linkem et al. 2011). In addition to this restructuring of forest skink taxa, new species have been described on Luzon, Palawan, and Panay islands (Brown 1995; Brown et al. 1995, 1999; Ferner et al. 1997; Linkem et al. 2010; Brown et al. 2010) bringing the total number of Philippine forest skink species to 29.

The *Parvoscincus decipiens* complex has troubled taxonomists for nearly a century. The species was originally described by Boulenger (1894) based on two specimens collected in Isabella Province of the Sierra Madre range of Luzon (Fig 5.1). Taylor (1915) described *Sphenomorphus curtirostris* from Mindanao based on differences in anterior loreal condition, a character that later was found to be a variable; the species was synonymized with *P. decipiens* by Brown and Alcala (1980). Additionally,

Lygosoma moellendorffi Boettger 1897 was described from Tablas Island and synonymized by Brown and Alcala (1980) with *P. decipiens*. Brown and Alcala (1980) examined 40 specimens from Luzon and Polillo islands, seven from Tablas Island, and 23 from Mindanao Island and concluded that despite considerable variation in the extent of dark marking on the head and flanks, no significant differences in scale counts or size existed among populations. They identified the anterior loreal scale as being variably single or double, but not of use in diagnosing populations. Owing to the lack of differences, Brown and Alcala (1980) considered all populations as conspecific under the name *P. decipiens.*

Our recent revision of the Philippine *Sphenomorphus* included multiple samples of *Parvoscincus decipiens* and found that there are multiple distinct lineages that warrant morphological examination (Linkem et al. 2011). We expanded the sampling of the *Parvoscincus decipiens* complex to incorporate recent collections from throughout Luzon Island to ascertain whether phylogenetic relationships of Linkem et al. (2011) are consistent with morphologically diagnosable lineages that can be considered new species. Expanded taxon sampling identified six new lineages that can be diagnosed morphologically based on some scale characters and color pattern variation.

Materials and Methods

Morphology

Specimens were collected using multiple techniques including capture by hand, pitfall traps, and snap traps. All specimens were fixed in 10% buffered formalin to preserve them, and after a few months the specimens were transferred to 70% ethanol. CWL determined sex by gonadal inspection and performed measurements using Mitutoyo digital calipers to the nearest 0.01 mm.

Measurements used are snout–vent length (SVL) measured from the tip of the snout to the cloacal opening; axilla–groin distance (AGD) measured from the posterior margin of the forelimb insertion to the anterior margin of the hind-limb insertion; head–forelimb length (HFL) measured from the anterior tip of the rostrum to the anterior region of forelimb insertion; head length (HL) measured from the anterior margin of the ear opening to the tip of the snout; head width (HW) measured at the widest part of the temporal region; internarial distance (IND) measured between the dorsal margin of the two nares; rostrum length (RostL) measured from the anterior margin of the eye to the tip of the snout.

Scales were counted on the right side of the body (when appropriate) using a dissecting microscope. Scale counts include: number of paravertebral scales (PVSR), dorsoventral scales between the parietals and the scales at the cloaca on the dorsal side; number of midbody scale rows (MBSR), scale rows around the middle of the body; and number of subdigital lamellae on Toe IV (SDL). Presence and absence of apical pits were observed on the dorsal scales, lateral scales, forelimbs and hind

limbs. Apical pits can be seen on the distal margin of scales and appear as small holes and imperfections in the scale. The pits may occur in multiple rows on each scale or a single row.

For the recognition of the new species, we adopt the General Lineage Concept of de Quieroz (1998) as the natural extension of the Evolutionary Species Concept (Wiley 1978). We consider as new species morphologically diagnosable forms for which the hypothesis of conspecificity can be rejected.

Genetic Data

Tissue samples from specimens were extracted using protocols detailed in the previous chapters. The ND2 gene was amplified through Polymerase Chain Reaction (PCR) for the NADH subunit 2 gene. All samples were cleaned and sequenced using methods mentioned in Chapters1–4. Sequences were aligned using MAFFT v6.717b (Katoh et al. 2005) and the optimal model of evolution for each codon position was assessed using jModelTest v2.0.2 (Posada 2008). Partitioned Bayesian analysis was performed in MrBayes 3.2 (Huelsenbeck and Ronquist 2001). Two independent analyses each with four Markov chain Monte Carlo chains were run for 10 million generation sampling ever 1000 generations. Convergence of independent runs was assessed using Tracer v1.5 (Rambaut and Drummond 2007) and Are We There Yet (AWTY: Wilgenbusch et al. 2004; Nylander et al. 2007).

Results

Phylogenetic Relationships

Independent analyses converged within 1 million generations for all parameters and were combined and summarized in MrBayes 3.2 summing the sump and sumt commands. The majority rule consensus tree (Fig 5.2) from the partitioned MrBayes analysis agrees with previous estimates of Philippine skink relationships (Linkem et al. 2011; Chapter 3). There is strong support for *Parvoscincus* and *Pinoyscincus*. Members of the *Parvoscincus decipiens* appear in two separate clades; one consists of four species (3 new and true *P. decipiens*) and the other of three species that are nested within the high elevation *P. hadros, P. igorotorum, P. beyeri, P. laterimaculatus, P. boyingi* clade. Species of the *P. decipiens* complex species nested in the high elevation clade are also taxa that occur at high elevations on separate mountain-tops of Luzon (Fig 5.2); although closely related, the species are separated by long branches separating. There are significant genetic differences that correspond with morphological differences between these different clades of the *Parvoscincus decipiens* complex. These clades are described as new species below.

Descriptions of new species

Parvoscincus **spah1** *sp. nov.*

Figs. 5.2; 5.3A; 5.4B, J, R; 5.5B, I

Sphenomorphus decipiens: Brown and Alcala 1980: 186 (part)

Parvoscincus decipiens sp *1*: Linkem, Diesmos, Brown 2011

Holotype.—KU 330120 (RMB 14729): Female: Philippines, Luzon Island, Cagayan Province, Municipality of Gonzaga, Barangay Magrafil, Site 1, Mt. Cagua, 18.219º N, 122.111º E, 783m asl. Collected 9 July 2011 by RMB.

Paratypes.—Philippines, Luzon Island, Cagayan Province, Municipality of Gonzaga, Barangay Magrafil, Mt. Cagua: KU 330126 (RMB 15016), KU 330122 (RMB 14817) Males; KU 330128 (RMB 15048) Female. Nueva Vizcaya Province, Municipality of Quezon, Barangay Maddiangat: KU 325796 (RMB 13514) Male. Bulacan Province, Municipality of Dona Remedios Trinidad, Barangay Kabayunan: KU 329401 (DSM 1804). Ilocos Norte Province, Municipality of Adams, Barangay Adams: KU 329931 (RMB 14368), KU 329941 (RMB 14515), KU 329945 (RMB 14524), KU 329949 (RMB 14538) Females; KU 329935 (RMB 14394) Male.

Referred Specimens.—KU 323307, KU 323316–17, KU 323325–29, KU 323331–35, KU 325795, KU 326585–86, KU 326707–09, KU 326711–16, KU 327626, KU 328946, KU 329930, KU 329934, KU 329939, KU 329947, KU 329951, KU 330067–68, KU 330119, KU 330121, KU 330123–25, KU 330127, KU 330129–30, TNHC 62889.

Diagnosis.—Parvoscincus spah1 can be identified by the following combination of characters: (1) A small body size (SVL at maturity 33–49 mm); (2) MBSR = 31–37; (3) PVSR = 58–73; (4) dorsal scales non-striated with apical pits; (5) apical pits on forelimbs and hind limbs; (6) four enlarged supraoculars; (7) anterior and posterior loreals undivided laterally; (8) three preoculars; and (9) 17–22 Toe IV SDL.

Parvoscincus spah1 is most closely related to *Parvoscincus spah2, P. spah3,* and *P. decipiens* (Fig 5.2). *Parvoscincus spah1* can be distinguished from *P. spah3* by having: apical pits on dorsal scales (vs. weak to missing apical pits on dorsal scales); a white throat with mottled dark brown ticks (vs. a dark black throat in males or white throat without checks in females); darker vertebral brown checks; and broad, dark brown dorsolateral band bordered dorsally and ventrally by white flecks (vs. dorsolateral band thin, irregular, with small white flecks ventrally).

Parvoscincus spah1 differs from *P. spah2* by having: a wide head (IND/RostL > 0.50 vs < 0.50); a throat with dark brown mottling (vs. white throat without mottling); dorsolateral band bordered dorsally by large white checks and not extending onto dorsum (vs. dorsolateral band extending dorsally towards midline becoming broken up dorsally); ventral edge of dorsolateral band flecked with white and becoming a mix of dark brown spots ventrally (vs. ventral edge of dorsolateral band with abrupt transition to lateral ground cream color, ventral edge of band broken up by irregular boxes of lateral ground color.

Parvoscincus spah1 is sympatric with *P. decipiens* and can be distinguished from this species by usually having: more paravertebral scales (58–72 vs. 54–63); usually having more lamellae under the fourth tow (17–22 vs. 14–18); having dark mottling under the throat (vs. having a few light brown lines); having dark mottled labials, temporals, and nuchals (vs. cream labials and temporals; dorsolateral band broad and extending down length of body (vs. dorsolateral band broad anteriorly at posterior of eye and becoming a thin line of black bordered dorsally by tan posterior to forelimb).

Parvoscincus spah1 is distinguished from Group 1 *Parvoscincus* (*P. beyeri, P. boyingi, P. hadros,* and *P. igorotorum*) by having fewer paravertebrals (58–73 vs. > 88) and fewer MBSR (31–37 vs. > 37). The new species differs from *P. spah5*, *P. spah6*, and *P. spah7* by having apical pits on the scales of the forelimbs (vs. no apical pores on forelimbs) and the throat mottled by dark brown (vs. throat with infrequent light brown lines).

Description of holotype.—A small-sized *Parvoscincus*, SVL 45.0 mm, with clawed, pentadactyl limbs. Snout rounded in lateral profile with subterminal lower jaw; rostral wide forming an oval dorsal margin with the nasals and frontonasal scale; frontonasal wider than long, in contact with nasals, rostral, anterior loreals, and prefrontal scales; prefrontals in narrow medial contact, in contact with anterior and posterior loreals, frontal, frontonasal, 1st supraciliary, and 1st supraocular; frontal slightly

longer than wide, in contact with 2 supraoculars, posterior apex rounded and narrow; 4 enlarged supraoculars, 1st largest, 2nd widest; frontoparietals fused, in contact with 3 supraoculars; interparietal arrowhead-shaped with parietal eye in posterior third; parietals in broad overlap, right overlapping left, in contact with fourth supraocular, postsupraocular, primary and secondary temporal; nuchals same size as dorsals, not obliquely enlarged.

Nasal pierced in center by large naris, surrounded anteriorly by rostral, dorsally by frontonasal, posteriorly by anterior loreal, and ventrally by 1st supralabial; single anterior loreal, posterior loreal wider than anterior; preoculars 3; 7 supralabials, 5th widest and under center of eye; supraciliaries 11, anterior 3 and posterior 2 larger than rest of series; 11 ciliaries; lower eyelid scaly and transparent, lacking non-scaled "window"; suboculars 8, largest anteriorly; primary temporals 3, secondary temporals 2, lower overlapping upper; ear large (EarD [1.34]/ EyeD [2.08] = 0.644), round, and moderately sunk.

Infralabials 7, decreasing in size posteriorly in series; mental large, forming a straight suture with a single large postmental and first infralabials; postmental contacts anterior 2 infralabials; chin scales increasing in number posteriorly (1, 3) and then blending into size and shape of gular scales; gular scales slightly smaller than ventrals.

Body slightly elongate (AGD [24.74]/SVL [45.00] = 0.55), cylindrical, with 31 equal-sized midbody scales, limbs overlapping when

adpressed; lateral body scales with 2 or 3 rows of apical pits; paravertebral scales 65, imbricate, with one row of apical pits. Tail elongate, slightly longer than body (TL [56.0]/SVL [45.0] = 1.2) cylindrical at base, slightly thicker dorsally than ventrally; subcaudal scales nondifferentiated; distal half of tail regenerated.

Forelimbs smaller than hind limbs (FLL [4.61]/HLL [5.83] = 0.79), pentadactyl; dorsal forelimb scales slightly smaller than body scale, ventral forelimb scales much smaller than ventral scales, dorsal and ventral forelimb scales imbricate with multiple rows of apical pits; multiple rows of dorsal scales on digits. Relative digit length with lamellae (L/R) in parentheses IV(12/12) > III(11/11) > II(9/9) > V(7/7) > I(5/5). Palmar scales irregular, raised, forming ventral protrusions from palmar surface; large set of five scales on distolateral edge of Digit V to the wrist, largest scale at wrist.

Hind limbs small (HLL [5.83]/SVL [45.0] = 0.13), pentadactyl; dorsal and ventral hind limb scales smaller than body scales; dorsal scales covered in apical pits, ventral scales with single row of apical pits; multiple scale rows on dorsal side of digits. Lamellae slightly keeled. Relative digit length with lamellae (L/R) in parentheses: IV(18/18) > III(14/15) > V(11/12) > II(9/9) > I(6/6). Plantar scales irregular, slightly raised; four large, ventrally pointed scales along ankle/ plantar margin; ventrally raised scales along distolateral edge of Digit V to ankle, increasing in size toward ankle.

Precloacal region with series of enlarged scales between pelvic region and cloaca, more elongate than ventral scales; medial precloacal scales larger, overlapping lateral scales.

Coloration of holotype in preservative.—Dorsal ground color brown with a series of dark brown vertebral spots from nuchals to tail. Broad dorsolateral band beginning at the posterior margin of the eye, extending over the ear and forelimb to the anterior portion of the tail; band dark brown, bordered dorsally by a series of white spots and ventrally by irregular white spots; dorsolateral band extends ventrally through midbody with a ventral edge that diffuses into the lateral coloration of black mottling on a cream background. Ground color of labials white with dark brown mottling resembling irregular bands; brown mottling extends over throat and gular region to the forelimbs. Dorsal surfaces of limbs dark brown with irregularly arranged circular tan spots; ventral surfaces of limbs same color as venter. Coloration in life not recorded.

Reproductive condition of holotype.—Female with a single small oviductal egg.

Variation.—All paratypes resemble the holotype in overall color pattern, some with a lighter dorsal coloration . There is no sexual dimorphism in this species. Degree of throat mottling varies from very light (KU 329935) to heavy (KU 325796). For variation in meristic and continuous characters within the type series and referred specimens see Table 2.

Distribution and natural history.—Found in abundance in the Sierra Madre and Cordillera mountain ranges of northern Luzon Island (Fig. 5.1). This species is also found in Aurora Province. Little is known about the natural history of *Parvoscincus spah1*. Specimens have been collected in pitfall traps near streams and by hand in and under rotting logs.

Parvoscincus **spah2** *sp. nov.*

Figs. 5.2; 5.3D; 5.4C, K, S; 5.5C, J

Sphenomorphus decipiens: Brown and Alcala 1980: 186 (part)

Parvoscincus decipiens sp 2: Linkem, Diesmos, Brown 2011

Holotype.—KU 306559: CDS 2171: Male: Philippines, Luzon Island, Camarines del Norte Province, Municipality of Labo.

Paratypes.—KU 313866: Male; KU 306560: Juv.; KU 306561: Male; NMPH 8611 (RMB3656): Female; TNHC62679 (RMB3685): Female; TNHC 62890 (RMB3682): Female

Diagnosis.—*Parvoscincus spah2* can be identified by the following combination of characters: (1) A small body size (SVL at maturity 36–43 mm); (2) MBSR = 32–36; (3) PVSR = 65–74; (4) dorsal scales non-striated with apical pits; (5) apical pits on forelimbs and hind limbs; (6) four enlarged supraoculars; (7) anterior and posterior loreals undivided laterally; (8) three preoculars; (9) and 16–19 Toe IV SDL; (10) narrow snout (IND/RostL < 0.50).

Parvoscincus spah2 is most closely related to *P. spah1*, *P. spah3*, and *P. decipiens* (Fig 5.2). *Parvoscincus spah2* can be distinguished from all these species by its narrow snout (IND/RostL 0.44–0.49 vs. > 0.50) and unique color pattern. It also differs from *P. spah1* by: lacking throat mottling (vs. heavy throat mottling); having dorsolateral band extending dorsally towards midline and discontinuous along dorsum (vs. dorsolateral band bordered dorsally by large white checks, restricted to lateral regions; andventral edge of dorsolateral band abruptly transitioning to lateral body color (vs. ventral edge of dorsolateral band flecked with white and becoming a mix of dark brown and white spots ventrally).

Parvoscincus spah2 differs from *P. spah3* by having: a single anterior loreal (vs. laterally divided anterior loreal) and apical pits on the dorsal scales (vs. weak to missing apical pits); a white throat in males and light brown streaking in females (vs. throat black in males and white in females); a broad dorsolateral band from the head to the tail (vs. dorsolateral band a thin strip along dorsal margin); and dorsal coloration with brown mottling extending from the dorsolateral band (vs. dorsal coloration without mottling other than vertebral spots).

Parvoscincus spah2 can be distinguished from *P. decipiens* by having: dark brown mottling on the dorsal surface (vs. light brown ground color without mottling); and labials spotted with dark brown extending posteriorly to the forelimbs (vs. labials white without spotting).

Parvoscincus spah2 differs from the high elevation *Parvoscincus spah5*, *P. spah6*, and *P. spah7* by the presence of distinct apical pits on the dorsal scales and forelimb scales (vs. without apical pits on dorsal and forelimb scales).

Description of Holotype.—A small *Parvoscincus*, SVL 36.5 mm, with clawed, pentadactyl limbs. Snout pointed in lateral profile; rostral wide forming an oval dorsal margin with the nasals and frontonasal scale; frontonasal wider than long, in contact with nasals, rostral, anterior loreals, and prefrontal scales; prefrontals in narrow medial contact, in contact with anterior and posterior loreals, frontal, frontonasal, and 1st supraciliary; frontal slightly longer than wide, in contact with 2 supraoculars, posterior apex rounded; 4 enlarged supraoculars, 1st largest, 2nd widest; frontoparietals fused, in contact with 3 supraoculars; interparietal arrowhead-shaped with parietal eye in posterior third; parietals in narrow overlap, left overlapping right, in contact with fourth supraocular, postsupraocular, primary and secondary temporal; nuchals same size as dorsals, not obliquely enlarged.

Nasal pierced in center by large naris, surrounded anteriorly by rostral, dorsally by frontonasal, posteriorly by anterior loreal, and ventrally by 1st supralabial; single anterior loreal, posterior loreal wider than anterior; preoculars 2; 7 supralabials, 5th widest and under center of eye; supraciliaries 13, anterior 3 and posterior 2 larger than rest of series; 14 ciliaries; lower eyelid scaly and transparent, lacking non-scaled

"window;" suboculars 8, largest anteriorly; primary temporals 3, secondary temporals 2, lower overlapping upper; ear large (EarD [1.22]/ EyeD [2.00] = 0.61), round, and moderately sunk.

Infralabials 7, decreasing in size posteriorly in series; mental large, forming a straight suture with a single large postmental and first infralabials; postmental contacts anterior 2 infralabials; chin scales increasing in number posteriorly (1, 2, 5) and then blending into size and shape of gular scales; gular scales slightly smaller than ventrals.

Body non-elongate (AGD [16.55]/SVL [36.5] = 0.45), cylindrical, with 36 equal-sized midbody scales, limbs overlapping when adpressed; lateral body scales with 2 or 3 rows of apical pits; paravertebral scales 65, imbricate, with one row of apical pits. Tail elongate, slightly longer than body (TL [50.0]/SVL [36.5] = 1.37) triangular at base, thicker dorsally than ventrally, becoming dorsoventrally compressed; subcaudal scales not differentiated.

Forelimbs smaller than hind limbs (FLL [3.44]/HLL [4.51] = 0.76), pentadactyl; dorsal forelimb scales smaller than body scale, ventral forelimb scales much smaller than ventral scales, dorsal and ventral forelimb scales imbricate with multiple rows of apical pits; multiple rows of dorsal scales on digits. Relative digit length with lamellae (L/R) in parentheses IV(12/12) > III(10/10) > II(9/9) > V(7/7) > I(5/5). Palmar scales irregular, raised, forming ventral protrusions from palmar surface;

large set of five scales on distolateral edge of Digit V to the wrist, largest scale at wrist.

Hind limbs small (HLL [4.51]/SVL [36.5] = 0.12), pentadactyl; dorsal and ventral hind limb scales smaller than body scales; dorsal scales covered in apical pits, ventral scales with single row of apical pits; multiple scale rows on dorsal side of digits. Lamellae slightly keeled. Relative digit length with lamellae (L/R) in parentheses: IV(17/18) > III(14/15) > V(--/11) > II(10/11) > I(6/6). Plantar scales irregular, slightly raised; four large, ventrally pointed scales along ankle/ plantar margin; ventrally raised scales along distolateral edge of Digit V to ankle, increasing in size toward ankle.

Precloacal region with series of enlarged scales between pelvic region and cloaca, more elongate than ventral scales; medial precloacal scales larger, overlapping lateral scales.

Coloration of holotype.—(Figs. 5.3C, K, S; 5.4C, J) Dorsal ground color light-tan medially, with dark brown laterally and a series of vertebral dark brown checks. Lateral brown extends along length of body from post ocular to base of tail and ventrally to the dorsal margin of limbs. Ventral margin of dorsolateral stripe checked with white. Venter white with spot on the distal half of tail and a few flecks on gular region; otherwise immaculate. Dorsum of limbs dark brown with white spots that extend onto the dorsal surface of the manus and pes. Ventral limb coloration white.

Variation.—Gravid females (TNHC 62679, PNM 8611) have brown streaking on the throat instead of white without pattern, non-gravid females have light brown spotting on the throat. Males have no spots on the throat, same as the holotype. Dorsal and lateral coloration same as holotype. Variation in scale counts and measurements are in Table 2.

Distribution.—PNM 8611, TNHC 62679, and TNHC 62890 found on Mt. Banahao at 600m a.s.l.; Municipality of Tayabas, Barangay Lalo. KU 313866 Mt. Labo at 212m a.s.l.; Municipality of Labo, Barangay Tulay Na Lupa (14.0394º, 122.787º) ; KU 306559, KU 306560–1 Mt. Labo at 211m a.s.l.; Municipality of Labo (14.089º, 122.782º).

Natural History.—Found under logs on stream banks, inside rotten logs and under logs and in leaf litter.

Parvoscincus **spah3** *sp. nov.*

Figs. 5.2; 5.3B, C; 5.4D, E, L, M, T, U; 5.5D, K

Sphenomorphus decipiens: Brown and Alcala 1980: 186 (part)

Parvoscincus decipiens sp 3: Linkem, Diesmos, Brown 2011

Holotype.—KU 320071 (ACD 4646): Male: Philippines, Luzon Island, Laguna Province, Los Banos, Mt. Makiling

Paratypes.—KU 304073 (Female), KU 313859 (Male), KU 313861 (Female), KU 313864 (Female), KU 313868–9 (Males), KU 320063 (Female), KU 320065–7 (Females), KU 320068–71 (Males), KU 326588–9 (Males), KU 326590–1 (Females), KU 330743 (Female), KU

330744 (Male), KU 331676 (Male), KU 331678–9 (Females), KU 331680–1 (Males), PMNH 2087 (Male), TNHC 62883 (Male), TNHC 62885 (Female), TNHC 62886 (Males), TNHC 62887 (Female), TNHC 62888 (Males), TNHC 62896 (Male), TNHC 62897–8 (Females).

Diagnosis.—*Parvoscincus spah3* can be identified by the following combination of characters: (1) A small body size (SVL at maturity 32–45 mm); (2) MBSR = 33–38; (3) PVSR = 58–69; (4) dorsal scales non-striated with weak apical pits or lacking apical pits; (5) apical pits on forelimbs and hind limbs; (6) four enlarged supraoculars; (7) anterior loreal divided laterally; (8) three preoculars; (9) and 15–19 Toe IV SDL.

Parvoscincus spah3 is most closely related to *P. spah1*, *P. spah2*, and *P. decipiens* (Fig 5.2). *P. spah3* can be distinguished from *P. spah1* by lacking or only having weak apical pits on dorsal scales (vs. multiple rows of apical pits on dorsal scales); by having two anterior loreals (vs. one anterior loreal); having a black throat in males and white throat in females (vs. white throat with dark brown mottling); dorsolateral band thin and weakly differentiated from flank color (vs. dorsolateral band broad and bordered dorsally and ventrally by white flecks).

Parvoscincus spah3 can be distinguished from *P. spah2* by the presence of a divided anterior loreal (vs. a single anterior loreal); by the presence of weakly developed apic pits on the dorsal scales or lacking apical pits (vs. multiple rows of apical pits on dorsal scales); having a

black throat in males and a white throat in females (vs. a white throat in males and a light brown streaked throat in females); having a weak dorsolateral band (vs. a broad dorsolateral band that extends onto the dorsum.

Parvoscincus spah3 can be distinguished from *P. decipiens* by the presence of two anterior loreals (vs. one anterior loreal); males having black throats and females having white throats (vs. throats white with a few light brown flecks); usually having more MBSR (33–36 vs. 30–34).

Parvoscincus spah3 can be distinguished from the high elevation *P. spah5, P. spah6,* and *P. spah7* by the presence of apical pits on the forelimbs (vs. absent); males having black throats and females white throats (vs. white throats with light brown streaks in both sexes); dorsolateral band thin and irregular (vs. moderately wide and bordered dorsally by light strip).

Description of Holotype.—A small *Parvoscincus*, SVL 41.01 mm, with clawed, pentadactyl limbs. Snout rounded in lateral profile with lower jaw slightly sunk; rostral wide forming an oval dorsal margin with the nasals and frontonasal scale; frontonasal wider than long, in contact with nasals, rostral, anterior loreals, and prefrontal scales; prefrontals in broad medial contact, in contact with anterior and posterior loreals, frontal, frontonasal, 1st supraciliary, and 1st supraocular; frontal slightly longer than wide, in contact with two supraoculars, posterior apex rounded and wide; four enlarged supraoculars, 1st largest, 2nd widest;

frontoparietals fused, in contact with three supraoculars; interparietal triangular with parietal eye in posterior third; parietals in broad overlap, left overlapping right, in contact with fourth supraocular, postsupraocular, primary and secondary temporal; nuchals same size as dorsals, not obliquely enlarged.

Nasal pierced in center by large naris, surrounded anteriorly by rostral, dorsally by frontonasal, posteriorly by two anterior loreals, and ventrally by 1st supralabial; two anterior loreals, anteriodorsal loreal twice as large as anterioventral loreal, posterior loreal wider than anterior, similar in size to anteriodorsal loreal; preoculars 3; 6 supralabials, 4th widest and under center of eye; supraciliaries 11, anterior 4 and posterior 2 larger than rest of series; 16 ciliaries; lower eyelid scaly and transparent, lacking non-scaled "window;" suboculars 10, largest anteriorly; primary temporals 3, secondary temporals 2, lower overlapping upper; ear large (EarD [1.74]/EyeD [2.64] = 0.659), round, and moderately sunk.

Infralabials 7, decreasing in size posteriorly in series; mental large, forming a straight suture with a single large postmental and first infralabials; postmental contacts anterior 2 infralabials; chin scales increasing in number posteriorly (1, 3) and then blending into size and shape of gular scales; gular scales slightly smaller than ventrals.

Body slightly elongate (AGD [21.12]/SVL [41.01] = 0.51), cylindrical, with 38 equal-sized midbody scales, limbs overlapping when adpressed; lateral body scales with 2 or 3 rows of apical pits; paravertebral

scales 64, imbricate, with one row of weak apical pits on some scales. Tail elongate, slightly longer than body (TL [51.87]/SVL [41.01] = 1.3) cylindrical at base, slightly thicker dorsally than ventrally; subcaudal scales nondifferentiated; tail original and complete.

Forelimbs smaller than hind limbs (FLL [3.80]/HLL [4.58] = 0.83), pentadactyl; dorsal forelimb scales slightly smaller than body scale, ventral forelimb scales much smaller than ventral scales, dorsal and ventral forelimb scales imbricate with multiple rows of apical pits; multiple rows of dorsal scales on digits. Relative digit length with lamellae (L/R) in parentheses IV(11/10) > III(10/10) > II(8/8) > V(8/8) > I(5/5). Palmar scales irregular, raised, forming ventral protrusions from palmar surface; large set of four scales on distolateral edge of Digit V to the wrist, largest scale at wrist.

Hind limbs small (HLL [4.58]/SVL [41.01] = 0.11), pentadactyl; dorsal and ventral hind limb scales smaller than body scales; dorsal scales covered in apical pits, ventral scales without apical pits; multiple scale rows on dorsal side of digits. Lamellae slightly keeled. Relative digit length with lamellae (L/R) in parentheses: IV(17/16) > III(11/11) > V(9/9) > II(8/8) > I(5/5). Plantar scales irregular, slightly raised; four large, ventrally pointed scales along ankle/plantar margin; ventrally raised scales along distolateral edge of Digit V to ankle, increasing in size toward ankle.

Precloacal region with series of enlarged scales between pelvic region and cloaca, more elongate than ventral scales; medial precloacal scales larger, overlapping lateral scales.

Coloration of Holotype.—Dorsal ground color brown, dark brown vertebral spots from the head to tail. Head black, throat black to gular region, venter white (Fig 5.4 D, L). Lateral head black with white spots; thin white line from the ventral portion of eye extending over the ear and terminating at axilla. Thin, intermittent dorsolateral band restricted to the dorsal margin. Flanks light brown. Forelimbs and hind limbs brown dorsally, white ventrally, posterior portion with large white spots on black.

Variation.—Males with black heads and throats females with white throats and light brown heads (Fig. 5.4 D, E, L, M, T, U). Occasionally, throats on females with brown flecking and males with white spots on the black throat. White spots on males in life are bluish (Fig 5.3B). Lateral division of the anterior loreal is variable within and between populations. Most samples have a divided loreal, but some have a single anterior loreal.

Distribution.—TNHC 62883 Municipality of Naga City, Barangay Panicuason, Mt. Isarog National Park, Mt. Isarog, 800m a.s.l., (TNHC 62885–6) 450m a.s.l.; TNHC 62887–8 Municipality of Tiwi, Barangay Banhaw, Sitio Purok 7, Mt. Malinao, 550m a.s.l.; TNHC 62896–8 Municipality of Malinao, Barangay Tagoytoy, Sitio Kumanging King, Mt. Malinao, 700m a.s.l.; KU 304073 Quezon Province, Polillo Is.; KU 313859, KU 313861, KU 313864, KU 313868–9 Camarines Norte

Province, Municipality of Labo, Mt. Labo; KU 320063, KU 320065–71, KU 326588–91, KU 331676, KU 331678–81 Laguna Province, Municipality of Los Banos, Mt Makiling.

Natural History.—Found under logs and in leaf litter in secondary growth forest. Males and females are found in abundance on Mt. Makiling outside of the Los Banos College campus. Breeding males and females found in January, though detailed survey of reproductive behavior has not been done.

Parvoscincus **spah 5** *sp. nov.*

Figs. 5.2; 5.3E; 5.4F, N, V; 5.5E, L

Sphenomorphus decipiens: Brown and Alcala 1980: 186 (part)

Parvoscincus decipiens sp 4: Linkem, Diesmos, Brown 2011

Holotype.— PNM 6759 (ACD 1015): Male: Philippines, Luzon Island, Laguna Province, Mt. Banahao.

Paratypes.—PNM 6761 (ACD 1020); PNM 6762 (ACD 1021); PNM 6760 (ACD 1016); TNHC 62892 (RMB 3727); TNHC 62893 (RMB 3731); TNHC 62894 (RMB 3732)

Diagnosis.—*Parvoscincus spah5* can be identified by the following combination of characters: (1) A small size (SVL at maturity 39–45 mm); (2) MBSR = 28–32; (3) PVSR = 62–66; (4) dorsal scales non-striated without apical pits; (5) apical pits on hind limbs, none on

forelimbs; (6) four enlarged supraoculars; (7) anterior loreal single; (8) three preoculars; (9) and 14–17 Toe IV SDL.

Parvoscincus spah5 is most closely related to *P. spah6* and *P. spah7* (Fig 5.2), and these three species are related to other high-elevation species of *Parvoscincus* species (*P. boyingi*, *P. laterimaculatus*, *P. igorotorum*, *P. beyeri*, and *P. hadros*). *Parvoscincus spah5* can be distinguished from *P. boyingi, P. laterimaculatus, P. igorotorum, P. beyeri, P. hadros* by having PV 62–66 (vs. > 74) and by being smaller (SVL 39.3–45.09 vs. 42–86.7).

Parvoscincus spah5 can be distinguished from *P. spah6* by having fewer PV scales (62–66 vs. 73); by having white flanks (vs. flanks brown with white spots); dorsolateral band bordered dorsally by straight light line (vs. dorsolateral band irregular dorsally with inverted hooks of dorsal color interrupting the dark brown band).

Parvoscincus spah5 can be distinguished from *P. spah7* by usually having fewer MBSR (28–32 vs 31–35) and fewer PV (62–66 vs 65–73) scales; by having white flanks (vs. flanks brown with white spots); dorsolateral band bordered dorsally by straight light line (vs. dorsolateral band irregular dorsally with half circles of dorsal color interrupting the dark brown band).

Description of holotype.—A small-sized *Parvoscincus*, SVL 42.41 mm, with clawed, pentadactyl limbs. Snout pointed in lateral profile; rostral wide forming an oval dorsal margin with the nasals and frontonasal

scales; frontonasal divided with right overlapping left and a small azygous scale between frontonasals and prefrontals, in contact with nasals, rostral, anterior loreals, and prefrontal scales; prefrontals in broad medial overlap, right overlapping left, in contact with anterior and posterior loreals, frontal, frontonasals, azygous frontonasal, 1st supraciliary and 1st supraoccular; frontal slightly longer than wide, in contact with 3 supraoculars, posterior apex rounded; 4 enlarged supraoculars, 1st largest, 3rd widest; frontoparietals fused, in contact with 2 supraoculars; interparietal acutely triangular with parietal eye in posterior third; parietals in narrow overlap, right overlapping left, in contact with fourth supraocular, postsupraocular, primary and secondary temporal; nuchals same size as dorsals, not obliquely enlarged.

Nasal pierced in center by large naris, surrounded anteriorly by rostral, dorsally by frontonasal, posteriorly by anterior loreal, and ventrally by 1st and 2nd supralabial; single anterior loreal, posterior loreal wider than anterior; preoculars 2; 7 supralabials, 5th widest and under center of eye; supraciliaries 10, anterior 3 and posterior 2 larger than rest of series; 12 ciliaries; lower eyelid scaly and transparent, lacking non-scaled "window;" suboculars 7, largest anteriorly; primary temporals 3, secondary temporals 2, lower overlapping upper; ear large (EarD [1.59]/ EyeD [2.16] = 0.74), round, and moderately sunk.

Infralabials 7, decreasing in size posteriorly in series; mental large, forming a straight suture with a single large postmental and first

infralabials; postmental contacts anterior 2 infralabials; chin scales increasing in number posteriorly (1, 2, 5) and then blending into size and shape of gular scales; gular scales slightly smaller than ventrals.

Body non-elongate (AGD [20.24]/SVL [42.41] = 0.48), cylindrical, with 28 equal-sized midbody scales, limbs overlapping when adpressed; lateral body scales with 1 row of faint apical pits; paravertebral scales 65, imbricate, with no apical pits. Tail original, slightly elongate, not complete, slightly longer than body (TL [44.2]/SVL [42.41] = 1.04) square at base, becoming dorsoventrally compressed distally; subcaudal scales nondifferentiated.

Forelimbs smaller than hind limbs (FLL [3.50]/HLL [4.88] = 0.72), pentadactyl; dorsal forelimb scales smaller than body scale, ventral forelimb scales much smaller than ventral scales, dorsal and ventral forelimb scales imbricate without apical pits; multiple rows of dorsal scales on digits. Relative digit length with lamellae (L/R) in parentheses IV(11/11) > III(10/10) > II(8/8) > V(8/8) > I(5/5). Palmar scales irregular, raised, forming ventral protrusions from palmar surface; large set of four scales on distolateral edge of Digit V to the wrist, largest scale at wrist.

Hind limbs small (HLL [4.88]/SVL [42.41] = 0.11), pentadactyl; dorsal and ventral hind limb scales smaller than body scales; dorsal scales with single row of apical pits, ventral scales without apical pits; multiple scale rows on dorsal side of digits. Lamellae slightly keeled. Relative digit length with lamellae (L/R) in parentheses:

IV(16/16) > III(12/13) > V(10/10) > II(9/9) > I(6/6). Plantar scales irregular, slightly raised; three large, ventrally pointed scales along ankle/ plantar margin; ventrally raised scales along distolateral edge of Digit V to ankle, increasing in size toward ankle.

Precloacal region with series of enlarged scales between pelvic region and cloaca, more elongate than ventral scales; medial precloacal scales larger, overlapping lateral scales.

Coloration of holotype (in preservative).—Dorsal ground color brown; series of small dark brown dorsovertebral spots from nuchals to base of the tail. Broad dorsolateral line near head, from posterior midline of ear to nuchal region tapering irregularly on ventral margin to forelimb and blending in midbody; bordered anteriorly by a tan line half a scale wide continuing down the entire length of the body and anterior of tail; dark brown dorsolateral line commencing at hind limb as a series of large blotches that terminates posterior to the cloacal opening. Anterior to the forelimb and ventral to the dorsolateral line is some brown ticking that continues around the gular region. Ground color of the gular and ventral region cream. The mental, postmental, infralabials scale margins with concentration of brown ticking that blend in with the gular streaks. The venter from the gular region posteriorly and the ventral sides of limbs are immaculate cream. Distal portion of ventral tail with some brown ticking. Dorsal aspects of limbs dark brown with random tan spots that decrease in size and increase in frequency towards the solar surfaces of feet.

Variation.—Paratypes primarily resemble the holotype. Two paratypes (TNHC 62894 and PNMH 6760) have a divided frontonasal like the holotype, the other paratypes have a single frontonasal. Coloration is the same across the type series. Variation in measurements and scale counts are in Table 5.2.

Distribution.—Collected above 1275 m a.s.l. on Mt. Banahao, Quezon Province, Municipality of Tayabas, Barangay Lalo. The species seems to be a high-elevation endemic.

Natural History.—Found in primary forest in loose soil under rocks and logs above 1000 m elevation.

Parvoscincus **spah6** *sp. nov.*

Figs. 5.2; 5.4G, O, W; 5.5F, G

Sphenomorphus decipiens: Brown and Alcala 1980: 186 (part)

Holotype.—KU 308693 (ELR 1158): Female: Luzon Island, Nueva Viscaya Province, Municipality of Quezon, Barangay Maddiangat, Mt. Palali, 1374 m a.s.l (16º 26’ 21.9”, 121º 13’ 24.1”): Collected by E. Rico on 15 March 2007 at 2 pm.

Paratypes.—KU 308651, KU 308690–92: all juveniles from same locality as holotype.

Diagnosis.—*Parvoscincus spah6* can be identified by the following combination of characters: (1) A small body size (SVL at maturity 39.28 mm); (2) MBSR = 32; (3) PVSR = 73; (4) dorsal scales

non-striated without apical pits; (5) apical pits on hind limbs, none on forelimbs; (6) four enlarged supraoculars; (7) anterior loreal single; (8) three preoculars; (9) and 14 Toe IV SDL.

Parvoscincus spah6 is most closely related to *P. spah5* and *P. spah7* (Fig 5.2), and these three species are related to other high elevation *Parvoscincus* species (*P. boyingi*, *P. laterimaculatus*, *P. igorotorum*, *P. beyeri*, and *P. hadros*). *Parvoscincus spah6* can be distinguished from *P. boyingi, P. laterimaculatus, P. igorotorum, P. beyeri, P. hadros* by being smaller (SVL 39.28 vs. 42–86.7) and having fewer PV (< 88) than all species but *P. laterimaculatus*.

Parvoscincus spah6 can be distinguished from *P. spah5* by having more PV scales (73 vs. 62–66); by having brown flanks with white spots (vs. white flanks); dorsolateral band irregular dorsally with inverted hooks of dorsal color interrupting the dark brown band (vs. dorsolateral band bordered dorsally by straight light line).

Parvoscincus spah6 and *P. spah7* are most similar morphologically with overlapping scale counts (Table 5.1, and 5.2). *P. spah6* has a slightly lower profile head (3.44 mm vs. 3.8–4.5 mm) and shorter head–forelimb length (13.4 vs. 14.3–16.45). Coloration is very similar, though the patternof the dorsolateral band is different on the dorsal margin. *P. spah6* has a dark brown dorsolateral band broken dorsally by inverted “hook” or “claw” shaped marks of the dorsal color (Fig 5.5F, M). *P. spah7* has a dark

brown dorsolateral band broken up dorsally by half circles of dorsal coloration (Fig 5.5 G, N).

Description of Holotype.—A small-sized *Parvoscincus*, SVL 39.28 mm, with clawed, pentadactyl limbs. Snout rounded in lateral profile with lower jaw slightly sunk; rostral wide forming an oval dorsal margin with the nasals and frontonasal scale; frontonasal wider than long, in contact with nasals, rostral, anterior loreals, and prefrontal scales; prefrontals in broad medial contact, right overlapping left, in contact with anterior and posterior loreals, frontal, frontonasal, 1st supraciliary, and 1st supraocular; frontal slightly longer than wide, in contact with 3 supraoculars, posterior apex rounded and narrow; 4 enlarged supraoculars, 2nd largest, 2nd widest; frontoparietals fused, in contact with 2 supraoculars; interparietal tear-drop shaped with parietal eye in posterior third; parietals in broad overlap, right overlapping left, in contact with postsupraocular, primary and secondary temporal; nuchals same size as dorsals, not obliquely enlarged.

Nasal pierced in center by large naris, surrounded anteriorly by rostral, dorsally by frontonasal, posteriorly by anterior loreal, and ventrally by 1st supralabial; single anterior loreal, posterior loreal wider than anterior; preoculars 3; 7 supralabials, 5th widest and under center of eye; supraciliaries 10, anterior 3 and posterior 2 larger than rest of series; 15 ciliaries; lower eyelid scaly and transparent, lacking non-scaled "window;" suboculars 8, largest anteriorly; primary temporals 3,

secondary temporals 2, lower overlapping upper; ear moderately large (EarD [1.42]/EyeD [2.64] = 0.54), round, and moderately sunk.

Infralabials 7, decreasing in size posteriorly in series; mental large, forming a straight suture with a single large postmental and first infralabials; postmental contacts anterior 2 infralabials; chin scales increasing in number posteriorly (1, 3) and then blending into size and shape of gular scales; gular scales slightly smaller than ventrals.

Body slightly elongate (AGD [20.47]/SVL [39.28] = 0.52), cylindrical, with 32 equal-sized midbody scales, limbs overlapping when adpressed; lateral body scales with one row of apical pits; paravertebral scales 73, imbricate, without apical pits scales. Tail elongate, slightly longer than body (TL [53.0]/SVL [39.28] = 1.34) rectangular at base, slightly thicker dorsally than ventrally; subcaudal scales nondifferentiated; tail original and complete.

Forelimbs smaller than hind limbs (FLL [3.42]/HLL [4.26] = 0.80), pentadactyl; dorsal forelimb scales slightly smaller than body scale, ventral forelimb scales much smaller than ventral scales, dorsal and ventral forelimb scales imbricate without apical pits; multiple rows of dorsal scales on digits. Relative digit length with lamellae (L/R) in parentheses IV(9/9) > III(9/8) > II(8/7) > V(6/6) > I(4/4). Palmar scales irregular, raised, forming ventral protrusions from palmar surface; large set of three scales on distolateral edge of Digit V to the wrist, largest scale at wrist.

Hind limbs small (HLL [4.26]/SVL [39.28] = 0.11), pentadactyl; dorsal and ventral hind limb scales smaller than body scales; dorsal scales with apical pits, ventral scales without apical pits; multiple scale rows on dorsal side of digits. Lamellae slightly keeled. Relative digit length with lamellae (L/R) in parentheses: IV(14/14) > III(13/11) > V(9/10) > II(8/7) > I(5/5). Plantar scales irregular, slightly raised; three large, ventrally pointed scales along ankle/plantar margin; ventrally raised scales along distolateral edge of Digit V to ankle, increasing in size toward ankle.

Precloacal region with series of enlarged scales between pelvic region and cloaca, more elongate than ventral scales; medial precloacal scales larger, overlapping lateral scales.

Coloration of holotype.—Dorsal ground color brown throughout; a series of small dark brown dorsovertebral spots from the nuchals to the base of the tail. Dorsolateral line broad near head, from posterior midline of ear to nuchal region tapering irregularly on ventral margin to forelimb; bordered anteriorly by a tan line half a scale wide that irregularly breaks the dorsolateral band with small inverted “hooks” of dorsal color; dark brown dorsolateral line blends into flanks becoming lighter and blending in with small white flecks. Anterior to the forelimb and ventral to the dorsolateral line is some brown ticking that continues around the gular region. The ground color of the gular and ventral region is cream color. The mental, postmental, infralabials scale margins have a concentration of brown ticking that blend in with the gular streaks. The ventrum from the

gular region posteriorly and the ventral side of limbs are all cream without any markings. Distal portion of ventral tail has some brown ticking. Dorsal aspect of limbs are dark brown with random tan spots that decrease in size and increase in frequency towards the solar surface of the feet.

Variation.—There is only one adult specimen and the juveniles appear to be new hatchlings. The paratypes match the holotype in coloration, measurements and scale counts were not taken for the juveniles.

Distribution.—Found between 1374–1450 m a.s.l. on Mt. Palali

Natural History.—The species appears to be a high elevation endemic to Mt. Palali. All specimens were found in primary montane forest in the leaf litter or near rotting logs.

Parvoscincus spah7 *sp nov.*

Figs. 5.2; 5.4H, P, X; 5.5G, N

Sphenomorphus decipiens: Brown and Alcala 1980: 186 (part)

Holotype.—KU 323324 (ACD 4859): Female; Aurora Province, Municipality Maria Aurora, Barangay Villa, Mt. Dayap, 915 m a.s.l. (N 15.660, E 121.327).

Paratypes.—KU 323323 (Male), KU 323309, KU 32332–22 (Females).

Diagnosis.—*Parvoscincus spah7* can be identified by the following combination of characters: (1) A small body size (SVL at

maturity 39.5–46.6 mm); (2) MBSR = 31–35; (3) PVSR = 65–75; (4) dorsal scales non-striated without apical pits; (5) apical pits on hind limbs, none on forelimbs; (6) four enlarged supraoculars; (7) anterior loreal single; (8) three preoculars; (9) and 15–17 Toe IV SDL.

Description of Holotype.—A small-sized *Parvoscincus*, SVL 41.61 mm, with clawed, pentadactyl limbs. Snout rounded in lateral profile with lower jaw slightly sunk; rostral wide forming an oval dorsal margin with the nasals and frontonasal scale; frontonasal wider than long, in contact with nasals, rostral, anterior loreals, and prefrontal scales; prefrontals in broad medial contact, left overlapping right, in contact with anterior and posterior loreals, frontal, frontonasal, 1st supraciliary, and 1st supraocular; frontal slightly longer than wide, in contact with 2 supraoculars, posterior apex rounded and narrow; 4 enlarged supraoculars, 2nd largest, 2nd widest; frontoparietals fused, in contact with 3 supraoculars; interparietal tear-drop shaped with parietal eye in posterior third; parietals in broad overlap, right overlapping left, in contact with fourth supraocular, postsupraocular, primary and secondary temporal; nuchals same size as dorsals, not obliquely enlarged.

Nasal pierced in center by large naris, surrounded anteriorly by rostral, dorsally by frontonasal, posteriorly by anterior loreal, and ventrally by 1st supralabial; single anterior loreal, posterior loreal wider than anterior; preoculars 3; 7 supralabials, 5th widest and under center of eye; supraciliaries 10, anterior 3 and posterior 2 larger than rest of series; 14

ciliaries; lower eyelid scaly and transparent, lacking non-scaled "window;" suboculars 8, largest anteriorly; primary temporals 3, secondary temporals 2, lower overlapping upper; ear moderately large (EarD [1.60]/EyeD [2.64] = 0.61), round, and moderately sunk.

Infralabials 7, decreasing in size posteriorly in series; mental large, forming a straight suture with a single large postmental and first infralabials; postmental contacts anterior 2 infralabials; chin scales increasing in number posteriorly (1, 3) and then blending into size and shape of gular scales; gular scales slightly smaller than ventrals.

Body slightly elongate (AGD [21.48]/SVL [41.61] = 0.52), cylindrical, with 32 equal-sized midbody scales, limbs overlapping when adpressed; lateral body scales with one row of apical pits; paravertebral scales 71, imbricate, without apical pit scales. Tail elongate, slightly longer than body (TL [55.0]/SVL [41.61] = 1.32) rectangular at base, slightly thicker dorsally than ventrally; subcaudal scales nondifferentiated; tail complete, last 1/5 regenerated.

Forelimbs smaller than hind limbs (FLL [3.66]/HLL [4.76] = 0.77), pentadactyl; dorsal forelimb scales slightly smaller than body scale, ventral forelimb scales much smaller than ventral scales, dorsal and ventral forelimb scales imbricate without apical pits; multiple rows of dorsal scales on digits. Relative digit length with lamellae (L/R) in parentheses IV(11/11) > III(9/9) > II(7/7) > V(7/7) > I(5/5). Palmar scales irregular, raised, forming ventral protrusions from palmar surface; large

set of four scales on distolateral edge of Digit V to the wrist, largest scale at wrist.

Hind limbs small (HLL [4.76]/SVL [41.61] = 0.11), pentadactyl; dorsal and ventral hind limb scales smaller than body scales; dorsal scales with apical pits, ventral scales without apical pits; multiple scale rows on dorsal side of digits. Lamellae slightly keeled. Relative digit length with lamellae (L/R) in parentheses: IV(15/15) > III(11/11) > V(8/8) > II(8/8) > I(5/5). Plantar scales irregular, slightly raised; three large, ventrally pointed scales along ankle/plantar margin; ventrally raised scales along distolateral edge of Digit V to ankle, increasing in size toward ankle.

Precloacal region with series of enlarged scales between pelvic region and cloaca, more elongate than ventral scales; medial precloacal scales larger, overlapping lateral scales.

Coloration of holotype.—Dorsal ground color brown throughout; a series of small dark brown dorsovertebral spots from the nuchals to the base of the tail. Dorsolateral line broad near head, from posterior midline of ear to nuchal region tapering irregularly on ventral margin to forelimb; bordered anteriorly by a tan line one scale wide that irregularly breaks the dorsolateral band with small half circles of dorsal color; dark brown dorsolateral line blends into flanks becoming lighter and blending in with small white flecks. Anterior to the forelimb and ventral to the dorsolateral line is some brown ticking that continues around the gular region. The ground color of the gular and ventral region is cream color. The mental,

postmental, infralabials scale margins have a concentration of brown ticking that blend in with the gular streaks. The ventrum from the gular region posteriorly and the ventral side of limbs are all cream without any markings. Distal portion of ventral tail has some brown ticking. Dorsal aspect of limbs dark brown with random tan spots that decrease in size and increase in frequency towards the solar surface of the feet.

Variation.—Coloration is the same across the type series. Scale count and measurement differences are in Table 5.2.

Distribution.—Found at two sites in Aurora Province in the Municipality of San Luis, Barangay Lipimieutal (543 m a.s.l.) and the Municipality Maria Aurora, Barangay Villa, Mt. Dayap, (915 m a.s.l.).

Natural History.—This species is found at high elevation (915 m and mid elevation (543 m) on Mt. Dayap in Aurora Province. The species was found in leaf litter and under logs in the forested regions.

Redescription of **Parvoscincus decipiens**

Figs. 5.2; 5.3F; 5.4A, I, Q; 5.5A, H

Lygosoma decipiens: Boulenger 1894: 734

Lygosoma decipiens: Smith 1937: 220

Sphenomorphus decipiens: Taylor 1922a

Lygosoma (Homolepida) moellendorffi: Boettger 1897

Sphenomorphus moellendorffi: Taylor 1922a

Sphenomorphus curtirostris: Taylor 1915

Otosaurus curtirostris: Smith 1937

Lygosoma (Sphenomorphus) curtirostris: Brown and Alcala 1970

Sphenomorphus decipiens: Brown and Alcala 1980: 186 (part)

Parvoscincus decipiens: Linkem, Diesmos, Brown: 2011

Holotype.—BMNH1946.8.16.95

Referred specimens.—KU 326592–99, KU 326601, KU 326603, KU 326606, KU 326608–11.

Diagnosis.—*Parvoscincus decipiens* can be diagnosed by the following combination of characters: (1) A small body size (SVL at maturity 35.02–40.62 mm); (2) MBSR = 30–34; (3) PVSR = 54–63; (4) dorsal scales non-striated without apical pits; (5) apical pits on hind limbs, variably present on forelimbs; (6) four enlarged supraoculars; (7) anterior loreal single; (8) three preoculars; (9) and 14–18 Toe IV SDL.

Parvoscincus decipiens is most closely related to *P. spah1*, *P. spah2,* and *P. spah3* (Fig. 5.2). *Parvoscincus decipiens* can be distinguished from *P. spah1* by not having apical pits on the dorsum or forelimbs (vs. having apical pits on dorsum and forelimbs); by having white labials and throat (vs. dark brown mottling on labials and throat); having a thin dorsolateral band with a solid tan line dorsally (vs. broad dorsolateral band).

Parvoscincus decipiens can be distinguished from *P. spah2* by having a wider rostrum (IND/Rost > 0.50 vs. < 0.50); lacking apical pits on the dorsum and forelimbs (vs. apical pits present on forelimbs and

dorsum); dorsum brown without dark brown spots laterally (vs. dark brown spots extending dorsally from the dorsolateral line); dorsolateral line thin and flanks light tan (vs. dorsolateral line broad, dark brown, and extending ventrally to mid-flank).

Parvoscincus decipiens can be distinguished from *P. spah3* by lacking apical pits on dorsum and forelimbs (vs. apical pits weak or absent on dorsum and present on forelimbs); having a single anterior loreal (vs. single or divided anterior loreal); males ans females having white throat (vs. males with black throat and females with white throat); dorsolateral band thin with light tan line dorsally (vs. dorsolateral band thin, broken, and occasionally bordered by light tan dorsally).

Redescription of holotype.—Rostral scale wider than tall, in contact with nasal, first supralabial and frontonasal, forming a wide, straight suture with the frontonasal; frontonasal single, wider than long, in contact with the rostral, both nasals the prefrontals, and the anterior loreal; prefrontals in broad medial contact, left overlapping right, in contact with the frontal, first supracilliary, frontonasal, and both anterior and posterior loreals; frontal slightly longer than wide, posterior region acutely rounded, in contact with 2 supraocular scales, first supracilliary, and prefrontals; frontoparietal single, in contact with 3 supraoculars, parietal, and interparietal; interparietal kite-shaped, with posterior axis 6x longer than anterior axis, interparietal eye visible, positioned near posterior margin along the posterior axis; parietals in broad contact behind interparietal, left

overlapping right, in contact with two postsupraoculars, primary and secondary temporals and non-enlarged nuchal scales, in point contact with fourth supraocular.

Nasal scales pierced by nares in center of scale, in contact with rostral, frontonasal, anterior loreal, and the first supralabial, in point contact with second supralabial; two scales in the loreal region, anterior scale rectangular, taller than wide, in point contact with first supralabial and broad contact with second supralabial, nasal, prefrontal and frontonasal; posterior loreal large, as wide as tall, in contact with prefrontal, anterior loreal, second and third supralabial and two preoculars; two preoculars, ventral scale larger, semi-circular, in contact with third supralabial, dorsal prefrontal, and posterior loreal. Supralabial (7/7), seventh largest, 4 under center of eye. 10 cilliaries, 9 supracilliaries. Temporal region with one primary temporal and three secondary temporals. Postsupraocular region with two rows of small scales surrounding the posterior margin of the eye. Ear opening large, tympanum mildly sunk, but fully visible.

Mental wider than long, surrounded by infralabials and a single postmental; post mentals increase in number (1, 3, 5) and then blend into size and shape of gular scales. Seven infralabials, first postmental in contact with two infralabials.

Coloration.— Dorsal ground color brown throughout; a series of small dark brown dorsovertebral spots from the nuchals to the base of the

tail. Dorsolateral line broad near head, from posterior midline of eye to nuchal region tapering irregularly on ventral margin to forelimb and blending in midbody; bordered ventrally by narrow white line; bordered anteriorly by a tan line half a scale wide that continues down the entire length of the body and anterior of tail. Anterior to the forelimb and ventral to the dorsolateral line is some brown ticking that continues around the gular region. The ground color of the gular and ventral region is cream color. The ventrum from the gular region posteriorly and the ventral side of limbs are all cream without any markings. Distal portion of ventral tail has some brown ticking. Dorsal aspect of limbs are light brown with posterior portion having some dark brown reticulation.

Distribution.—Found in abundance in the Sierra Madre mountain range of northeast Luzon in the Provinces of Isabella and Cagayan. Occurs in sympatry with *Parvoscincus spah1*.

Natural History.—Found in mid-montane forest in leaf litter and under logs.

Discussion

The combination of our molecular results and morphological comparisons demonstrates that what has been considered one widespread species on Luzon is a complex of seven species. Surprisingly, these species do not share a most recent common ancestor, and instead, are composed of two independent clades that have converged on a similar

morphology (Fig 5.2). Examination of the type material in the British Natural History Museum allowed us to identify the true clade of *Parvoscincus decipiens* and we have described the other clades as new species. Among the species that share a most recent common ancestor with *P. decipiens* (*P. spah1, P. spah2, P. spah3*), there are significant differences in color pattern, along with some scale differences that can be used to distinguish the clades. There are some regions of sympatry between these species of Luzon, *Parvoscincus decipiens* and *Parvoscincus spah1* are sympatric in the Sierra Madre mountain range, *Parvoscincus spah1* also occurrs in Kalinga and Aurora provinces. *Parvoscincus spah2* occurs in the Bicol Peninsula on Mt. Labo and Mt. Banahao at lower elevations (< 700 m). *Parvoscincus spah3* occurs on the Bicol Peninsula and lake region of southern Luzon on Mt. Malinao, Mt. Isarog, Mt. Labo, and Mt. Makiling. *Parvoscincus spah3* also occurs on Polillo Island, which was connected to the Bicol Peninsula during the Pleistocene. *Parvoscincus spah2* and *Parvoscincus spah3* occur sympatrically on Mt. Labo.

The new species have greater genetic diversity (based on branch lengths) than true *P. decipiens*, showing deep splits between populations (Fig 5.2). Despite the genetic diversity, there are not large-scale morphological changes. The differences among the new species are primarily color-pattern differences; we found differentiation in traditional morphological characters, such as scale counts and body shape. We identified a new character state, the presence of apical pits on the scale and

coded the presence of this feature on the forelimb, hind limb, flank, and dorsum. All members of the *P. decipiens* Group have apical pits on the flanks and hind limbs, but apical pits are variably present on the dorsum and forelimbs. Both *P. spah3* and *P. decipiens* lack apical pits on the dorsum and forelimb, and are sister taxa, suggesting a shared evolution of these character states. The role of apical pits in the physiology and natural history of these species is unknown. They seem to be more prevalent in smaller species, in which they may be involved in water balance or a sensory function. Histological examination of these structures is warranted.

The second clade of new species is closely related to the *Parvoscincus beyeri* complex of high-elevation species (Brown et al. 2010). The three species are also high-elevation specialists suggesting a single origin of high elevation *Parvoscincus* on Luzon. *Parvoscincus spah5* occurs on Mt. Banahao and maybe sympatric with *Parvoscincus spah2,* depending on the range of elevation of the latter species. *Parvoscincus spah6* occurs on Mt. Palali in Nueva Viscaya Province, and *P. spah7* occurs at high and mid-elevation on Mt. Dayap. Each species seems to be endemic to its mountain range, though sampling of high elevation sites has been limited; future work may reveal new populations of these species or additional new species. These species lack apical pits on the dorsum and forelimbs, as do their close relatives (Table 5.1).

This revision of the *Parvoscincus decipiens* complex increases the number of species of the genus on Luzon to 18. This revision and Brown et al. (2010) show that there is a significant amount of undiscovered and/or cryptic diversity within the scincid lizard fauna of Luzon Island. With these new descriptions, Luzon now has the highest species richness for skinks of all Philippine islands with Mindanao being the second richest. Mindanao is composed of multiple independent lineages, which have colonized the island independently (Linkem et al. 2011) whereas our results for Luzon increase the endemic diversity of the island and degree of intra-island speciation. Comparing these large islands and what may drive species richness on each island is an area of future research.

Table 5.1 Ranges of size (SVL) and scale counts for *Parvoscincus* species including the new species. Presence (+) or absence (0) or apical pores on different parts of the body.

	SVL	PV	MBSR	TIV	Dorsal apical pores	Lateral apical pores	Fore-limb apical pores	Hind limb apical pores
spah 1	33.75–44.12	58–72	31–37	17–22	+	+	+	+
spah 2	30.89–43.14	65–74	32–36	16–19	+	+	+	+
spah 3	32.02–43.27	58–69	33–36	16–18	0, +	+	+	+
spah 5	39.3–45.09	62–66	28–32	14–17	0	+	0	0, +
spah 6	39.28	73	32	14	0	+	0	+
spah 7	39.55–46.64	65–75	31–35	15–17	0	+	0	+
decipiens	35.02–40.62	54–63	30–34	14–18	0	+	0, +	+
leucospilos	52–55	63–68	30–32	16–18	0	+	0	+
steerei	26.4–36.0	52–63	28–32	9–14	+	+	0	+
tagapayo	23.1–32.1	54–61	28–30	9–11	0	+	0	+
sisoni	26.5–33.6	62–68	24–26	11–12	?	?	?	?
palawanensis	28.1–34.3	48–54	22–24	10–12	?	?	?	?
lawtoni	33.1–47.0	58–64	28–29	12–15	0	+	0	+
luzonensis	39.9–47.8	65–73	27–29	9–12	?	?	?	?
kitangladensis	48.88–56.25	62–77	30–38	15–18	0	+	0	+
hadros	73.5–86.7	108–111	45–47	18–22	0	0	0	0
beyeri	57.8–72.9	88–102	38–42	18–21	0	0	0	0
boyingi	46.1–66.7	88–96	37–42	19–21	0	+	0	+
laterimaculatus	42.1–57.1	74–83	34–38	17–18	0	+	0	+
igorotorum	51.9–57.5	98–101	44–45	20	?	?	?	?

Table 5.2 Summary of continuous measurements and scale counts for the new species and *P. decipiens*. Separated by males and females summarizing the range, mean and standard deviation for each measurement.

	spah1	*spah2*	*spah3*	*spah5*	*spah6*	*spah7*	*decipiens*
	31 Males; 25 Females	3 Males; 3 females	18 Males; Females 16	5 Males; 2 Females	1 Female	1 Male; 5 Females	7 Males; 8 Females
PVSR male	58–73	65–71	58–69	64–66	—	65	56–61
	(64.3 ± 3.43)	(68 ± 3)	(63 ± 2.61)	(65 ± 0.84)	—	—	(58 ± 1.62)
female	61–73	67–74	58–67	62–66	73	68–75	54–63
	(65.8 ± 2.93)	(70 ± 3.5)	(63 ±2.38)	(64 ± 2.83)	—	(72 ± 2.74)	(60 ± 2.62)
MBSR male	31–37	33–36	35–38	28–32	—	33	31–34
	(34.2 ± 1.56)	(35 ± 1.73)	(36 ± 1.08)	(30 ± 1.48)	—	—	(32 ± 1.11)
female	31–37	32–35	33–37	28	32	31–35	30–34
	(33.6 ± 1.76)	(34 ± 1.73)	(36 ± 1.10)	(28 ± 0)	—	(33 ± 1.58)	(32 ± 1.46)
Lamellae male	17–22	16–19	15–19	14–17	—	16	14–17
	(18.9 ± 1.26)	(18 ± 1.53)	(17 ± 0.83)	(16 ± 1.14)	—	—	(16 ± 1.13)
female	17–22	18, 19	15–18	17	14	15–17	15–18
	(19.0 ± 1.50)	(18 ± 0.58)	(17 ± 0.83)	(17 ± 0)	—	(17 ± 0.89)	(16 ± 0.93)
SVL male	35.65–46.48	36.16–41.77	34.67–43.45	42.41–45.09	—	46.61	35.0–40.0
	(41.79 ± 2.60)	(38.14 ± 3.15)	(39.62 ± 2.43)	(43.72 ± 1.17)	—	—	(38.4 ± 1.60)
female	33.05–49.04	40.61–43.14	32.02–45.34	39.3–43.8	39.28	39.6–46.6	36.6–40.6
	(42.11 ± 3.93)	(42.49 ± 1.45)	(38.94 ± 3.95)	(41.6 ± 3.19)	—	(43.2 ± 2.73)	(38.5 ± 1.45)

AGD male	17.26–23.83	16.55–20.61	17.27–22.48	20.2–23.1	—	24.07	14.6–19.4
	(21.14 ± 1.75)	(18.15 ± 2.16)	(19.62 ± 1.33)	(22.3 ± 1.19)	—	—	(17.5 ± 1.51)
female	15.39–24.93	18.10–21.41	15.28–22.76	18.2–22.3	19.95	19.9–25.5	16.9–21.1
	(21.89 ± 2.69)	(20.29 ± 1.90)	(19.53 ± 2.69)	(20.3 ± 2.87)	—	(22.7 ± 2.26)	(19.1 ± 1.37)
HFL male	13.08–16.60	13.16–14.47	12.54–15.37	14.0–16.3	—	16.45	13.4–16.0
	(14.67 ± 0.90)	(13.67 ± 0.70)	(14.06 ± 0.77)	(15.3 ± 1.00)	—	—	(14.5 ± 0.84)
female	12.62–15.70	14.68–15.19	11.70–15.93	13.4–16.3	13.37	14.3–15.9	12.0–14.9
	(14.36 ± 0.92)	(14.90 ± 0.26)	(13.76 ± 1.18)	(14.9 ± 2.02)	—	(15.1 ± 0.67)	(13.2 ± 0.80)
HL male	7.84–9.33	7.51–8.17	7.37–9.29	8.6–9.0	—	9.46	7.8–8.9
	(8.63 ± 0.45)	(7.85 ± 0.33)	(8.51 ± 0.56)	(8.8 ± 0.15)	—	—	(8.5 ± 0.35)
female	6.99–9.49	8.39–8.90	7.28–9.22	7.6–8.2	8.35	8.1–8.9	7.4–8.5
	(8.53 ± 0.59)	(8.57 ± 0.29)	(8.22 ± 0.60)	(7.9 ± 0.46)	—	(8.6 ± 0.39)	(8.1 ± 0.34)
HW male	4.79–6.45	4.46–4.89	4.99–6.59	4.9–5.2	—	5.64	4.8–5.8
	(5.72 ± 0.39)	(4.69 ± 0.22)	(5.76 ± 0.48)	(5.1 ± 0.12)	—	—	(5.4 ± 0.35)
female	4.53–6.26	4.90–5.31	4.55–6.48	4.8–5.0	4.93	5.0–5.8	4.9–5.5
	(5.59 ± 0.45)	(5.17 ± 0.23)	(5.49 ± 0.56)	(4.9 ± 0.13)	—	(5.3 ± 0.32)	(5.2 ± 0.21)
HH male	3.64–5.44	3.40–3.81	3.78–5.31	4.0–4.3	—	4.47	3.7–4.3
	(4.40 ± 0.37)	(3.62 ± 0.21)	(4.51 ± 0.47)	(4.1 ± 0.14)	—	—	(4.0 ± 0.21)
female	3.16–5.11	3.83–4.22	3.38–4.96	3.5–4.0	3.44	3.8–4.5	3.5–4.1
	(4.30 ± 0.47)	(4.02 ± 0.20)	(4.13 ± 0.47)	(3.8 ± 0.33)	—	(4.1 ± 0.30)	(3.9 ± 0.20)
RostL male	2.49–3.34	2.69–3.00	2.54–3.74	2.9–3.2	—	3.24	2.8–3.5

	(3.00 ± 0.20)	(2.84 ± 0.16)	(3.11 ± 0.25)	(3.0 ± 0.11)	—	—	(3.1 ± 0.18)
female	2.58–3.42	2.95–3.16	2.40–3.72	2.9–3.1	2.78	2.8–3.2	2.7–3.3
	(2.97 ± 0.19)	(3.08 ± 0.12)	(2.88 ± 0.31)	(3.0 ± 0.12)	—	(3.0 ± 0.17)	(2.9 ± 0.18)
IND male	1.53–2.36	1.32–1.39	1.59–2.31	1.6–1.8	—	2.04	1.6–2.0
	(1.93 ± 0.21)	(1.35 ± 0.04)	(1.81 ± 0.17)	(1.7 ± 0.08)	—	—	(1.8 ± 0.13)
female	1.45–2.37	1.38–1.48	1.36–2.05	1.5–1.6	1.94	1.6–2.1	1.4–1.8
	(1.87 ± 0.23)	(1.43 ± 0.05)	(1.66 ± 0.21)	(1.6 ± 0.03)	—	(1.8 ± 0.19)	(1.7 ± 0.14)
AGD/ SVL male	0.47–0.55	0.45–0.49	0.47–0.51	0.48–0.54	—	0.52	0.42–0.51
	(0.51 ± 0.02)	(0.47 ± 0.02)	(0.50 ± 0.01)	(0.51 ± 0.02)	—	—	(0.46 ± 0.03)
female	0.46–0.57	0.45–0.50	0.46–0.55	0.46–0.51	0.51	0.50–0.55	0.46–0.53
	(0.52 ± 0.03)	(0.48 ± 0.03)	(0.50 ± 0.03)	(0.49 ± 0.03)	—	(0.52 ± 0.02)	(0.50 ± 0.02)
IND/ RostL male	0.50–0.85	0.46–0.49	0.51–0.72	0.52–0.56	—	0.63	0.53–0.63
	(0.65 ± 0.08)	(0.48 ± 0.01)	(0.59 ± 0.06)	(0.55 ± 0.01)	—	—	(0.58 ± 0.03)
female	0.52–0.78	0.44–0.48	0.53–0.68	0.52–0.53	0.69	0.53–0.69	0.52–0.63
	(0.63 ± 0.07)	(0.46 ± 0.02)	(0.58 ± 0.05)	(0.52 ± 0.01)	—	(0.62 ± 0.07)	(0.57 ± 0.04)

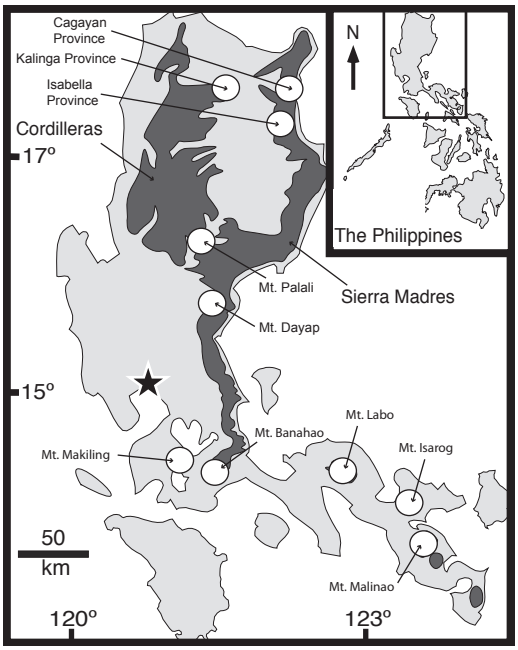

Figure 5.1 Map of Luzon Island (Philippines in inset) showing the localities where *P. decipiens* complex skinks can be found. The major mountain ranges of Northern Luzon are shown in dark gray.

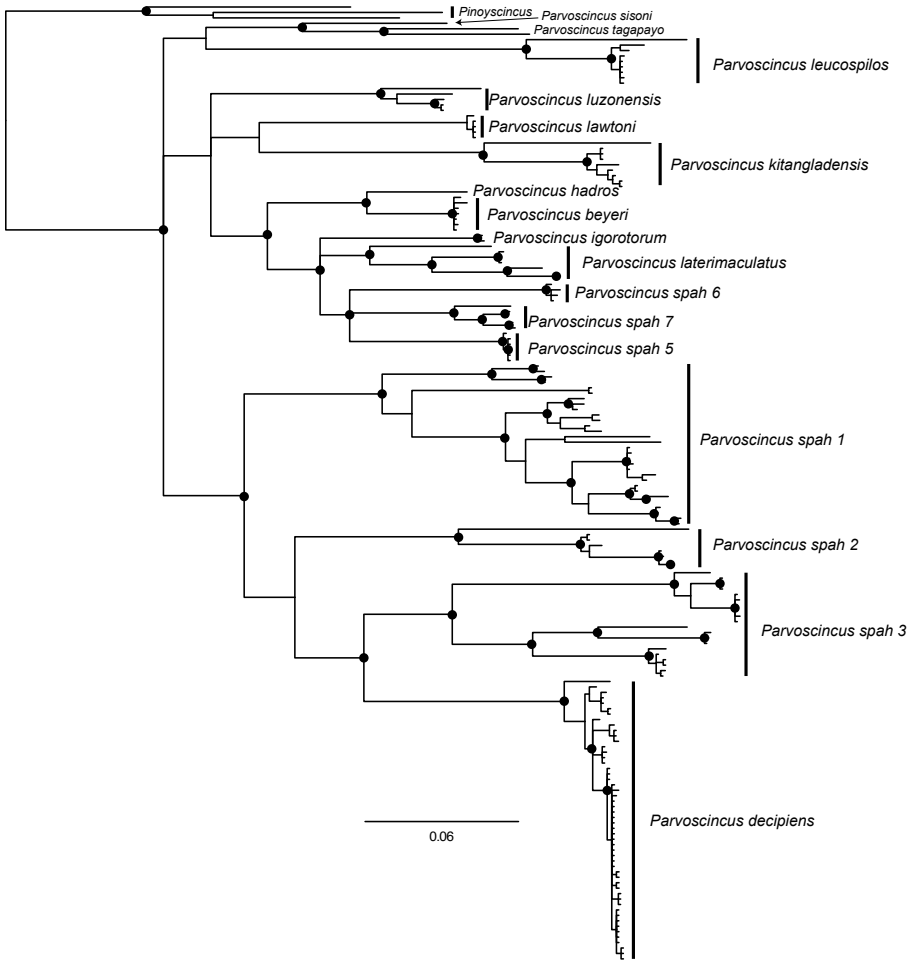

Figure 5.2 Partitioned Bayesian majority rule consensus estimate of molecular phylogeny from the ND2 data of *Parvoscincus*. Populations within the *P. decipiens* complex are genetically unique and are diagnosed as new species based on morphological differences. Black circles label nodes with posterior probabilities above 0.95.

Figure 5.3 Photos of the species in life. A) *Parvoscincus spah1* (ACD 2862); B) *Parvoscincus spah3* male; C) *Parvoscincus spah3* female; D) *Parvoscincus spah2* (CWL 486); E) *Parvoscincus spah5*; *Parvoscincus decipiens* (ACD 2146)

Figure 5.4 Photographs of heads from ventral, lateral, and dorsal perspective to show color pattern variation among species. Images A, I, Q *Parvoscincus decipiens*; B. J, R *Parvoscincus spah1* holotype; C, K, S, *Parvoscincus spah2* holotype; D, L, T *Parvoscincus spah3* holotype (male); E, M, U, *Parvoscincus spah3* (female); F, N, V, *Parvoscincus spah5* holotype; G, O, W, *Parvoscincus spah6* holotype; H, P, X, *Parvoscincus spah7* holotpye.

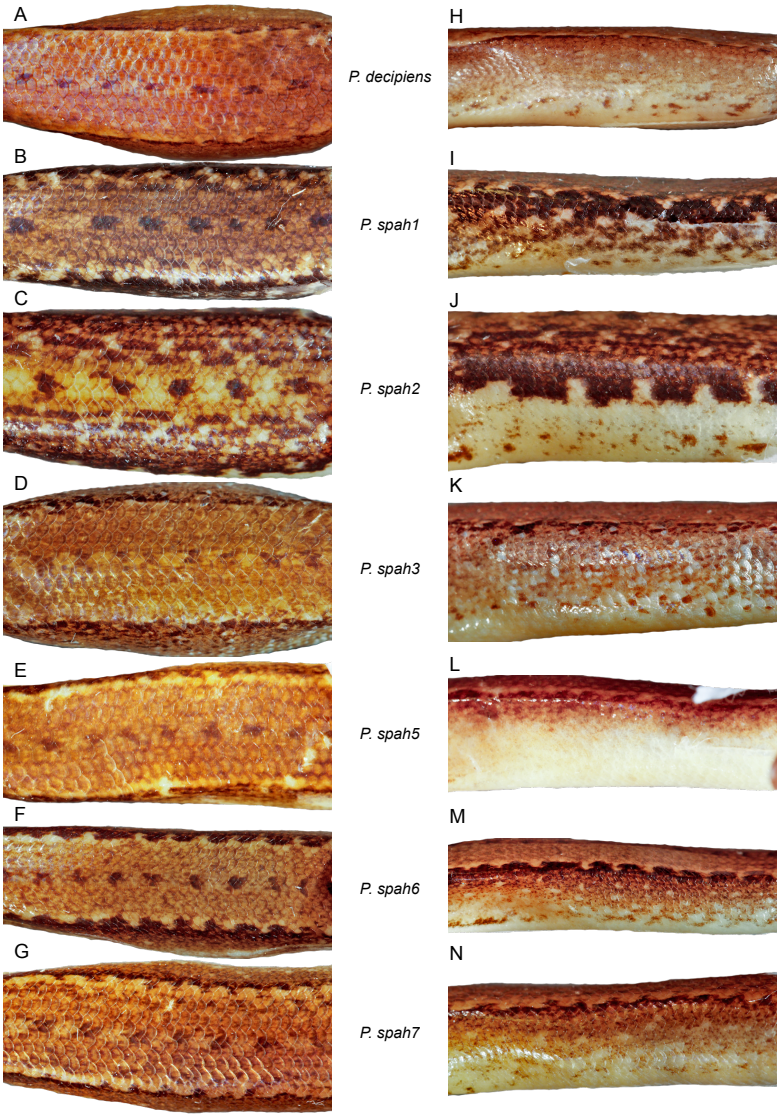

Figure 5.5 Photographs of dorsal and lateral views of the thorax to show color pattern variation among species.

Literature Cited

Allison A, Greer AE. 1986. Egg shells with pustulate surface structures: basis for a new genus of New Guinea skinks (Lacertilia: Scincidae). *Journal of Herpetology*. 20:116–119.

Arevalo E, Davis SK, Sites Jr. JW. 1994. Mitochondrial DNA sequence divergence and phylogentic relationships among eight chromosome races of the *Sceloporus grammicus* complex (Phrynosomatidae) in Central Mexico. *Systematic Biology* 43:387–418.

Blackburn DC, Bickford DP, Diesmos AC, Iskandar DT, Brown RM. 2010. An ancient origin for the enigmatic Flat-Headed Frogs (Bombinatoridae: Barbourula) from the islands of Southeast Asia. *PLoS ONE* 5:e12090.

Boulenger GA. 1894. Second report on additions to the lizard collections in the Natural History Museum. *Proceedings of the Zoological Society London* 1894:722–736.

Boulenger GA. 1887. *Catalogue of the Lizards of the British Museum (Natural History). III. Lacertidae, Gerrhosauridae, Scincidae, Anelytropisidae, Dibamidae, Chameleontidae*. Trustees of the British Museum, London, England.

Böhme W. 1981. A new lygosomine skink from Thailand (Reptilia: Scincidae). *Bollettino del Museo Civico di Storia Naturale di Verona* 8:375–382.

Brandley MC, Schmitz A, Reeder TW. 2005. Partitioned Bayesian analyses, partition choice, and the phylogenetic relationships of scincid lizards. *Systematic Biology* 54:373–390.

Brown RM. 2006. Recognition of Philippine Amphibian Diversity. In: Catibog-Sinha CS, Heaney LR (Eds.). *Philippine Biodiversity: Principles and Practice*. Haribon Foundation for Conservation of Natural Resources, Quezon City, Philippines, pp. 45

Brown RM, Diesmos AC. 2001 (2002). Application of lineage-based species concepts to oceanic island frog populations: the effects of differing taxonomic philosophies on the estimation of Philippine biodiversity. *The Silliman Journal* 42:133–162.

Brown RM, Diesmos AC. 2009. Philippines, Biology. In: Gillespie R, Clague D (Eds.). *Encyclopedia of Islands*. University of California Press, Berkeley, USA, pp. 723–732.

Brown RM, Guttman SI. 2002. Phylogenetic systematics of the *Rana signata* complex of Philippine and Bornean stream frogs: reconsideration of Huxley's modification of Wallace's Line at the Oriental–Australian faunal zone interface. *Biological Journal of the Linnean Society* 76:393–461.

Brown RM, Diesmos AC, Alcala AC. 2001 (2002). The state of Philippine herpetology and the challenges for the next decade. *The Silliman Journal* 42:18–87.

Brown RM, Ferner JW, Greer AE. 1995. A new species of lygosomine lizard (Reptilia: Lacertilia: Scincidae; *Sphenomorphus*) from Mt. Isarog, Luzon Island, Philippines. *Proceedings of the Biological Society of Washington* 108:18–28.

Brown RM, Linkem CW, Diesmos AC, Balete DS, Duya MV, Ferner JW. 2010. Species boundaries in Philippine montane forest skinks (Genus

Sphenomorphus): three new species from the mountains of Luzon and clarification of the status of the poorly known *Sphenomorphus beyeri*, *Sphenomorphus knollmanae*, and *Sphenomorphus laterimaculatus*. *Scientific Papers, Natural History Museum, University of Kansas* 42:1–27.

Brown RM, McGuire JA, Diesmos AC. 2000. Status of some Philippine frogs related to *Rana everetti* (Anura: Ranidae), description of a new species, and resurrection of *Rana igorota* Taylor 1922. *Herpetologica* 56:81–104.

Brown RM, McGuire JA, Ferner JW, Alcala AC. 1999. New species of diminutive scincid lizard (Squamata; Lygosominae; *Sphenomorphus*) from Luzon Island, Republic of the Philippines. *Copeia* 1999:362–370.

Brown RM, Stuart BL. In press. Patterns of biodiversity discovery through time: an historical analysis of amphibian species discoveries in the Southeast Asian mainland and island archipelagos. In: Gower DJ, Johnson KG, Richardson JE, Rosen BR, Rüber L, Williams ST (Eds.). *Biotic Evolution and Environmental Change in Southeast Asia*. Cambridge University Press, UK, pp. 348–389.

Brown RP, Yang Z. 2011. Rate variation and estimation of divergence times using strict and relaxed clocks. *BMC Evolutionary Biology* 11:271.

Brown WC. 1995. A new lizard of the genus *Sphenomorphus* (Reptilia: Scincidae) from Mt. Kitanglad, Mindanao Island, Philippine Islands. *Proceedings of the Biological Society of Washington* 108:388–391.

Brown WC, Alcala AC. 1970. The zoogeography of the Philippine Islands, a fringing archipelago. *Proceedings of the California Academy of Science* 38:105–130.

Brown WC, Alcala AC. 1980. *Philippine Lizards of the Family Scincidae*. Silliman University Press, Dumaguete City, Philippines.

Catibog-Sinha CS, Heaney LR. 2006. *Philippine Biodiversity: Principles and Practice*. Haribon Foundation for the Conservation of Natural Resources, Inc., Quezon City, Philippines.

Chapple DG, Ritchie PA, Daugherty CH. 2009. Origin, diversification, and systematics of the New Zealand skink fauna (Reptilia: Scincidae). *Molecular Phylogenetics and Evolution* 52:470–487.

Collar NJ, Mallari NAD, Tabaranza Jr. B. 1999. *Threatened Birds of the Philippines*. Bookmark, Inc., Makati City, Philippines.

Conrad JL. 2008. Phylogeny and systematics of Squamata (Reptilia) based on morphology. *Bulletin of the American Museum of Natural History* 310:1–182.

De Graciansky P-C, Hardenbol J, Jacquin T, and Vail PR. 1998. Mesozoic and Cenozoic sequence stratigraphy of European basins. *Society for Sedimentary Geology Special Publication No. 60*.

DENR. Department of Environmental Resources and United Nations Environment Programme. 1997. *Philippine biodiversity: as assessment and action plan*. Bookmark, Inc., Makati City, Philippines.

de Queiroz, K, 1998. The general lineage concept of species. Species criteria, and the process of speciation. In: Howard DJ, Berlocher SH (Eds.). *Endless Forms: Species and Speciation*. Oxford University Press, New York, New York, USA, pp. 57–75.

Dickerson, RE, Merrill, ER, McGregor, RC, Schultze, W, Taylor, EH, Herre, AWCT, 1928. *Distribution of Life in The Philippines*. Bureau of Science, Manila, Philippines.

Diesmos, AC, Brown, RM, Alcala, AC, Sison, RV, Afuang, LE, Gee, GVA, 2002. Philippine amphibians and reptiles. In: Ong PS, Afuang LE, Rosell-Ambal RG (Eds.) *Philippine Biodiversity Conservation Priorities: a Second Iteration of the National Biodiversity Strategy and Action Plan*. Department of the Environment and Natural Resources–Protected Areas and Wildlife Bureau, Conservation International Philippines, Biodiversity Conservation Program–University of the Philippines Center for Integrative and Developmental Studies, and Foundation for the Philippine Environment, Quezon City, Philippines, pp. 26–44.

Drummond AJ, Rambaut A. 2007. BEAST: Bayesian evolutionary analysis by sampling trees. *BMC Evolutionary Biology* 7:214.

Drummond AJ, Ho SYW, Phillips MJ, Rambaut A. 2006. Relaxed phylogenetics and dating with confidence. *PLoS Biology* 4:e88.

Edgar RC. 2004. MUSCLE: Multiple sequence alignment with high accuracy and high throughput. *Nucleic Acids Research* 32:1792–1797.

Esselstyn JA, Brown RM. 2009. The role of repeated sea-level fluctuations in the generation of shrew (Soricidae: *Crocidura*) diversity in the Philippine Archipelago. *Molecular Phylogenetics and Evolution* 53:171–181.

Esselstyn JA, Garcia HJD, Saulog MG, Heaney LR. 2008. A new species of *Desmalopex (Pteropodidae*) from the Philippines, with a phylogenetic analysis of the Pteropodini. *Journal of Mammalogy* 89:815–825.

Esselstyn JA, Timm RM, Brown RM. 2009. Do geological or climatic processes drive speciation in dynamic archipelagos? The evolution of shrew diversity on SE Asian Islands. *Evolution* 63:2595–2610.

Esselstyn JA, Widmann P, Heaney LR. 2004. The mammals of Palawan Island, Philippines. *Proceedings of the Biological Society of Washington* 117:271–302.

Evans BJ, Supriatna J, Andayani N, Setiadi MI, Cannatella DC, Melnick D. 2003a. Monkeys and toads define areas of endemism on the island of Sulawesi. *Evolution* 57:1436–1443.

Evans BJ, Brown RM, McGuire JA, Supriatna J, Andayani N, Diesmos AC, Iskandar D, Melnick DJ, Cannatella DC. 2003b. Phylogenetics of fanged frogs: testing biogeographic hypotheses at the interface of the Asian and Australian faunal zones. *Systematic Biology* 52:794–819.

Evans SE, Manabe M. 1999. Early Cretaceous lizards from the Okurodani Formation of Japan. *Geobios* 32:889–899.

Ferner JW, Brown RM, Greer AE. 1997. A new genus and species of moist closed canopy forest skinks from the Philippines. *Journal of Herpetology* 31:187–192.

Fitzinger, LJFJ. 1843. *Systema Reptilium*. Fasciculus Primus. Wien: Braumüller et Seidel.

Frost DR, Hillis DM. 1990. Species in concept and practice: herpetological applications. *Herpetologica* 46:87–104.

Gardner MG, Hugall AF, Donnellan SC, Hutchinson MN, Foster R. 2008. Molecular systematics of social skinks: phylogeny and taxonomy of the

Egernia group (Reptilia: Scincidae). *Zoological Journal of the Linnean Society* 154:781–794.

Goldman N, Anderson JP, Rodrigo AG. 2000. Likelihood-based tests of topologies in Phylogenetics. *Systematic Biology* 49:652–670.

Graybeal A, Cannatella DC. 1995. A new taxon of Bufonidae from Peru, with descriptions of two new species and a review of the phylogenetic status of supraspecific bufonid taxa. *Herpetologica* 51:105–131.

Greer AE. 1974. The generic relationships of the scincid lizard genus *Leiolepisma* and its relatives. *Australian Journal of Zoology Supplement* **31**:1–67.

Greer AE. 1979. A phylogenetic subdivision of Australian skinks. *Records of the Australian Museum* 32:339–371.

Greer AE. 1991. *Lankascincus*, a new genus of scincid lizards from Sri Lanka, with descriptions of three new species. *Journal of Herpetology* 25:59–64.

Greer AE. 1997. *Leptoseps*: a new genus of scincid lizards from Southeast Asia. *Journal of Herpetology* 31:393–398.

Greer AE, Biswas S. 2004. A generic diagnosis for the Southeast Asian scincid lizard genus *Tropidophorus* Duméril & Bibron, 1839 (Reptilia: Scincidae). *Journal of Herpetology* 38:426–430.

Greer AE, Parker F. 1967. A new scincid lizard from the northern Solomon Islands. *Breviora* 275:1–20.

Greer AE, Parker F. 1974. The *fasciatus* species group of *Sphenomorphus* (Lacertilia: Scincidae): notes on eight previously described species and

descriptions of three new species. *Papua New Guinea Scince Society Proceedings* 25:31–61.

Greer AE, Simon M. 1982. An unusual new genus and species of scincid lizard from New Guinea. *Journal of Herpetology* 16:131–139.

Greer AE, Shea G. 2003. A new character within the taxonomically difficult *Sphenomorphus* group of lygosomine skinks, with a description of a new species from New Guinea. *Journal of Herpetology* 38:79–87.

Greer AE, David P, Teynié A. 2006. The Southeast Asian scincid lizard *Siaphos tridigitus* Bourret, 1939 (Reptilia, Scincidae): a second specimen. *Zoosystema* 28:785–790.

Grismer JL, Leong TM, Norsham SY. 2003. Two new Southeast Asian skinks of the genus *Larutia* and intrageneric phylogenetic relationships. *Herpetologica* 59:554–566.

Grismer LL. 2006. Two new species of skinks (Genus *Sphenomorphus* Fitzinger 1843) from the Seribuat Archipelago West Malaysia. *Herpetological Natural History* 9:151–162.

Grismer LL. 2007a. A new species of small montane forest floor skink (Genus *Spenomorphus* Fitzinger 1843) from southern peninsular Malaysia. *Herpetologica* 63:544–551.

Grismer LL. 2007b. A new species of insular skink (Genus *Sphenomorphus* Fitzinger 1843) from the Langkawi Archipelago, Kedah, West Malaysia with the first report of the herpetofauna of Pulau Singa Besar and an updated checklist of the herpetofauna of Pulau Langkawi. *Zootaxa* 1691:53–56.

Grismer LL, Wood Jr. PL, Grismer JL. 2009a. A new insular species of skink of the genus *Sphenomorphus* Strauch 1887 (Squamata: Scincidae) from Pulau Perhentian Besar, Terengganu, Peninsular Malaysia. *Tropical Life Sciences Research* 20:51–69.

Grismer LL, Ahmad N, Onn CK. 2009b. A new, diminutive, upland *Sphenomorphus* Fitzinger 1843 (Squamata: Scincidae) from Belum-Temengor Forest complex, Peninsular Malaysia. *Zootaxa* 2312:27–38.

Hall R. 1997. Cenozoic plate tectonic reconstructions of SE Asia. In: Fraser AJ, Matthews SJ, Murphy RW (Eds.). *Petroleum geology of Southeast Asia*. Geological Society, London, UK, pp. 11–23.

Hall R. 1998. The plate tectonics of Cenozoic SE Asia and the distribution of land and sea. In: Hall R, Holloway JD (Eds.). *Biogeography and geological evolution of SE Asia*. Backhuys Publishers, Leiden, Neitherlands, pp. 99–131.

Hall R. 2001. Cenozoic reconstructions of SE Asia and the SW Pacific: changing patterns of land and sea. In: Metcalfe I, Smith JMB, Morwood M, Davidson I (Eds.). *Faunal and floral migrations and evolution in SE Asia-Australasia*. Balkema, Lisse, pp. 35–56.

Hall R. 2002. Cenozoic geological and plate tectonic evolution of SE Asia and the SW Pacific: computer-based reconstructions and animations. *Journal of Asian Earth Sciences* 20:353–434.

Hall R. 2011. Australia-SE Asia collision: plate tectonics and crustal flow. In: Hall R, Cottam MA, Wilson MEJ (Eds.). *The SE Asian gateway: history*

and tectonics of Australia-Asia collision. The Geological Society of London, London, pp. 75–109.

Heaney LR. 2009. Southeast Asia's changing palaeogeography. *Blumea* 54:148–161.

Heaney LR. 1985. Zoogeographic evidence for middle and late Pleistocene land bridges to the Philippine Islands. *Modern Quaternary Research in SE Asia* 9:127–144.

Heaney LR. 1986. Biogeography of small mammals in SE Asia: estimates of rates of colonization, extinction and speciation. *Biological Journal of the Linnean Society* 28:127–165.

Heaney LR, Mittermeier RA. 1997. The Philippines. In: Mittermeier RA, Robles Gil P, Mittermeier GG (Eds.). *Megadiversity: earth's biologically wealthiest nations*. CEMEX, Monterrey, Mexico, pp 236–255.

Heaney LR, Regalado JC. 1998. *Vanishing treasures of the Philippine rain forest*. The Field Museum, Chicago. IL, USA.

Heaney LR, Rickart EA. 1990. Correlation of clades and clines: geographic, elevational, and phylogenetic distribution patterns among Philippine mammals. In: Peters G, Hutterer R (Eds.). *Vertebrates in the Tropics*. Museum Alexander Koenig, Bonn, Germany, pp. 321–332.

Heaney LR, Balete DS, Dolar ML, Alcala AC, Dans ATL, Gonzales PC, Ingle NR, Lepiten MV, Oliver WLR, Ong PS, Rickart EA, Tabaranza BR, Utzurrum RB. 1998. A synopsis of the mammalian fauna of the Philippine Islands. *Fieldiana* 88:1–61.

Heaney LR, Walsh JS, Peterson AT. 2005. The roles of geological history and

colonization abilities in genetic differentiation between mammalian populations in the Philippine archipelago. *Journal of Biogeography* 32:229–247.

Honda M, Ota H, Kobayashi M, Nabhitabhata J, Yong H, Hikida T. 2000. Phylogenetic relationships, character evolution, and biogeography of the subfamily Lygosominae (Reptilia: Scincidae) inferred from mitochondrial DNA sequences. *Molecular Phylogenetics and Evolution* 15:452–461.

Honda M, Ota H, Kohler G, Ineich I, Chirio L, Chen S-L, Hikida T. 2003. Phylogeny of the lizard subfamily Lygosominae (Reptilia: Scincidae), with special reference to the origin of the New World taxa. *Genes Genetics Systematics* 78:71–80.

Honda M, Ota H, Murphy RW, Hikida T. 2006. Phylogeny and biogeography of water skinks of the genus *Tropidophorus* (Reptilia: Scincidae): a molecular approach. *Zoologica Scripta* 35:85–95.

Huelsenbeck JP, Ronquist F. 2001. MRBAYES: Bayesian inference of phylogenetic trees. *Bioinformatics* 17:754–755.

Huelsenbeck JP, Suchard MA. 2007. A nonparametric method for accommodating and testing across-site rate variation. *Systematic Biology* 56:975–987.

Hugall AF, Lee MSY. 2004. Molecular claims of Gondwanan age for Australian agamid lizards are untenable. *Molecular Biology and Evolution* 21:2102–2110.

Hugall AF, Foster R, Lee MSY. 2007. Calibration choice, rate smoothing, and the pattern of tetrapod diversification according to the long nuclear gene RAG-1. *Systematic Biology* 56:543–563.

Hutchinson MN. 1992. Origins of the Australian scincid lizards: a preliminary report on the skinks of Riversleigh. *Records of the Northern Territory Museum of Arts and Sciences (The Beagle)* 9:61–70.

Inger RF. 1954. Systematics and zoogeography of Philippine Amphibia. *Fieldiana* 33:181–531.

Inger RF. 1958. Three new skinks related to *Sphenomorphus variegatus* (Peters). *Fieldiana: Zoology* 39:257–268.

Inger RF, Lian TF, Lakim M, Yambun P. 2001. New species of the lizard genus *Sphenomorphus*, (Lacertilia: Scincidae), with notes on ecological and geographic distribution of species in Sabah, Malaysia. *The Raffles Bulletin of Zoology* 49:181–189.

Jansa SA, Barker FK, Heaney LR. 2006. The pattern and timing of diversification of Philippine endemic rodents: evidence from mitochondrial and nuclear gene sequences. *Systematic Biology* 55:73–88.

Jones AW, Kennedy RS. 2008. Evolution in a tropical archipelago: comparative phylogeography of Philippine fauna and flora reveals complex patterns of colonization and diversification. *Biological Journal of the Linnean Society* 95:620–639.

Katoh K, Kuma K-I, Toh H, Miyata T. 2005. MAFFT version 5: improvement in accuracy of multiple sequence alignment. *Nucleic Acids Research* 33:511–518.

Kennedy R.S., Gonzales P.C., Dickinson E.C., Miranda H.C., Fisher T.H., 2000. *A guide to the birds of the Philippines*. Oxford University Press: Oxford.

Kloss CB. 1929. The zoo-geographic boundaries between Asia and Australia and some Oriental sub-regions. *Bulletin of the Raffles Museum* 1929:1–10.

Kocher TD, Thomas WK, Meyer A, Edwards SV, Paabo S, Villablanca FX, Wilson AC. 1989. Dynamics of mitochondrial DNA evolution in animals: amplification and sequencing with conserved primers. *Procedings of the National Academy of Sciences USA* **86**:6196–6200.

Landis CA, Campbell HJ, Begg JG, Mildenhall DC, Paterson AM, Trewick SA. 2008 The Waipounamu Erosion Surface: questioning the antiquity of the New Zealand land surface and terrestrial fauna and flora. *Geological Magazine* 145:173–197.

Lartillot N, Lepage T, Blanquart S. 2009. PhyloBayes 3: a Bayesian software package for phylogenetic reconstruction and molecular dating. *Bioinformatics* 25:2286–2288.

Leaché AD. 2009. Species tree discordance traces to phylogeographic clade boundaries in North American fence lizards (Sceloporus). *Systematic Biology* 58:547–559.

Lee MSY, Hutchinson MN, Worthy TH, Archer M, Tennyson AJD, Worthy JP, Scofield RP. 2009. Miocene skinks and geckos reveal long-term conservatism of New Zealand's lizard fauna. *Biology Letters* 5:833–837.

Linkem CW, Diesmos AC, Brown RM. 2010a. A new species of scincid lizards (Genus: *Sphenomorphus*) from Palawan Island, Philippines. *Herpetologica* 66:67–79.

Linkem CW, Hesed KM, Diesmos AC, Brown RM. 2010b. Species boundaries and cryptic lineage diversity in a Philippine forest skink complex (Reptilia;

Squamata; Scincidae: Lygosominae). *Molecular Phylogenetics and Evolution* 56:572–585.

Linkem CW, Diesmos AC, Brown RM. 2011. Molecular systematics of the Philippine forest skinks (Squamata: Scincidae: *Sphenomorphus*): testing morphological hypotheses of interspecific relationships. *Zoological Journal of the Linnean Society* 163:1217–1243.

Lydekker R. 1896. *A geographical history of mammals*. Cambridge University Press, Cambridge, UK.

Macey JR, Larson A, Ananjeva NB, Fang Z, Papenfuss TJ. 1997. Two novel gene orders and the role of light-strand replication in rearrangement of the vertebrate mitochondrial genome. *Molecular Biology and Evolution* 14:91–104.

Mackness BS, Hutchinson MN. 2000. Fossil lizards from the early Pliocene Bluff Downs Local Fauna. *Transactions of the Royal Society of South Australia* 124:17–30.

Maddison DR, Maddison WP. 2004. Batch Architect: automation of simulations and replicated analyses. A package of modules for Mesquite. Version 1.01.

Maddison DR, Maddison WP. 2005. MacClade, Available from: http://macclade.org

Maddison WP, Maddison DR. 2010. Mesquite: a modular system for evolutionary analysis. http://mesquiteproject.org

Mallari NAD, Tabaranza Jr. BR, Crosby MJ. 2001. *Key Conservation Sites in the Philippines*. The Department of Environmental Resources and Bookmark, Inc., Makati City, Philippines.

Marshall DC. 2010. Cryptic failure of partitioned Bayesian phylogenetic analyses: lost in the land of long trees. *Systematic Biology* 59:108–117.

Marshall DC, Simon C, Buckley TR. 2006. Accurate branch length estimation in partitioned Bayesian analyses requires accommodation of among-partition rate variation and attention to branch length priors. *Systematic Biology* 55:993–1003.

Martin JE, Hutchinson MN, Meredith R, Case JA, Pledge NS. 2004. The oldest genus of scincid lizard (Squamata) from the Tertiary Etadunna Formation of South Australia. *Journal of Herpetology* 38:180–187.

McGuire JA, Kiew BH. 2001. Phylogenetic systematics of Southeast Asian flying lizards (Iguania: Agamidae: *Draco*) as inferred from mitochondrial DNA sequence data. *Biological Journal of the Linnean Society* 72:203–229.

Mittermeier RA, Myers N, Mittermeier CG. 2000. *Hotspots: Earth's Biologically Richest and Most Endangered Terrestrial Ecoregions*. Cemex, Conservation International, Mexico City, Mexico

Mittleman MB. 1952. A generic synopsis of the lizards of the subfamily Lygosominae. *Smithsonian Miscellaneous Collections* 117:1–35.

Moyle RG, Anderson MJ, Oliveros CH, Steinheimer F, Reddy S. 2012. Phylogeny and biogeography of the Core Babblers (Aves: Timaliidae). *Systematic Biology* doi: 10.1093/sysbio/sys027

Myers WC, Donnelly MA. 1991. The lizard genus *Sphenomorphus* (Scincidae) in Panama, with a description of a new species. *American Museum Novitates* 3027:1–12.

Myers N, Mittermeier RA, Mittermeier CG, da Fonseca GAB, Kent J. 2000.

Biodiversity hotspots for conservation priorities. *Nature* 403:853–858.

Near TJ, Bossu CM, Bradburd GS, Carlson RL, Harrington RC, Hollingsworth Jr. PR, Keck BP, Etnier DA. Phylogeny and temporal diversification of darters (Percidae: Etheostomatinae). *Systematic Biology* 60:565–595.

Nguyen TQ, Schmitz A, Nguyen TT, Orlov NL, Böhme W, Ziegler T. 2011. Review of the genus *Sphenomorphus* Fitzinger, 1843 (Squamata: Sauria: Scincidae) in Vietnam with description of a new species from northern Vietnam and southern China and the first record of *Sphenomorphus mimicus* Taylor, 1962 from Vietnam. *Journal of Herpetology* 45:145–154.

Nylander JAA. 2004. MrModeltest v2. Program distributed by the author. Evolutionary Biology Centre, Uppsala University. Sweden.

Nylander JAA, Wilgenbusch JC, Warren DL, Swofford DL. 2007. AWTY (Are We There Yet?) a system for graphical exploration of MCMC convergence in Bayesian phylogenetics. *Bioinformatics* 24:581–583.

Ong PS, Afuang LE, Rosell-Ambal RG. (Eds.). 2002. *Philippine Biodiversity Conservation Priorities: a Second Iteration of the National Biodiversity Strategy and Action Plan*. Department of the Environment and Natural Resources–Protected Areas and Wildlife Bureau, Conservation International Philippines, Biodiversity Conservation Program–University of the Philippines Center for Integrative and Developmental Studies, and Foundation for the Philippine Environment, Quezon City, Philippines.

Palumbi, S.R., 1996. The polymerase chain reaction. In: Hillis DM, Moritz C, Mable BK (Eds.). *Molecular Systematics, 2nd edition*. Sinauer Associates, Sunderland, Massachusetts, USA, pp. 205–247.

Philippe H, Snell EA, Bapteste E, Lopez P, Holland PWH, Casane D. 2004. Phylogenomics of eukaryotes: impacts of missing data on large alignments. *Molecular Biology and Evolution* 21:1740–1752.

Posada D. 2008. jModelTest: Phylogenetic Model Averaging. *Molecular Biology and Evolution* 25: 1253-1256.

Rambaut A, Drummond AJ. 2007. Tracer v1.5, Available from http://beast.bio.ed.ac.uk/Tracer.

Ree RH, Sanmartín I. 2009. Prospects and challenges for parametric models in historical biogeographical inference. *Journal of Biogeography* 36:1211–1220.

Ree RH, Smith SA. 2008. Maximum likelihood inference of geographic range evolution by dispersal, local extinction, and cladogenesis. *Systematic Biology* 57:4–14.

Reeder TW. 2003. A phylogeny of the Australian *Sphenomorphus* group (Scincidae: Squamata) and the phylogenetic placement of the crocodile skinks (*Tribolonotus*): Bayesian approaches to assessing congruence and obtaining confidence in maximum likelihood inferred relationships. *Molecular Phylogenetics and Evolution* 27:384–397.

Rice WR. 1989. Analyzing tables of statistical tests. *Evolution* 43:223–225.

Roberts TE. 2006a. History, ocean channels, and distance determine phylogeographic patterns in three widespread Philippine fruit bats (Pteropodidae). *Molecular Ecology* 15:2183–2199.

Roberts TE. 2006b. Multiple levels of allopatric divergence in the endemic Philippine fruit bat *Haplonycteris fischeri* (Pteropodidae). *Biological Journal of the Linnean Society* 88:329–349.

Sanderson MJ, Shaffer HB. 2002. Troubleshooting molecular phylogenetic analyses. *Annual Review of Ecology and Systematics* 33:49–72.

Sanderson MJ, Boss D, Chen D, Cranston KA, Wehe A. 2008. The PhyLoTA Browser: processing GenBank for molecular phylogenetics research. *Systematic Biology* 57:335–346.

Sarasin P. and Sarasin F. 1901. *Ueber die geologische Geschichte der Insel Celebes auf Grund der Thierverbreitung*. Kreidel, Wiesbaden.

Schmitz A. 2003. Taxonomic and phylogenetic studies on scincid lizards (Reptilia: Scincidae). Unpublished Thesis, University Bonn, Germany

Shea GM, Hutchinson MN. 1992. A new species of lizard (*Tiliqua*) from the Miocene of Riversleigh, Queensland. *Memoirs of the Queensland Museum* 32:303–310.

Shi X, Gu H, Field C. 2006. Test a clade in phylogenetic trees. *Molecular Biology and Evolution* 23:1976–1983.

Shimodaira H. 2002. An approximately unbiased test of phylogenetic tree selection. *Systematic Biology* 51:492–508.

Siler CD, Brown RM. 2010. Phylogeny-based species delimitation in Philippine slender skinks (Reptilia: Squamata: Scincidae: *Brachymeles*): taxonomic revision of pentadactyl species groups and description of three new species. *Herpetological Monographs* 24:1–54.

Siler CD, Oaks JR, Esselstyn JA, Diesmos AC, Brown RM. 2010. Phylogeny and biogeography of Philippine bent-toed geckos (Gekkonidae: *Cyrtodactylus*) contradict a prevailing model of Pleistocene diversification. *Molecular Phylogenetics and Evolution* 55:699–710.

Siler CD, Oaks JR, Welton LJ, Linkem CW, Swab JC, Diesmos AC, Brown RM. 2012. Did geckos ride the Palawan raft to the Philippines? *Journal of Biogeography* DOI: 10.1111/j.1365-2699.2011.02680.x

Simpson GG. 1961. *Principles of animal taxonomy*. Columbia University Press, New York, New York, USA.

Skinner A. 2007. Phylogenetic relationships and rate of early diversification of Australian *Sphenomorphus* group scincids (Scincoidea, Squamata). *Biological Journal of the Linnean Society* 92:347–366.

Skinner A, Hugall AF, Hutchinson MN. 2011. Lygosomine phylogeny and the origins of Australian scincid lizards. *Journal of Biogeography* 38:1044–1058.

Smith MA. 1937. A review of the genus *Lygosoma* (Scincidae, Reptilia) and its allies. *Records of the Indian Museum* 39:213–234.

Sokal R, Michner C. 1958. A statistical method for evaluating systematic relationships. *University of Kansas Science Bulletin* 38:1409–1438.

Spakman W, Hall R. 2010. Surface deformation and slab-mantle interaction during Banda Arc subduction rollback. *Nature Geosciences* 3:562–566.

Stamatakis A. 2006. RAxML-VI-HPC: Maximum Likelihood-based Phylogenetic Analyses with Thousands of Taxa and Mixed Models. *Bioinformatics* 22:2688–2690.

Stelbrink B, Albrecht C, Hall R, and Rintelen T. 2012. The Biogeography of Sulawesi revisited: is there evidence for a vicariant origin of taxa on Wallaces "anomalous island"? *Evolution* doi:10.1111/j. 1558-5646.2012.01588.x

Steppan SJ, Zawadzki C, Heaney LR. 2003. Molecular phylogeny of the endemic Philippine rodent *Apomys* (Muridae) and the dynamics of diversification in an oceanic archipelago. *Biological Journal of the Linnean Society* 80:699–715.

Sukumaran J, Holder MT. 2010. DendroPy: A Python library for phylogenetic computing. *Bioinformatics* 26:1569–1571.

Swofford DL, Olsen GJ, Waddell PJ, Hillis DM. 1996. Phylogenetic inference. In: Hillis DM, Moritz C, Mable BK (Eds.). *Molecular Systematics, 2nd edition*. Sinauer Associates, Sunderland, Massachusetts, USA, pp. 407–514.

Taylor EH. 1915. New species of Philippine lizards. *Philippine Journal of Science* 10:89–109.

Taylor EH. 1917. *Brachymeles*, a genus of Philippine lizards. *Philippine Journal of Science* 12:267–279.

Taylor EH. 1922a. *The lizards of the Philippine Islands*. Philippine Bureau of Science. Manila, Philippines.

Taylor EH. 1922*b*. Additions to the herpetological fauna of the Philippine Islands, I. *Philippine Journal of Science* 21:161–206.

Taylor EH. 1922*c*. Additions to the herpetological fauna of the Philippine Islands, II. *Philippine Journal of Science* 21:257–303.

Taylor EH. 1923. Additions to the herpetological fauna of the Philippine Islands, III. *Philippine Journal of Science* 22:515–557.

Taylor EH. 1925. Additions to the herpetological fauna of the Philippine Islands, IV. *Philippine Journal of Science* 26:97–111.

Thomson RC, Shaffer HB. 2010. Sparse supermatrices for phylogenetic inference: Taxonomy, alignment, rogue taxa, and the phylogeny of living turtles. *Systematic Biology* 59:42–58.

Townsend TM, Larson A, Louis E, Macey JR. 2004. Molecular phylogenetics of Squamata: the position of snakes, amphisbaenians, and dibamids, and the root of the squamate tree. *Systematic Biology* 53:735–757.

Townsend TM, Alegre RE, Kelley ST, Wiens JJ, Reeder TW. 2008. Rapid development of multiple nuclear loci for phylogenetic analysis using genomic resources: an example from squamate reptiles. *Molecular Phylogenetics and Evolution* 47:129–142.

Uetz P. 2011. The reptile database. http://www.reptile-database.org/

Utzurrum RCB. 1991. Philippine island biogeographic patterns: practical considerations for resource conservation and management. *Association of Systematic Biologists of the Philippines Communication* 3:19–32.

Voris HK. 2000. Maps of Pleistocene sea levels in Southeast Asia: shorelines, river systems and time durations. *Journal of Biogeography* 27:1153–1167.

Wallace AR. 1863. On the physical geography of the Malay Archipelago. *Journal of the Royal Geographic Society* 33:217–234.

Whiting AS, Bauer AM, Sites Jr. JW. 2003. Phylogenetic relationships and limb loss in sub-Saharan African scincine lizards (Squamata: Scincidae). *Molecular Phylogenetics and Evolution* 29:582–598.

Whitmore TC. 1987. *Biogeographical evolution of the Malay Archipelago*. Clarendon Press, Oxford.

Whitten AJ, Mustafa M, and Henderson GS. 2002. *The ecology of Sulawesi*. Periplus, Singapore.

Wiens JJ. 1998. Does adding characters with missing data increase or decrease phylogenetic accuracy? *Systematic Biology* 47:625–640.

Wiens JJ. 2003. Missing data, incomplete taxa, and phylogenetic accuracy. *Systematic Biology* 52:528–538.

Wiens JJ. 2006. Missing data and the design of phylogenetic analyses. *Journal of Biomedical Informatics* 39:34–42.

Wiens JJ, Moen DS. 2008. Missing data and the accuracy of Bayesian phylogenetics. *Journal of Systematic Evolution* 46:307–314.

Wiens JJ, Brandley MC, Reeder TW. 2006. Why does a trait evolve multiple times within a clade? Repeated evolution of snake-like body form in squamate reptiles. *Evolution* 60:123–141.

Wiley EO. 1978. The evolutionary species concept reconsidered. *Systematic Zoology* 21:17–26.

Wilgenbusch JC, Warren DL, Swofford DL. 2004. AWTY: A system for graphical exploration of MCMC convergence in Bayesian phylogenetic inference. http://ceb.csit.fsu.edu/awty.

Yang Z. 1996. Maximum likelihood models for combined analyses of multiple sequence data. *Journal Molecular Evolution* 42:587–596.

Yu Y, Harris AJ, He XJ. In review. A novel Bayesian method for reconstructing geographic ranges and ancestral states on phylogenies. *Systematic Biology*.

Yumul Jr. G, Dimilanta C, Queaño K, Marquez E. 2009. Philippines, geology. In: Gillespie R, Clague D (Eds.). *Encyclopedia of Islands*. University of California Press, Berkeley, USA, pp. 732–738.

Zwickl DJ. 2006. Genetic algorithm approaches for the phylogenetic analysis of large biological sequence datasets under the maximum likelihood criterion. Ph.D. dissertation, The University of Texas at Austin, USA.

Appendix 1 Voucher specimen catalog numbers (KU = University of Kansas Natural History Museum; TNHC = Texas Natural History Collection; RMB = R. Brown field series; ACD = A. Diesmos field series; GVAG = G. Gee). Genbank accession numbers and full locality data for specimens included in this study. Abbreviations: Is. = Island, Prov. = Province. All GPS data are in the WGS84 datum an decimal degree units.

Museum	Taxon	Genbank	Island	Latitude	Longitude
	Eutropis multifasciata	GU573553			
	Scincella potanini	AY607287			
	Scincella rupicola	AY607284			
	Scincella tsinlingensis	AY607286			
Sphenomorphus					
KU 306538	*S. abdictus abdictus*	GU573559	Dinagat Is., Dinagat Is. Prov.	10.3636111	125.5730556
KU 306540	*S. abdictus abdictus*	GU573562	Dinagat Is., Dinagat Is. Prov.	10.3636111	125.5730556
KU 306542	*S. abdictus abdictus*	GU573560	Dinagat Is., Dinagat Is. Prov.	10.3636111	125.5730556
KU 306544	*S. abdictus abdictus*	GU573561	Dinagat Is., Dinagat Is. Prov.	10.3636111	125.5730556
ACD 1755	*S. abdictus aquilonius*	GU573684	Luzon Is., Isabela Prov.	16.9833333	122.0161111
ACD 1865	*S. abdictus aquilonius*	GU573686	Luzon Is., Isabela Prov.	16.9833333	122.0161111
ACD 1922	*S. abdictus aquilonius*	GU573685	Luzon Is., Isabela Prov.	16.9833333	122.0161111
ACD 1957	*S. abdictus aquilonius*	GU573678	Luzon Is., Isabela Prov.	16.9833333	122.0161111
ACD 2038	*S. abdictus aquilonius*	GU573679	Luzon Is., Isabela Prov.	16.9833333	122.0161111
ACD 2169	*S. abdictus aquilonius*	GU573680	Luzon Is., Isabela Prov.	16.9833333	122.0161111
ACD 2170	*S. abdictus aquilonius*	GU573677	Luzon Is., Isabela Prov.	16.9833333	122.0161111
ACD 2283	*S. abdictus aquilonius*	GU573689	Luzon Is., Isabela Prov.	16.8497222	121.7491667
ACD 2293	*S. abdictus aquilonius*	GU573687	Luzon Is., Isabela Prov.	16.8497222	121.7491667
ACD 2359	*S. abdictus aquilonius*	GU573693	Luzon Is., Isabela Prov.	16.8497222	121.7491667
ACD 2360	*S. abdictus aquilonius*	GU573688	Luzon Is., Isabela Prov.	16.8497222	121.7491667
ACD 2468	*S. abdictus aquilonius*	GU573682	Luzon Is., Isabela Prov.	16.8497222	121.7491667

ACD 2490	*S. abdictus aquilonius*	GU573675	Luzon Is., Isabela Prov.	17.4122222	121.8027778
ACD 3079	*S. abdictus aquilonius*	GU573692	Luzon Is., Isabela Prov.	16.9833333	122.0161111
ACD 3080	*S. abdictus aquilonius*	GU573690	Luzon Is., Isabela Prov.	16.9833333	122.0161111
ACD 3083	*S. abdictus aquilonius*	GU573681	Luzon Is., Isabela Prov.	16.9833333	122.0161111
ACD 3105	*S. abdictus aquilonius*	GU573674	Luzon Is., Isabela Prov.	16.9833333	122.0161111
ACD 3132	*S. abdictus aquilonius*	GU573694	Luzon Is., Isabela Prov.	16.9833333	122.0161111
ACD 3138	*S. abdictus aquilonius*	GU573683	Luzon Is., Isabela Prov.	16.9833333	122.0161111
ACD 3171	*S. abdictus aquilonius*	GU573691	Luzon Is., Isabela Prov.	16.9833333	122.0161111
ACD 3237	*S. abdictus aquilonius*	GU573672	Luzon Is., Cagayan Prov.	18.0630556	121.6438889
ACD 3348	*S. abdictus aquilonius*	GU573673	Luzon Is., Cagayan Prov.	18.0630556	121.6438889
KU302911	*S. abdictus aquilonius*	GU573655	Polillo Is., Quezon Prov.	14.7525833	121.9682
KU302912	*S. abdictus aquilonius*	GU573653	Polillo Is., Quezon Prov.	14.7525833	121.9682
KU302913	*S. abdictus aquilonius*	GU573662	Polillo Is., Quezon Prov.	14.7525833	121.9682
KU302914	*S. abdictus aquilonius*	GU573657	Polillo Is., Quezon Prov.	14.7525833	121.9682
KU302915	*S. abdictus aquilonius*	GU573661	Polillo Is., Quezon Prov.	14.7525833	121.9682
KU302916	*S. abdictus aquilonius*	GU573652	Polillo Is., Quezon Prov.	14.7525833	121.9682
KU302917	*S. abdictus aquilonius*	GU573654	Polillo Is., Quezon Prov.	14.7525833	121.9682
KU302919	*S. abdictus aquilonius*	GU573656	Polillo Is., Quezon Prov.	14.7525833	121.9682
KU302920	*S. abdictus aquilonius*	GU573666	Polillo Is., Quezon Prov.	14.7525833	121.9682
KU 302921	*S. abdictus aquilonius*	GU573651	Polillo Is., Quezon Prov.	14.7525833	121.9682
KU 302922	*S. abdictus aquilonius*	GU573664	Polillo Is., Quezon Prov.	14.7525833	121.9682
RMB 3438	*S. abdictus aquilonius*	GU573648	Luzon Is., Camarines Sur Prov.	13.6191667	123.1813889
TNHC 63108	*S. abdictus aquilonius*	GU573635	Luzon Is., Zambales Prov.	14.8291667	120.2827778
TNHC 63109	*S. abdictus aquilonius*	GU573636	Luzon Is., Zambales Prov.	14.8291667	120.2827778
KU 304050	*S. abdictus aquilonius*	GU573695	Luzon Is., Isabela Prov.	16.9833333	122.0161111
KU 304047	*S. abdictus aquilonius*	GU573631	Lubang Is., Occidental Mindoro Prov.	13.8577778	120.1233333
RMB 5538	*S. abdictus aquilonius*	GU573633	Lubang Is., Occidental Mindoro Prov.	13.8577778	120.1233333
KU 304048	*S. abdictus aquilonius*	GU573632	Lubang Is., Occidental Mindoro Prov.	13.8577778	120.1233333
KU 304049	*S. abdictus aquilonius*	GU573634	Lubang Is., Occidental Mindoro Prov.	13.8577778	120.1233333
KU 304555	*S. abdictus aquilonius*	GU573703	Camiguin Norte Is., Cagayan Prov.	19.2641667	121.4797222

KU 304556	*S. abdictus aquilonius*	GU573696	Camiguin Norte Is., Cagayan Prov.	19.2641667	121.4797222
KU 304560	*S. abdictus aquilonius*	GU573698	Camiguin Norte Is., Cagayan Prov.	19.2641667	121.4797222
KU 304561	*S. abdictus aquilonius*	GU573704	Camiguin Norte Is., Cagayan Prov.	19.2641667	121.4797222
KU 304568	*S. abdictus aquilonius*	GU573701	Camiguin Norte Is., Cagayan Prov.	19.2641667	121.4797222
KU 304570	*S. abdictus aquilonius*	GU573699	Camiguin Norte Is., Cagayan Prov.	19.2641667	121.4797222
KU 304576	*S. abdictus aquilonius*	GU573697	Camiguin Norte Is., Cagayan Prov.	19.2641667	121.4797222
KU 304577	*S. abdictus aquilonius*	GU573705	Camiguin Norte Is., Cagayan Prov.	19.2641667	121.4797222
KU 304621	*S. abdictus aquilonius*	GU573702	Camiguin Norte Is., Cagayan Prov.	19.2641667	121.4797222
KU 304622	*S. abdictus aquilonius*	GU573700	Camiguin Norte Is., Cagayan Prov.	19.2641667	121.4797222
KU 304787	*S. abdictus aquilonius*	GU573629	Camiguin Norte Is., Cagayan Prov.	19.2641667	121.4797222
KU 304788	*S. abdictus aquilonius*	GU573637	Camiguin Norte Is., Cagayan Prov.	19.2641667	121.4797222
KU 304789	*S. abdictus aquilonius*	GU573638	Camiguin Norte Is., Cagayan Prov.	19.2641667	121.4797222
KU 304790	*S. abdictus aquilonius*	GU573628	Camiguin Norte Is., Cagayan Prov.	19.2641667	121.4797222
KU 304898	*S. abdictus aquilonius*	GU573622	Camiguin Norte Is., Cagayan Prov.	19.2641667	121.4797222
KU 304901	*S. abdictus aquilonius*	GU573619	Camiguin Norte Is., Cagayan Prov.	19.2641667	121.4797222
KU 304904	*S. abdictus aquilonius*	GU573625	Camiguin Norte Is., Cagayan Prov.	19.2641667	121.4797222
KU 304911	*S. abdictus aquilonius*	GU573620	Camiguin Norte Is., Cagayan Prov.	19.2641667	121.4797222
KU 304912	*S. abdictus aquilonius*	GU573623	Camiguin Norte Is., Cagayan Prov.	19.2641667	121.4797222
KU 304913	*S. abdictus aquilonius*	GU573624	Camiguin Norte Is., Cagayan Prov.	19.2641667	121.4797222
KU 304914	*S. abdictus aquilonius*	GU573627	Camiguin Norte Is., Cagayan Prov.	19.2641667	121.4797222
KU 304922	*S. abdictus aquilonius*	GU573626	Camiguin Norte Is., Cagayan Prov.	19.2641667	121.4797222
KU 304928	*S. abdictus aquilonius*	GU573621	Camiguin Norte Is., Cagayan Prov.	19.2641667	121.4797222
KU 304930	*S. abdictus aquilonius*	GU573630	Camiguin Norte Is., Cagayan Prov.	19.2641667	121.4797222
KU 307677	*S. abdictus aquilonius*	GU573676	Luzon Is., Isabela Prov.	17.4261111	121.7625
KU 307678	*S. abdictus aquilonius*	GU573667	Polillo Is., Quezon Prov.	14.7525833	121.9682
KU 307679	*S. abdictus aquilonius*	GU573649	Polillo Is., Quezon Prov.	14.7525833	121.9682
KU 307680	*S. abdictus aquilonius*	GU573659	Polillo Is., Quezon Prov.	14.7525833	121.9682
KU 307681	*S. abdictus aquilonius*	GU573660	Polillo Is., Quezon Prov.	14.7525833	121.9682
KU 307682	*S. abdictus aquilonius*	GU573668	Polillo Is., Quezon Prov.	14.7525833	121.9682
KU 307683	*S. abdictus aquilonius*	GU573663	Polillo Is., Quezon Prov.	14.7525833	121.9682

KU 307684	*S. jagori jagori*	GU573600	Polillo Is., Quezon Prov.	14.7525833	121.9682
KU 307685	*S. jagori jagori*	GU573604	Polillo Is., Quezon Prov.	14.7525833	121.9682
KU 307686	*S. abdictus aquilonius*	GU573665	Polillo Is., Quezon Prov.	14.7525833	121.9682
KU 307687	*S. jagori jagori*	GU573612	Polillo Is., Quezon Prov.	14.7525833	121.9682
KU 307688	*S. abdictus aquilonius*	GU573650	Polillo Is., Quezon Prov.	14.7525833	121.9682
KU 307689	*S. abdictus aquilonius*	GU573658	Polillo Is., Quezon Prov.	14.7525833	121.9682
KU 307690	*S. jagori jagori*	GU573607	Polillo Is., Quezon Prov.	14.7525833	121.9682
KU 307691	*S. abdictus aquilonius*	GU573670	Polillo Is., Quezon Prov.	14.8447333	121.9193
KU 307692	*S. jagori jagori*	GU573609	Polillo Is., Quezon Prov.	14.8447333	121.9193
KU 307693	*S. abdictus aquilonius*	GU573669	Polillo Is., Quezon Prov.	14.8447333	121.9193
KU 307694	*S. abdictus aquilonius*	GU573671	Polillo Is., Quezon Prov.	14.8447333	121.9193
KU 308074	*S. abdictus aquilonius*	GU573706	Camiguin Norte Is., Cagayan Prov.	19.2641667	121.4797222
KU 307970	*S. abdictus aquilonius*	GU573707	Camiguin Norte Is., Cagayan Prov.	19.2641667	121.4797222
KU 307977	*S. abdictus aquilonius*	GU573710	Camiguin Norte Is., Cagayan Prov.	19.2641667	121.4797222
KU 307987	*S. abdictus aquilonius*	GU573708	Camiguin Norte Is., Cagayan Prov.	19.2641667	121.4797222
KU 307988	*S. abdictus aquilonius*	GU573711	Camiguin Norte Is., Cagayan Prov.	19.2641667	121.4797222
KU 308016	*S. abdictus aquilonius*	GU573713	Camiguin Norte Is., Cagayan Prov.	19.2641667	121.4797222
KU 308028	*S. abdictus aquilonius*	GU573709	Camiguin Norte Is., Cagayan Prov.	19.2641667	121.4797222
KU 308029	*S. abdictus aquilonius*	GU573712	Camiguin Norte Is., Cagayan Prov.	19.2641667	121.4797222
RMB 949	*S. abdictus aquilonius*	GU573639	Luzon Is., Aurora Prov., Munic. San Luis	15.7213889	121.5205556
KU 309908	*S. coxi coxi*	GU573562	Camiguin Sur Is.		
ACD 2602	*S. coxi coxi*	GU573566	Mindanao Is., Davao Oriental Prov.	7.2338889	126.5575
ACD 2684	*S. coxi coxi*	GU573565	Mindanao Is., Davao Oriental Prov.	7.2338889	126.5575
ACD 2685	*S. coxi coxi*	GU573564	Mindanao Is., Davao Oriental Prov.	7.2338889	126.5575
ACD 925	*S. coxi divergens*	GU573640	Luzon Is., Laguna Prov.	14.1788889	121.2255556
KU308349	*S. coxi divergens*	GU573645	Mindoro Is., Occidental Mindoro Prov.	13.4180556	120.4672222
KU308380	*S. coxi divergens*	GU573641	Mindoro Is., Occidental Mindoro Prov.	13.4180556	120.4672222
KU308410	*S. coxi divergens*	GU573644	Mindoro Is., Occidental Mindoro Prov.	13.4180556	120.4672222
KU308411	*S. coxi divergens*	GU573642	Mindoro Is., Occidental Mindoro Prov.	13.4180556	120.4672222
KU308412	*S. coxi divergens*	GU573646	Mindoro Is., Occidental Mindoro Prov.	13.4180556	120.4672222
KU308413	*S. coxi divergens*	GU573643	Mindoro Is., Occidental Mindoro Prov.	13.4180556	120.4672222

KU307008	*S. coxi divergens*	GU573647	Panay Is., Antique Prov.	10.8333333	122.1
TNHC 60017	*S. fasciatus*	AF373264 DQ675240			
KU302926	*S. jagori grandis*	GU573592	Panay Is., Antique Prov.	11.7222222	122.0963889
KU302927	*S. jagori grandis*	GU573594	Panay Is., Antique Prov.	11.7222222	122.0963889
KU302928	*S. jagori grandis*	GU573596	Panay Is., Antique Prov.	11.7222222	122.0963889
KU302924	*S. jagori grandis*	GU573593	Panay Is., Antique Prov.	11.7222222	122.0963889
KU302925	*S. jagori grandis*	GU573595	Panay Is., Antique Prov.	11.7222222	122.0963889
KU308219	*S. jagori jagori*	GU573615	Catanduanes Is., Catanduanes Prov.	13.7794444	124.3897222
KU308220	*S. jagori jagori*	GU573613	Catanduanes Is., Catanduanes Prov.	13.7794444	124.3897222
KU308221	*S. jagori jagori*	GU573617	Catanduanes Is., Catanduanes Prov.	13.7794444	124.3897222
KU308222	*S. jagori jagori*	GU573618	Catanduanes Is., Catanduanes Prov.	13.7794444	124.3897222
KU308223	*S. jagori jagori*	GU573616	Catanduanes Is., Catanduanes Prov.	13.7794444	124.3897222
KU 308238	*S. jagori jagori*	GU573614	Catanduanes Is., Catanduanes Prov.	13.7794444	124.3897222
GVAG 266	*S. jagori grandis*	GU573597	Panay Is., Antique Prov.	10.7883333	122.0197222
GVAG 275	*S. jagori grandis*	GU573591	Panay Is., Antique Prov.	10.7883333	122.0197222
TNHC 62860	*S. jagori grandis*	GU573598	Negros Is., Negros Oriental Prov.	9.2902778	123.26
TNHC 62861	*S. jagori grandis*	GU573599	Negros Is., Negros Oriental Prov.	9.2902778	123.26
TNHC 63094	*S. jagori jagori*	GU573567	Luzon Is., Camarines Sur Prov.	13.6191667	123.1813889
TNHC 63095	*S. jagori jagori*	GU573568	Luzon Is., Camarines Sur Prov.	13.6191667	123.1813889
TNHC 63098	*S. jagori jagori*	GU573570	Luzon Is., Albay Prov.	13.4013889	123.7075
TNHC 63099	*S. jagori jagori*	GU573569	Luzon Is., Albay Prov.	13.4013889	123.7075
TNHC 63100	*S. jagori jagori*	GU573573	Luzon Is., Sorsogon Prov.	12.7013889	124.0386111
RMB3947	*S. jagori jagori*	GU573575	Luzon Is., Sorsogon Prov.	12.7013889	124.0386111
TNHC 63102	*S. jagori jagori*	GU573571	Luzon Is., Sorsogon Prov.	12.7013889	124.0386111
TNHC 63105	*S. jagori jagori*	GU573574	Luzon Is., Sorsogon Prov.	12.7013889	124.0386111
TNHC 63106	*S. jagori jagori*	GU573572	Luzon Is., Sorsogon Prov.	12.7013889	124.0386111
KU 302929	*S. jagori jagori*	GU573610	Polillo Is., Quezon Prov.	14.7525833	121.9682
KU 302930	*S. jagori jagori*	GU573601	Polillo Is., Quezon Prov.	14.7525833	121.9682
KU 302931	*S. jagori jagori*	GU573602	Polillo Is., Quezon Prov.	14.7525833	121.9682
KU 302932	*S. jagori jagori*	GU573605	Polillo Is., Quezon Prov.	14.7525833	121.9682

KU 302933	*S. jagori jagori*	GU573603	Polillo Is., Quezon Prov.	14.7525833	121.9682
KU 302934	*S. jagori jagori*	GU573611	Polillo Is., Quezon Prov.	14.7525833	121.9682
KU 302935	*S. jagori jagori*	GU573606	Polillo Is., Quezon Prov.	14.7525833	121.9682
KU 302918	*S. jagori jagori*	GU573608	Polillo Is., Quezon Prov.	14.7525833	121.9682
KU 306548	*S. jagori jagori*	GU573579	Samar Is., Western Samar Prov.	12.0544444	125.0269444
KU 306459	*S. jagori jagori*	GU573583	Samar Is., Western Samar Prov.	12.0544444	125.0269444
KU 306550	*S. jagori jagori*	GU573576	Samar Is., Western Samar Prov.	12.0544444	125.0269444
KU 306551	*S. jagori jagori*	GU573582	Samar Is., Eastern Samar Prov.	11.9011111	125.4188889
KU 306545	*S. jagori jagori*	GU573584	Dinagat Is., Dinagat Is. Prov.	10.3636111	125.5730556
KU 306552	*S. jagori jagori*	GU573581	Samar Is., Western Samar Prov.	12.0544444	125.0269444
KU 306553	*S. jagori jagori*	GU573580	Samar Is., Western Samar Prov.	12.0544444	125.0269444
KU 306554	*S. jagori jagori*	GU573578	Samar Is., Eastern Samar Prov.	11.9011111	125.4188889
KU 306555	*S. jagori jagori*	GU573577	Samar Is., Eastern Samar Prov.	11.9011111	125.4188889
KU 306546	*S. jagori jagori*	GU573587	Dinagat Is., Dinagat Is. Prov.	10.3636111	125.5730556
KU 306547	*S. jagori jagori*	GU573588	Dinagat Is., Dinagat Is. Prov.	10.3636111	125.5730556
TNHC 56380	*S. jagori jagori*	GU573585	Bohol Is., Bohol Prov.	9.8241667	124.1975
RMB 2888	*S. jagori jagori*	GU573586	Bohol Is., Bohol Prov.	9.7088889	124.105
KU 315067	*S. jagori jagori*	GU573589	Mindanao Is., Zamboanga City Prov.		
KU 315069	*S. jagori jagori*	GU573590	Mindanao Is., Zamboanga City Prov.		
	S. jobiensis	DQ675258			
TNHC 62682	*S. leucospilos*	GU573554	Luzon Is., Quezon Prov.	14.0288889	121.5911111
KU 306556	*S. llanosi*	GU573557	Samar Is., Western Samar Prov.	12.0544444	125.0269444
KU 306557	*S. llanosi*	GU573558	Samar Is., Eastern Samar Prov.	11.9011111	125.4188889
GVAG 228	*S. steerei*	GU573556	Panay Is.. Antique Prov.		
GVAG 248	*S. steerei*	GU573555	Panay Is.. Antique Prov.		

Appendix 2 Gene and taxon sampling from chapter 2.

Taxonomic identification	Voucher number	Genebank Numbers					
		ND2	12S	16S	ND4	NGFB	R35
Lacertidae							
Tachydromus sexilineatus	KU 311512	HQ907420	—	JF498098	—	JF498325	HQ907624
Xantusiidae							
Xantusia vigilis	KU 220088	JF498215	JF497976	JF498107	—	JF498334	JF498458
X. vigilis	KU 220090	JF498216	JF497977	JF498108	—	JF498335	JF498459
Scincidae							
Scincinae							
Plestiodon quadrilineatus	KU 311490	HQ907422	JF497945	JF498073	JF498547	JF498301	HQ907628
P. fasciatus	KU 289462	HQ907423	JF497944	JF498072	JF498546	JF498300	HQ907629
P. anthracinus	KU 290718	HQ907424	JF497943	JF498071	JF498545	JF498299	HQ907630
Lygosominae							
Dasia grisea	KU 305573	HQ907425	JF497855	JF497978	JF498460	JF498217	HQ907631
E. caeruleocauda	KU 307154	JF498109	JF497857	JF497980	JF498462	JF498219	JF498336
E. cyanogaster	KU 307235	JF498111	JF497859	JF497982	JF498464	JF498221	JF498338
E. cyanura	TNHC 58932	JF498110	JF497858	JF497981	JF498463	JF498220	JF498337
E. schmidti	KU 307133	—	JF497860	JF497983	JF498465	JF498222	JF498339
Emoia atrocostata	KU 304896	HQ907421	JF497856	JF497979	JF498461	JF498218	HQ907627

Eremiascincus richardsonii	—	—	AY169582	AY169619	AY169657	—	—
Eulamprus murrayi	—	—	AY169584	AY169621	AY169659	—	—
Eutropis multifasciata	KU 302890	JF498112	JF497861	JF497984	JF498466	JF498223	JF498340
Glaphyromorphus darwiniensis	—	—	DQ915286	DQ915310	DQ915334	—	—
Hemiergis peroni	—	—	AY169590	AY169627	AY169665	—	—
Insulasaurus arborens	KU 306712	JF498114	JF497863	JF497986	JF498468	JF498225	JF498342
Insulasaurus arborens	KU 306805	JF498113	JF497862	JF497985	JF498467	JF498224	JF498341
Insulasaurus traanorum	KU 311442	JF498115	JF497864	JF497987	JF498469	—	JF498343
Insulasaurus traanorum	KU 311443	JF498116	JF497865	JF497988	JF498470	JF498226	JF498344
Insulasaurus victoria	KU 309443	JF498117	—	JF497989	—	—	JF498345
Insulasaurus wrighti	KU 311422	JF498118	JF497866	JF497990	JF498471	JF498227	JF498346
Insulasaurus wrighti	KU 311438	JF498119	JF497867	JF497991	JF498472	JF498226	JF498347
Lipinia noctua	CAS 236454	JF498120	JF497868	JF497992	JF498473	—	JF498348
Lipinia pulchella	TNHC 56378	JF498121	JF497869	JF497993	JF498474	JF498228	JF498349
Lipinia pulchella	TNHC 56379	JF498122	JF497870	JF497994	JF498475	JF498229	HQ907625
Mabuya mabouia	KU 214970	JF498123	JF497871	JF497995	—	JF498230	JF498350
Mabuya unimarginata	KU 291283	JF498124	JF497943	JF497996	JF498476	JF498231	JF498351
Otosaurus cumingi	RMB 808	JF498125	JF497873	JF497997	JF498477	JF498232	JF498352

Otosaurus cumingi	RMB 985	JF498126	JF497874	JF497998	JF498478	—	JF498353
Panaspis togoensis	KU 290440	JF498127	JF497875	JF497999	—	JF498233	JF498354
Papuascincus stanleyanus	RNF 0065	JF498128	JF497876	—	JF498479	JF498234	JF498355
Papuascincus stanleyanus	RNF 0067	JF498129	JF497877	JF498000	JF498480	JF498235	JF498356
Parvoscincus beyeri	FMNH 266118	JF498130	—	JF498001	JF498481	JF498236	JF498357
Parvoscincus beyeri	TNHC 06267	JF498131	JF497878	JF498002	JF498482	JF498237	JF498358
Parvoscincus boyingi	FMNH 267561	JF498133	JF497880	JF498004	JF498484	JF498239	JF498360
Parvoscincus boyingi	FMNH 267664	JF498132	JF497879	JF498003	JF498483	JF498238	JF498359
Parvoscincus cf. beyeri	KU 308666	JF498134	JF497881	JF498005	JF498485	JF498240	JF498361
Parvoscincus cf. decipiens sp. 1	KU 306558	JF498135	JF497882	JF498006	JF498486	JF498241	JF498362
Parvoscincus cf. decipiens sp. 1	TNHC 62889	JF498136	JF497883	—	JF498487	—	—
Parvoscincus cf. decipiens sp. 2	KU 306560	JF498137	JF497884	JF498007	JF498488	JF498242	JF498363
Parvoscincus cf. decipiens sp. 2	TNHC 62679	JF498138	JF497885	JF498008	JF498489	—	JF498364
Parvoscincus cf. decipiens sp. 3	TNHC 62883	JF498139	JF497886	JF498009	JF498490	JF498243	JF498365
Parvoscincus cf. decipiens sp. 3	TNHC 62897	JF498140	JF497887	JF498010	JF498491	JF498244	JF498366
Parvoscincus cf. decipiens sp. 4	TNHC 62893	JF498142	JF497888	JF498012	JF498493	JF498246	JF498368
Parvoscincus cf. decipiens sp. 4	ACD 1020	JF498141	—	JF498011	JF498492	JF498245	JF498367
Parvoscincus cf. lawtoni	FMNH 266278	JF498143	JF497889	JF498013	JF498494	JF498247	JF498369

Parvoscincus decipiens	ACD 2233	JF498144	—	JF498014	JF498495	JF49824 8	JF498370
Parvoscincus decipiens	ACD 2423	JF498145	JF497890	JF498015	JF498496	JF49824 9	JF498371
Parvoscincus hadros	PNM 9618	—	—	JF498016	—	—	JF498372
Parvoscincus hadros	PNM 9620	—	—	JF498017	—	—	JF498373
Parvoscincus igorotorum	FMNH 259448	JF498146	JF497891	JF498018	JF498497	JF49825 0	JF498374
Parvoscincus igorotorum	PNM 9623	JF498147	JF497892	JF498019	JF498498	—	JF498375
Parvoscincus kitangladensis	KU 326618	JF498148	JF497893	JF498020	JF498499	JF49825 1	JF498376
Parvoscincus kitangladensis	KU 326619	JF498149	JF497894	JF498021	JF498500	JF49825 2	JF498377
Parvoscincus kitangladensis	KU 326627	JF498150	JF497895	JF498022	JF498501	JF49825 3	JF498378
Parvoscincus laterimaculatus	TNHC 62675	JF498151	JF497896	JF498023	JF498502	JF49825 4	JF498379
Parvoscincus laterimaculatus	TNHC 62676	JF498152	JF497897	JF498024	JF498503	JF49825 5	JF498380
Parvoscincus lawtoni	KU 308668	JF498153	JF497898	JF498025	JF498504	JF49825 6	JF498381
Parvoscincus leucospilos	KU 320522	JF498154	JF497899	JF498026	JF498505	JF49825 7	JF498382
Parvoscincus leucospilos	TNHC 62682	JF498155	JF497900	JF498027	JF498506	JF49825 8	JF498383
Parvoscincus luzonensis	FMNH 258990	JF498156	JF497901	JF498028	JF498507	JF49825 9	JF498384
Parvoscincus luzonensis	FMNH 263506	JF498157	—	JF498029	JF498508	JF49826 0	JF498385
Parvoscincus sisoni	RMB 700	JF498158	JF497902	JF498030	JF498509	JF49826 1	JF498386
Parvoscincus steerei 1	RMB 3944	JF498160	JF497904	JF498032	JF498511	—	JF498388

Parvoscincus steerei 1	TNHC 63091	JF498159	JF497903	JF498031	JF498510	—	JF498387
Parvoscincus steerei 2	ACD 1203	JF498161	JF497905	JF498033	JF498512	JF498262	JF498389
Parvoscincus steerei 3	ACD 2696	JF498162	JF497906	JF498034	—	JF498263	JF498390
Parvoscincus steerei 3	ACD 2709	JF498163	—	JF498035	—	JF498264	JF498391
Parvoscincus steerei 4	EMD 429	JF498164	JF497908	JF498036	—	JF498265	JF498392
Parvoscincus steerei 5	KU 306736	JF498165	JF497909	JF498037	—	JF498266	JF498393
Parvoscincus steerei4	TNHC 56356	JF498166	JF497910	JF498038	JF498513	JF498267	JF498394
Parvoscincus steerei5	KU 302937	JF498167	JF497911	JF498039	JF498514	JF498268	JF498395
Parvoscincus steerei5	KU 302938	JF498168	JF497912	JF498040	JF498515	JF498269	JF498396
Parvoscincus steerei6	KU 306840	JF498169	JF497913	JF498041	JF498516	JF498270	JF498397
Parvoscincus steerei6	GVAG 273	JF498170	JF497914	JF498042	JF498517	JF498271	JF498398
Parvoscincus steerei7	TNHC 63086	JF498171	JF497915	JF498043	JF498518	JF498272	JF498399
Parvoscincus steerei7	TNHC 63093	JF498172	JF497916	JF498044	JF498519	JF498273	JF498400
Parvoscincus tagapayo	KU 308926	JF498173	JF497917	JF498045	JF498520	JF498274	JF498401
Parvoscincus tagapayo	KU 326400	JF498174	JF497918	JF498046	JF498521	JF498275	JF498402
Pinoyscincus abdictus abdictus	ACD 2687	JF498175	JF497920	JF498048	JF498523	JF498277	JF498404
Pinoyscincus abdictus abdictus	KU 306538	GU573559	JF497919	JF498047	JF498522	JF498276	JF498403

Pinoyscincus abdictus aquilonius10	FMNH 266115	JF498176	JF497921	JF498049	JF498524	JF498278	JF498405
Pinoyscincus abdictus aquilonius10	KU 302920	GU573666	JF497922	JF498050	JF498525	JF498279	JF498406
Pinoyscincus abdictus aquilonius10	TNHC 62758	GU573648	JF497923	JF498051	JF498526	JF498280	JF498407
Pinoyscincus abdictus aquilonius11	RMB 953	JF498177	JF497924	JF498052	JF498527	JF498281	JF498408
Pinoyscincus abdictus aquilonius8	KU 307018	JF498178	JF497925	JF498053	JF498528	JF498282	JF498409
Pinoyscincus abdictus aquilonius8	TNHC 63108	JF498179	JF497926	JF498054	JF498529	JF498283	JF498410
Pinoyscincus coxi coxi	KU 309908	GU573562	JF497927	JF498055	JF498530	JF498284	JF498411
Pinoyscincus coxi coxi	ACD 2685	GU573564	JF497928	JF498056	JF498531	JF498285	JF498412
Pinoyscincus coxi divergens	KU 308380	GU573561	JF497929	JF498057	JF498532	—	JF498413
Pinoyscincus coxi divergens	ACD 925	GU573640	JF497930	JF498058	JF498533	JF498286	JF498414
Pinoyscincus jagori grandis	GVAG 266	GU573597	JF497931	JF498059	JF498534	JF498287	JF498415
Pinoyscincus jagori grandis	TNHC 62860	JF498180	JF497932	JF498060	JF498535	JF498288	JF498416
Pinoyscincus jagori jagori 3	TNHC 63095	JF498181	JF497933	JF498061	JF498536	JF498289	JF498417
Pinoyscincus jagori jagori 3	TNHC 63102	GU573571	JF497934	JF498062	JF498537	JF498290	JF498418
Pinoyscincus jagori jagori 4	KU 306546	GU573587	JF497935	JF498063	JF498538	JF498291	JF498419
Pinoyscincus jagori jagori 4	TNHC 56380	JF498182	JF497936	JF498064	JF498539	JF498292	JF498420

Pinoyscincus jagori jagori 6	KU 302929	GU573610	JF497937	JF498065	JF498540	JF498293	JF498421
Pinoyscincus jagori jagori 6	KU 307684	JF498183	JF497938	JF498066	—	JF498294	JF498422
Pinoyscincus llanosi	KU 306556	GU573557	JF497939	JF498067	JF498541	JF498295	JF498423
Pinoyscincus llanosi	KU 306557	GU573558	JF497940	JF498068	JF498542	JF498296	JF498424
Pinoyscincus mindanensis	KU 310135	JF498184	JF497941	JF498069	JF498543	JF498297	JF498425
Pinoyscincus mindanensis	TNHC 56351	JF498185	JF497942	JF498070	JF498544	JF498298	JF498426
Scincella assatus	KU 289795	—	JF497946	JF498074	JF498548	JF498302	JF498427
Scincella assatus	KU 291286	JF498186	—	JF498075	JF498549	JF498303	JF498428
Scincella cherrei	—	—	JF497947	JF498076	JF498550	JF498304	JF498429
Scincella lateralis	KU 289460	JF498187	JF497948	JF498077	—	JF498305	JF498430
Scincella reevesii	FMNH 255540	HQ907428	JF497949	JF498078	JF498551	—	HQ907634
Sphenomorphus acutus	KU 319962	JF498188	JF497950	JF498079	JF498552	JF498306	JF498431
Sphenomorphus concinnatus	KU 307213	JF498189	—	JF498080	JF498553	JF498307	JF498432
Sphenomorphus concinnatus	KU 307348	JF498190	JF497951	JF498081	JF498554	JF498308	JF498433
Sphenomorphus cranei	KU 307167	JF498191	JF497952	JF498082	JF498555	JF498309	JF498434
Sphenomorphus cranei	KU 307168	JF498192	JF497953	JF498083	JF498556	JF498310	JF498435
Sphenomorphus cyanolaemus	FMNH 239867	JF498193	JF497954	JF498084	JF498557	JF498311	JF498436
Sphenomorphus diwata	EMD 368	JF498194	JF497955	JF498085	JF498558	JF498312	JF498437

Sphenomorphus diwata	EMD 428	JF498195	JF497956	JF498086	JF498559	JF498313	JF498438
Sphenomorphus fasciatus	KU 310807	JF498196	JF497957	JF498087	JF498560	JF498314	JF498439
Sphenomorphus fasciatus	KU 315061	JF498197	JF497958	JF498088	JF498561	JF498315	JF498440
Sphenomorphus indicus	CAS 214892	JF498198	JF497959	JF498089	JF498562	JF498316	JF498441
Sphenomorphus maculatus	FMNH 261863	JF498199	JF497960	JF498090	JF498563	JF498317	JF498442
Sphenomorphus multisquamatus	FMNH 243828	JF498200	JF497961	JF498091	JF498564	JF498318	JF498443
Sphenomorphus sabanus	FMNH 239881	JF498201	JF497962	JF498092	JF498565	JF498319	JF498444
Sphenomorphus scutatus	CAS 236398	JF498202	JF497963	JF498093	JF498566	JF498320	JF498445
Sphenomorphus solomonis	KU 307173	JF498203	JF497964	JF498094	JF498567	JF498321	JF498446
Sphenomorphus solomonis	KU 307349	JF498204	JF497965	JF498095	JF498568	JF498322	JF498447
Sphenomorphus variegatus	KU 309900	JF498205	JF497966	JF498096	—	JF498323	JF498448
Sphenomorphus variegatus	KU 315087	JF498206	JF497967	JF498097	JF498569	JF498324	JF498449
Trachylepis perroteti	KU 291923	JF498207	JF497968	JF498099	—	JF498326	JF498450
Tytthoscincus aesculeticola	SP 06913	JF498208	JF497969	JF498100	JF498570	JF498327	JF498451
Tytthoscincus aesculeticola	FMNH 239839	JF498209	JF497970	JF498101	JF498571	JF498328	JF498452
Tytthoscincus atrigularis	KU 315055	JF498210	JF497971	JF498102	JF498572	JF498329	JF498453
Tytthoscincus atrigularis	KU 315060	JF498211	JF497972	JF498103	JF498573	JF498330	JF498454
Tytthoscincus hallieri	FMNH 230184	JF498212	JF497973	JF498104	JF498574	JF498331	JF498455

Tytthoscincus parvus	RMB 4707	JF498213	JF497974	JF498105	JF498575	JF498332	JF498456
Tytthoscincus parvus	JAM6275	JF498214	JF497975	JF498106	JF498576	JF498333	JF498457

This Page Intentionally left blank